United States Nuclear Regulatory Commission

Protecting People and the Environment

NUREG/CR-XXXX
ANL-10/27

Verification of RESRAD-OFFSITE

Office of Nuclear Regulatory Research

United States Nuclear Regulatory Commission

Protecting People and the Environment

NUREG/CR-XXXX
ANL-10/27

Verification of RESRAD-OFFSITE

Manuscript Completed: July 2009
Date Published: June 2010

Prepared by
C. Yu, E.K. Gnanapragasam, J.-J. Cheng, S. Kamboj, B.M. Biwer, and D.J. LePoire

Argonne National Laboratory
9700 South Cass Avenue
Argonne, IL 60439

John Randall, NRC Project Manager

NRC Job Code N6731

Office of Nuclear Regulatory Research

ABSTRACT

This report documents the procedures used and the results obtained regarding the verification of the RESRAD-OFFSITE computer code. The RESRAD-OFFSITE code is an extension of the original RESRAD (onsite) code. The RESRAD-OFFSITE and RESRAD (onsite) codes share the same database and many models and modules. The RESRAD (onsite) code has already been extensively tested, verified, and validated. Many parameter values used in the RESRAD-OFFSITE code were taken from the RESRAD (onsite) database. These parameters include soil-plant transfer factors, meat and milk transfer factors, bioaccumulation factors, dose conversion factors, decay half-lives, and scenario-specific occupancy factors. The RESRAD (onsite) database is well documented and verified. Components of the RESRAD-OFFSITE code were verified by separately developed spreadsheets or benchmarked against the RESRAD (onsite) code. Independent verification was performed using calculations external to the RESRAD-OFFSITE code. Microsoft Excel® spreadsheets were used to verify all the major portions of the RESRAD-OFFSITE code, including the source term model, groundwater transport model, air dispersion model, and accumulation in offsite soil and in food models.

Paperwork Reduction Act Statement

NEED TEXT

Public Protection Notification

The NRC may not conduct or sponsor, and a person is not required to respond to, a request for information or an information collection requirement unless the requesting document displays a current valid OMB control number.

CONTENTS

ABSTRACT iii

FIGURES vi

TABLES xi

EXECUTIVE SUMMARY xv

1.0 INTRODUCTION 1.1

2.0 SOURCE TERM 2.1

2.1 Mixing Model 2.1
2.1.1 Thicknesses of Clean Cover, Contaminated Mixing Zone, and Undisturbed Primary Contamination 2.4
2.1.2 Composite Modification Factor for the Concentration of Nuclides in the Mixing Zone 2.9
2.2 Release by Surface Runoff 2.11
2.2.1 Concentrations of Nuclide in the Unmixed Portion of the Primary Contamination 2.16
2.2.2 Release Rates of Nuclide through Runoff 2.23
2.3 Release to Groundwater 2.23
2.4 Release to Air 2.29

3.0 GROUNDWATER TRANSPORT MODEL 3.1

3.1 Verification of Transport in the Unsaturated Zone 3.1
3.1.1 Output Flux from a Decreasing Triangular Input Flux 3.5
3.1.2 Output Flux from an Increasing Triangular Input Flux 3.5
3.1.3 Description of the Excel Files Used in This Verification 3.10
3.2 Verification of Transport in the Saturated Zone to the Surface Water Body 3.15
3.2.1 Output Flux from a Decreasing Triangular Input Flux 3.16
3.2.2 Output Flux from an Increasing Triangular Input Flux 3.22
3.2.3 Description of the Excel Files Used in This Verification 3.23
3.3 Verification of Transport in the Saturated Zone to the Well 3.23
3.3.1 Output Flux from a Decreasing Triangular Input Flux 3.28
3.3.2 Output Flux from an Increasing Triangular Input Flux 3.29
3.3.3 Description of the Excel Files Used in This Verification 3.34

4.0 ATMOSPHERIC TRANSPORT MODEL 4.1

4.1 Sector-Average Gaussian Plume Model 4.1
4.2 Area Model 4.2

5.0 ACCUMULATION AT OFFSITE LOCATIONS AND IN FOOD 5.1

CONTENTS (Cont.)

5.1 Accumulation in Offsite Surface Soil 5.1
5.1.1 Accumulation in Offsite Surface Soil from Irrigation 5.1
5.1.2 Accumulation in Offsite Surface Soil from Deposition of Contaminated Dust 5.5
5.1.3 Accumulation in Offsite Surface Soil for the Second Member of the Transformation Chain 5.10
5.2 Accumulation in Surface Water 5.13
5.3 Accumulation in Plants 5.20
5.4 Accumulation in Meat and Milk 5.28
5.5 Accumulation in Fish and Aquatic Foods 5.30

6 REFERENCES 6.1

FIGURES

2-1 Comparison of the RESRAD-OFFSITE Results and Spreadsheet Results for the Release Rates of Nuclide through Surface Runoff for Case I Concerning U-238 and Its Progenies 2.24

2-2 Comparison of the RESRAD-OFFSITE Results and the Spreadsheet Results for Release Rates of Nuclide through Surface Runoff for Case VIII Concerning Ra-226 and Its Progenies 2.27

2-3 Comparison of the RESRAD-OFFSITE Results and the Spreadsheet Results for the Release Rates of Nuclide to Groundwater for Case I Concerning U-238 and Its Progenies 2.30

3-1 Time Varying Flux Profile Represented as a Combination of Two Triangular Flux Distributions Shifted in Time 3.2

3-2 Decreasing Triangular Input Flux Profile 3.5

3-3 Verification of RESRAD-OFFSITE Computed Flux Exiting an Unsaturated Zone Resulting from a Triangular Input Flux of ^{60}Co of Unity at Time Zero and of Zero at the First Time Point at the Top of the Unsaturated Zone Using Spreadsheet Calculations 3.6

3-4 Verification of RESRAD-OFFSITE Computed Flux Exiting an Unsaturated Zone Resulting from a Triangular Input Flux of ^{90}Sr of Unity at Time Zero and of Zero at the First Time Point at the Top of the Unsaturated Zone Using Spreadsheet Calculations 3.7

3-5 Verification of RESRAD-OFFSITE Computed Flux Exiting an Unsaturated Zone Resulting from a Triangular Input Flux of ^{63}Ni of Unity at Time Zero and of Zero at the First Time Point at the Top of the Unsaturated Zone Using Spreadsheet Calculations 3.8

FIGURES (Cont.)

3-6 Verification of RESRAD-OFFSITE Computed Flux Exiting an Unsaturated Zone Resulting from a Triangular Input Flux of ^{14}C of Unity at Time Zero and of Zero at the First Time Point at the Top of the Unsaturated Zone Using Spreadsheet Calculations 3.9

3-7 Increasing Triangular Input Flux Profile 3.10

3-8 Double Triangular Input Flux Profile 3.10

3-9 Verification of RESRAD-OFFSITE Computed Flux Exiting an Unsaturated Zone Resulting from a Triangular Input Flux of ^{3}H of Zero at Time Zero and of Unity at the First Time Point at the Top of the Unsaturated Zone Using Spreadsheet Calculations 3.11

3-10 Verification of RESRAD-OFFSITE Computed Flux Exiting an Unsaturated Zone Resulting from a Triangular Input Flux of ^{137}Cs of Zero at Time Zero and of Unity at the First Time Point at the Top of the Unsaturated Zone Using Spreadsheet Calculations 3.12

3-11 Verification of RESRAD-OFFSITE Computed Flux Exiting an Unsaturated Zone Resulting from a Triangular Input Flux of ^{226}Ra of Zero at Time Zero and of Unity at the First Time Point at the Top of the Unsaturated Zone Using Spreadsheet Calculations 3.13

3-12 Verification of RESRAD-OFFSITE Computed Flux Exiting an Unsaturated Zone Resulting from a Triangular Input Flux of ^{238}U of Zero at Time Zero and of Unity at the First Time Point at the Top of the Unsaturated Zone Using Spreadsheet Calculations 3.14

3-13 Decreasing Triangular Input Flux Profile 3.17

3-14 Verification of RESRAD-OFFSITE Computed Flux to the Surface Water Body Resulting from a Triangular Input Flux of ^{60}Co of Unity at Time Zero and of Zero at the First Time Point at the Water Table Using Spreadsheet Calculations 3.18

3-15 Verification of RESRAD-OFFSITE Computed Flux to the Surface Water Body Resulting from a Triangular Input Flux of ^{90}Sr of Unity at Time Zero and of Zero at the First Time Point at the Water Table Using Spreadsheet Calculations 3.19

3-16 Verification of RESRAD-OFFSITE Computed Flux to the Surface Water Body Resulting from a Triangular Input Flux of ^{63}Ni of Unity at Time Zero and of Zero at the First Time Point at the Water Table Using Spreadsheet Calculations 3.20

3-17 Verification of RESRAD-OFFSITE Computed Flux to the Surface Water Body Resulting from a Triangular Input Flux of ^{14}C of Unity at Time Zero and of Zero at the First Time Point at the Water Table Using Spreadsheet Calculations 3.21

FIGURES (Cont.)

3-18 Increasing Triangular Input Flux Profile 3.22

3-19 Double Triangular Input Flux Profile 3.22

3-20 Verification of RESRAD-OFFSITE Computed Flux to the Surface Water Body Resulting from a Triangular Input Flux of ^{3}H of Zero at Time Zero and of Unity at the First Time Point at the Water Table Using Spreadsheet Calculations 3.24

3-21 Verification of RESRAD-OFFSITE Computed Flux to the Surface Water Body Resulting from a Triangular Input Flux of ^{137}Cs of Zero at Time Zero and of Unity at the First Time Point at the Water Table Using Spreadsheet Calculations 3.25

3-22 Verification of RESRAD-OFFSITE Computed Flux to the Surface Water Body Resulting from a Triangular Input Flux of ^{226}Ra of Zero at Time Zero and of Unity at the First Time Point at the Water Table Using Spreadsheet Calculations 3.26

3-23 Verification of RESRAD-OFFSITE Computed Flux to the Surface Water Body Resulting from a Triangular Input Flux of ^{238}U of Zero at Time Zero and of Unity at the First Time Point at the Water Table Using Spreadsheet Calculations 3.27

3-24 Decreasing Triangular Input Flux Profile 3.29

3-25 Verification of RESRAD-OFFSITE Computed Concentration in the Well Resulting from a Triangular Input Flux of ^{60}Co of Unity at Time Zero and of Zero at the First Time Point at the Water Table Using Spreadsheet Calculations 3.30

3-26 Verification of RESRAD-OFFSITE Computed Flux Concentration in the Well Resulting from a Triangular Input Flux of ^{90}Sr of Unity at Time Zero and of Zero at the First Time Point at the Water Table Using Spreadsheet Calculations 3.31

3-27 Verification of RESRAD-OFFSITE Computed Concentration in the Well Resulting from a Triangular Input Flux of ^{63}Ni of Unity at Time Zero and of Zero at the First Time Point at the Water Table Using Spreadsheet Calculations 3.32

3-28 Verification of RESRAD-OFFSITE Computed Concentration in the Well Resulting from a Triangular Input Flux of ^{14}C of Unity at Time Zero and of Zero at the First Time Point at the Water Table Using Spreadsheet Calculations 3.33

3-29 Increasing Triangular Input Flux Profile 3.34

3-30 Double Triangular Input Flux Profile 3.34

3-31 Verification of RESRAD-OFFSITE Computed Flux Concentration in the Well Resulting from a Triangular Input Flux of ^{3}H of Zero at Time Zero and of Unity at the First Time Point at the Water Table Using Spreadsheet Calculations 3.35

FIGURES (Cont.)

3-32 Verification of RESRAD-OFFSITE Computed Flux Concentration in the Well Resulting from a Triangular Input Flux of ^{137}Cs of Zero at Time Zero and of Unity at the First Time Point at the Water Table Using Spreadsheet Calculations 3.36

3-33 Verification of RESRAD-OFFSITE Computed Flux Concentration in the Well Resulting from a Triangular Input Flux of ^{226}Ra of Zero at Time Zero and of Unity at the First Time Point at the Water Table Using Spreadsheet Calculations 3.37

3-34 Verification of RESRAD-OFFSITE Computed Flux Concentration in the Well Resulting from a Triangular Input Flux of ^{238}U of Zero at Time Zero and of Unity at the First Time Point at the Water Table Using Spreadsheet Calculations 3.38

4-1 Effective Release Height Calculation in RESRAD-OFFSITE 4.5

4-2 Calculation of the Effective Wind Speed..... 4.6

4-3 Vertical Dispersion Coefficient Calculation..... 4.6

4-4 Calculation of the Depleted Source Strength Due to Wet and Dry Deposition 4.6

4-5 Normalized Air Concentration Calculation in RESRAD-OFFSITE 4.7

4-6 Site Layout for Verification of the Area Averaged Normalized Air Concentration..... 4.8

5-1 Accumulation of C-14 in Offsite Soil from Irrigation from Spreadsheet Calculations and from RESRAD-OFFSITE Code..... 5.7

5-2 Offsite Surface Soil Accumulation from Irrigation 5.8

5-3 Accumulation of C-14 in Offsite Soil from Deposition from Spreadsheet Calculations and from RESRAD-OFFSITE Code..... 5.10

5-4 Offsite Surface Soil Accumulation from Deposition..... 5.11

5-5 Accumulation of Sr-90 in Offsite Soil from Both Irrigation and Deposition from Spreadsheet Calculations and from RESRAD-OFFSITE Code..... 5.13

5-6 Offsite Surface Soil Accumulation from both Irrigation and Particulate Deposition for the First Member of Transformation Chain..... 5.15

5-7 Accumulation of Y-90 in Offsite Soil from Both Irrigation and Deposition from Spreadsheet Calculations and from RESRAD-OFFSITE Code..... 5.17

5-8 Offsite Surface Soil Accumulation from Both Irrigation and Particulate Deposition in the Second Member of the Chain..... 5.18

FIGURES (Cont.)

5-9 Accumulation of Ra-226 in Surface Water from Spreadsheet Calculations and from RESRAD-OFFSITE Code 5.22

5-10 Accumulation in Surface Water for the First Member of Transformation Chain 5.23

5-11 Accumulation of Pb-210 in Surface Water from Spreadsheet Calculations and from RESRAD-OFFSITE Code 5.25

5-12 Accumulation of U-238 in Fruit, Grain, and Nonleafy Vegetables from Spreadsheet Calculations and from RESRAD-OFFSITE Code 5.30

5-13 Plant Concentration Calculations for Fruit, Grain, and Nonleafy Vegetables 5.31

5-14 Accumulation of U-238 in Leafy Vegetables from Spreadsheet Calculations and from RESRAD-OFFSITE Code 5.32

5-15 Plant Concentration Calculations for Leafy Vegetables 5.33

5-16 Accumulation of U-238 in Pasture and Silage from Spreadsheet Calculations and from RESRAD-OFFSITE Code 5.34

5-17 Plant Concentration Calculations for Pasture and Silage 5.35

5-18 Accumulation of U-238 in Grain from Spreadsheet Calculations and from RESRAD-OFFSITE Code 5.36

5-19 Plant Concentration Calculations for Grain 5.37

5-20 Accumulation of Cs-137 in Meat from Spreadsheet Calculations and from RESRAD-OFFSITE Code 5.40

5-21 Accumulation of Cs-137 in Milk from Spreadsheet Calculations and from RESRAD-OFFSITE Code 5.40

5-22 Meat Concentration Calculations 5.41

5-23 Milk Concentration Calculations 5.42

5-24 Fish and Aquatic Foods Concentration Calculations 5.44

5-25 Accumulation of Co-60 in Fish from Spreadsheet Calculations and from RESRAD-OFFSITE Code 5.44

5-26 Accumulation of Co-60 in Crustacea from Spreadsheet Calculations and from RESRAD-OFFSITE Code 5.45

TABLES

2-1 Parameters Used for Different Test Cases 2.3

2-2 Comparison of the RESRAD-OFFSITE Results and the Spreadsheet Results for the Thicknesses of Clean Cover, Contaminated Mixing Zone, and Unmixed Portion of the Primary Contamination for Case III Concerning H-3, with Disagreements Highlighted 2.6

2-3 Comparison of the RESRAD-OFFSITE Results and the Spreadsheet Results for the Thicknesses of Clean Cover, Contaminated Mixing Zone, and Unmixed Portion of the Primary Contamination for Case IV Concerning C-14, with Disagreements Highlighted 2.7

2-4 Comparison of the RESRAD-OFFSITE Results and the Spreadsheet Results for the Thicknesses of Clean Cover, Contaminated Mixing Zone, and Unmixed Portion of the Primary Contamination for Case VIII Concerning Ra-226, with Disagreements Highlighted 2.8

2-5 Comparison of the RESRAD-OFFSITE Results and the Spreadsheet Results for the Modification Factor for the Concentration of Nuclides in the Mixing Zone for Case II Concerning Cs-137 ..... 2.12

2-6 Comparison of the RESRAD-OFFSITE Results and the Spreadsheet Results for the Modification Factor for the Concentration of Nuclides in the Mixing Zone for Case III Concerning H-3 ..... 2.13

2-7 Comparison of the RESRAD-OFFSITE Results and the Spreadsheet Results for the Modification Factor for the Concentration of Nuclides in the Mixing Zone for Case VI Concerning Ni-63 ..... 2.14

2-8 Comparison of the RESRAD-OFFSITE Results and the Spreadsheet Results for the Modification Factor for the Concentration of Nuclides in the Mixing Zone for Case VIII Concerning Ra-226 ..... 2.15

2-9 Calculations of the Radiological Decay Constants and Leach Rate Constants 2.18

2-10 Comparison of the RESRAD-OFFSITE Results and the Spreadsheet Results for the Concentration of Nuclide in the Unmixed Portion of the Primary Contamination for Case I Concerning U-238 and Its Progenies, with Notable Disagreements Highlighted 2.19

2-11 Comparison of the RESRAD-OFFSITE Results and the Spreadsheet Results for the Concentration of Nuclide in the Unmixed Portion of the Primary Contamination for Case III Concerning H-3, with Notable Disagreements Highlighted 2.20

2-12 Comparison of the RESRAD-OFFSITE Results and the Spreadsheet Results for the Concentration of Nuclide in the Unmixed Portion of the Primary Contamination for Case IV Concerning C-14, with Notable Disagreements Highlighted 2.21

TABLES (Cont.)

2-13 Comparison of the RESRAD-OFFSITE Results and the Spreadsheet Results for the Concentration of Nuclide in the Unmixed Portion of the Primary Contamination for Case V Concerning Co-60 ..... 2.22

2-14 Comparison of the RESRAD-OFFSITE Results and the Spreadsheet Results for the Release Rates of Nuclide through Surface Runoff for Case I Concerning U-238 and Its Progenies, with Notable Disagreements Highlighted 2.26

2-15 Comparison of the RESRAD-OFFSITE Results and the Spreadsheet Results for the Release Rates of Nuclide through Surface Runoff for Case VIII Concerning Ra-226 and Its Progenies 2.28

2-16 Comparison of the RESRAD-OFFSITE Results and the Spreadsheet Results for the Release Rates of Nuclide to Groundwater for Case I Concerning U-238 and Its Progenies, with Notable Disagreements Highlighted 2.32

2-17 Comparison of the RESRAD-OFFSITE Results and the Spreadsheet Results for the Release Rates of Nuclide to Groundwater for Case III Concerning H-3, with Notable Disagreements Highlighted 2.33

2-18 Comparison of the RESRAD-OFFSITE Results and the Spreadsheet Results for the Release Rates of Nuclide to Groundwater for Case IV Concerning C-14, with Notable Disagreements Highlighted 2.34

2-19 Comparison of the RESRAD-OFFSITE Results and the Spreadsheet Results for the Release Rates of Nuclide to Groundwater for Case VII Concerning Sr-90 ..... 2.35

2-20 Comparison of the RESRAD-OFFSITE Results and Spreadsheet Results for the Release Rates of Nuclide in the Form of Dust to the Air for Case I Concerning U-238 and Its Progenies, with Notable Disagreements Highlighted 2.36

2-21 Comparison of the RESRAD-OFFSITE Results and the Spreadsheet Results for the Release Rates of Nuclide in the Form of Dust to the Air for Case VIII Concerning Ra-226 and Its Progenies 2.37

3-1 Nuclides Used in This Verification and Their Transformation Rates 3.3

3-2 RESRAD-OFFSITE Inputs and Intermediate Calculations That Pertain to Transport in the Unsaturated Zone 3.3

3-3 Value of the Two Exponentials for the Cases Used in This Verification 3.4

3-4 RESRAD-OFFSITE Inputs and Intermediate Calculations That Pertain to Transport in the Saturated Zone to the Surface Water Body 3.17

3-5 RESRAD-OFFSITE Inputs and Intermediate Calculations That Pertain to Transport in the Saturated Zone to the Well 3.29

TABLES (Cont.)

4-1 Baseline Site Layout and Atmospheric Transport Parameters Used to Verify RESRAD-OFFSITE Point-to-Point Air Dispersion Calculations 4.2

4-2 Comparison of RESRAD-OFFSITE Normalized Air Concentrations with Spreadsheet Verification Calculations 4.3

4-3 Additional Comparison of RESRAD-OFFSITE Normalized Air Concentrations with Spreadsheet Verification Calculations 4.4

5-1 Parameters Used in the Verification of Accumulation in Offsite Soil, Surface Water, Plant, Meat, Milk, and Aquatic Food 5.2

5-2 Radionuclide Specific Parameters Used in the Verification of Accumulation in Offsite Soil, Surface Water Body, Plant, Meat, Milk, and Aquatic Food 5.3

5-3 Spreadsheet Calculations for C-14 Accumulation in Offsite Surface Soil from Irrigation 5.6

5-4 Spreadsheet Calculations for C-14 Accumulation in Offsite Surface Soil from Deposition 5.9

5-5 Spreadsheet Calculations for Sr-90 Accumulation in Offsite Surface Soil from both Irrigation and Deposition 5.12

5-6 Spreadsheet Calculations for Y-90 Accumulation in Offsite Surface Soil from Both Irrigation and Deposition 5.16

5-7 Spreadsheet Calculations for Ra-226 Accumulation in Surface Water 5.21

5-8 Spreadsheet Calculations for Pb-210 Accumulation in Surface Water 5.24

5-9 Spreadsheet Calculations for U-238 Accumulation in Fruit, Grain, and Nonleafy Vegetables – Grown in Area 1 ..... 5.26

5-10 Spreadsheet Calculations for U-238 Accumulation in Leafy Vegetables – Grown in Area 2 ..... 5.27

5-11 Spreadsheet Calculations for U-238 Accumulation in Pasture and Silage – Grown in Area 3 ..... 5.28

5-12 Spreadsheet Calculations for U-238 Accumulation in Grain – Grown in Area 4 ..... 5.29

5-13 Spreadsheet Calculations for Cs-137 Meat Concentration 5.38

TABLES (Cont.)

5-14 Spreadsheet Calculations for Cs-137 Milk Concentration 5.39

5-15 Spreadsheet Calculations for Co-60 Accumulation in Fish and Aquatic Foods 5.43

EXECUTIVE SUMMARY

The RESRAD-OFFSITE computer code evaluates the radiological dose and excess cancer risk to an individual who is exposed while located within or outside the area of initial (primary) contamination. The RESRAD-OFFSITE code was developed by adding offsite transport and offsite accumulation modules to the original and well established RESRAD (onsite) code, which was designed for the evaluation of radiological doses to an onsite receptor from exposure to RESidual RADioactive materials in soil. The RESRAD code has been extensively verified. The modules in RESRAD-OFFSITE that are also in RESRAD had already been verified by benchmarking an onsite exposure scenario against RESRAD. This verification report focuses on the verification of the modules that were added or modified when RESRAD-OFFSITE was developed; namely, the source term module which was modified by the incorporation of a surface soil mixing model to maintain (onsite and offsite) mass balance; the groundwater transport module which was modified to model dispersive transport and to allow the source of water to be away from the centerline of the plume; the new atmospheric transport module; the new modules to model the accumulation in surface soil at offsite locations and in the surface water body and the transfer to plant, meat, milk, and aquatic foods which were modified to include the transfer of nuclides from offsite locations in addition to the transfer from onsite locations. Spreadsheets were created using the formulations in the user's manual. The code was verified by comparing its output against the spreadsheet calculations.

The verification of the source term module consisted of verifying the temporal variation of the thicknesses of the clean cover, the contaminated mixing layer, and the undisturbed initial contamination; the temporal variation of the concentration in the undisturbed initial contamination; the temporal variation of the multiplication factor used to compute the concentration in the mixing layer; and the temporal variation of the rates at which the nuclides are released to the various media. Eight cases that covered a range of initial thicknesses of cover, mixing layer, and contamination and a range of erosion rates of the cover and contamination were used in this verification. A different nuclide was chosen for each case to cover a range of half-lives and a range of distribution coefficients, which are a measure of the affinity of the nuclides to the soil matrix. The two nuclides for which the code considers a vapor release, C-14 and H-3, were also included. There was mostly very good agreement between the RESRAD-OFFSITE output and spreadsheet output. Inconsequential differences were sometimes observed at specific times; namely, at the times at which the cover or the initial contamination eroded down to the thickness of the mixing layer and near time zero. These differences were due to the precision used by the code and the spreadsheet calculations for stored variables. All of the spreadsheet calculations were performed at double precision. Most of the variables in the computational code of RESRAD-OFFSITE are in single precision; only those variables that need to be at a higher precision are set to either double or quadruple precision.

The RESRAD-OFFSITE temporal outputs of the flux out of the unsaturated zone, the flux to the surface water body, and the concentration in the well were verified by comparison with the spreadsheet calculations. The same eight nuclides that were used for the verification of the source term module were used for the verification of the groundwater transport module. At least three different simulations with three different distribution coefficients were used for the verification, to cover a wide range of transport velocities. The precision of the error function built into the spreadsheet calculations was not sufficient at the range of arguments that were needed for the RESRAD-OFFSITE simulations. The evaluation algorithm used by RESRAD-OFFSITE for the error function had to be written into the spreadsheet calculations in order to perform the verification. The peak fluxes and peak concentrations computed by RESRAD-OFFSITE were verified by the Excel® calculations.

The point-source-to-point-receptor normalized air concentrations (χ/Q values) computed by RESRAD-OFFSITE for five different combinations of distance, direction, wind speed, and stability classes were

compared with spreadsheet-calculated values. The five χ/Q values were calculated under six different cases: three dispersion coefficient depositions combinations – using Brigg's dispersion coefficients without either wet or dry deposition, using the Pasquill-Gifford dispersion coefficient with only dry deposition, and using the Pasquill-Gifford dispersion coefficient with both wet and dry deposition – in conjunction with zero and non-zero heat release fluxes. The results for the thirty cases agreed within 2%; the difference was attributed to the fact that the spreadsheet calculations use a Simpson's integration while RESRAD-OFFSITE uses Romberg integration. The spatial integration of the χ/Q value over the receptor area was verified for a case in which the receptor location straddled the wind sector boundary; the numbers agreed to within 0.2%.

The accumulation in offsite soil was verified for the eight parent nuclides and selected progeny nuclides from the atmospheric deposition of dust and from irrigation water. The accumulation in the surface water body was also verified. The contamination of plants by root uptake, by foliar interception of dust, and by interception of irrigation water computed by RESRAD-OFFSITE agreed with the spreadsheet calculations. The calculations of the contamination of meat and milk by ingestion of the two types of livestock feed – grain and pasture and silage – by ingestion of soil associated with those two types of feed, and by the ingestion of livestock water were also verified. The spreadsheet-computed concentrations of nuclides in fish and crustacea agreed with the RESRAD-OFFSITE output.

1.0 INTRODUCTION

The RESRAD-OFFSITE computer code evaluates the radiological dose and excess cancer risk to an individual who is exposed while located within or outside the area of initial (primary) contamination. The models and parameters used in the RESRAD-OFFSITE code are described in detail in the RESRAD-OFFSITE User's Manual (Yu et al. 2007). The RESRAD-OFFSITE code is an extension of the original RESRAD (onsite) code, which was designed for the evaluation of radiological doses to an onsite receptor from exposure to RESidual RADioactive materials in soil (Yu et al. 1993, 2001).

The RESRAD-OFFSITE and RESRAD (onsite) codes share the same database and many models and modules. The RESRAD (onsite) code has already been extensively tested, verified, and validated, as documented in the RESRAD User's Manual and other documents (Yu et al. 2001; Halliburton NUS 1994; Cheng et al. 1995; Gnanapragasam et al. 2000; Mills et al. 1997; Whelan et al. 1999a,b).

Many parameter values used in the RESRAD-OFFSITE code were taken from the RESRAD (onsite) database. These parameters include soil-plant transfer factors, meat and milk transfer factors, bioaccumulation factors, dose conversion factors, decay half-lives, and scenario-specific occupancy factors. The RESRAD (onsite) database is well documented and verified (Yu et al. 2000, 2001, 2003).

The RESRAD-OFFSITE code was developed following the RESRAD program's quality assurance (QA) and quality control (QC) procedures. Some components of the code were verified by separately developed spreadsheets, or benchmarked against the RESRAD (onsite) code with respect to most of the equations used in the code. Additional benchmarking of the RESRAD-OFFSITE code against other peer codes was performed over the past several years. Some of the results were documented in the benchmarking report (Yu et al. 2006) and in other reports and peer-reviewed articles (Gnanapragasam and Yu 1997, Gnanapragasam et al. 2000; BIOMOVS II 1995, 1996).

The purpose of this report had two objectives: (1) verify the proper operation of the code and (2) document the results using calculations outside the RESRAD-OFFSITE code. Independent verification was performed using calculations external to the RESRAD-OFFSITE code; Microsoft Excel® spreadsheets were used to verify all the major portions of the program, including the source term (Chapter 2), groundwater transport model (Chapter 3), air dispersion model (Chapter 4), and accumulation in offsite soil and in food models (Chapter 5). All references cited are listed in Chapter 6.

2.0 SOURCE TERM

RESRAD-OFFSITE analyzes the changes in radioactivity of the contamination source over time by accounting for the erosion, mixing, and leaching mechanisms, as well as the radiological ingrowth and decay factors. For gaseous radionuclides (H-3, C-14, and radon), the loss of radioactivity through gas diffusion is also considered in addition to the above mechanisms and factors. The effects of erosion and mixing are quantified in RESRAD-OFFSITE by tracking the changes in three thicknesses — the clean cover thickness, the penetration depth of mixing to the primary contaminated zone, and the thickness of the undisturbed primary contamination — as well as changes in the density of the mixing zone and in the volume fraction of the primary contaminated soil in the mixing zone. The effects of leaching, radiological ingrowth and decay, and loss through gas diffusion are analyzed independently of the erosion and mixing mechanisms, and are quantified by tracking the changes in radionuclide concentrations in the undisturbed primary contaminated soil. With the results obtained from quantifying the effects of the various mechanisms, the release rates of radionucludes from the contamination source to the surrounding environment are then calculated.

This chapter documents the efforts to verify the release rate calculations in RESRAD-OFFSITE. Section 2.1 discusses the verification of the intermediate results related to the soil mixing model. Section 2.2 focuses on the release rates of radionuclides through surface runoff. Release rates of radionuclides to the underlying soils below the contamination source are the focus of Section 2.3, and the release rates of radionuclides to the air are the focus in Section 2.4.

To verify the RESRAD-OFFSITE results, calculation spreadsheets were designed to implement the mathematical equations developed to model the changes in the contamination source, which are discussed in Chapter 2 of the RESRAD-OFFSITE User's Manual (Yu et al. 2007). These spreadsheets simulate eight different test cases, each designed to consider a specific decay chain with different leaching potentials, erosion rates, and mixing depths. For most cases, the spreadsheets perform calculations for intermediate variables and radionuclide release rates every year for 1,000 years. To generate results for comparison with the spreadsheets, the RESRAD-OFFSITE code was executed with an input selection of 1,024 graphic points and a maximum input time point of 994 years, which, along with an exposure duration of 30 years, instruct RESRAD-OFFSITE to record the intermediate and final results every year for 1,024 years. For the cases involving short-lived radionuclides, the time interval was reduced to ½ or ¼ of a year, so that additional results were obtained for a one-year interval.

2.1 Mixing Model

RESRAD-OFFSITE considers mixing of soil at the surface level due to plowing or other human activities. Soils within the mixing depth are assumed to be homogeneously mixed and to have the same properties. In addition to mixing, surface soil could be eroded away; the erosion rate is determined by several parameters including the annual rainfall erosion index, soil erodability factor, slope length-steepness factor, cropping-management factor, and the conservation practice factor. Because of erosion, the mixing zone, which is of constant depth, could be driven deeper into the soil column as time progresses. Depending on the initial thickness of the cover material and the cover erosion rate, the mixing zone could penetrate into the primary contamination zone and even to the uncontaminated vadose zone that lies underneath the primary contamination. As a result, the mixing zone could become contaminated with varying radionuclide concentrations over time. The radionuclide concentrations in the mixing zone determine the release rates of radionuclides through surface runoff and dust suspension/ resuspension, which result in releases of contaminated dust particles to the air.

Soil mixing is modeled as a continuous process in RESRAD-OFFSITE. By considering mass balance, analytical equations were derived for the calculations of radionuclide concentrations in the mixing zone and in the undisturbed primary contamination zone, as well as several intermediate variables (see Chapter 2 of Yu et al. 2007). During the execution of RESRAD-OFFSITE, two output files are generated that record the calculations undertaken to model the soil mixing. These two files are CZTHICK3.DAT and SFSIN.DAT. CZTHICK3.DAT stores temporal data of the composite modification factor for the concentration of nuclides in the mixing zone and of the thicknesses of clean cover, the contaminated mixing zone, and the unmixed portion of the contaminated zone. SFSIN.DAT stores temporal data of the concentration of each initially present radionuclide and its principal progeny nuclide in the unmixed portion of the primary contamination. To verify the mixing model, the equations implemented by RESRAD-OFFSITE were coded into Microsoft Excel® spreadsheets so that temporal data for the same variables recorded in the two output files were generated for comparison.

Eight different test cases were developed for the verification of source term modeling. All eight test cases consider a contaminated area of 10,000 m^2 with an initial parent nuclide concentration of 100 pCi/g. The specific conditions considered in these test cases are listed in Table 2-1 and are discussed as follows:

- Case I considers U-238 and its progeny nuclides. The half-life of U-238 is 4.47×10^9 years, and the RESRAD-OFFSITE default K_d value for U-238 is 50 cm^3/g, which is a measure of how readily U-238 adsorbs to soil particles. Because of the long half-life and the moderately large K_d value, changes in U-238 concentration in soil for the first 1,000 years would be primarily caused by soil mixing. There is no clean cover, so penetration of the mixing zone (with a mixing depth of 15 cm) to the primary contamination starts at time 0. A high erosion rate of approximately 0.01 m/yr is assumed for the primary contamination zone; therefore, at approximately 185 years, the mixing zone would start to penetrate to the vadose zone that lies beneath the primary contamination. To verify RESRAD-OFFSITE's ability to handle soil layers with different properties, the density of the primary contamination zone is set to a different value from that of the vadose zone; the contaminated zone has a density of 1.5 g/cm^3, while the vadose zone has a density of 1.7 g/cm^3.

- Case II considers Cs-137, which has a short half-life of 30 years. The RESRAD-OFFSITE default K_d value for Cs-137 is 4,600 cm^3/g. Because of the large K_d value, release of Cs-137 through leaching is insignificant. The concentration of Cs-137 in the primary contamination zone would decrease quickly through radiological decay. In addition to radiological decay, soil mixing would also affect the concentration; however, with a clean cover of 1 m on top of the contaminated zone and a mixing depth of 0.3 m, the effect of soil mixing would not be observed until 350 years later, when the erosion has reduced the cover thickness to 0.3 m. The erosion would continue even after the cover layer is gone and would completely remove the primary contaminated zone at the end of the simulation, which is 1,000 years.

- Case III deals with H-3, which could be converted to tritiated water (HTO) upon contact with the environment; in turn, HTO can diffuse out from the contaminated area. RESRAD-OFFSITE employs the same special model as RESRAD (onsite) to deal with the loss of H-3 through gas diffusion, and the equations used to evaluate the loss were also coded into the spreadsheet. The loss through gas diffusion affects the remaining H-3 concentration in the primary contaminated zone. The RESRAD-OFFSITE default evasion depth of HTO was used in this test case, which is 0.3 m and equivalent to the thickness of the cover layer, so gas diffusion was inhibited at time 0. However, as soon as the cover layer starts to erode away, gas diffusion begins to proceed. The RESRAD-OFFSITE default K_d value for H-3 is 0 cm^3/g, which means that H-3 does not adsorb to soil particles; therefore, loss of H-3 through leaching is significant. Under this condition, the radioactivity of H-3 in soil is expected to be depleted in a short period of time.

Table 2-1 Parameters Used for Different Test Cases

Parameter	Case I	Case II	Case III	Case IV	Case V	Case VI	Case VII	Case VIII
Radionuclide	U-238	Cs-137	H-3	C-14	Co-60	Ni-63	Sr-90	Ra-226
K_d of radionuclide (cm^3/g)	50	4,600	0	0	1,000	1,000	30	70
Time interval (yr)	1	1	1	1	0.25	1	0.5	1
Thickness of clean cover (m)	0	1	0.3	0.3	0	0.1	0.1	0.3
Thickness of primary contamination (m)	2	1	1	1	1	0.1	1	0.5
Thickness of vadose zone (m)	4	4	4	4	4	10	4	4
Density of clean cover (g/cm^3)	NA	1.6	1.6	1.6	NA	1.6	1.5	1.7
Density of primary contaminated zone (g/cm^3)	1.5	1.6	1.5	1.5	1.8	1.8	1.8	1.5
Density of vadose zone (g/cm^3)	1.7	1.7	1.7	1.7	1.6	1.6	1.6	1.6
Nominal erosion rate of cover (m/yr)	NA	0.002	0.001	0.001	NA	0.001	0	0.001
Nominal erosion rate of primary contaminated zone (m/yr)	0.01	0.002	0	0	0.01	0.001	0	0.0005
Soil mixing depth (m)	0.15	0.3	0.15	0.15	0.15	0.3	0.15	0.2
Evasion depth for H-3 and C-14 (m)	NA	NA	0.3	0.5	NA	NA	NA	NA
Evasion rate for C-14 (1/yr)	NA	NA	NA	2.0	NA	NA	NA	NA

NA — Not applicable.

- Case IV deals with C-14. Like H-3, C-14 could be converted to CO_2 and escape the contaminated zone through gas diffusion. The special model employed by RESRAD-OFFSITE to address the loss of C-14 through gas diffusion is the same as that employed by RESRAD (onsite). The equations used were coded into the spreadsheet. Because the default K_d value for C-14 is also 0 cm^3/g, the radioactivity of C-14 in soil is expected to diminish quickly. The other input parameters used for this test case are the same as those used for Case III.

- Case V concerns Co-60, which has a short decay half-life of 5.27 years. Because the activity of Co-60 decreases quickly with time, a smaller time interval was chosen to obtain more recorded data for comparison. To observe the effect of soil mixing on the concentration of Co-60 in the mixing zone, no cover layer was considered above the primary contaminated zone. In this way, the mixing zone would penetrate to the primary contaminated zone immediately at time 0.

- Case VI concerns Ni-63, which has a half-life of 96 years and a RESRAD-OFFSITE default K_d value of 1,000 g/cm^3. Like Cs-137, loss of radioactivity through leaching is insignificant because of the strong adsorption to soil particles. A thin cover layer and primary contamination zone, each with a thickness of 0.1 m, are specifically selected so that the mixing zone penetrates not only to the primary contamination zone but also to the vadose zone underneath the primary contamination from the very beginning. The soil mixing depth for this case is 0.3 m.

- Case VII considers Sr-90, a pure β emitter. The half-life of Sr-90 (29.12 years) is about the same as that of Cs-137; however, the default K_d value (30 g/cm^3) is much smaller than that of Cs-137 (4,600 g/cm^3). As a result, the remaining radioactivity in the primary contaminated zone is affected by both leaching and radiological decay. No erosion is assumed for both the cover layer and the primary contaminated zone, so the mixing zone would penetrate 0.05 m to the primary contaminated zone, but would not go farther as time passes. A time interval of 0.5 year is used for this case.

- The last case, Case VIII, considers Ra-226, which generates radon by radiological decay. Like HTO for H-3 and CO_2 for C-14, the formed radon gas can diffuse through the cover layer to the atmosphere. However, because the half-lives of radon and its progeny nuclides are short, they are treated as associated nuclides and do not affect the concentration of the next principal nuclide in the decay chain, Pb-210. The radon model incorporated in the RESRAD-OFFSITE code is the same as that in the RESRAD (onsite) code and does not affect the operation of the mixing model. Furthermore, the calculations associated with the radon model have been verified before (Halliburton NUS 1994); therefore, they are not repeated in this chapter. The thickness of the cover layer selected for this case is 1 m, followed by a thickness of 0.3 m for the primary contamination zone. Erosion rates for the cover layer and the primary contamination are different: the former is approximately 0.001 m/yr, while the latter is 0.0005 m/yr. The mixing depth is selected to be 0.2 m.

2.1.1 Thicknesses of Clean Cover, Contaminated Mixing Zone, and Undisturbed Primary Contamination

To calculate the thicknesses of clean cover, contaminated mixing zone, and undisturbed primary contamination, the thicknesses of the cover and primary contamination at each time point must be calculated first. Equations 2.19 and 2.20 from the RESRAD-OFFSITE User's Manual (Yu et al. 2007) were used for calculating the thicknesses of the cover and primary contamination. Then Eq. 2.21 was used to obtain the target thicknesses listed in the CZTHICK3.DAT file. The equations used are listed

here: Eq. 2.1 is Eq. 2.19 in the RESRAD-OFFSITE User's Manual, Eq. 2.2 here is Eq. 2.20, and Eq. 2.3 is Eq. 2.21.

$$T_{cv}(t) = T_{cv}(0) - \varepsilon_{cv} t \text{ when } t \le t_{cv} = T_{cv}(0)/\varepsilon_{cv}, \text{ and}$$
$$T_{cv}(t) = 0 \text{ when } t > t_{cv} \qquad \text{(Eq. 2.1)}$$

$$T_{pc}(t) = T_{pc}(0) \text{ when } t \le t_{cv},$$
$$T_{pc}(t) = T_{pc}(0) - \varepsilon_{pc}(t - t_{cv}) \text{ when } t_{cv} \le t \le t_{cv} + t_{pc} = T_{cv}(0)/\varepsilon_{cv} + T_{pc}(0)/\varepsilon_{pc}, \text{ and} \qquad \text{(Eq. 2.2)}$$
$$T_{pc}(t) = 0 \text{ when } t > t_{cv} + t_{pc}$$

$$T_{cv}^{c}(t) = T_{cv}(t),\ T_{mix}^{c}(t) = 0,\ T_{pc}^{um}(t) = T_{pc}(0) \text{ when } T_{cv}(t) \ge d_{mix},$$
$$T_{cv}^{c}(t) = 0,\ T_{mix}^{c}(t) = d_{mix}, \text{ and } T_{pc}^{um}(t) = T_{pc}(t) + T_{cv}(t) - d_{mix}$$
$$\text{when } T_{cv}(t) < d_{mix} \le T_{cv}(t) + T_{pc}(t), \text{ and} \qquad \text{(Eq. 2.3)}$$
$$T_{cv}^{c}(t) = 0,\ T_{mix}^{c}(t) = d_{mix} \text{ and } T_{pc}^{um}(t) = 0 \text{ when } T_{cv}(t) + T_{pc}(t) < d_{mix}$$

where:

$T_{cv}(t)$ = thickness of cover at time t (m),
$T_{cv}(0)$ = thickness of cover at time 0 (m),
ε_{cv} = cover erosion rate (m/yr),
t_{cv} = time required for complete erosion of cover (yr),
$T_{pc}(t)$ = thickness of primary contamination at time t (m),
$T_{pc}(0)$ = thickness of primary contamination at time 0 (m),
ε_{pc} = primary contamination erosion rate (m/yr),
t_{pc} = time required for complete erosion of primary contamination (yr),
$T_{cv}^{c}(t)$ = thickness of clean cover at time t (m),
$T_{mix}^{c}(t)$ = thickness of contaminated mixing zone at time t (m),
d_{mix} = depth of mixing zone (m), and
$T_{pc}^{um}(t)$ = thickness of unmixed portion of the primary contamination (m).

Comparison of the clean cover thickness, the thickness of the contaminated mixing zone, and the thickness of the unmixed portion of the primary contamination between those values listed in CZTHICK3.DAT and those calculated by the spreadsheets shows good agreement. Tables 2-2 to 2-4 show the comparisons for Cases III, IV, and VIII where some disagreements were identified. These differences occur around the time at which the thickness of either the cover or the contaminated zone becomes equal to the thickness of the mixing layer; they are due to the differences in the precision to which the erosion rate is computed in the Excel spread sheet and the RESRAD-OFFSITE code. Excel uses double precision while RESRAD-OFFSITE uses single precision for most variables.

Although these tables do not show it, one inconsequential difference between equation 2.3 (equation 2.21 of the RESRAD-OFFSITE User's manual) and the RESRAD-OFFSITE code was observed during this

Table 2-2 Comparison of the RESRAD-OFFSITE Results and the Spreadsheet Results for the Thicknesses of Clean Cover, Contaminated Mixing Zone, and Unmixed Portion of the Primary Contamination for Case III Concerning H-3, with Disagreements Highlighted

	Thickness of Clean Cover (m)		Thickness of Contaminated Mixing Zone (m)		Thickness of the Unmixed Portion of Primary Contamination (m)	
Time (yr)	RESRAD-OFFSITE	Spreadsheet	RESRAD-OFFSITE	Spreadsheet	RESRAD-OFFSITE	Spreadsheet
0	0.3	0.3	0	0	1	1
1	0.299	0.299	0	0	1	1
10	0.29	0.29	0	0	1	1
20	0.28	0.28	0	0	1	1
50	0.25	0.25	0	0	1	1
100	0.2	0.2	0	0	1	1
149	0.151	0.151	0	0	1	1
150	0.15	0	0	0.15	1	1
151	0	0	0.15	0.15	0.999	0.999
200	0	0	0.15	0.15	0.95	0.95
250	0	0	0.15	0.15	0.9	0.9
300	0	0	0.15	0.15	0.85	0.85
350	0	0	0.15	0.15	0.85	0.85
400	0	0	0.15	0.15	0.85	0.85
450	0	0	0.15	0.15	0.85	0.85
500	0	0	0.15	0.15	0.85	0.85
550	0	0	0.15	0.15	0.85	0.85
600	0	0	0.15	0.15	0.85	0.85
650	0	0	0.15	0.15	0.85	0.85
700	0	0	0.15	0.15	0.85	0.85
750	0	0	0.15	0.15	0.85	0.85
800	0	0	0.15	0.15	0.85	0.85
850	0	0	0.15	0.15	0.85	0.85
900	0	0	0.15	0.15	0.85	0.85
950	0	0	0.15	0.15	0.85	0.85
1000	0	0	0.15	0.15	0.85	0.85

Table 2-3 Comparison of the RESRAD-OFFSITE Results and the Spreadsheet Results for the Thicknesses of Clean Cover, Contaminated Mixing Zone, and Unmixed Portion of the Primary Contamination for Case IV Concerning C-14, with Disagreements Highlighted

	Thickness of Clean Cover (m)		Thickness of Contaminated Mixing Zone (m)		Thickness of the Unmixed Portion of Primary Contamination (m)	
Time (yr)	RESRAD-OFFSITE	Spreadsheet	RESRAD-OFFSITE	Spreadsheet	RESRAD-OFFSITE	Spreadsheet
135	0.165	0.165	0	0	1	1
136	0.164	0.164	0	0	1	1
137	0.163	0.163	0	0	1	1
138	0.162	0.162	0	0	1	1
139	0.161	0.161	0	0	1	1
140	0.16	0.16	0	0	1	1
141	0.159	0.159	0	0	1	1
142	0.158	0.158	0	0	1	1
143	0.157	0.157	0	0	1	1
144	0.156	0.156	0	0	1	1
145	0.155	0.155	0	0	1	1
146	0.154	0.154	0	0	1	1
147	0.153	0.153	0	0	1	1
148	0.152	0.152	0	0	1	1
149	0.151	0.151	0	0	1	1
150	0.15	0	0	0.15	1	1
151	0	0	0.15	0.15	0.999	0.999
152	0	0	0.15	0.15	0.998	0.998
153	0	0	0.15	0.15	0.997	0.997
154	0	0	0.15	0.15	0.996	0.996
155	0	0	0.15	0.15	0.995	0.995
156	0	0	0.15	0.15	0.994	0.994
157	0	0	0.15	0.15	0.993	0.993
158	0	0	0.15	0.15	0.992	0.992
159	0	0	0.15	0.15	0.991	0.991
160	0	0	0.15	0.15	0.99	0.99
161	0	0	0.15	0.15	0.989	0.989
162	0	0	0.15	0.15	0.988	0.988
163	0	0	0.15	0.15	0.987	0.987
164	0	0	0.15	0.15	0.986	0.986
165	0	0	0.15	0.15	0.985	0.985
166	0	0	0.15	0.15	0.984	0.984

Table 2-4 Comparison of the RESRAD-OFFSITE Results and the Spreadsheet Results for the Thicknesses of Clean Cover, Contaminated Mixing Zone, and Unmixed Portion of the Primary Contamination for Case VIII Concerning Ra-226, with Disagreement Highlighted

	Thickness of Clean Cover (m)		Thickness of Contaminated Mixing Zone (m)		Thickness of the Unmixed Portion of Primary Contamination (m)	
Time (yr)	RESRAD-OFFSITE	Spreadsheet	RESRAD-OFFSITE	Spreadsheet	RESRAD-OFFSITE	Spreadsheet
0	0.3	0.3	0	0	0.5	0.5
1	0.299	0.299	0	0	0.5	0.5
10	0.29	0.29	0	0	0.5	0.5
30	0.27	0.27	0	0	0.5	0.5
50	0.25	0.25	0	0	0.5	0.5
99	0.201	0.201	0	0	0.5	0.5
100	0	0	0.2	0.2	0.5	0.5
101	0	0	0.2	0.2	0.499	0.499
150	0	0	0.2	0.2	0.45	0.45
200	0	0	0.2	0.2	0.4	0.4
250	0	0	0.2	0.2	0.35	0.35
300	0	0	0.2	0.2	0.3	0.3
350	0	0	0.2	0.2	0.275	0.275
400	0	0	0.2	0.2	0.25	0.25
450	0	0	0.2	0.2	0.225	0.225
500	0	0	0.2	0.2	0.2	0.2
550	0	0	0.2	0.2	0.175	0.175
600	0	0	0.2	0.2	0.15	0.15
650	0	0	0.2	0.2	0.125	0.125
700	0	0	0.2	0.2	0.1	0.1
750	0	0	0.2	0.2	0.075	0.075
800	0	0	0.2	0.2	0.05	0.05
850	0	0	0.2	0.2	0.025	0.025
900	0	0	0.2	0.2	4.47E-08	6.59E-08
950	0	0	0.2	0.2	0	0
1000	0	0	0.2	0.2	0	0

verification. The first line of equation 2.3 applies when the thickness of the cover is greater than the thickness of the mixing layer. The second line of equation 2.3 is applicable when the thickness of the cover is less than the thickness of the mixing layer. At the transition from the first to the second line, when the thickness of the cover is equal to the thickness of the mixing layer, both the first and second lines of equation 2.3 are equivalent. While the Users' Manual places the equality on the first line of equation 2.21 (equation 2.3 here), the code uses the second line at the point of transition. Because both forms are equivalent at the transition point, this does not affect the other results as seen in the remaining tables of this section.

2.1.2 Composite Modification Factor for the Concentration of Nuclides in the Mixing Zone

The composite modification factor for the concentration of nuclides in the mixing zone is used to obtain the concentration of nuclides in the mixing zone, which then can be used to calculate the nuclide release rates through runoff and to the atmosphere. The calculation of the composite modification factor involves several steps. First of all, the depths of penetration of the mixing zone into the primary contamination and into the vadose zone need to be known. These depths of penetration can be calculated with Eqs. 2.23 and 2.24 of the RESRAD-OFFSITE User's Manual (Yu et al. 2007), which are shown as Eqs. 2.4 and 2.5 below:

$$d_{pc}(t) = T_{cv}(t_{im}) + T_{pc}(t_{im}) - [T_{cv}(t) + T_{pc}(t)] \geq 0 \text{ while } d_{mix} \leq T_{cv}(t) + T_{pc}(t), \qquad \text{(Eq. 2.4)}$$

where:

$$T_{cv}(t_{im}) + T_{pc}(t_{im}) = T_{pc}(0) + d_{mix} \text{ if } d_{mix} \leq T_{cv}(0),$$
$$T_{cv}(t_{im}) + T_{pc}(t_{im}) = T_{pc}(0) + T_{cv}(0) \text{ if } d_{mix} > T_{cv}(0),$$
$$d_{pc}(t) = \text{depth of penentration of the mixng zone to the primary contamination at time } t \text{ after initial mixing (m), and}$$
$$t_{im} = \text{time of initial mixing (yr).}$$

$$d_{upc}(t) = T_{cv}(t_{pm}) + T_{pc}(t_{pm}) - [T_{cv}(t) + T_{pc}(t)] \text{ when } d_{mix} > T_{cv}(t) + T_{pc}(t), \qquad \text{(Eq. 2.5)}$$

where:

$$T_{cv}(t_{pm}) + T_{pc}(t_{pm}) = d_{mix} \text{ if } d_{mix} \leq T_{cv}(0) + T_{pc}(0),$$
$$T_{cv}(t_{pm}) + T_{pc}(t_{pm}) = T_{pc}(0) + T_{cv}(0) \text{ if } d_{mix} > T_{cv}(0) + T_{pc}(0),$$
$$d_{upc}(t) = \text{depth of penetration of the mixing zone to the vadose zone at time } t \text{ after intial penetration (m), and}$$
$$t_{pm} = \text{time of initial penetration of the mixing zone to the vadose zone, i.e., time when the mixing layer contains the highest amount of soil from the primary contamination (yr).}$$

After the penetration depths are known, the density of soil in the mixing zone is calculated (Eq. 2.26 in the RESRAD-OFFSITE User's Manual) (Yu et al. 2007). The depth of penetration is used as an independent variable in the expression.

$$\rho_{mix}(d_{pc}) = \rho_{pc} + (\rho_{mix}(0) - \rho_{pc})\exp(-d_{pc}/d_{mix})$$
$$\text{while } d_{pc} \le T_{cv}(t) + T_{pc}(t), \qquad \text{(Eq. 2.6)}$$

where:

$\rho_{mix}(d_{pc})$ = density of soil in the mixing zone when the penetration depth to the primary contamination is d_{pc} (g/cm^3).

The initial density of soil in the mixing zone is calculated with Eq. 2.25 (Yu et al. 2007), which is listed as Eq. 2.7 as follows:

$$\rho_{mix}(0) = \rho_{cv} \text{ if } T_{cv}(0) \ge d_{mix},$$
$$\rho_{mix}(0) = \rho_{pc} + \tfrac{T_{cv}(0)}{d_{mix}}(\rho_{cv} - \rho_{pc}) \text{ if } T_{cv}(0) < d_{mix} \le T_{cv}(0) + T_{pc}(0), \text{ and}$$
$$\rho_{mix}(0) = \rho_{pc} + \tfrac{T_{cv}(0)}{d_{mix}}(\rho_{cv} - \rho_{pc}) + \sum_{is}^{N_s} \tfrac{H_{dm}(is)}{d_{mix}}(\rho_{us}(is) - \rho_{pc}) + \tfrac{T_{dm}^{sat}}{d_{mix}}(\rho_{sat} - \rho_{pc}) \qquad \text{(Eq. 2.7)}$$
$$\text{if } T_{cv}(0) + T_{pc}(0) < d_{mix},$$

where:

$\rho_{mix}(0)$ = density of soil in the mixing zone at time 0 (g/cm^3),
$H_{dm}(is)$ = thickness of each vadose zone that is within the mixing zone (m) at time 0,
$\rho_{us}(is)$ = dry bulk density of the vadose zone (g/cm^3),
T_{dm}^{sat} = thickness of the vadose zone that is within the mixing layer (m) at time 0,
ρ_{sat} = dry bulk density of the saturated zone (g/cm^3).

It should be noted that due to its complexity, the calculation of $\rho_{mix}(d_{pc})$ is not carried out further by RESRAD-OFFSITE after the mixing zone reaches the bottom of the primary contamination. The density after that is kept constant as the last calculated value.

With the density of soil in the mixing zone known, the volume fraction of soil from the primary contamination in the mixing zone can be calculated. The equation used depends on whether the mixing zone has penetrated to the vadose zone. If it has not penetrated the vadose zone, the volume fraction is calculated as:

$$f_{vm}(d_{pc}) = 1 - (1 - f_{vm}(0))\exp(-d_{pc}/d_{mix}) \text{ when } d_{mix} \le T_{cv}(t) + T_{pc}(t), \text{ with}$$
$$f_{vm}(0) = 0 \text{ if } T_{cv}(0) \ge d_{mix},$$
$$f_{vm}(0) = 1 - \tfrac{T_{cv}(0)}{d_{mix}} \text{ if } T_{cv}(0) < d_{mix} \le T_{cv}(0) + T_{pc}(0), \text{ and} \qquad \text{(Eq. 2.8)}$$
$$f_{vm}(0) = \tfrac{T_{pc}(0)}{d_{mix}} \text{ if } T_{cv}(0) + T_{pc}(0) < d_{mix}.$$

where:

$f_{vm}(d_{pc})$ = volume fraction of soil from the primary contamination in the mixing zone when the penetration depth to the primary contamination is d_{pc}, and

$f_{vm}(0)$ = the initial value of f_{vm} when $d_{pc} = 0$, i.e., at the beginning of penetration.

If the mixing zone has penetrated to the uncontaminated vadoze zone, then the following equations are used:

$$
\begin{aligned}
f_{vm}(d_{upc}) &= f_{vm}^{p} \exp(-d_{upc} / d_{mix}) \text{ when } d_{mix} > T_{cv}(t) + T_{pc}(t), \text{ with} \\
f_{vm}^{p} &= 1 - \exp(-T_{pc}(0) / d_{mix}) \text{ if } T_{cv}(0) \geq d_{mix}, \\
f_{vm}^{p} &= 1 - \frac{T_{cv}(0)}{d_{mix}} \exp\left(-\frac{T_{cv}(0)+T_{pc}(0)-d_{mix}}{d_{mix}}\right) \text{ if } T_{cv}(0) < d_{mix} \leq T_{cv}(0) + T_{pc}(0), \text{ and} \\
f_{vm}^{p} &= \frac{T_{pc}(0)}{d_{mix}} \text{ if } T_{cv}(0) + T_{pc}(0) < d_{mix}.
\end{aligned}
\qquad \text{(Eq. 2.9)}
$$

where:

$f_{vm}^{p}(d_{upc})$ = volume fraction of soil from the primary contamination in the mixing zone when the penetration depth to the vadose zone is d_{upc}, and

f_{vm}^{p} = the initial value of f_{vm} when $d_{upc} = 0$, i.e., at the beginning of penetration to the vadose zone.

Finally, after f_{vm} is calculated, the composite modification factor for the concentration of nuclides in the mixing zone, M_{mix}, can be calculated as

$$M_{mix}(t) = f_{vm}(t)\, \rho_{pc} / \rho_{mix}(t) \qquad \text{(Eq. 2.10)}$$

Tables 2-5 to 2-8 compare values of the modification factor listed in the CZTHICK3.DAT file with those obtained with the spreadsheets. Table 2-5 shows the comparison for Case II concerning Cs-137. Table 2-6 shows the comparison for Case III concerning H-3. Tables 2-7 and 2-8 show comparisons for Case VI and Case VIII concerning Ni-63 and Ra-226, respectively. In general, the results are identical; the few exceptions where there is a discrepancy are highlighted in yellow in the tables. These discrepancies appear at the time when the mixing zone just penetrates the primary contamination. At this time, the volume fraction of soil from the primary contamination in the mixing zone is very small. These discrepancies are explained by the different precisions used by RESRAD-OFFSITE and the Excel spreadsheets for storing numerical values. The Excel spreadsheet uses double precision while RESRAD-OFFSITE uses single precision for most variables. Double and quadruple precision is used for a few selected variables in RESRAD-OFFSITE.

2.2 RELEASE BY SURFACE RUNOFF

To know the release rates of radionuclides through surface runoff, the concentrations of nuclides in the mixing zone need to be calculated first. In RESRAD-OFFSITE, this is done by multiplying the concentrations of nuclides in the unmixed portion of the primary contamination with the composite modification factor for the concentration of nuclides in the mixing zone, which was discussed in the previous section. The concentrations of nuclides in the unmixed portion of primary contamination are

Table 2-5 Comparison of the RESRAD-OFFSITE Results and the Spreadsheet Results for the Modification Factor for the Concentration of Nuclides in the Mixing Zone for Case II Concerning Cs-137, with Notable Disagreement Highlighted

Time (yr)	RESRAD-OFFSITE	Spreadsheet
349	0	0
350	0	1.510E-07
351	6.644E-03	6.645E-03
352	1.324E-02	1.324E-02
353	1.980E-02	1.980E-02
354	2.631E-02	2.631E-02
355	3.278E-02	3.278E-02
375	1.535E-01	1.535E-01
400	2.835E-01	2.835E-01
425	3.935E-01	3.935E-01
450	4.866E-01	4.866E-01
475	5.654E-01	5.654E-01
500	6.321E-01	6.321E-01
525	6.886E-01	6.886E-01
550	7.364E-01	7.364E-01
575	7.769E-01	7.769E-01
600	8.111E-01	8.111E-01
625	8.401E-01	8.401E-01
650	8.647E-01	8.647E-01
675	8.854E-01	8.854E-01
700	9.030E-01	9.030E-01
725	9.179E-01	9.179E-01
750	9.305E-01	9.305E-01
775	9.412E-01	9.412E-01
800	9.502E-01	9.502E-01
825	9.579E-01	9.579E-01
850	9.643E-01	9.643E-01
851	9.579E-01	9.579E-01
852	9.516E-01	9.516E-01
853	9.452E-01	9.452E-01
854	9.389E-01	9.390E-01
855	9.327E-01	9.327E-01
875	8.163E-01	8.163E-01
900	6.910E-01	6.910E-01
925	5.849E-01	5.849E-01
950	4.951E-01	4.951E-01
1000	3.548E-01	3.548E-01

Table 2-6 Comparison of the RESRAD-OFFSITE Results and the Spreadsheet Results for the Modification Factor for the Concentration of Nuclides in the Mixing Zone for Case III Concerning H-3, with Notable Disagreement Highlighted

Time (yr)	RESRAD-OFFSITE	Spreadsheet
149	0	0
150	0	6.066E-08
151	6.231E-03	6.232E-03
152	1.243E-02	1.243E-02
153	1.859E-02	1.859E-02
154	2.471E-02	2.471E-02
155	3.080E-02	3.080E-02
160	6.071E-02	6.071E-02
165	8.975E-02	8.975E-02
170	1.179E-01	1.179E-01
175	1.453E-01	1.453E-01
180	1.719E-01	1.719E-01
185	1.977E-01	1.977E-01
190	2.227E-01	2.227E-01
200	2.705E-01	2.705E-01
210	3.156E-01	3.156E-01
220	3.579E-01	3.579E-01
230	3.978E-01	3.978E-01
240	4.353E-01	4.353E-01
250	4.705E-01	4.705E-01
260	5.036E-01	5.036E-01
270	5.347E-01	5.347E-01
280	5.638E-01	5.638E-01
290	5.913E-01	5.913E-01
300	6.170E-01	6.170E-01
350	6.170E-01	6.170E-01
400	6.170E-01	6.170E-01
500	6.170E-01	6.170E-01
600	6.170E-01	6.170E-01
700	6.170E-01	6.170E-01
800	6.170E-01	6.170E-01
900	6.170E-01	6.170E-01
1000	6.170E-01	6.170E-01

Table 2-7 Comparison of the RESRAD-OFFSITE Results and the Spreadsheet Results for the Modification Factor for the Concentration of Nuclides in the Mixing Zone for Case VI Concerning Ni-63

Time (yr)	RESRAD-OFFSITE	Spreadsheet
0	3.60E-01	3.60E-01
1	3.59E-01	3.59E-01
2	3.58E-01	3.58E-01
3	3.56E-01	3.56E-01
4	3.55E-01	3.55E-01
5	3.54E-01	3.54E-01
6	3.53E-01	3.53E-01
7	3.52E-01	3.52E-01
8	3.51E-01	3.50E-01
9	3.49E-01	3.49E-01
10	3.48E-01	3.48E-01
11	3.47E-01	3.47E-01
12	3.46E-01	3.46E-01
13	3.45E-01	3.45E-01
14	3.44E-01	3.43E-01
15	3.42E-01	3.42E-01
16	3.41E-01	3.41E-01
17	3.40E-01	3.40E-01
18	3.39E-01	3.39E-01
19	3.38E-01	3.38E-01
20	3.37E-01	3.37E-01
21	3.36E-01	3.35E-01
22	3.34E-01	3.34E-01
23	3.33E-01	3.33E-01
24	3.32E-01	3.32E-01
25	3.31E-01	3.31E-01
26	3.30E-01	3.30E-01
27	3.29E-01	3.29E-01
28	3.28E-01	3.28E-01
29	3.27E-01	3.27E-01
30	3.26E-01	3.25E-01
31	3.24E-01	3.24E-01
32	3.23E-01	3.23E-01

Table 2-8 Comparison of the RESRAD-OFFSITE Results and the Spreadsheet Results for the Modification Factor for the Concentration of Nuclides in the Mixing Zone for Case VIII Concerning Ra-226, with Notable Disagreement Highlighted

Time (yr)	RESRAD-OFFSITE	Spreadsheet
99	0	0
100	0	2.491E-07
101	4.404E-03	4.404E-03
102	8.790E-03	8.790E-03
103	1.316E-02	1.316E-02
104	1.751E-02	1.751E-02
105	2.185E-02	2.185E-02
125	1.051E-01	1.051E-01
150	2.004E-01	2.004E-01
175	2.865E-01	2.865E-01
200	3.640E-01	3.640E-01
225	4.338E-01	4.338E-01
250	4.964E-01	4.964E-01
275	5.524E-01	5.524E-01
325	6.256E-01	6.256E-01
375	6.679E-01	6.679E-01
425	7.055E-01	7.055E-01
475	7.391E-01	7.391E-01
525	7.689E-01	7.689E-01
575	7.954E-01	7.954E-01
625	8.189E-01	8.189E-01
675	8.398E-01	8.398E-01
725	8.583E-01	8.583E-01
775	8.747E-01	8.747E-01
825	8.892E-01	8.892E-01
875	9.021E-01	9.021E-01
899	9.077E-01	9.077E-01
900	9.080E-01	9.080E-01
901	9.057E-01	9.057E-01
925	8.530E-01	8.530E-01
950	8.013E-01	8.013E-01
975	7.527E-01	7.527E-01
1000	7.071E-01	7.071E-01

calculated at each time point by taking into account loss through leaching and gas diffusion as well as changes through radiological ingrowth and decay. These concentrations are recorded for the principal nuclides in each decay chain and saved in the output file SFSIN.DAT.

The release rates of nuclides through surface runoff can be obtained by multiplying the concentrations of nuclides in the mixing zone with the total mass of soil eroded away. This is equivalent to multiplying the

eroded mass of soil that is from the primary contamination with the concentrations of nuclides in the unmixed portion of primary contamination. Temporal data of the eroded masses of soil that are from the primary contamination are recorded by RESRAD-OFFSITE and are saved, along with the data of the release rates of nuclide through surface runoff, in the output file named SWFLUXIN.DAT.

2.2.1 Concentrations of Nuclide in the Unmixed Portion of the Primary Contamination

Concentrations of nuclides in the unmixed portion of the primary contamination are adjusted constantly to account for loss through leaching and gas diffusion as well as changes through radiological ingrowth and decay. The following equations are used to consider each principal nuclide in a decay chain when there's no loss through gas diffusion:

$$A_k(t) = \sum_{i=1}^{k} a_{k,i} \exp(-\lambda_i t - L_i t), \qquad \text{(Eq. 2.11)}$$

where:

$A_k(t)$ = concentration of kth principal nuclide in a decay chain in the unmixed portion of primary contamination at time t (pCi/g),

$a_{k,i}$ = set of coefficients defined by $a_{1,1} = A_1(0)$,

$a_{k,i} = \frac{\lambda_k a_{k-1,i}}{\lambda_k + L_k - \lambda_i - L_i}$ for all $1 \le i \le k$,

$a_{k,k} = -\sum_{i=1}^{k-1} a_{k,i}$,

$A_1(0)$ = concentration of the parent nuclide at time 0 (pCi/g),

λ_i = radiological decay constant for ith principal nuclide in a decay chain (1/yr), and

L_i = leach rate constant for ith principal nuclide in a decay chain (1/yr).

The radiological decay constant for a nuclide is calculated as $\lambda_i = \ln(2)/t_{1/2,i}$, with $t_{1/2}$ (yr) being the radiological decay half-life. The leach rate constant is a function of the water infiltration rate, volumetric water content, thickness, and retardation factor, and can be calculated with Eqs. E.3 to E.8 from the RESRAD User's Manual (Yu et al. 2001).

$$\begin{aligned}
L_i &= \frac{I}{\theta T_0 R_{d_i}}, \\
I &= (1 - C_e)\left[(1 - C_r) P_r + I_{rr}\right], \\
\theta &= \theta_{sat} R_s = P_t R_s, \qquad \text{(Eq. 2.12)} \\
R_s &= \left(\frac{I}{K_{sat}}\right)^{\frac{1}{2b+3}}, \\
R_{d_i} &= 1 + \frac{\rho_{pc} K_{d_i}}{\theta},
\end{aligned}$$

where:

I = water infiltration rate (m/yr),
C_e = evapotranspiration coefficient,
C_r = runoff coefficient,
P_r = precipitation rate (m/yr),
I_{rr} = irrigation rate (m/yr),
θ = volumetric water content in the primary contamination,
θ_{sat} = saturated water content in the primary contamination,
P_t = total porosity in the primary contamination,
R_s = saturation ratio,
K_{sat} = saturated hydraulic conductivity in the primary contamination (m/yr),
b = soil-specific exponential parameter for the primary contamination,
T_0 = initial thickness of the primary contamination (m),
R_{d_i} = retardation factor for nuclide *i*, and
K_{d_i} = soil/water distribution coefficient for nuclide *i* in the primary contamination (cm^3/g).

Table 2-9 shows calculations of the radiological decay and leach rate constants for the parents and their principal progeny nuclides concerned in Cases I-VIII when the density of the primary contamination is 1.5 g/cm^3.

For H-3 and C-14, Eq. 2.11 needs some modification to account for the loss through gas diffusion. The evasion rate constant, E, is introduced:

$$\begin{aligned} A(t) &= A(0)\exp\left(-\lambda t - Lt - E_c t\right), \\ E_c(t) &= 0 \text{ when } d_{ref} - C_d < 0, \\ &= E \times \frac{d_{ref} - C_d(t)}{T(t)} \text{ when } 0 \le d_{ref} - C_d \le T(t), \\ &= E \text{ when } d_{ref} - C_d(t) > T(t). \end{aligned} \qquad \text{(Eq. 2.13)}$$

where:

E_c = evasion rate constant adjusted for cover thickness (yr^{-1}),
E = evasion rate constant, and
d_{ref} = reference evasion depth (0.3) (m).

E_{H-3} is calculated by taking into account the loss of HTO through evapotranspiration; therefore, the evapotranspiration rate, E_t, is used:

$$\begin{aligned} E_t &= C_e \times \left[(1 - C_r)P_r + I_{rr}\right] \\ E_{H-3} &= \frac{E_t}{P_t \; R_s \; d_{ref}} \end{aligned} \qquad \text{(Eq. 2.14)}$$

Table 2-9 Calculations of the Radiological Decay Constants and Leach Rate Constants[a]

Radionuclide	Half-life $t_{1/2}$ (yr)	Kd (cm^3/g)	Rd	Leach Rate Constant L (1/yr)	Radiological Decay Constant λ (1/yr)
U-238	4.47E+09	50	234.70	3.32E-03	1.55E-10
U-234	2.45E+05	50	234.70	3.32E-03	2.83E-06
Th-230	7.70E+04	60000	280445.22	2.78E-06	9.00E-06
Ra-226	1600	70	328.18	2.37E-03	4.33E-04
Pb-210	22.3	100	468.41	1.66E-03	3.11E-02
Po-210	0.379	10	47.74	1.63E-02	1.83E+00
Cs-137	30	4600	21501.72	3.62E-05	2.31E-02
Sr-90	29.12	30	141.22	5.52E-03	2.38E-02
Ni-63	96	1000	4675.07	1.67E-04	7.22E-03
Co-60	5.271	1000	4675.07	1.67E-04	1.32E-01
C-14	5730	0	1.00	7.79E-01	1.21E-04
H-3	12.35	0	1.00	7.79E-01	5.61E-02

[a] The parameters used in the calculations are:

Initial thickness of the contaminated zone (T_0)	2 m
Evapotranspiration coefficient (C_e)	0.5
Runoff coefficient (C_r)	0.2
Irrigation (Irr)	0.2 m/yr
Precipitation (P_r)	1 m/yr
Infiltration rate (I)	0.5 m/yr
Saturated hydraulic conductivity (K_{sat})	10 m/yr
b parameter of the contaminated zone (b)	5.3
Total porosity of the contaminated zone (P_t)	0.4
Dry soil bulk density (r)	1.5 g/cm^3
Saturation ratio (R_s)	0.802
Moisture content (q)	0.321

For C-14, E_{C-14} is set to an empirical constant of 22/yr. Appendix L of the RESRAD User's Manual (Yu et al. 2001) provides more information on the calculation of the evasion rates for H-3 and C-14.

Tables 2-10 to 2-13 compare the concentrations of nuclides in the unmixed portion of the primary contamination listed in SFSIN.DAT with those obtained from the spreadsheets. Table 2-10 concerns U-238 and its progeny nuclides in Case I; Tables 2-11 and 2-12 concern H-3 in Case III and C-14 in Case IV, respectively; and Table 2-13 concerns Co-60 in Case V. In general, the results agree very well with each other except when the concentrations are very small. The discrepancies result from different precisions used for storing real numbers in RESRAD-OFFSITE and the spreadsheets. However, the discrepancies do not compromise agreement in the final dose results because the concentrations involved are extremely low and essentially make no dose contribution.

Table 2-10 Comparison of the RESRAD-OFFSITE Results and the Spreadsheet Results for the Concentration of Nuclide in the Unmixed Portion of the Primary Contamination for Case I Concerning U-238 and Its Progenies, with Notable Disagreement Highlighted

	U-238		U-234		Th-230		Ra-226		Pb-210		Po-210	
Time (yr)	RESRAD-OFFSITE	Spread-sheet	RESRAD-OFFSITE	Spread-sheet	RESRAD-OFFSITE	Spread-sheet	RESRAD-OFFSITE	Spread-sheet	RESRAD-OFFSITE	Spread-sheet	RESRAD-OFFSITE	Spread-sheet
0	100	100	0	0	0	0	0	0	0	0	0	0
1	9.97E+01	9.97E+01	2.83E-04	2.83E-04	1.27E-09	1.27E-09	1.84E-13	1.84E-13	1.40E-15	1.40E-15	3.71E-16	4.01E-16
2	9.93E+01	9.93E+01	5.63E-04	5.63E-04	5.08E-09	5.08E-09	1.47E-12	1.47E-12	2.25E-14	2.25E-14	9.98E-15	1.00E-14
3	9.90E+01	9.90E+01	8.42E-04	8.42E-04	1.14E-08	1.14E-08	4.94E-12	4.94E-12	1.13E-13	1.13E-13	6.21E-14	6.22E-14
4	9.87E+01	9.87E+01	1.12E-03	1.12E-03	2.02E-08	2.02E-08	1.17E-11	1.17E-11	3.54E-13	3.54E-13	2.21E-13	2.21E-13
5	9.84E+01	9.84E+01	1.39E-03	1.39E-03	3.15E-08	3.15E-08	2.28E-11	2.28E-11	8.58E-13	8.58E-13	5.80E-13	5.80E-13
50	8.47E+01	8.47E+01	1.20E-02	1.20E-02	2.86E-06	2.86E-06	2.05E-08	2.05E-08	6.04E-09	6.04E-09	5.76E-09	5.76E-09
75	7.80E+01	7.80E+01	1.66E-02	1.66E-02	6.09E-06	6.09E-06	6.52E-08	6.52E-08	2.56E-08	2.56E-08	2.47E-08	2.47E-08
100	7.18E+01	7.18E+01	2.03E-02	2.03E-02	1.03E-05	1.03E-05	1.46E-07	1.46E-07	6.84E-08	6.84E-08	6.66E-08	6.66E-08
125	6.60E+01	6.60E+01	2.34E-02	2.34E-02	1.52E-05	1.52E-05	2.69E-07	2.69E-07	1.43E-07	1.43E-07	1.39E-07	1.39E-07
150	6.08E+01	6.08E+01	2.58E-02	2.58E-02	2.07E-05	2.07E-05	4.38E-07	4.38E-07	2.54E-07	2.54E-07	2.49E-07	2.49E-07
175	5.59E+01	5.59E+01	2.77E-02	2.77E-02	2.68E-05	2.68E-05	6.57E-07	6.57E-07	4.08E-07	4.08E-07	4.01E-07	4.01E-07
200	5.15E+01	5.15E+01	2.92E-02	2.92E-02	3.32E-05	3.32E-05	9.26E-07	9.26E-07	6.07E-07	6.07E-07	5.97E-07	5.97E-07
225	4.74E+01	4.74E+01	3.02E-02	3.02E-02	3.98E-05	3.98E-05	1.25E-06	1.25E-06	8.53E-07	8.53E-07	8.40E-07	8.40E-07
250	4.36E+01	4.36E+01	3.09E-02	3.09E-02	4.67E-05	4.67E-05	1.61E-06	1.61E-06	1.15E-06	1.15E-06	1.13E-06	1.13E-06
275	4.01E+01	4.01E+01	3.13E-02	3.13E-02	5.37E-05	5.37E-05	2.03E-06	2.03E-06	1.48E-06	1.48E-06	1.46E-06	1.46E-06
300	3.69E+01	3.69E+01	3.14E-02	3.14E-02	6.07E-05	6.07E-05	2.49E-06	2.49E-06	1.87E-06	1.87E-06	1.84E-06	1.84E-06
350	3.13E+01	3.13E+01	3.10E-02	3.10E-02	7.48E-05	7.48E-05	3.54E-06	3.54E-06	2.76E-06	2.76E-06	2.73E-06	2.73E-06
400	2.65E+01	2.65E+01	3.00E-02	3.00E-02	8.85E-05	8.85E-05	4.73E-06	4.73E-06	3.81E-06	3.81E-06	3.76E-06	3.76E-06
450	2.25E+01	2.25E+01	2.86E-02	2.86E-02	1.02E-04	1.02E-04	6.04E-06	6.04E-06	4.98E-06	4.98E-06	4.92E-06	4.92E-06
500	1.90E+01	1.90E+01	2.69E-02	2.69E-02	1.14E-04	1.14E-04	7.43E-06	7.43E-06	6.25E-06	6.25E-06	6.18E-06	6.18E-06
550	1.61E+01	1.61E+01	2.51E-02	2.51E-02	1.26E-04	1.26E-04	8.88E-06	8.88E-06	7.60E-06	7.60E-06	7.51E-06	7.51E-06
600	1.36E+01	1.36E+01	2.32E-02	2.32E-02	1.37E-04	1.37E-04	1.04E-05	1.04E-05	8.99E-06	8.99E-06	8.89E-06	8.89E-06
650	1.16E+01	1.16E+01	2.13E-02	2.13E-02	1.46E-04	1.46E-04	1.19E-05	1.19E-05	1.04E-05	1.04E-05	1.03E-05	1.03E-05
700	9.79E+00	9.79E+00	1.94E-02	1.94E-02	1.56E-04	1.56E-04	1.34E-05	1.34E-05	1.18E-05	1.18E-05	1.17E-05	1.17E-05
750	8.30E+00	8.30E+00	1.76E-02	1.76E-02	1.64E-04	1.64E-04	1.49E-05	1.49E-05	1.32E-05	1.32E-05	1.31E-05	1.31E-05
800	7.03E+00	7.03E+00	1.59E-02	1.59E-02	1.71E-04	1.71E-04	1.63E-05	1.63E-05	1.46E-05	1.46E-05	1.45E-05	1.45E-05
850	5.95E+00	5.95E+00	1.43E-02	1.43E-02	1.78E-04	1.78E-04	1.77E-05	1.77E-05	1.60E-05	1.60E-05	1.58E-05	1.58E-05
900	5.04E+00	5.04E+00	1.28E-02	1.28E-02	1.84E-04	1.84E-04	1.90E-05	1.90E-05	1.73E-05	1.73E-05	1.71E-05	1.71E-05
950	4.27E+00	4.27E+00	1.15E-02	1.15E-02	1.89E-04	1.89E-04	2.03E-05	2.03E-05	1.85E-05	1.85E-05	1.84E-05	1.84E-05
1000	3.62E+00	3.62E+00	1.02E-02	1.02E-02	1.94E-04	1.94E-04	2.15E-05	2.15E-05	1.97E-05	1.97E-05	1.95E-05	1.95E-05

Table 2-11 Comparison of the RESRAD-OFFSITE Results and the Spreadsheet Results for the Concentration of Nuclide in the Unmixed Portion of the Primary Contamination for Case III Concerning H-3, with Notable Disagreements Highlighted

Time (yr)	RESRAD-OFFSITE	Spreadsheet
0	1.00E+02	1.00E+02
1	1.98E+01	1.98E+01
2	3.88E+00	3.88E+00
3	7.53E-01	7.53E-01
4	1.44E-01	1.44E-01
5	2.74E-02	2.74E-02
6	5.16E-03	5.16E-03
7	9.60E-04	9.60E-04
8	1.77E-04	1.77E-04
9	3.22E-05	3.22E-05
10	5.81E-06	5.81E-06
11	1.04E-06	1.04E-06
12	1.83E-07	1.83E-07
14	5.54E-09	5.54E-09
16	1.61E-10	1.61E-10
18	4.48E-12	4.48E-12
20	1.20E-13	1.20E-13
22	3.06E-15	3.06E-15
24	7.52E-17	7.52E-17
26	1.77E-18	1.77E-18
28	4.01E-20	4.01E-20
30	8.70E-22	8.70E-22
32	1.81E-23	1.81E-23
34	3.62E-25	3.62E-25
36	6.92E-27	6.92E-27
38	1.27E-28	1.27E-28
40	2.24E-30	2.24E-30
42	3.79E-32	3.79E-32
44	6.15E-34	6.15E-34
46	9.57E-36	9.57E-36
48	1.43E-37	1.43E-37
50	2.04E-39	2.04E-39
52	2.81E-41	2.81E-41
54	0.00E+00	3.70E-43
56	0.00E+00	4.68E-45
58	0.00E+00	5.67E-47
60	0.00E+00	6.60E-49

Table 2-12 Comparison of the RESRAD-OFFSITE Results and the Spreadsheet Results for the Concentration of Nuclide in the Unmixed Portion of the Primary Contamination for Case IV Concerning C-14, with Notable Disagreements Highlighted

Time (yr)	RESRAD-OFFSITE	Spreadsheet
0	1.00E+02	1.00E+02
1	1.41E+01	1.41E+01
2	1.98E+00	1.98E+00
3	2.76E-01	2.76E-01
4	3.84E-02	3.84E-02
5	5.32E-03	5.32E-03
6	7.35E-04	7.35E-04
7	1.01E-04	1.01E-04
8	1.38E-05	1.38E-05
9	1.89E-06	1.89E-06
10	2.56E-07	2.56E-07
11	3.47E-08	3.47E-08
12	4.68E-09	4.68E-09
14	8.39E-11	8.39E-11
16	1.48E-12	1.48E-12
18	2.58E-14	2.58E-14
20	4.41E-16	4.41E-16
22	7.42E-18	7.42E-18
24	1.23E-19	1.23E-19
26	2.00E-21	2.01E-21
28	3.21E-23	3.22E-23
30	5.08E-25	5.08E-25
32	7.89E-27	7.90E-27
34	1.21E-28	1.21E-28
36	1.82E-30	1.82E-30
38	2.69E-32	2.69E-32
40	3.92E-34	3.92E-34
42	5.62E-36	5.63E-36
44	7.94E-38	7.95E-38
46	1.10E-39	1.10E-39
48	1.51E-41	1.51E-41
50	2.03E-43	2.03E-43
52	2.80E-45	2.69E-45
54	0.00E+00	3.51E-47
56	0.00E+00	4.50E-49
58	0.00E+00	5.68E-51
60	0.00E+00	7.05E-53

Table 2-13 Comparison of the RESRAD-OFFSITE Results and the Spreadsheet Results for the Concentration of Nuclide in the Unmixed Portion of the Primary Contamination for Case V Concerning Co-60

Time (yr)	RESRAD-OFFSITE	Spreadsheet
0.00	1.00E+02	1.00E+02
0.25	9.68E+01	9.68E+01
0.50	9.36E+01	9.36E+01
0.75	9.06E+01	9.06E+01
1.00	8.77E+01	8.77E+01
1.25	8.48E+01	8.48E+01
1.50	8.21E+01	8.21E+01
1.75	7.94E+01	7.94E+01
2.00	7.68E+01	7.68E+01
2.25	7.43E+01	7.43E+01
2.50	7.19E+01	7.19E+01
2.75	6.96E+01	6.96E+01
3.00	6.73E+01	6.73E+01
3.25	6.52E+01	6.52E+01
3.50	6.31E+01	6.31E+01
3.75	6.10E+01	6.10E+01
4.00	5.90E+01	5.90E+01
4.25	5.71E+01	5.71E+01
4.50	5.53E+01	5.53E+01
4.75	5.35E+01	5.35E+01
5.00	5.17E+01	5.17E+01
.	.	.
.	.	.
.	.	.
30.00	1.92E+00	1.92E+00
30.25	1.86E+00	1.86E+00
30.50	1.80E+00	1.80E+00
30.75	1.74E+00	1.74E+00
31.00	1.68E+00	1.68E+00
31.25	1.63E+00	1.63E+00
31.50	1.57E+00	1.57E+00
31.75	1.52E+00	1.52E+00
32.00	1.47E+00	1.47E+00

2.2.2 Release Rates of Nuclide through Runoff

The rate at which soil from the primary contamination is eroded is computed at each intermediate time point with the following equation:

$$m_{pc}(t) = 10^6\ \varepsilon\ A\ f_{vm}(t)\ \rho_{pc}, \qquad \text{(Eq. 2.15)}$$

where:

$\varepsilon = \varepsilon_{cv}$ when $T_{cv}(t) > 0$, and

$\varepsilon = \varepsilon_{pc}$ when $T_{cv}(t) = 0$,

$m_{pc}(t)$ = eroded mass that is from the primary contamination at time t (g/yr),

A = area of contamination (m^2)

After the calculation of $m_{pc}(t)$, nuclide release rates through surface runoff, $R_k^{sr}(t)$, can be easily calculated as:

$$R_k^{sr}(t) = m_{pc}(t) A_k(t) \qquad \text{(Eq. 2.16)}$$

The release rates of nuclide through surface runoff for Cases III (H-3), IV (C-14), and VII (Sr-90) are all zero. For Cases III and IV, it takes some time to erode the cover thickness to be less than the mixing depth, and by then the nuclides in the primary contamination had either diffused out or leached to the underlying vadose zone. For Case VII, the release rate is zero because there is no erosion of surface soil (erosion rate of cover is 0 m/yr).

Listed records in SWFLUXIN.DAT are the same as those obtained with spreadsheets for Case II (Cs-137), Case V (Co-60), and Case VI (Ni-63). For Cases I (U-238) and Case VIII (Ra-226), discrepancies are found for a short period of time; they eventually disappear as time progresses. Figure 2-1 compares time profiles of the release rates of U-238 and its progeny nuclides in Case I. Table 2-14 highlights the comparison of the numerical values with which the graphics in Figure 2-1 are obtained. Figure 2-2 and Table 2-15 display comparisons of the release rates of Ra-226 and its progeny nuclides in Case VIII.

Because the calculations in RESRAD-OFFSITE are sequential; any discrepancies observed in the earlier results can lead to discrepancies in the later results. In this section, the discrepancies in the release rates of nuclides through surface runoff are related to the discrepancies observed in Sections 2.1.1, 2.1.2, and 2.2.1. For both Tables 2-8 and 2-15, the observed discrepancy occurs at 100 years, while for both Tables 2-10 and 2-14, the observed discrepancy occurs at 1 year.

2.3 RELEASE TO GROUNDWATER

Radionuclides in both the mixing zone and the unmixed portion of the primary contamination can dissolve in pore water and be carried through the vadose zone to the underlying groundwater table. The calculations of the release rates of nuclides, R_k^{gw}, to the groundwater are performed using Eq. 2.32 in the RESRAD-OFFSITE User's Manual (Yu et al. 2007):

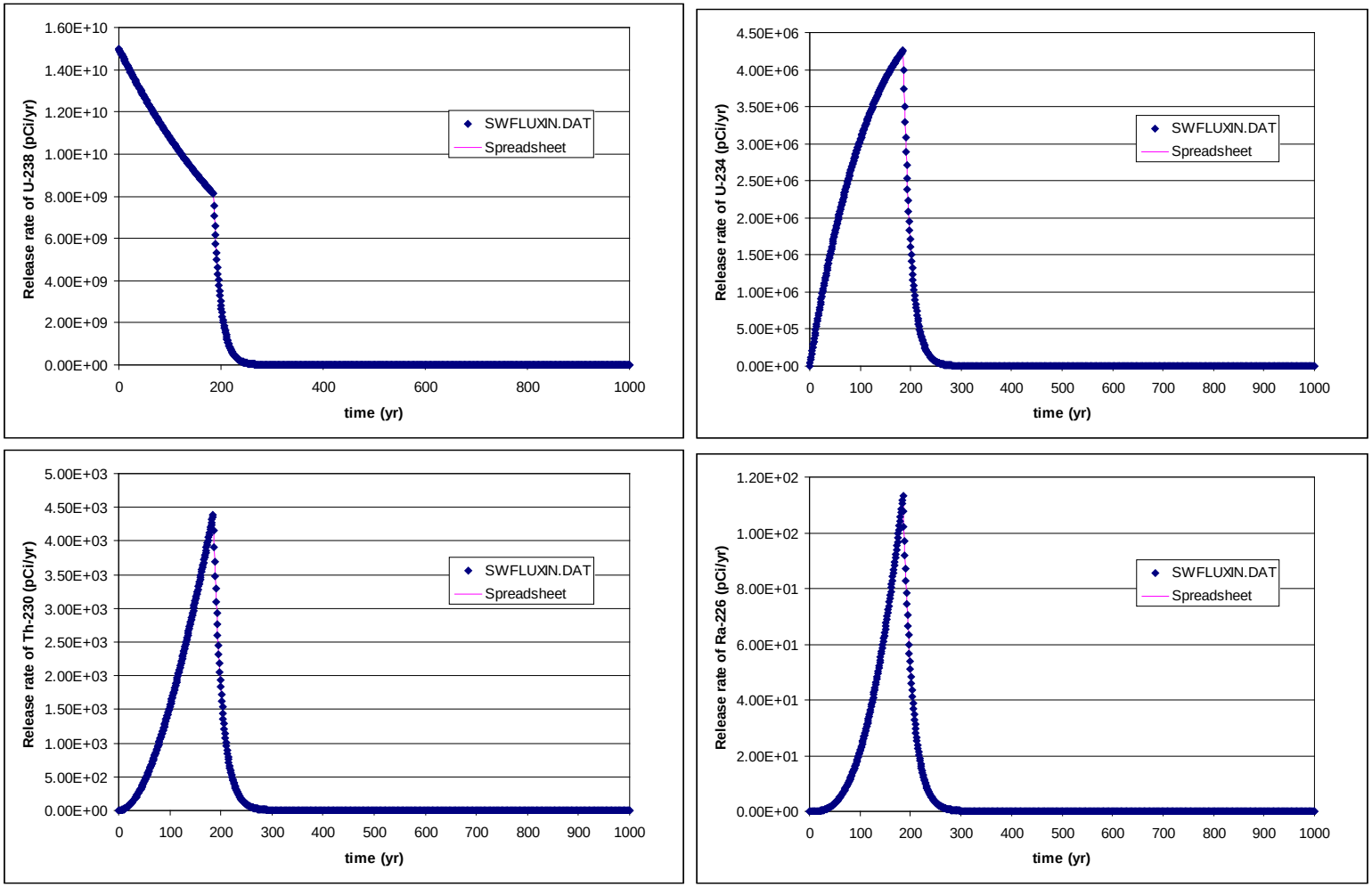

Figure 2-1 Comparison of the RESRAD-OFFSITE Results and Spreadsheet Results for the Release Rates of Nuclide through Surface Runoff for Case I Concerning U-238 and Its Progenies

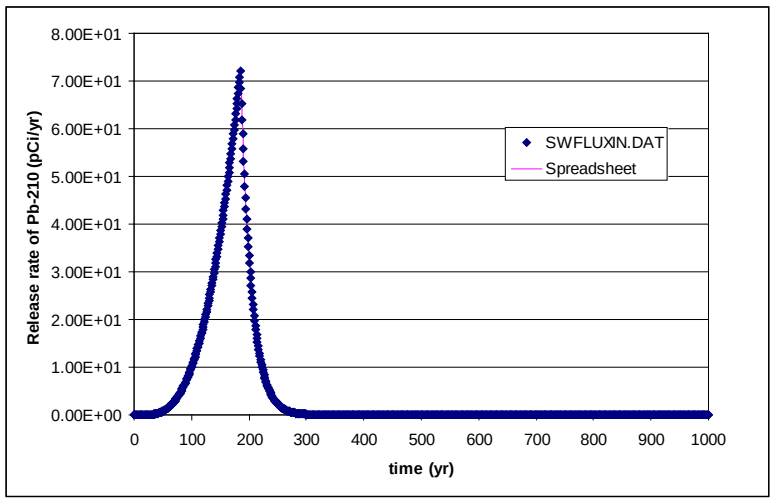

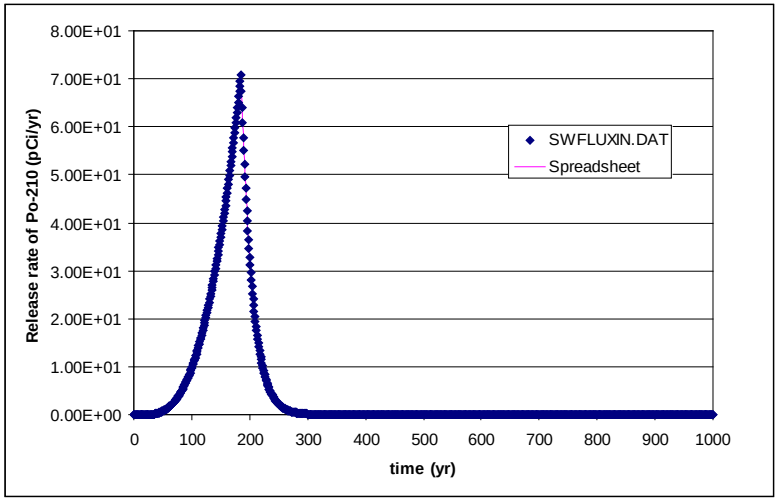

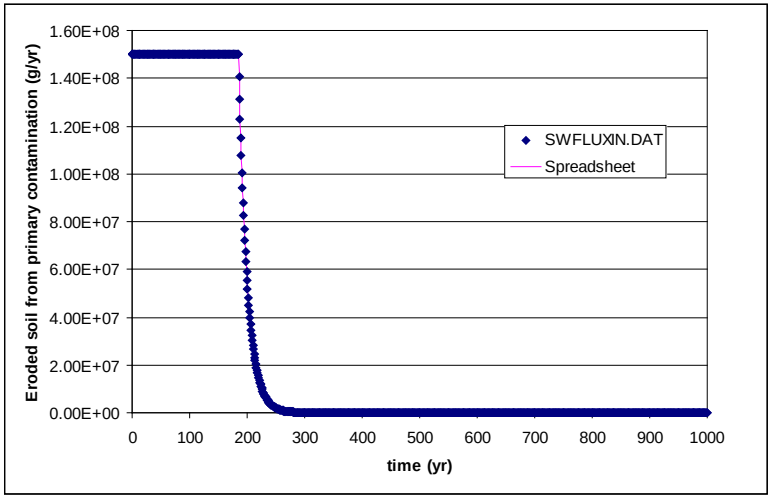

Figure 2-1 (Cont.)

Table 2-14 Comparison of the RESRAD-OFFSITE Results and the Spreadsheet Results for the Release Rates of Nuclide through Surface Runoff for Case I Concerning U-238 and Its Progenies, with Notable Disagreement Highlighted

	U-238		U-234		Th-230		Ra-226		Pb-210		Po-210	
Time (yr)	RESRAD-OFFSITE	Spread-sheet	RESRAD-OFFSITE	Spread-sheet	RESRAD-OFFSITE	Spread-sheet	RESRAD-OFFSITE	Spread-sheet	RESRAD-OFFSITE	Spread-sheet	RESRAD-OFFSITE	Spread-sheet
0	1.50E+10	1.50E+10	0	0	0	0	0	0	0	0	0	0
1	1.50E+10	1.49E+10	4.24E+04	4.24E+04	1.91E-01	1.91E-01	2.76E-05	2.76E-05	2.10E-07	2.10E-07	6.02E -08	5.57E -08
2	1.49E+10	1.49E+10	8.45E+04	8.45E+04	7.62E-01	7.62E-01	2.20E-04	2.20E-04	3.38E-06	3.38E-06	1.50E-06	1.50E-06
3	1.49E+10	1.49E+10	1.26E+05	1.26E+05	1.71E+00	1.71E+00	7.41E-04	7.41E-04	1.70E-05	1.70E-05	9.32E-06	9.32E-06
4	1.48E+10	1.48E+10	1.68E+05	1.68E+05	3.04E+00	3.04E+00	1.75E-03	1.75E-03	5.32E-05	5.32E-05	3.31E-05	3.31E-05
5	1.48E+10	1.48E+10	2.09E+05	2.09E+05	4.73E+00	4.73E+00	3.41E-03	3.41E-03	1.29E-04	1.29E-04	8.70E-05	8.71E-05
50	1.27E+10	1.27E+10	1.80E+06	1.80E+06	4.29E+02	4.29E+02	3.07E+00	3.07E+00	9.06E-01	9.06E-01	8.63E-01	8.63E-01
75	1.17E+10	1.17E+10	2.49E+06	2.49E+06	9.13E+02	9.13E+02	9.78E+00	9.78E+00	3.84E+00	3.84E+00	3.71E+00	3.71E+00
100	1.08E+10	1.08E+10	3.05E+06	3.05E+06	1.54E+03	1.54E+03	2.19E+01	2.19E+01	1.03E+01	1.03E+01	9.98E+00	9.98E+00
125	9.91E+09	9.91E+09	3.51E+06	3.51E+06	2.28E+03	2.28E+03	4.03E+01	4.03E+01	2.14E+01	2.14E+01	2.09E+01	2.09E+01
150	9.12E+09	9.12E+09	3.88E+06	3.88E+06	3.11E+03	3.11E+03	6.57E+01	6.57E+01	3.81E+01	3.81E+01	3.74E+01	3.74E+01
175	8.39E+09	8.39E+09	4.16E+06	4.16E+06	4.01E+03	4.01E+03	9.85E+01	9.85E+01	6.12E+01	6.12E+01	6.01E+01	6.01E+01
200	2.84E+09	2.84E+09	1.61E+06	1.61E+06	1.83E+03	1.83E+03	5.11E+01	5.11E+01	3.35E+01	3.35E+01	3.30E+01	3.30E+01
225	4.94E+08	4.94E+08	3.15E+05	3.15E+05	4.15E+02	4.15E+02	1.30E+01	1.30E+01	8.89E+00	8.89E+00	8.75E+00	8.75E+00
250	8.59E+07	8.59E+07	6.08E+04	6.08E+04	9.20E+01	9.20E+01	3.18E+00	3.18E+00	2.26E+00	2.26E+00	2.22E+00	2.22E+00
275	1.49E+07	1.49E+07	1.16E+04	1.16E+04	2.00E+01	2.00E+01	7.55E-01	7.55E-01	5.52E-01	5.52E-01	5.44E-01	5.44E-01
300	2.59E+06	2.59E+06	2.21E+03	2.21E+03	4.27E+00	4.27E+00	1.75E-01	1.75E-01	1.31E-01	1.31E-01	1.29E-01	1.29E-01
350	7.84E+04	7.84E+04	7.78E+01	7.78E+01	1.87E-01	1.87E-01	8.86E-03	8.86E-03	6.92E-03	6.92E-03	6.84E-03	6.84E-03
400	2.37E+03	2.37E+03	2.69E+00	2.69E+00	7.91E-03	7.91E-03	4.23E-04	4.23E-04	3.40E-04	3.40E-04	3.36E-04	3.36E-04
450	7.16E+01	7.16E+01	9.13E-02	9.13E-02	3.24E-04	3.24E-04	1.92E-05	1.92E-05	1.59E-05	1.59E-05	1.57E-05	1.57E-05
500	2.16E+00	2.16E+00	3.06E-03	3.06E-03	1.30E-05	1.30E-05	8.45E-07	8.45E-07	7.11E-07	7.11E-07	7.03E-07	7.03E-07
550	6.54E-02	6.54E-02	1.02E-04	1.02E-04	5.10E-07	5.10E-07	3.61E-08	3.61E-08	3.08E-08	3.08E-08	3.05E-08	3.05E-08
600	1.98E-03	1.98E-03	3.36E-06	3.36E-06	1.98E-08	1.98E-08	1.50E-09	1.50E-09	1.30E-09	1.30E-09	1.29E-09	1.29E-09
650	5.97E-05	5.97E-05	1.10E-07	1.10E-07	7.56E-10	7.56E-10	6.14E-11	6.14E-11	5.37E-11	5.37E-11	5.32E-11	5.32E-11
700	1.80E-06	1.80E-06	3.58E-09	3.58E-09	2.87E-11	2.87E-11	2.46E-12	2.46E-12	2.18E-12	2.18E-12	2.16E-12	2.16E-12
750	5.45E-08	5.45E-08	1.16E-10	1.16E-10	1.08E-12	1.08E-12	9.76E-14	9.76E-14	8.71E-14	8.71E-14	8.62E-14	8.62E-14
800	1.65E-09	1.65E-09	3.73E-12	3.73E-12	4.01E-14	4.01E-14	3.82E-15	3.82E-15	3.43E-15	3.43E-15	3.40E-15	3.40E-15
850	4.98E-11	4.98E-11	1.20E-13	1.20E-13	1.49E-15	1.49E-15	1.48E-16	1.48E-16	1.34E-16	1.34E-16	1.32E-16	1.32E-16
900	1.50E-12	1.50E-12	3.83E-15	3.83E-15	5.49E-17	5.49E-17	5.68E-18	5.68E-18	5.16E-18	5.16E-18	5.11E-18	5.11E-18
950	4.55E-14	4.55E-14	1.22E-16	1.22E-16	2.01E-18	2.01E-18	2.16E-19	2.16E-19	1.97E-19	1.97E-19	1.95E-19	1.95E-19
1000	1.37E-15	1.37E-15	3.89E-18	3.89E-18	7.37E-20	7.37E-20	8.18E-21	8.18E-21	7.49E-21	7.49E-21	7.42E-21	7.42E-21

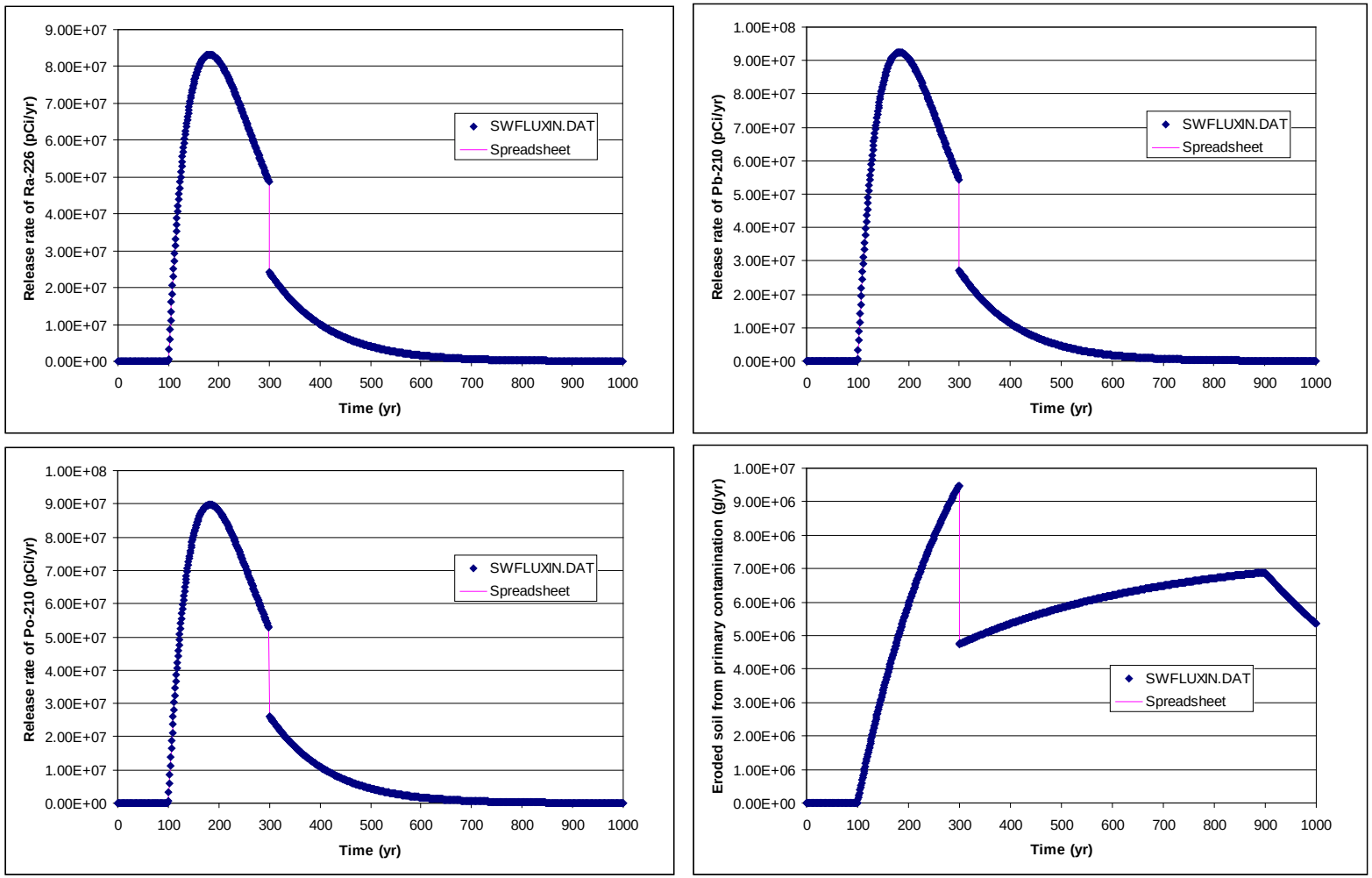

Figure 2-2 Comparison of the RESRAD-OFFSITE Results and the Spreadsheet Results for Release Rates of Nuclide through Surface Runoff for Case VIII Concerning Ra-226 and Its Progenies

Table 2-15 Comparison of the RESRAD-OFFSITE Results and the Spreadsheet Results for the Release Rates of Nuclide through Surface Runoff for Case VIII Concerning Ra-226 and Its Progenies, with Notable Disagreements Highlighted

	Ra-226		Pb-210		Po-210	
Time (yr)	RESRAD-OFFSITE	Spread-sheet	RESRAD-OFFSITE	Spread-sheet	RESRAD-OFFSITE	Spread-sheet
99	0	0	0	0	0	0
100	0	1.57E+02	0	1.65E+02	0	1.60E+02
101	2.74E+06	2.74E+06	2.88E+06	2.88E+06	2.80E+06	2.80E+06
102	5.42E+06	5.42E+06	5.71E+06	5.71E+06	5.53E+06	5.53E+06
103	8.03E+06	8.03E+06	8.47E+06	8.47E+06	8.21E+06	8.21E+06
104	1.06E+07	1.06E+07	1.12E+07	1.12E+07	1.08E+07	1.08E+07
105	1.31E+07	1.31E+07	1.38E+07	1.38E+07	1.34E+07	1.34E+07
125	5.10E+07	5.10E+07	5.52E+07	5.52E+07	5.35E+07	5.35E+07
150	7.48E+07	7.48E+07	8.24E+07	8.24E+07	7.99E+07	7.99E+07
175	8.25E+07	8.25E+07	9.16E+07	9.16E+07	8.89E+07	8.89E+07
200	8.10E+07	8.10E+07	9.02E+07	9.02E+07	8.76E+07	8.76E+07
225	7.47E+07	7.47E+07	8.33E+07	8.33E+07	8.09E+07	8.09E+07
250	6.61E+07	6.61E+07	7.39E+07	7.39E+07	7.17E+07	7.17E+07
275	5.70E+07	5.70E+07	6.37E+07	6.37E+07	6.19E+07	6.19E+07
300	2.41E+07	2.41E+07	2.70E+07	2.70E+07	2.62E+07	2.62E+07
325	1.95E+07	1.95E+07	2.18E+07	2.18E+07	2.11E+07	2.11E+07
350	1.57E+07	1.57E+07	1.75E+07	1.75E+07	1.70E+07	1.70E+07
375	1.26E+07	1.26E+07	1.41E+07	1.41E+07	1.37E+07	1.37E+07
400	1.01E+07	1.01E+07	1.13E+07	1.13E+07	1.09E+07	1.09E+07
425	8.06E+06	8.06E+06	9.01E+06	9.01E+06	8.75E+06	8.75E+06
450	6.43E+06	6.43E+06	7.19E+06	7.19E+06	6.98E+06	6.98E+06
475	5.12E+06	5.12E+06	5.72E+06	5.72E+06	5.55E+06	5.55E+06
500	4.07E+06	4.07E+06	4.55E+06	4.55E+06	4.42E+06	4.42E+06
525	3.23E+06	3.23E+06	3.61E+06	3.61E+06	3.51E+06	3.51E+06
550	2.56E+06	2.56E+06	2.86E+06	2.86E+06	2.78E+06	2.78E+06
575	2.03E+06	2.03E+06	2.27E+06	2.27E+06	2.20E+06	2.20E+06
600	1.60E+06	1.60E+06	1.79E+06	1.79E+06	1.74E+06	1.74E+06
625	1.27E+06	1.27E+06	1.42E+06	1.42E+06	1.37E+06	1.37E+06
650	1.00E+06	1.00E+06	1.12E+06	1.12E+06	1.09E+06	1.09E+06
675	7.89E+05	7.89E+05	8.82E+05	8.82E+05	8.56E+05	8.56E+05
700	6.22E+05	6.22E+05	6.95E+05	6.95E+05	6.75E+05	6.75E+05
725	4.90E+05	4.90E+05	5.48E+05	5.48E+05	5.31E+05	5.31E+05
750	3.86E+05	3.86E+05	4.31E+05	4.31E+05	4.18E+05	4.18E+05
775	3.03E+05	3.03E+05	3.39E+05	3.39E+05	3.29E+05	3.29E+05
800	2.38E+05	2.38E+05	2.67E+05	2.67E+05	2.59E+05	2.59E+05
825	1.87E+05	1.87E+05	2.09E+05	2.09E+05	2.03E+05	2.03E+05
850	1.47E+05	1.47E+05	1.64E+05	1.64E+05	1.60E+05	1.60E+05
875	1.16E+05	1.16E+05	1.29E+05	1.29E+05	1.25E+05	1.25E+05
900	9.06E+04	9.06E+04	1.01E+05	1.01E+05	9.83E+04	9.83E+04
925	6.64E+04	6.64E+04	7.43E+04	7.43E+04	7.21E+04	7.21E+04
950	4.87E+04	4.87E+04	5.44E+04	5.44E+04	5.28E+04	5.28E+04
975	3.57E+04	3.57E+04	3.99E+04	3.99E+04	3.87E+04	3.87E+04
1000	2.62E+04	2.62E+04	2.92E+04	2.92E+04	2.84E+04	2.84E+04

$$R_k^{gw} = L_k \; A_k(t) \, \rho_{pc} \; A\left(f_{vm} \; T_{mix}^{c}(t) + T_{pc}^{um}(t)\right) \times 10^6 \qquad \text{(Eq. 2.17)}$$

The output file, AQFLUXIN.DAT, contains the calculation results.

Comparison of the RESRAD-OFFSITE results and spreadsheet results are displayed in Figure 2-3 showing the temporal profiles for Case I concerning U-238 and its progeny nuclides and in Tables 2-16 to 2-19 showing numerical values for Case I, Case III (concerning H-3), Case IV (concerning C-14), and Case VII (concerning Sr-90), respectively. Overall, the agreement between the RESRAD-OFFSITE results and the spreadsheet results is very good. Differences are found when the release rates are very small and/or when they involve a distant progeny nuclide along the decay chain. The differences are caused by the different precisions used in RESRAD-OFFSITE and spreadsheets. For other cases, the release rates of nuclides to groundwater calculated by RESRAD-OFFSITE and the spreadsheets are the same.

2.4 RELEASE TO AIR

The release rates of nuclides to the atmosphere in the form of dust are calculated by RESRAD-OFFSITE using nuclide concentrations in the mixing zone and the dust loading factor, as presented by Eq. 2.33 in the RESRAD-OFFSITE User's Manual (Yu et al. 2007):

$$R_k^{du}(t) = f_{vm}(t) \; \frac{\rho_{pc}}{\rho_{mix}(t)} \; A_k(t) \; m_{du} \; A \; v_{du} \times 3.15576 \times 10^7 \qquad \text{(Eq. 2.18)}$$

where:

$R_k^{du}(t) =$ release rate of nuclide k in the form of dust to the air at time t (pCi/y),

m_{du} = mass loading factor of dust particles (1×10^{-4} g/m^3),

v_{du} = deposition velocity of dust (0.001 m/s), and

3.15576×10^7 = conversion factor (s/yr).

The calculated release rates for each time point are saved in the output file AIFLUXIN.DAT.

For Cases III (concerning H-3) and IV (concerning C-14), the releases in the form of dust to the air are zero, because the initial cover thickness is greater than the mixing depth, and by the time the cover thickness reduces to less than the mixing depth, the concentrations of H-3 and C-14 in the primary contamination become zero due to loss through gas diffusion and leaching. For Cases II (concerning Cs-137), Case V (concerning Co-60), Case VI (concerning Ni-63), and Case VII (concerning Sr-90), the release rates calculated by RESRAD-OFFSITE match those calculated by the spreadsheets.

Discrepancies between the RESRAD-OFFSITE results and the spreadsheet results are observed for Case I (concerning U-238) and Case VIII (concerning Ra-226). These discrepancies occur at the same times as those observed in the release rates through runoff (Section 2.2). The coincidence is understandable because both release rates are calculated using the same information, the concentrations of nuclides in the mixing layer. Therefore, the explanations for the discrepancies in the release rates to the air are the same as those for the discrepancies in the release rates through runoff. Table 2-20 shows the comparison between RESRAD-OFFSITE results and the spreadsheet results for Case I, and Table 2-21 shows the comparison for Case VIII.

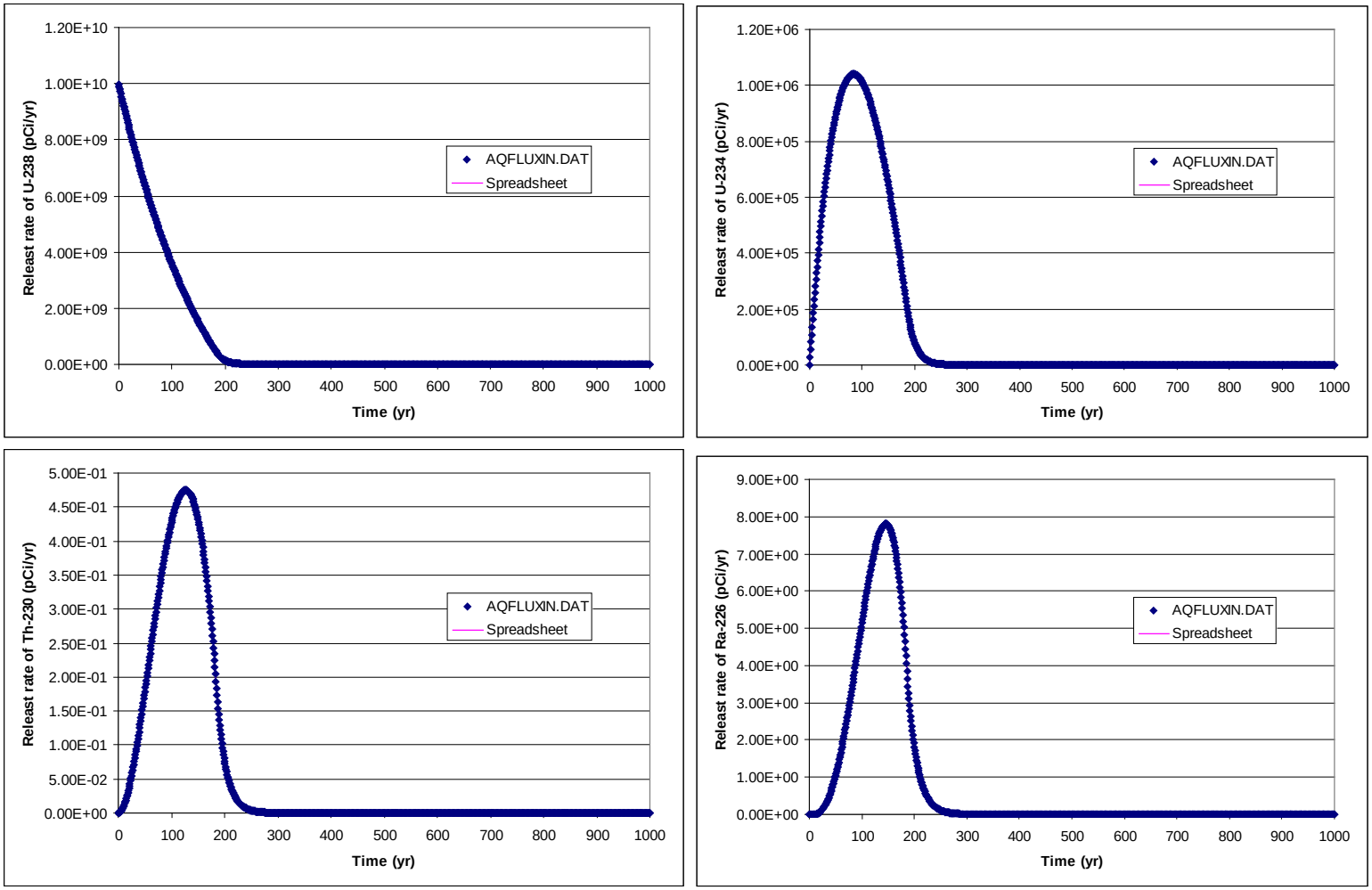

Figure 2-3 Comparison of the RESRAD-OFFSITE Results and the Spreadsheet Results for the Release Rates of Nuclide to Groundwater for Case I Concerning U-238 and Its Progenies

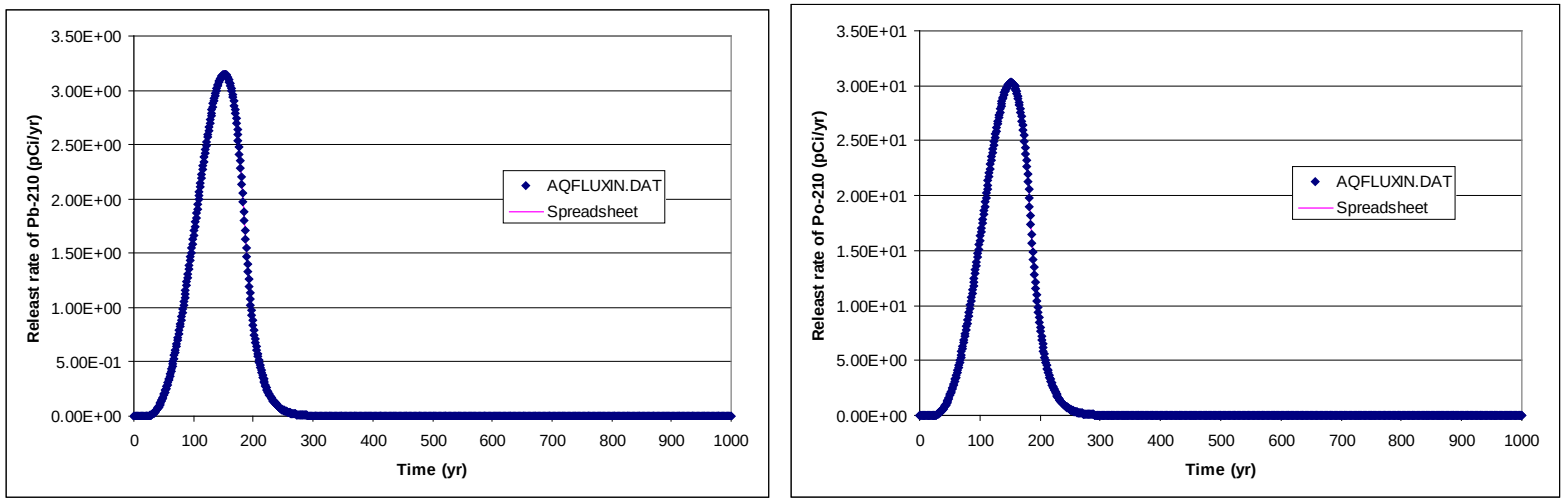

Figure 2-3 (Cont.)

Table 2-16 Comparison of the RESRAD-OFFSITE Results and the Spreadsheet Results for the Release Rates of Nuclide to Groundwater for Case I Concerning U-238 and Its Progenies, with Notable Disagreement Highlighted

	U-238		U-234		Th-230		Ra-226		Pb-210		Po-210	
Time (yr)	RESRAD-OFFSITE	Spread-sheet	RESRAD-OFFSITE	Spread-sheet	RESRAD-OFFSITE	Spread-sheet	RESRAD-OFFSITE	Spread-sheet	RESRAD-OFFSITE	Spread-sheet	RESRAD-OFFSITE	Spread-sheet
0	9.96E+09	9.96E+09	0.00E+00	0.00E+00	0.00E+00	0.00E+00	0.00E+00	0.00E+00	0.00E+00	0.00E+00	0.00E+00	0.00E+00
1	9.87E+09	9.87E+09	2.80E+04	2.80E+04	1.06E-04	1.06E-04	1.30E-05	1.30E-05	6.94E-08	6.94E-08	1.95E-07	1.81E-07
2	9.79E+09	9.79E+09	5.55E+04	5.55E+04	4.19E-04	4.19E-04	1.03E-04	1.03E-04	1.11E-06	1.11E-06	4.84E-06	4.85E-06
3	9.71E+09	9.71E+09	8.26E+04	8.26E+04	9.36E-04	9.36E-04	3.46E-04	3.46E-04	5.56E-06	5.56E-06	3.00E-05	3.00E-05
4	9.63E+09	9.63E+09	1.09E+05	1.09E+05	1.65E-03	1.65E-03	8.15E-04	8.15E-04	1.73E-05	1.73E-05	1.06E-04	1.06E-04
5	9.55E+09	9.55E+09	1.35E+05	1.35E+05	2.56E-03	2.56E-03	1.58E-03	1.58E-03	4.17E-05	4.17E-05	2.77E-04	2.77E-04
25	8.02E+09	8.02E+09	5.68E+05	5.68E+05	5.50E-02	5.50E-02	1.69E-01	1.69E-01	1.99E-02	1.99E-02	1.79E-01	1.79E-01
50	6.33E+09	6.33E+09	8.97E+05	8.97E+05	1.79E-01	1.79E-01	1.09E+00	1.09E+00	2.26E-01	2.26E-01	2.11E+00	2.11E+00
75	4.85E+09	4.85E+09	1.03E+06	1.03E+06	3.17E-01	3.17E-01	2.90E+00	2.90E+00	7.98E-01	7.98E-01	7.57E+00	7.57E+00
100	3.57E+09	3.57E+09	1.01E+06	1.01E+06	4.27E-01	4.27E-01	5.19E+00	5.19E+00	1.71E+00	1.71E+00	1.63E+01	1.63E+01
150	1.51E+09	1.51E+09	6.43E+05	6.43E+05	4.32E-01	4.32E-01	7.80E+00	7.80E+00	3.17E+00	3.17E+00	3.05E+01	3.05E+01
200	1.41E+08	1.41E+08	8.02E+04	8.02E+04	7.63E-02	7.63E-02	1.82E+00	1.82E+00	8.36E-01	8.36E-01	8.07E+00	8.07E+00
250	4.27E+06	4.27E+06	3.03E+03	3.03E+03	3.83E-03	3.83E-03	1.13E-01	1.13E-01	5.63E-02	5.63E-02	5.44E-01	5.44E-01
300	1.29E+05	1.29E+05	1.10E+02	1.10E+02	1.78E-04	1.78E-04	6.23E-03	6.23E-03	3.27E-03	3.27E-03	3.17E-02	3.17E-02
350	3.90E+03	3.90E+03	3.87E+00	3.87E+00	7.81E-06	7.81E-06	3.16E-04	3.16E-04	1.73E-04	1.73E-04	1.67E-03	1.67E-03
400	1.18E+02	1.18E+02	1.34E-01	1.34E-01	3.30E-07	3.30E-07	1.50E-05	1.50E-05	8.49E-06	8.49E-06	8.23E-05	8.23E-05
450	3.56E+00	3.56E+00	4.54E-03	4.54E-03	1.35E-08	1.35E-08	6.85E-07	6.85E-07	3.96E-07	3.96E-07	3.84E-06	3.84E-06
500	1.08E-01	1.08E-01	1.53E-04	1.53E-04	5.41E-10	5.41E-10	3.01E-08	3.01E-08	1.77E-08	1.77E-08	1.72E-07	1.72E-07
550	3.26E-03	3.25E-03	5.07E-06	5.07E-06	2.13E-11	2.13E-11	1.28E-09	1.28E-09	7.69E-10	7.69E-10	7.46E-09	7.46E-09
600	9.84E-05	9.84E-05	1.67E-07	1.67E-07	8.24E-13	8.24E-13	5.35E-11	5.35E-11	3.25E-11	3.25E-11	3.15E-10	3.15E-10
650	2.97E-06	2.97E-06	5.47E-09	5.47E-09	3.15E-14	3.15E-14	2.18E-12	2.18E-12	1.34E-12	1.34E-12	1.30E-11	1.30E-11
700	8.98E-08	8.98E-08	1.78E-10	1.78E-10	1.19E-15	1.19E-15	8.78E-14	8.78E-14	5.44E-14	5.44E-14	5.28E-13	5.28E-13
750	2.71E-09	2.71E-09	5.77E-12	5.77E-12	4.48E-17	4.48E-17	3.48E-15	3.48E-15	2.17E-15	2.17E-15	2.11E-14	2.11E-14
800	8.20E-11	8.20E-11	1.86E-13	1.86E-13	1.67E-18	1.67E-18	1.36E-16	1.36E-16	8.56E-17	8.56E-17	8.32E-16	8.32E-16
850	2.48E-12	2.48E-12	5.97E-15	5.97E-15	6.20E-20	6.20E-20	5.27E-18	5.27E-18	3.34E-18	3.34E-18	3.24E-17	3.24E-17
900	7.49E-14	7.49E-14	1.91E-16	1.91E-16	2.29E-21	2.29E-21	2.02E-19	2.02E-19	1.29E-19	1.29E-19	1.25E-18	1.25E-18
950	2.26E-15	2.26E-15	8.81E+05	8.81E+05	8.39E-23	8.40E-23	7.70E-21	7.70E-21	4.92E-21	4.92E-21	4.78E-20	4.78E-20
1000	6.84E-17	6.84E-17	8.74E+05	8.74E+05	3.07E-24	3.07E-24	2.91E-22	2.91E-22	1.87E-22	1.87E-22	1.82E-21	1.82E-21

Table 2-17 Comparison of the RESRAD-OFFSITE Results and the Spreadsheet Results for the Release Rates of Nuclide to Groundwater for Case III Concerning H-3, with Notable Disagreements Highlighted

	Modification Factor	
Time (yr)	RESRAD-OFFSITE	Spreadsheet
0	2.34E+12	2.34E+12
1	4.63E+11	4.63E+11
2	9.07E+10	9.07E+10
3	1.76E+10	1.76E+10
4	3.38E+09	3.38E+09
5	6.42E+08	6.42E+08
6	1.21E+08	1.21E+08
7	2.24E+07	2.24E+07
8	4.13E+06	4.13E+06
9	7.53E+05	7.53E+05
10	1.36E+05	1.36E+05
11	2.42E+04	2.42E+04
12	4.28E+03	4.28E+03
14	1.30E+02	1.30E+02
16	3.76E+00	3.76E+00
18	1.05E-01	1.05E-01
20	2.79E-03	2.79E-03
22	7.16E-05	7.16E-05
24	1.76E-06	1.76E-06
26	4.15E-08	4.15E-08
28	9.37E-10	9.37E-10
30	2.03E-11	2.03E-11
32	4.23E-13	4.23E-13
34	8.45E-15	8.45E-15
36	1.62E-16	1.62E-16
38	2.97E-18	2.97E-18
40	5.24E-20	5.24E-20
42	8.86E-22	8.86E-22
44	1.44E-23	1.44E-23
46	2.24E-25	2.24E-25
48	3.34E-27	3.34E-27
50	4.78E-29	4.78E-29
52	6.56E-31	6.56E-31
54	0.00E+00	8.65E-33
56	0.00E+00	1.09E-34
58	0.00E+00	1.33E-36
60	0.00E+00	1.54E-38

Table 2-18 Comparison of the RESRAD-OFFSITE Results and the Spreadsheet Results for the Release Rates of Nuclide to Groundwater for Case IV Concerning C-14, with Notable Disagreements Highlighted

	Modification Factor	
Time (yr)	RESRAD-OFFSITE	Spreadsheet
0	2.34E+12	2.34E+12
1	3.29E+11	3.29E+11
2	4.62E+10	4.62E+10
3	6.45E+09	6.45E+09
4	8.98E+08	8.98E+08
5	1.24E+08	1.24E+08
6	1.72E+07	1.72E+07
7	2.36E+06	2.36E+06
8	3.23E+05	3.23E+05
9	4.41E+04	4.41E+04
10	5.99E+03	5.99E+03
11	8.11E+02	8.11E+02
12	1.09E+02	1.09E+02
14	1.96E+00	1.96E+00
16	3.46E-02	3.47E-02
18	6.02E-04	6.02E-04
20	1.03E-05	1.03E-05
22	1.73E-07	1.73E-07
24	2.87E-09	2.87E-09
26	4.68E-11	4.69E-11
28	7.51E-13	7.52E-13
30	1.19E-14	1.19E-14
32	1.84E-16	1.85E-16
34	2.82E-18	2.82E-18
36	4.24E-20	4.25E-20
38	6.29E-22	6.29E-22
40	9.16E-24	9.17E-24
42	1.31E-25	1.32E-25
44	1.86E-27	1.86E-27
46	2.58E-29	2.58E-29
48	3.52E-31	3.53E-31
50	4.75E-33	4.75E-33
52	6.55E-35	6.29E-35
54	0.00E+00	8.20E-37
56	0.00E+00	1.05E-38
58	0.00E+00	1.33E-40
60	0.00E+00	1.65E-42

Table 2-19 Comparison of the RESRAD-OFFSITE Results and the Spreadsheet Results for the Release Rates of Nuclide to Groundwater for Case VII Concerning Sr-90

	Modification Factor	
Time (yr)	RESRAD-OFFSITE	Spreadsheet
0.0	1.66E+10	1.66E+10
0.5	1.63E+10	1.63E+10
1.0	1.60E+10	1.60E+10
1.5	1.58E+10	1.58E+10
2.0	1.55E+10	1.55E+10
2.5	1.53E+10	1.53E+10
3.0	1.50E+10	1.50E+10
3.5	1.48E+10	1.48E+10
4.0	1.45E+10	1.45E+10
4.5	1.43E+10	1.43E+10
5.0	1.40E+10	1.40E+10
.	.	.
.	.	.
.	.	.
150.0	1.17E+08	1.17E+08
150.5	1.15E+08	1.15E+08
151.0	1.13E+08	1.13E+08
151.5	1.12E+08	1.12E+08
152.0	1.10E+08	1.10E+08
152.5	1.08E+08	1.08E+08
153.0	1.06E+08	1.06E+08
153.5	1.04E+08	1.04E+08
154.0	1.03E+08	1.03E+08
154.5	1.01E+08	1.01E+08
.	.	.
.	.	.
.	.	.
300.0	8.29E+05	8.29E+05
300.5	8.16E+05	8.16E+05
301.0	8.02E+05	8.02E+05
301.5	7.89E+05	7.89E+05
302.0	7.76E+05	7.76E+05
302.5	7.64E+05	7.64E+05
303.0	7.51E+05	7.51E+05
303.5	7.39E+05	7.39E+05
304.0	7.27E+05	7.27E+05
304.5	7.15E+05	7.15E+05

Table 2-20 Comparison of the RESRAD-OFFSITE Results and Spreadsheet Results for the Release Rates of Nuclide in the Form of Dust to the Air for Case I Concerning U-238 and Its Progenies, with Notable Disagreement Highlighted

	U-238		U-234		Th-230		Ra-226		Pb-210		Po-210	
Time (yr)	RESRAD-OFFSITE	Spread-sheet	RESRAD-OFFSITE	Spread-sheet	RESRAD-OFFSITE	Spread-sheet	RESRAD-OFFSITE	Spread-sheet	RESRAD-OFFSITE	Spread-sheet	RESRAD-OFFSITE	Spread-sheet
0	3.16E+06	3.16E+06	0	0	0	0	0	0	0	0	0	0
1	3.15E+06	3.15E+06	8.92E+00	8.92E+00	4.02E-05	4.02E-05	5.80E-09	5.80E-09	4.41E-11	4.41E-11	1.27E-11	1.17E-11
2	3.13E+06	3.13E+06	1.78E+01	1.78E+01	1.60E-04	1.60E-04	4.63E-08	4.63E-08	7.11E-10	7.11E-10	3.16E-10	3.15E-10
3	3.12E+06	3.12E+06	2.66E+01	2.66E+01	3.60E-04	3.60E-04	1.56E-07	1.56E-07	3.57E-09	3.57E-09	1.96E-09	1.96E-09
4	3.11E+06	3.11E+06	3.53E+01	3.53E+01	6.39E-04	6.39E-04	3.69E-07	3.69E-07	1.12E-08	1.12E-08	6.97E-09	6.97E-09
5	3.10E+06	3.10E+06	4.40E+01	4.40E+01	9.96E-04	9.96E-04	7.18E-07	7.18E-07	2.71E-08	2.71E-08	1.83E-08	1.83E-08
25	2.90E+06	2.90E+06	2.06E+02	2.06E+02	2.38E-02	2.38E-02	8.56E-05	8.56E-05	1.44E-05	1.44E-05	1.32E-05	1.32E-05
50	2.67E+06	2.67E+06	3.79E+02	3.79E+02	9.02E-02	9.02E-02	6.46E-04	6.46E-04	1.91E-04	1.91E-04	1.82E-04	1.82E-04
75	2.46E+06	2.46E+06	5.23E+02	5.23E+02	1.92E-01	1.92E-01	2.06E-03	2.06E-03	8.07E-04	8.07E-04	7.80E-04	7.80E-04
100	2.26E+06	2.26E+06	6.42E+02	6.42E+02	3.24E-01	3.24E-01	4.60E-03	4.60E-03	2.16E-03	2.16E-03	2.10E-03	2.10E-03
125	2.08E+06	2.08E+06	7.38E+02	7.38E+02	4.79E-01	4.79E-01	8.48E-03	8.48E-03	4.50E-03	4.50E-03	4.40E-03	4.40E-03
150	1.92E+06	1.92E+06	8.15E+02	8.15E+02	6.54E-01	6.54E-01	1.38E-02	1.38E-02	8.02E-03	8.02E-03	7.86E-03	7.86E-03
175	1.77E+06	1.77E+06	8.76E+02	8.76E+02	8.45E-01	8.45E-01	2.07E-02	2.07E-02	1.29E-02	1.29E-02	1.26E-02	1.26E-02
200	5.98E+05	5.98E+05	3.39E+02	3.39E+02	3.85E-01	3.85E-01	1.07E-02	1.07E-02	7.05E-03	7.05E-03	6.93E-03	6.93E-03
225	1.04E+05	1.04E+05	6.63E+01	6.63E+01	8.74E-02	8.74E-02	2.73E-03	2.73E-03	1.87E-03	1.87E-03	1.84E-03	1.84E-03
250	1.81E+04	1.81E+04	1.28E+01	1.28E+01	1.93E-02	1.93E-02	6.68E-04	6.68E-04	4.74E-04	4.74E-04	4.67E-04	4.67E-04
275	3.14E+03	3.14E+03	2.45E+00	2.45E+00	4.20E-03	4.20E-03	1.59E-04	1.59E-04	1.16E-04	1.16E-04	1.15E-04	1.15E-04
300	5.46E+02	5.46E+02	4.64E-01	4.64E-01	8.97E-04	8.97E-04	3.68E-05	3.68E-05	2.76E-05	2.76E-05	2.72E-05	2.72E-05
325	9.49E+01	9.49E+01	8.74E-02	8.74E-02	1.89E-04	1.89E-04	8.36E-06	8.36E-06	6.41E-06	6.41E-06	6.32E-06	6.32E-06
350	1.65E+01	1.65E+01	1.64E-02	1.64E-02	3.94E-05	3.94E-05	1.86E-06	1.86E-06	1.46E-06	1.46E-06	1.44E-06	1.44E-06
400	4.98E-01	4.98E-01	5.65E-04	5.65E-04	1.66E-06	1.66E-06	8.89E-08	8.89E-08	7.16E-08	7.16E-08	7.08E-08	7.08E-08
450	1.51E-02	1.51E-02	1.92E-05	1.92E-05	6.82E-08	6.82E-08	4.05E-09	4.05E-09	1.56E-08	1.56E-08	3.30E-09	3.30E-09
500	4.55E-04	4.55E-04	6.45E-07	6.45E-07	2.73E-09	2.73E-09	1.78E-10	1.78E-10	3.34E-09	3.34E-09	1.48E-10	1.48E-10
550	1.38E-05	1.38E-05	2.14E-08	2.14E-08	1.07E-10	1.07E-10	7.58E-12	7.58E-12	1.50E-10	1.50E-10	6.41E-12	6.41E-12
600	4.16E-07	4.16E-07	7.06E-10	7.06E-10	4.16E-12	4.16E-12	3.16E-13	3.16E-13	6.48E-12	6.48E-12	2.71E-13	2.71E-13
650	1.26E-08	1.26E-08	2.31E-11	2.31E-11	1.59E-13	1.59E-13	1.29E-14	1.29E-14	2.74E-13	2.74E-13	1.12E-14	1.12E-14
700	3.80E-10	3.80E-10	7.52E-13	7.52E-13	6.03E-15	6.03E-15	5.19E-16	5.19E-16	1.13E-14	1.13E-14	4.54E-16	4.54E-16
750	1.15E-11	1.15E-11	2.44E-14	2.44E-14	2.26E-16	2.26E-16	2.05E-17	2.05E-17	4.59E-16	4.59E-16	1.81E-17	1.81E-17
800	3.47E-13	3.47E-13	7.85E-16	7.85E-16	8.45E-18	8.45E-18	8.04E-19	8.04E-19	1.83E-17	1.83E-17	7.15E-19	7.15E-19
850	1.05E-14	1.05E-14	2.52E-17	2.52E-17	3.13E-19	3.13E-19	3.11E-20	3.11E-20	7.22E-19	7.22E-19	2.79E-20	2.79E-20
900	3.17E-16	3.17E-16	8.07E-19	8.07E-19	1.15E-20	1.15E-20	1.20E-21	1.20E-21	2.81E-20	2.81E-20	1.07E-21	1.07E-21
950	9.57E-18	9.56E-18	2.57E-20	2.57E-20	4.24E-22	4.24E-22	4.55E-23	4.55E-23	1.09E-21	1.09E-21	4.11E-23	4.11E-23

Table 2-21 Comparison of the RESRAD-OFFSITE Results and the Spreadsheet Results for the Release Rates of Nuclide in the Form of Dust to the Air for Case VIII Concerning Ra-226 and Its Progenies, with Notable Disagreements Highlighted

	Ra-226		Pb-210		Po-210	
Time (yr)	RESRAD-OFFSITE	Spread-sheet	RESRAD-OFFSITE	Spread-sheet	RESRAD-OFFSITE	Spread-sheet
99	0	0	0	0	0	0
100	0	2.91E-01	0	3.05E-01	0	2.96E-01
101	5.10E+03	5.10E+03	5.36E+03	5.36E+03	5.19E+03	5.19E+03
102	1.01E+04	1.01E+04	1.06E+04	1.06E+04	1.03E+04	1.03E+04
103	1.49E+04	1.49E+04	1.57E+04	1.57E+04	1.53E+04	1.53E+04
104	1.97E+04	1.97E+04	2.08E+04	2.08E+04	2.02E+04	2.02E+04
105	2.43E+04	2.43E+04	2.57E+04	2.57E+04	2.49E+04	2.49E+04
125	9.59E+04	9.59E+04	1.04E+05	1.04E+05	1.01E+05	1.01E+05
150	1.43E+05	1.43E+05	1.57E+05	1.57E+05	1.52E+05	1.52E+05
175	1.59E+05	1.59E+05	1.76E+05	1.76E+05	1.71E+05	1.71E+05
200	1.58E+05	1.58E+05	1.76E+05	1.76E+05	1.70E+05	1.70E+05
225	1.47E+05	1.47E+05	1.64E+05	1.64E+05	1.59E+05	1.59E+05
250	1.31E+05	1.31E+05	1.46E+05	1.46E+05	1.42E+05	1.42E+05
275	1.14E+05	1.14E+05	1.27E+05	1.27E+05	1.23E+05	1.23E+05
300	9.67E+04	9.67E+04	1.08E+05	1.08E+05	1.05E+05	1.05E+05
325	7.84E+04	7.84E+04	8.76E+04	8.76E+04	8.50E+04	8.50E+04
350	6.33E+04	6.33E+04	7.07E+04	7.07E+04	6.86E+04	6.86E+04
375	5.09E+04	5.09E+04	5.69E+04	5.69E+04	5.52E+04	5.52E+04
400	4.09E+04	4.09E+04	4.57E+04	4.57E+04	4.44E+04	4.44E+04
425	3.27E+04	3.27E+04	3.66E+04	3.66E+04	3.55E+04	3.55E+04
450	2.62E+04	2.62E+04	2.93E+04	2.93E+04	2.84E+04	2.84E+04
475	2.09E+04	2.09E+04	2.33E+04	2.33E+04	2.27E+04	2.27E+04
500	1.66E+04	1.66E+04	1.86E+04	1.86E+04	1.80E+04	1.80E+04
525	1.32E+04	1.32E+04	1.48E+04	1.48E+04	1.43E+04	1.43E+04
550	1.05E+04	1.05E+04	1.17E+04	1.17E+04	1.14E+04	1.14E+04
575	8.33E+03	8.33E+03	9.31E+03	9.31E+03	9.03E+03	9.03E+03
600	6.60E+03	6.60E+03	7.37E+03	7.37E+03	7.16E+03	7.16E+03
625	5.22E+03	5.22E+03	5.83E+03	5.83E+03	5.66E+03	5.66E+03
650	4.12E+03	4.12E+03	4.61E+03	4.61E+03	4.48E+03	4.48E+03
675	3.26E+03	3.26E+03	3.64E+03	3.64E+03	3.53E+03	3.53E+03
700	2.57E+03	2.57E+03	2.87E+03	2.87E+03	2.79E+03	2.79E+03
725	2.03E+03	2.03E+03	2.27E+03	2.27E+03	2.20E+03	2.20E+03
750	1.60E+03	1.60E+03	1.78E+03	1.78E+03	1.73E+03	1.73E+03
775	1.26E+03	1.26E+03	1.41E+03	1.41E+03	1.36E+03	1.36E+03
800	9.89E+02	9.89E+02	1.11E+03	1.11E+03	1.07E+03	1.07E+03
825	7.78E+02	7.78E+02	8.70E+02	8.70E+02	8.44E+02	8.44E+02
850	6.12E+02	6.12E+02	6.84E+02	6.84E+02	6.64E+02	6.64E+02
875	4.80E+02	4.80E+02	5.37E+02	5.37E+02	5.21E+02	5.21E+02
900	3.77E+02	3.77E+02	4.22E+02	4.22E+02	4.09E+02	4.09E+02
925	2.77E+02	2.77E+02	3.09E+02	3.09E+02	3.00E+02	3.00E+02
950	2.03E+02	2.03E+02	2.27E+02	2.27E+02	2.20E+02	2.20E+02
975	1.49E+02	1.49E+02	1.66E+02	1.66E+02	1.61E+02	1.61E+02
1000	1.09E+02	1.09E+02	1.22E+02	1.22E+02	1.18E+02	1.18E+02

3.0 GROUNDWATER TRANSPORT MODEL

Groundwater transport has three components: flux-to-flux transport in the unsaturated zone, pulse-to-flux transport in the saturated zone to the surface water body, and pulse-to-concentration transport in the saturated zone to the well.

3.1 Verification of Transport in the Unsaturated Zone

The equation for transport in the unsaturated zone that needs to be verified is the dispersive-advective transport Eq. 3.59 of the RESRAD-OFFSITE User's Manual (Yu et al. 2007). This equation is reproduced below as Eq. 3.1.

$$\begin{aligned} f_{t_2}^{t_1}(z,t_n) = \; & \frac{1}{2}\left(a + \frac{bz}{\sqrt{V_c^2 + 4D_z^c\lambda}}\right)\exp\left(\frac{z\left(V_c - \sqrt{V_c^2 + 4D_z^c\lambda}\right)}{2D_z^c}\right)\left[erf\left(\frac{z - \sqrt{V_c^2 + 4D_z^c\lambda}(t_n - t_2)}{\sqrt{4D_z^c(t_n - t_2)}}\right) - erf\left(\frac{z - \sqrt{V_c^2 + 4D_z^c\lambda}(t_n - t_1)}{\sqrt{4D_z^c(t_n - t_1)}}\right)\right] \\ & + \frac{1}{2}\left(a - \frac{bz}{\sqrt{V_c^2 + 4D_z^c\lambda}}\right)\exp\left(\frac{z\left(V_c + \sqrt{V_c^2 + 4D_z^c\lambda}\right)}{2D_z^c}\right)\left[erf\left(\frac{z + \sqrt{V_c^2 + 4D_z^c\lambda}(t_n - t_2)}{\sqrt{4D_z^c(t_n - t_2)}}\right) - erf\left(\frac{z + \sqrt{V_c^2 + 4D_z^c\lambda}(t_n - t_1)}{\sqrt{4D_z^c(t_n - t_1)}}\right)\right] \end{aligned}$$

(Eq. 3.1)

This is the output flux at a distance z at time $t_n > t_2 > t_1$, due to the input flux entering between times t_1 and t_2, and was obtained by the convolution

$$f(z,t_n) = \int_{t_n - t_2}^{t_n - t_1} f(0, t_n - \tau)\frac{z}{\tau}\sqrt{\frac{1}{4\pi D_z^c \tau}}\exp\left(-\frac{(z - V_c\tau)^2}{4D_z^c\tau} - \lambda\tau\right)d\tau$$ using a linear interpolation

between the known input fluxes at times t_1 and t_2.

The coefficients a and b in Eq. 3.1 are given by Eq. 3.57 of the RESRAD-OFFSITE User's Manual, which is reproduced below as Eq. 3.2.

$$f(0, t_1 \le t_n - \tau \le t_2) = f(0,t_1)\frac{t_2 - (t_n - \tau)}{t_2 - t_1} + f(0,t_2)\frac{(t_n - \tau) - t_1}{t_2 - t_1} \qquad \text{(Eq. 3.2)}$$

Rearranging in terms of τ, $f(0, t_1 \le t_n - \tau \le t_2) = a + b\tau$,

where $a = f(0,t_1)\frac{t_2 - t_n}{t_2 - t_1} + f(0,t_2)\frac{t_n - t_1}{t_2 - t_1}$ and $b = \frac{f(0,t_1) - f(0,t_2)}{t_2 - t_1}$.

Any time-dependent input flux can be expressed as linear combination of two triangular flux distributions shifted in time, as illustrated in Figure 3-1. Thus, it is sufficient to verify the output flux from two triangular input fluxes, the first going from one to zero and the second going from zero to one in the first time interval.

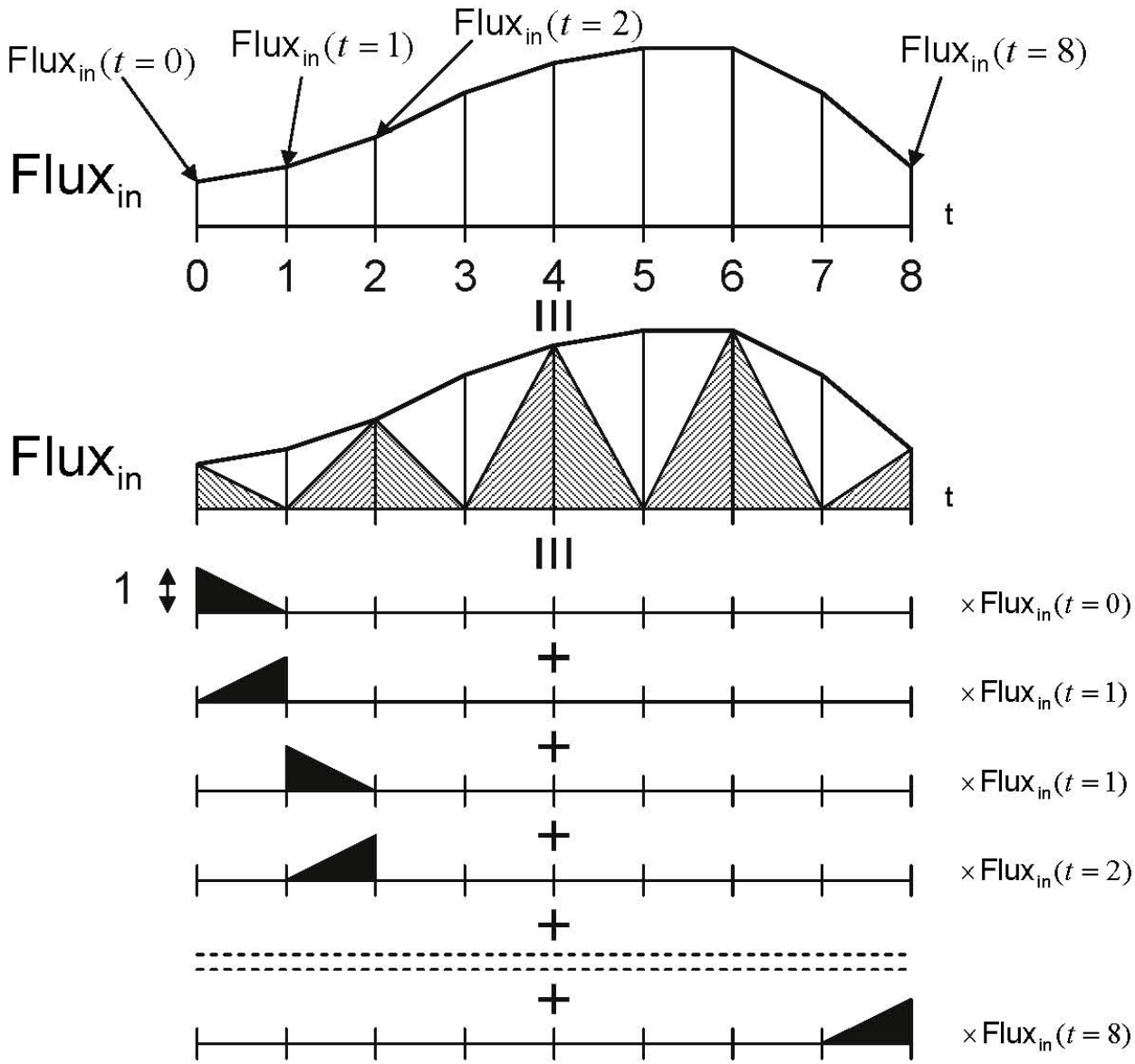

Figure 3-1 Time Varying Flux Profile Represented as a Combination of Two Triangular Flux Distributions Shifted in Time

The output fluxes of eight different nuclides (Table 3-1) that represent a wide spectrum of half-lives were verified. The values used for the RESRAD-OFFSITE inputs that pertain to modeling the transport in the unsaturated zone are in Table 3-2. The inputs are in bold while the intermediate calculations are in italics. Four different runs with four different distribution coefficients were used for each of the nuclides to cover a wide range of conditions in this verification of transport in the unsaturated zone. Even so, this verification is not exhaustive; the Excel file that was used in this verification is available to verify other cases, should the need arise.

Table 3-1 Nuclides Used in This Verification and Their Transformation Rates

Nuclide	^{60}Co	^{3}H	^{90}Sr	^{137}Cs	^{63}Ni	^{226}Ra	^{14}C	^{238}U
Half-life, years	5.271	12.35	29.12	30	96	1600	5730	$4.468\ 10^{9}$
Transformation rate, 1/year	0.132	.0561	.0238	.0231	.00722	.000433	.000121	$1.55\ 10^{-10}$

Table 3-2 RESRAD-OFFSITE Inputs and Intermediate Calculations That Pertain to Transport in the Unsaturated Zone

Transport distance	z (m)	**4**			
Darcy velocity	V_d (m/yr)	**0.5**			
Saturated hydraulic conductivity	K_{sat} (m/yr)	**10**			
Parameter b of Clapp-Hornberger equation	b	**5.3**			
Saturation ratio	R_s	*0.8023*			
Field capacity	f_c	**0.3**			
Total porosity	p_t	**0.4**			
Total moisture content	θ_t	*0.3209*			
Effective porosity	p_e	**0.2**			
Effective moisture content	θ_e	*0.1605*			
Dry bulk density	ρ_b (g/cc)	**1.5**			
Distribution coefficient	K_d (cc/g)	**0**	**1**	**10**	**100**
Retardation factor	R_d	*1*	*5.674*	*47.74*	*468.4*
Contaminant transport velocity	V_c (m/yr)	*3.1160*	*0.5492*	*0.06527*	*0.006652*
Dispersivity	D (m)	**0.1**			
Dispersion coefficient of contaminant	D_c (m^2/yr)	*0.3116*	*0.0549*	*0.00653*	*0.000665*
Time horizon	(years)	**4**	**20**	**200**	**2000**
Number of time points		**128**			

The expression of output flux contains two exponentials, a couple of differences between pairs of error functions, and two terms that involve the temporal variation of the input flux. The argument of the first exponential, $\frac{z\left(V_c - \sqrt{V_c^2 + 4D_z^c\lambda}\right)}{2D_z^c}$, is negative and can be zero in cases where the transformation rate or the dispersion coefficient is miniscule compared to the contaminant transport rate. Thus, the first exponential is less than or equal to unity, as shown in the second column of Table 3-3. The argument of the second exponential, $\frac{z\left(V_c + \sqrt{V_c^2 + 4D_z^c\lambda}\right)}{2D_z^c}$, is positive and is greater than $\frac{z}{d}$. Thus, the value of the second exponential can be and is usually very large, as shown in the third column of Table 3-3. The second pair of error functions have to be evaluated to a much higher precision than the first pair. This is because the small differences between these two error functions are magnified by the much larger exponential multiplier. The error function that is available in Excel is not sufficiently precise for this purpose. The arguments of the second pair of error functions are typically large. Thus, the expression

Table 3-3 Value of the Two Exponentials for the Cases Used in This Verification

	$\exp\left(\frac{z\left(V_c - \sqrt{V_c^2 + 4D_z^c\lambda}\right)}{2D_z^c}\right)$	$\exp\left(\frac{z\left(V_c + \sqrt{V_c^2 + 4D_z^c\lambda}\right)}{2D_z^c}\right)$
^{238}U		
$K_d = 0$	1	2.354E+17
$K_d = 1$	0.999999999	2.354E+17
$K_d = 10$	0.99999999	2.354E+17
$K_d = 100$	0.999999907	2.354E+17
^{14}C		
$K_d = 0$	0.999844729	2.354E+17
$K_d = 1$	0.999119315	2.356E+17
$K_d = 10$	0.992615405	2.371E+17
$K_d = 100$	0.929968694	2.531E+17
^{226}Ra		
$K_d = 0$	0.999444051	2.355E+17
$K_d = 1$	0.996849808	2.361E+17
$K_d = 10$	0.973817337	2.417E+17
$K_d = 100$	0.771968359	3.049E+17
^{63}Ni		
$K_d = 0$	0.99077643	2.376E+17
$K_d = 1$	0.948834155	2.481E+17
$K_d = 10$	0.645521954	3.646E+17
$K_d = 100$	0.019232592	1.224E+19
^{137}Cs		
$K_d = 0$	0.970797583	2.425E+17
$K_d = 1$	0.845703411	2.783E+17
$K_d = 10$	0.254337486	9.255E+17
$K_d = 100$	1.81932E-05	1.294E+22
^{90}Sr		
$K_d = 0$	0.969929157	2.427E+17
$K_d = 1$	0.84144947	2.797E+17
$K_d = 10$	0.244362118	9.633E+17
$K_d = 100$	1.38824E-05	1.696E+22
^{3}H		
$K_d = 0$	0.930607698	2.529E+17
$K_d = 1$	0.667174394	3.528E+17
$K_d = 10$	0.041344072	5.693E+18
$K_d = 100$	3.30086E-10	7.131E+26
^{60}Co		
$K_d = 0$	0.845269484	2.785E+17
$K_d = 1$	0.392224955	6.001E+17
$K_d = 10$	0.00103154	2.282E+20
$K_d = 100$	5.79693E-18	4.061E+34

$erf(x) \approx 1 - \frac{e^{-x^2}}{\sqrt{\pi}x}\left(1 + \sum_{i=1}\left(-1\right)^i \frac{\prod_{j=1}^{i}(2j+1)}{x^{2i}}\right)$ is used to evaluate the error functions in this case in both the RESRAD-OFFSITE code and in the Excel spreadsheet used for the verification.

3.1.1 Output Flux from a Decreasing Triangular Input Flux

The coefficients a and b for the input flux shown in Figure 3-2 are evaluated as:

$a = f(0,t_1)\frac{t_2 - t_n}{t_2 - t_1} + f(0,t_2)\frac{t_n - t_1}{t_2 - t_1} = \frac{t_2 - t_n}{t_2 - t_1}$ and $b = \frac{f(0,t_1) - f(0,t_2)}{t_2 - t_1} = \frac{1}{t_2 - t_1}$. The expression for the output flux then becomes

$$
\begin{aligned}
f(z,t_n) = \; & \frac{1}{2}\left(\frac{t_2 - t_n}{t_2 - t_1} + \frac{z/(t_2 - t_1)}{\sqrt{V_c^2 + 4D_z^c\lambda}}\right)\exp\left(\frac{z\left(V_c - \sqrt{V_c^2 + 4D_z^c\lambda}\right)}{2D_z^c}\right) \times \\
& \left[erf\left(\frac{z}{\sqrt{4D_z^c}}\frac{1}{\sqrt{(t_n - t_2)}} - \frac{\sqrt{V_c^2 + 4D_z^c\lambda}}{\sqrt{4D_z^c}}\sqrt{(t_n - t_2)}\right) - erf\left(\frac{z}{\sqrt{4D_z^c}}\frac{1}{\sqrt{(t_n - t_1)}} - \frac{\sqrt{V_c^2 + 4D_z^c\lambda}}{\sqrt{4D_z^c}}\sqrt{(t_n - t_1)}\right)\right] \\
& + \frac{1}{2}\left(\frac{t_2 - t_n}{t_2 - t_1} - \frac{z/(t_2 - t_1)}{\sqrt{V_c^2 + 4D_z^c\lambda}}\right)\exp\left(\frac{z\left(V_c + \sqrt{V_c^2 + 4D_z^c\lambda}\right)}{2D_z^c}\right) \times \\
& \left[erf\left(\frac{z}{\sqrt{4D_z^c}}\frac{1}{\sqrt{(t_n - t_2)}} + \frac{\sqrt{V_c^2 + 4D_z^c\lambda}}{\sqrt{4D_z^c}}\sqrt{(t_n - t_2)}\right) - erf\left(\frac{z}{\sqrt{4D_z^c}}\frac{1}{\sqrt{(t_n - t_1)}} + \frac{\sqrt{V_c^2 + 4D_z^c\lambda}}{\sqrt{4D_z^c}}\sqrt{(t_n - t_1)}\right)\right]
\end{aligned}
\qquad \text{(Eq. 3.3)}
$$

This equation was evaluated in Excel files for 128 different values of time, t_n; the Excel files are described later. The situation was also modeled in the RESRAD-OFFSITE using the inputs shown in Table 3-2. In addition, the erosion rate of the contaminated zone was increased so that the contaminated zone erodes away before the second time point. This produces the desired triangular input flux. Thirty-two (eight nuclides, each at four different distribution coefficients) temporal profiles of output flux were verified. The verification of four of these flux profiles is illustrated in Figures 3-3, 3-4, 3-5, and 3-6.

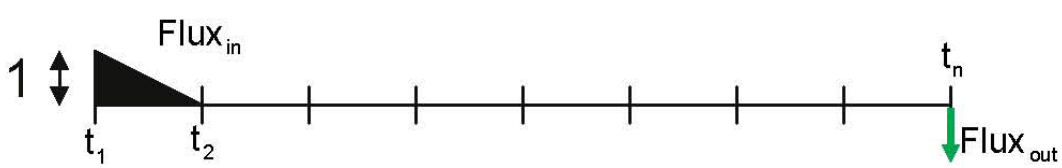

Figure 3-2 Decreasing Triangular Input Flux Profile

3.1.2 Output Flux from an Increasing Triangular Input Flux

The coefficients a and b for the input flux shown in Figure 3-7 are evaluated as

$a = f(0,t_1)\frac{t_2 - t_n}{t_2 - t_1} + f(0,t_2)\frac{t_n - t_1}{t_2 - t_1} = \frac{t_n - t_1}{t_2 - t_1}$ and $b = \frac{f(0,t_1) - f(0,t_2)}{t_2 - t_1} = \frac{-1}{t_2 - t_1}$. The expression for the output flux then becomes

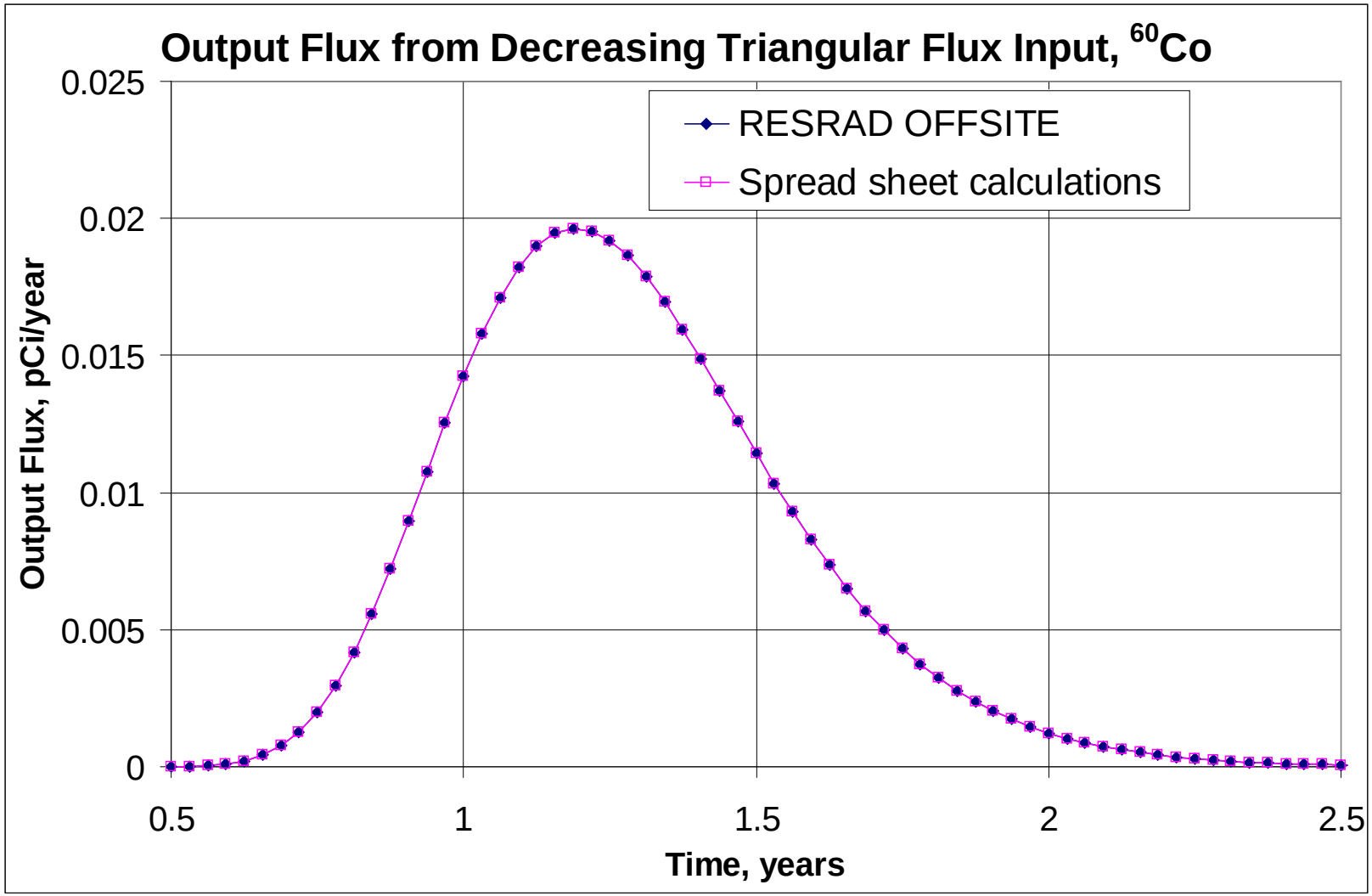

Figure 3-3 Verification of RESRAD-OFFSITE Computed Flux Exiting an Unsaturated Zone Resulting from a Triangular Input Flux of ^{60}Co of Unity at Time Zero and of Zero at the First Time Point at the Top of the Unsaturated Zone Using Spreadsheet Calculations

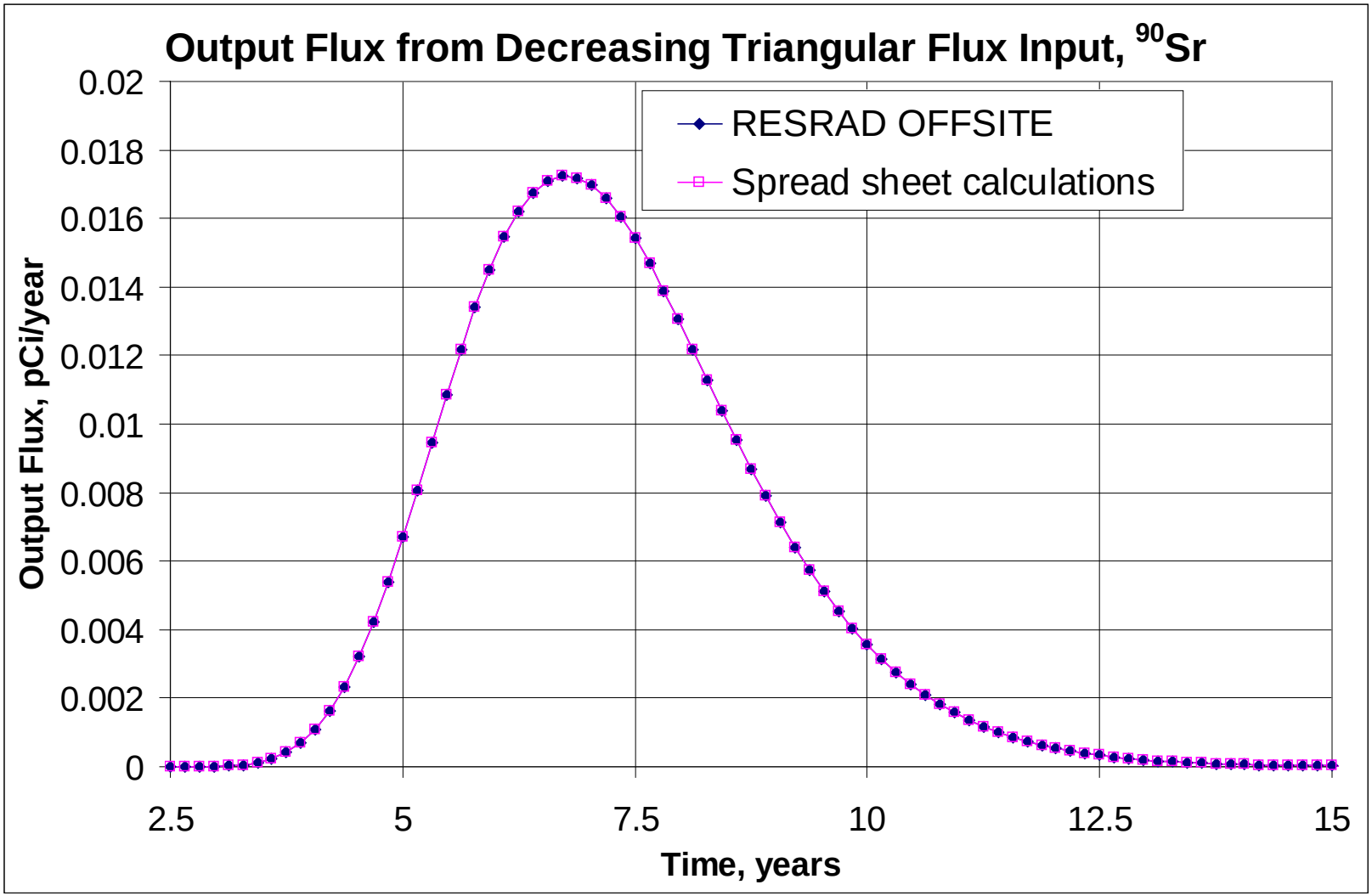

Figure 3-4 Verification of RESRAD-OFFSITE Computed Flux Exiting an Unsaturated Zone Resulting from a Triangular Input Flux of ^{90}Sr of Unity at Time Zero and of Zero at the First Time Point at the Top of the Unsaturated Zone Using Spreadsheet Calculations

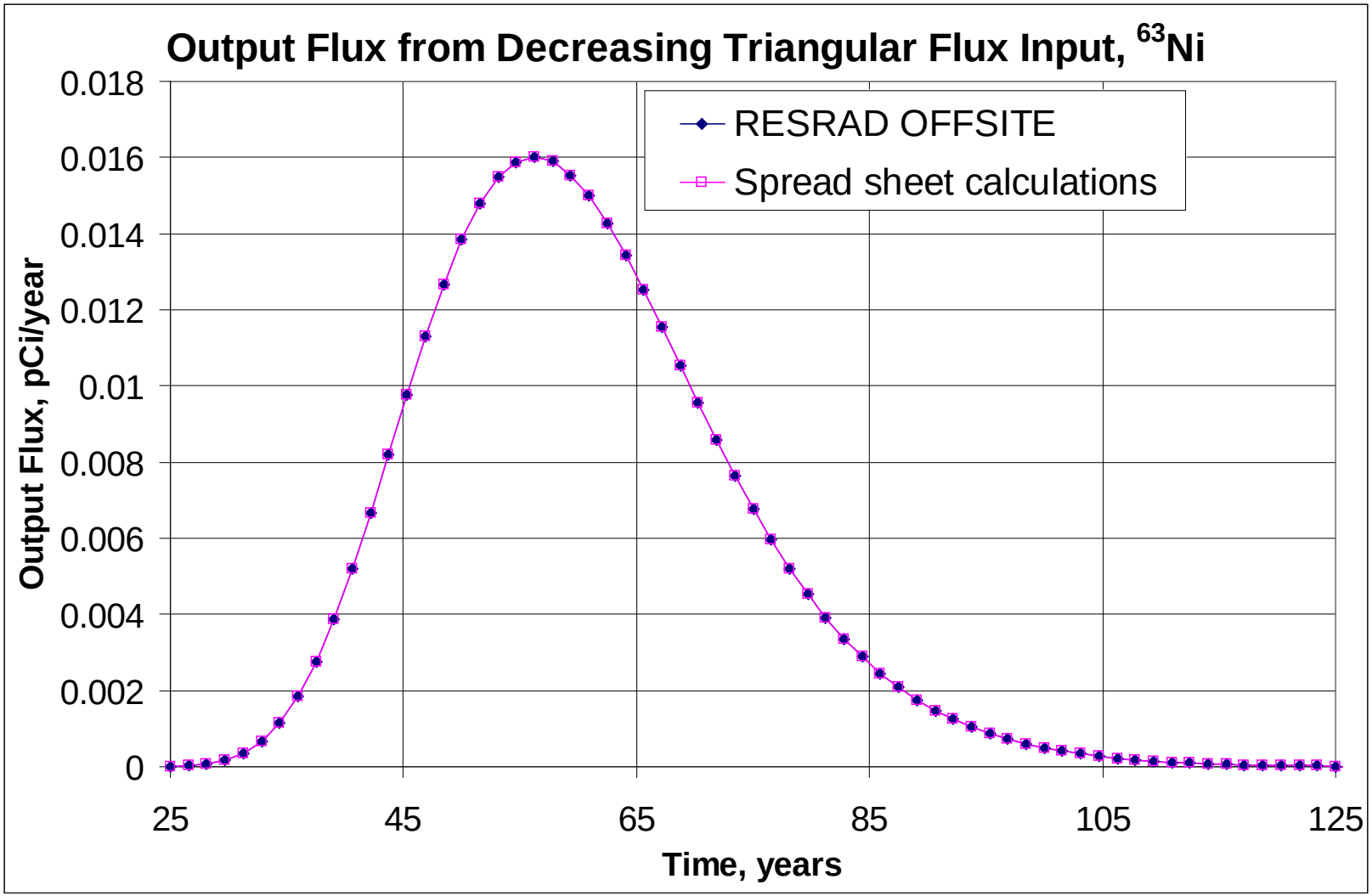

Figure 3-5 Verification of RESRAD-OFFSITE Computed Flux Exiting an Unsaturated Zone Resulting from a Triangular Input Flux of ^{63}Ni of Unity at Time Zero and of Zero at the First Time Point at the Top of the Unsaturated Zone Using Spreadsheet Calculations

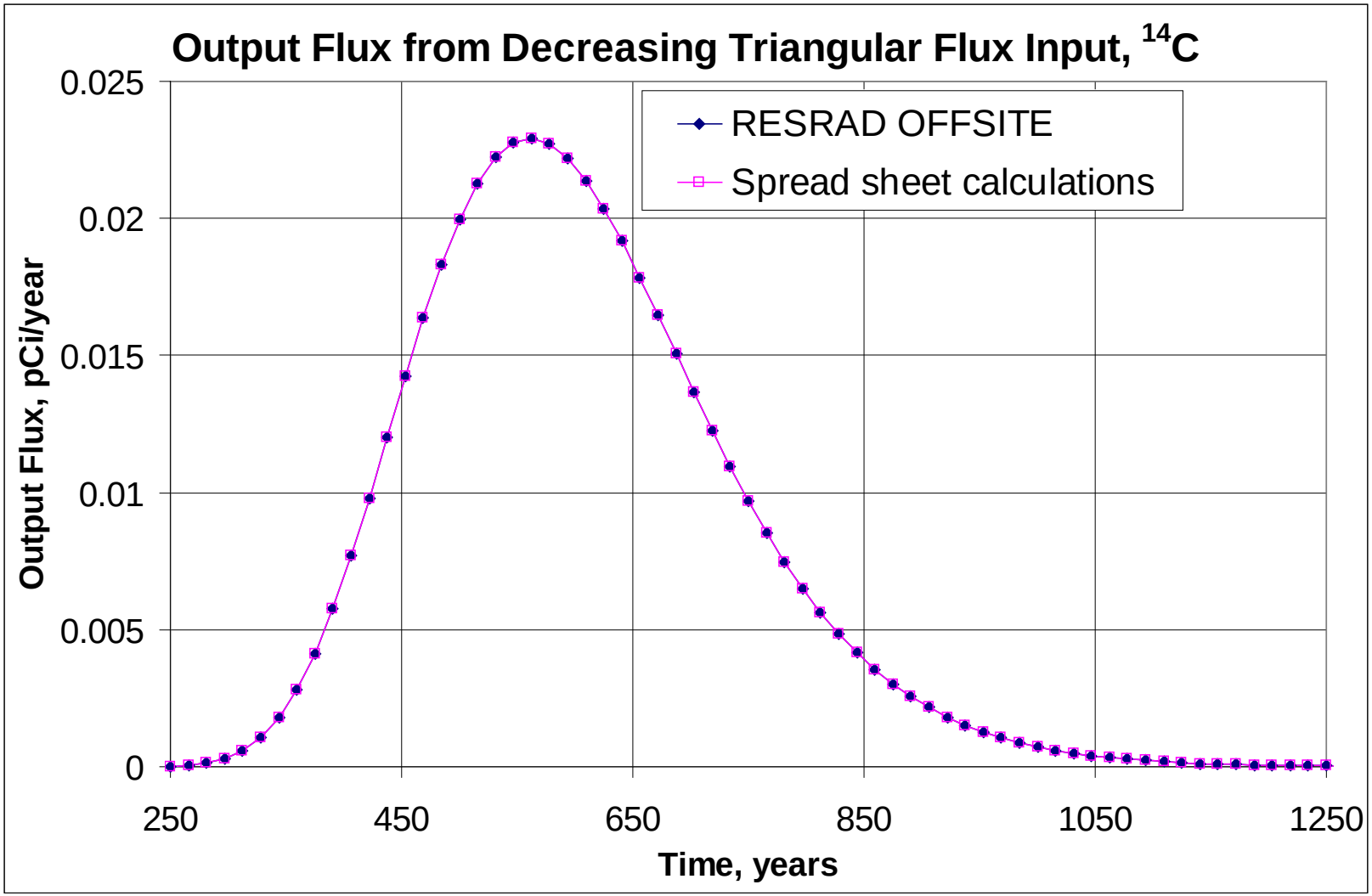

Figure 3-6 Verification of RESRAD-OFFSITE Computed Flux Exiting an Unsaturated Zone Resulting from a Triangular Input Flux of ^{14}C of Unity at Time Zero and of Zero at the First Time Point at the Top of the Unsaturated Zone Using Spreadsheet Calculations

$$
\begin{aligned}
f(z,t_n) = \; & \frac{1}{2}\left(\frac{t_n - t_1}{t_2 - t_1} - \frac{z/(t_2 - t_1)}{\sqrt{V_c^2 + 4D_z^c\lambda}}\right)\exp\left(\frac{z\left(V_c - \sqrt{V_c^2 + 4D_z^c\lambda}\right)}{2D_z^c}\right)\times \\
& \left[erf\left(\frac{z}{\sqrt{4D_z^c}}\frac{1}{\sqrt{(t_n - t_2)}} - \frac{\sqrt{V_c^2 + 4D_z^c\lambda}}{\sqrt{4D_z^c}}\sqrt{(t_n - t_2)}\right) - erf\left(\frac{z}{\sqrt{4D_z^c}}\frac{1}{\sqrt{(t_n - t_1)}} - \frac{\sqrt{V_c^2 + 4D_z^c\lambda}}{\sqrt{4D_z^c}}\sqrt{(t_n - t_1)}\right)\right] \\
& + \frac{1}{2}\left(\frac{t_n - t_1}{t_2 - t_1} + \frac{z/(t_2 - t_1)}{\sqrt{V_c^2 + 4D_z^c\lambda}}\right)\exp\left(\frac{z\left(V_c + \sqrt{V_c^2 + 4D_z^c\lambda}\right)}{2D_z^c}\right)\times \\
& \left[erf\left(\frac{z}{\sqrt{4D_z^c}}\frac{1}{\sqrt{(t_n - t_2)}} + \frac{\sqrt{V_c^2 + 4D_z^c\lambda}}{\sqrt{4D_z^c}}\sqrt{(t_n - t_2)}\right) - erf\left(\frac{z}{\sqrt{4D_z^c}}\frac{1}{\sqrt{(t_n - t_1)}} + \frac{\sqrt{V_c^2 + 4D_z^c\lambda}}{\sqrt{4D_z^c}}\sqrt{(t_n - t_1)}\right)\right]
\end{aligned}
\qquad \text{(Eq. 3.4)}
$$

This equation was evaluated in Excel files for 128 different values of time, t_n; the Excel files are described later. The situation was also modeled in the RESRAD-OFFSITE using the inputs shown in Table 3-2. It is not possible to obtain the desired increasing triangular input flux profile (Figure 3-7) using the release model of RESRAD-OFFSITE. The RESRAD-OFFSITE feature allowing an informed user to override the internal release model was utilized for this verification of the transport in the unsaturated zone. A double triangular input flux shown in Figure 3-8 was specified for the run. The increasing triangular input flux depicted in Figure 3-7 is equivalent to the difference between the double triangular input flux in Figure 3-8 and the decreasing triangular input flux in Figure 3-2 shifted by a time interval. Thus, the output flux corresponding to the increasing triangular input flux (Figure 3-7) is obtained as the difference between the output flux from the double triangular input flux (Figure 3-8) and the output flux from the decreasing triangular flux (Figure 3-2) shifted by a time interval. Thirty-two (eight nuclides, each at four different distribution coefficients) temporal profiles of output flux were verified. The verification of four of these flux profiles is illustrated in Figures 3-9, 3-10, 3-11, and 3-12.

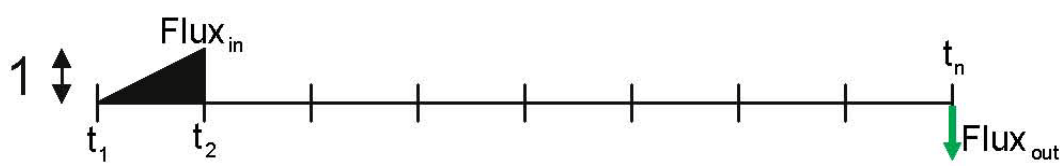

Figure 3-7 Increasing Triangular Input Flux Profile

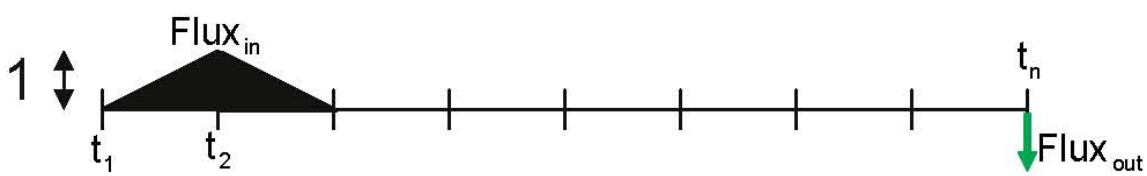

Figure 3-8 Double Triangular Input Flux Profile

3.1.3 Description of the Excel Files Used in This Verification

Four Excel files, unsaturated 0.xls, unsaturated 1.xls, unsaturated 10.xls, and unsaturated 100.xls, one for each value of the distribution coefficient, were used to verify the transport in the unsaturated zone. The first tab, "Ti," contains the inputs that pertain to transport in the unsaturated zone and some intermediate calculations; the inputs are in bold. The tabs "AQ 1," "AQ 2," and "AQ 21" are the temporal input fluxes used in RESRAD-OFFSITE and correspond to Figures 3-2, 3-7, and 3-8. Tabs "WT 1" and "WT 21" are

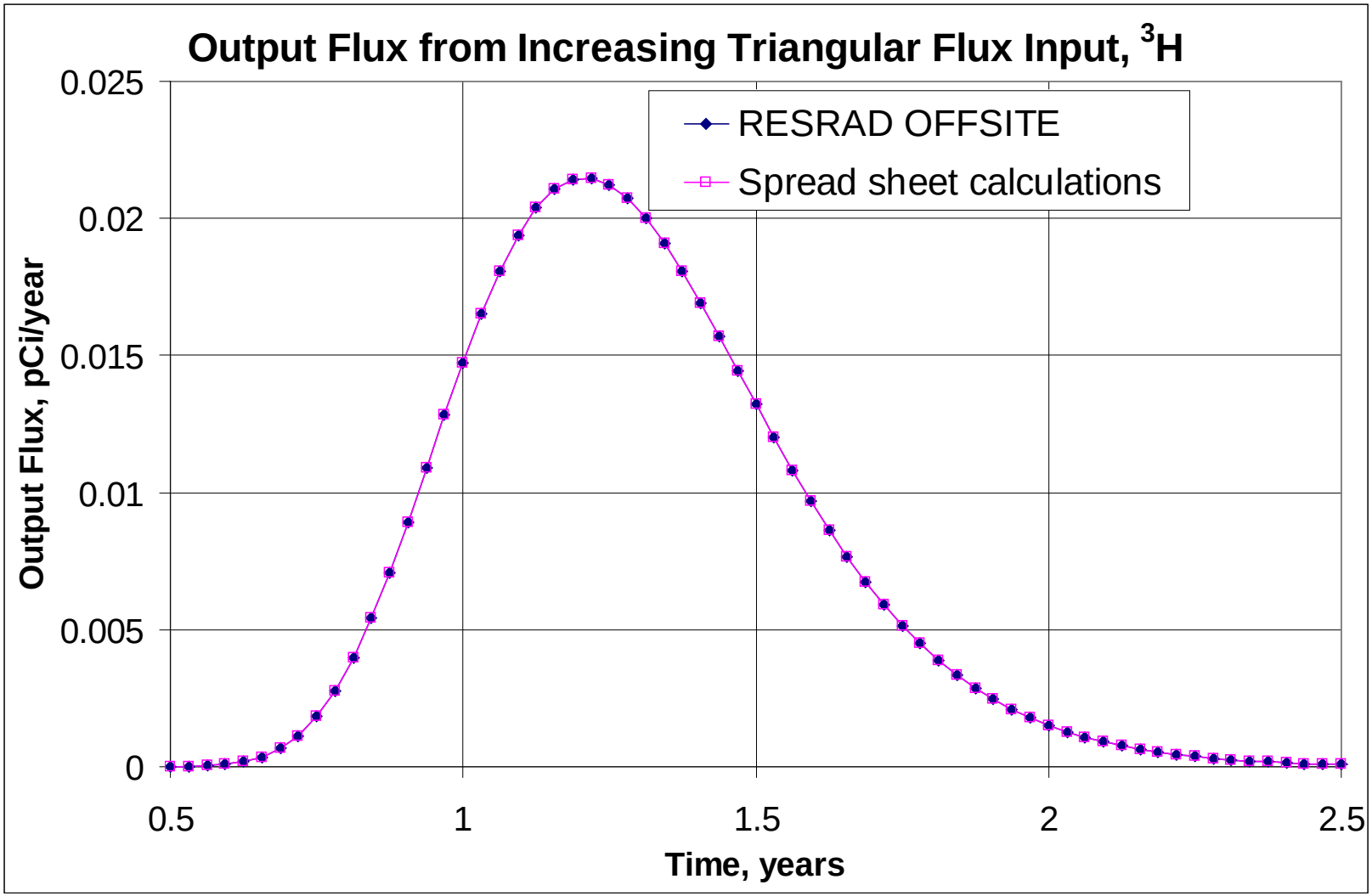

Figure 3-9 Verification of RESRAD-OFFSITE Computed Flux Exiting an Unsaturated Zone Resulting from a Triangular Input Flux of ^{3}H of Zero at Time Zero and of Unity at the First Time Point at the Top of the Unsaturated Zone Using Spreadsheet Calculations

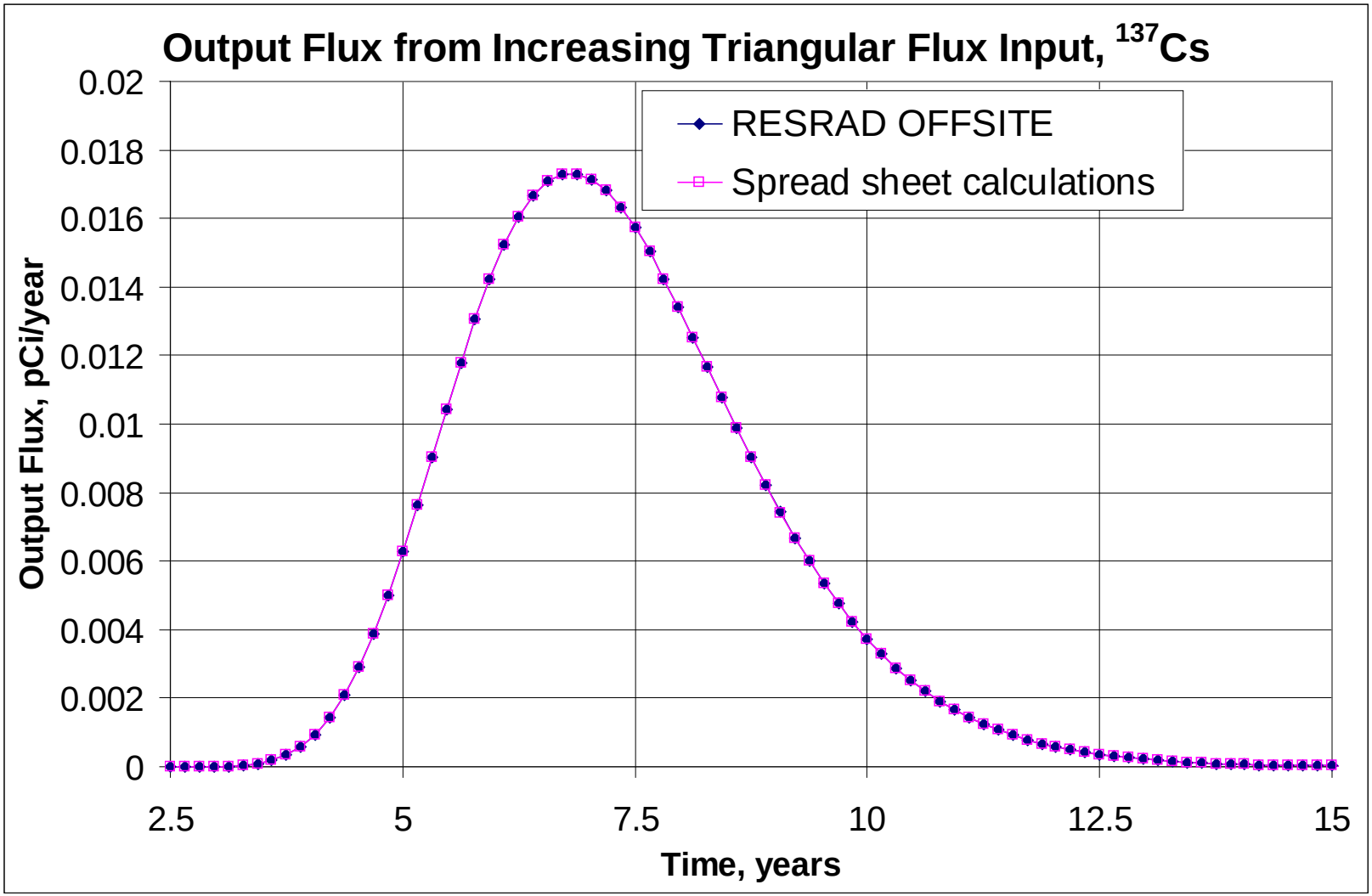

Figure 3-10 Verification of RESRAD-OFFSITE Computed Flux Exiting an Unsaturated Zone Resulting from a Triangular Input Flux of ^{137}Cs of Zero at Time Zero and of Unity at the First Time Point at the Top of the Unsaturated Zone Using Spreadsheet Calculations

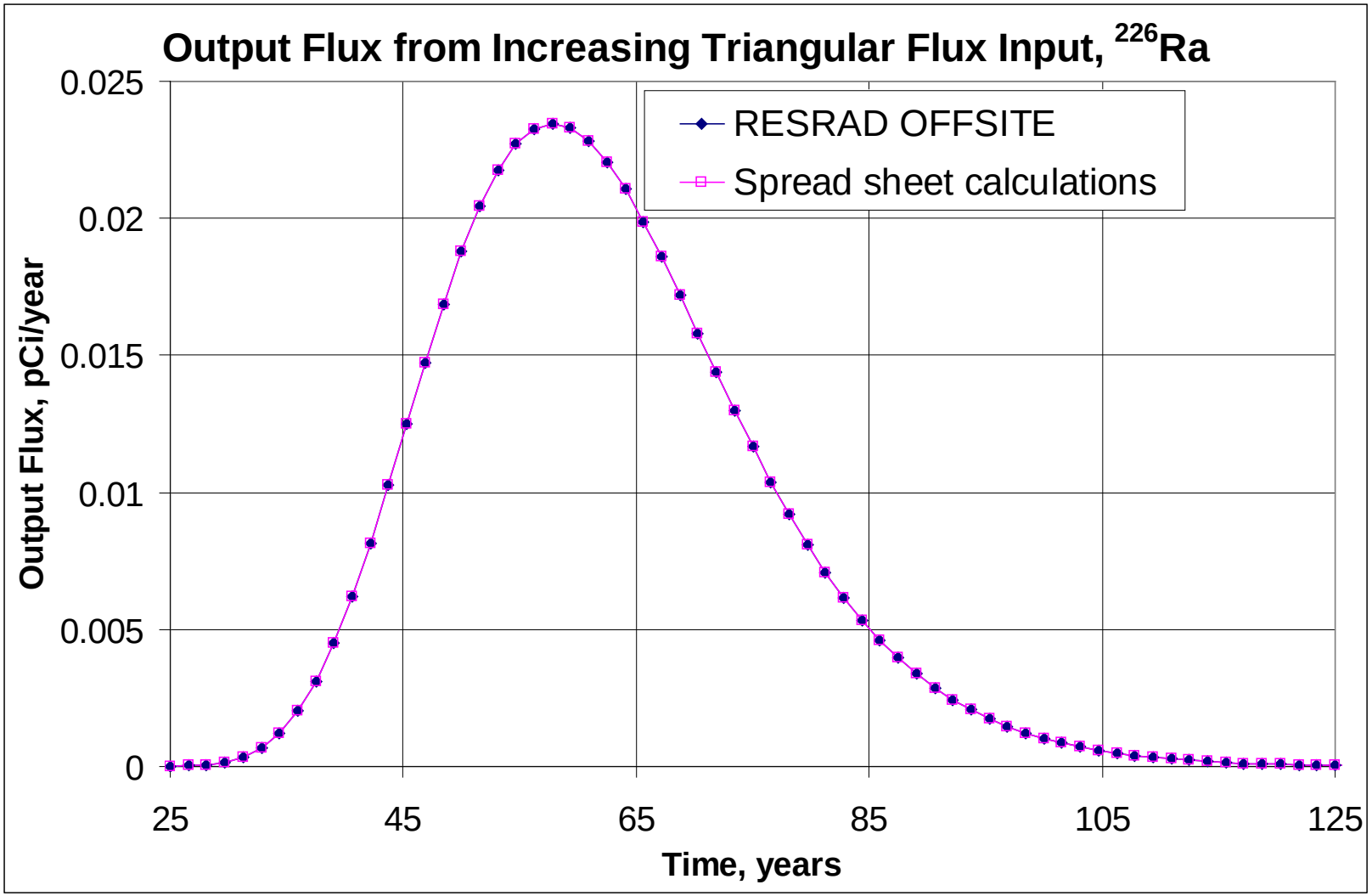

Figure 3-11 Verification of RESRAD-OFFSITE Computed Flux Exiting an Unsaturated Zone Resulting from a Triangular Input Flux of ^{226}Ra of Zero at Time Zero and of Unity at the First Time Point at the Top of the Unsaturated Zone Using Spreadsheet Calculations

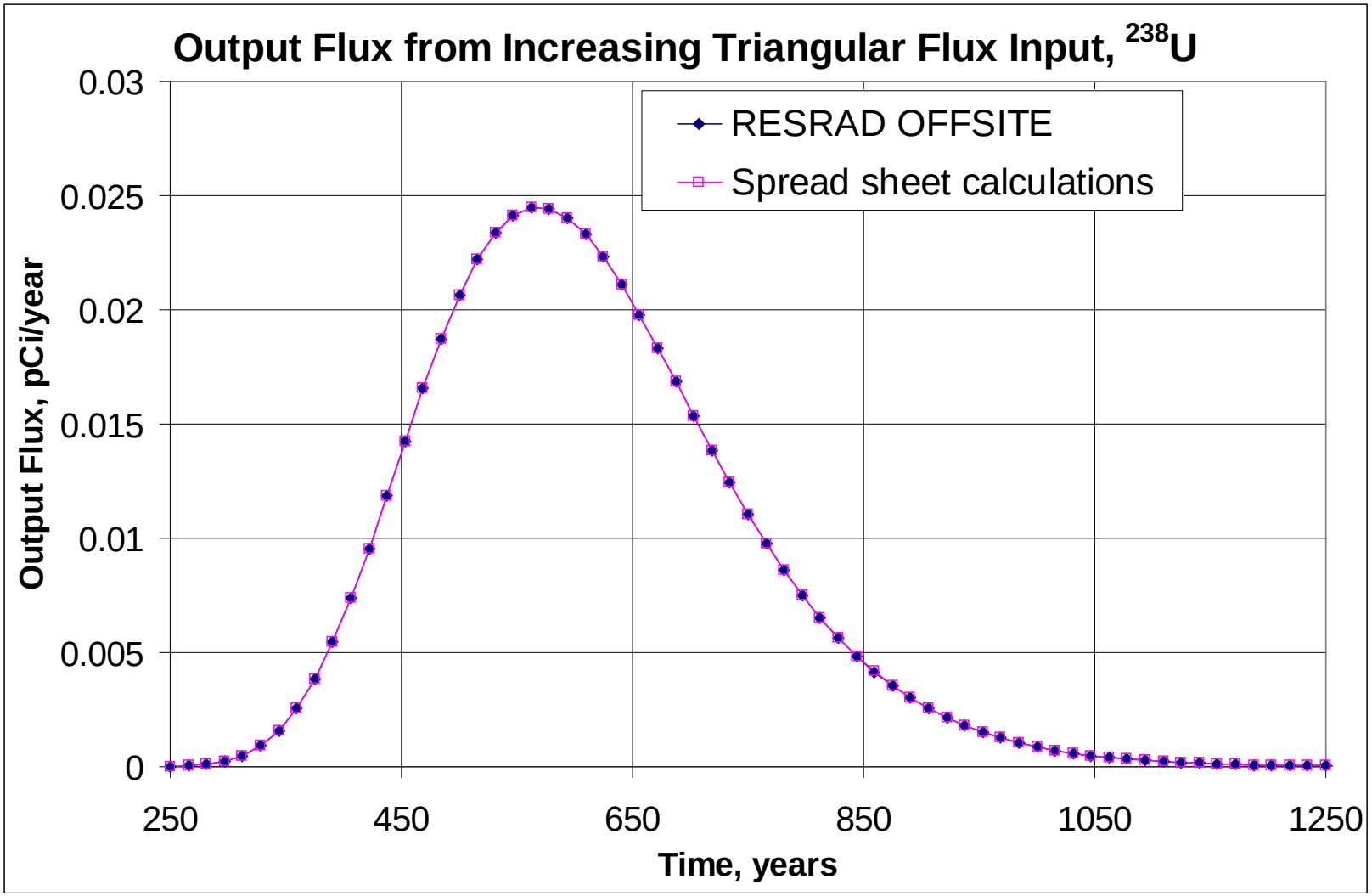

Figure 3-12 Verification of RESRAD-OFFSITE Computed Flux Exiting an Unsaturated Zone Resulting from a Triangular Input Flux of ^{238}U of Zero at Time Zero and of Unity at the First Time Point at the Top of the Unsaturated Zone Using Spreadsheet Calculations

the RESRAD-OFFSITE outputs of flux out of the unsaturated zone corresponding to the input fluxes in tabs “AQ 1” and “AQ 21.” The temporal flux in tab “WT 2” was obtained by subtracting from the fluxes in tab “WT 21” the fluxes in tab “WT 1” shifted by a time step.

The tab “Single Nuclide graph” compares the temporal output flux from RESRAD-OFFSITE with that calculated in the spreadsheet. The comparisons are captured in three plots: the first one, the one at the top anchored in cell “H4,” compares the output flux from a uniform input flux over the first time interval; the second plot in the middle, anchored in cell “H35,” compares the output flux from a decreasing triangular input flux over the first time interval; and the third plot at the bottom, anchored in cell “H66,” compares the output flux from a increasing triangular input flux over the first time interval. The plots pertain to the nuclide shown in cell “C1”; plots that pertain to the eight nuclides ^{60}Co, ^{3}H, ^{90}Sr, ^{137}Cs, ^{63}Ni, ^{226}Ra, ^{14}C, and ^{238}U can be viewed by typing in the numbers, 2, 4, 9, 3, 5, 6, 1, and 11, respectively, in cell “A1.” Note that the nuclide name will change in cell “C1” but not in the title of the plots. Plots of all 64 verifications that were performed can be viewed in turn in this fashion. A subset of these plots were shown in Figures 3-3 to 3-6 and 3-9 to 3-12.

3.2 Verification of Transport in the Saturated Zone to the Surface Water Body

Two of the three equations of transport in the saturated zone to the surface water body that need to be verified are the dispersive-advective transport Eqs. 3.67 and 3.68 of the RESRAD-OFFSITE User’s Manual. These equations are reproduced below.

$$f_1(x,t_n-t_m)=\int_{t_n-t_m}^{t_n-t_{m-1}}\left(\frac{t_n-t_{m-1}-\tau}{t_m-t_{m-1}}\right)\frac{V_c e^{-\lambda\tau}}{2L_x}\left[erf\left(\frac{x+\frac{L_x}{2}-V_c\tau}{\sqrt{4D_x^c\tau}}\right)-erf\left(\frac{x-\frac{L_x}{2}-V_c\tau}{\sqrt{4D_x^c\tau}}\right)\right]d\tau$$
$$-\int_{t_n-t_m}^{t_n-t_{m-1}}\left(\frac{t_n-t_{m-1}-\tau}{t_m-t_{m-1}}\right)\sqrt{\frac{D_x^c}{4\pi\tau}}\frac{e^{-\lambda\tau}}{L_x}\left[e^{-\frac{\left(x+\frac{L_x}{2}-V_c\tau\right)^2}{4D_x^c\tau}}-e^{-\frac{\left(x-\frac{L_x}{2}-V_c\tau\right)^2}{4D_x^c\tau}}\right]d\tau \qquad \text{(Eq. 3.5)}$$

$$f_2(x,t_n-t_{m-1})=\int_{t_n-t_m}^{t_n-t_{m-1}}\left(\frac{\tau-t_n+t_m}{t_m-t_{m-1}}\right)\frac{V_c e^{-\lambda\tau}}{2L_x}\left[erf\left(\frac{x+\frac{L_x}{2}-V_c\tau}{\sqrt{4D_x^c\tau}}\right)-erf\left(\frac{x-\frac{L_x}{2}-V_c\tau}{\sqrt{4D_x^c\tau}}\right)\right]d\tau$$
$$-\int_{t_n-t_m}^{t_n-t_{m-1}}\left(\frac{\tau-t_n+t_m}{t_m-t_{m-1}}\right)\sqrt{\frac{D_x^c}{4\pi\tau}}\frac{e^{-\lambda\tau}}{L_x}\left[e^{-\frac{\left(x+\frac{L_x}{2}-V_c\tau\right)^2}{4D_x^c\tau}}-e^{-\frac{\left(x-\frac{L_x}{2}-V_c\tau\right)^2}{4D_x^c\tau}}\right]d\tau$$

The first is the spatially integrated flux across a vertical plane in the saturated zone, at a distance x downgradient of the center of the primary contamination, at time $t_n > t_m > t_{m-1}$, due to an input flux that increases linearly from zero at time t_{m-1} to one at time t_m. The second is the spatially integrated flux across the same vertical plane in the saturated zone, at the same time, due to the input flux that decreases linearly from one at time t_{m-1} to zero at time t_m.

The third equation that needs to be verified is Eq. 3.70 of the RESRAD-OFFSITE User's Manual; this relates the spatially integrated fluxes in Eqs. 3.68 and 3.69 to the flux that enters a surface water body through a rectangular section of the aquifer of dimensions $y_f - y_n$ by d_s. This is reproduced below.

$$f_{sw}(x) = f(x)\frac{f_{s,y}(y_n, y_f)}{L_y}\frac{f_{s,z}}{L_z} \qquad \text{(Eq. 3.6)}$$

where:

$$f_{s,y}(y_n, y_f) = \sqrt{D_y^c t_p}\left(Interf\,\frac{2y_f + L_y}{\sqrt{16D_y^c t_p}} - Interf\,\frac{2y_f - L_y}{\sqrt{16D_y^c t_p}} - Interf\,\frac{2y_n + L_y}{\sqrt{16D_y^c t_p}} + Interf\,\frac{2y_n - L_y}{\sqrt{16D_y^c t_p}} \right)$$

and

$$f_{s,z} = \sqrt{D_z^c t_p}\left(Interf\,\frac{d_s + L_z}{\sqrt{4D_z^c t_p}} - Interf\,\frac{d_s - L_z}{\sqrt{4D_z^c t_p}} - Interf\,\frac{L_z}{\sqrt{4D_z^c t_p}} + Interf\,\frac{-L_z}{\sqrt{4D_z^c t_p}} \right)$$

t_p in these expressions is obtained from Eq. 3.49 of the RESRAD-OFFSITE User's Manual:

$$t_p = \frac{-nD_x^c + \sqrt{\left(nD_x^c\right)^2 + \left(4\lambda D_x^c + V_c^2\right)x^2}}{\left(4\lambda D_x^c + V_c^2\right)}. \qquad \text{(Eq. 3.7)}$$

The fluxes of eight different nuclides (Table 3-1) that represent a wide spectrum of half-lives were verified. The values used for the RESRAD-OFFSITE inputs that pertain to modeling the transport in the saturated zone to the surface water body are in Table 3-4. The inputs are in bold while the intermediate calculations are in italics. Three different runs with three different distribution coefficients were used for each of the nuclides to cover a wide range of conditions in this verification of transport in the saturated zone. Even so this verification is not exhaustive; the excel file that was used in this verification is available to verify other cases should the need arise.

3.2.1 Output Flux from a Decreasing Triangular Input Flux

For the input flux shown in Figure 3-13, the expression for the output flux becomes

$$f_2(x,t_n) = \frac{V_c}{2L_x}\int_{t_n-t_2}^{t_n-t_1}\left(\frac{\tau - t_n + t_2}{t_2 - t_1}\right)e^{-\lambda\tau}\left[erf\left(\frac{x + \frac{L_x}{2} - V_c\tau}{\sqrt{4D_x^c\tau}}\right) - erf\left(\frac{x - \frac{L_x}{2} - V_c\tau}{\sqrt{4D_x^c\tau}}\right)\right]d\tau$$
$$- \frac{V_c}{2L_x}\int_{t_n-t_2}^{t_n-t_1}\left(\frac{\tau - t_n + t_2}{t_2 - t_1}\right)e^{-\lambda\tau}\sqrt{\frac{D_x^c}{\pi V_c^2}}\,\frac{e^{-\frac{\left(x+\frac{L_x}{2}-V_c\tau\right)^2}{4D_x^c\tau}} - e^{-\frac{\left(x-\frac{L_x}{2}-V_c\tau\right)^2}{4D_x^c\tau}}}{\sqrt{\tau}}\,d\tau \qquad \text{(Eq. 3.8)}$$

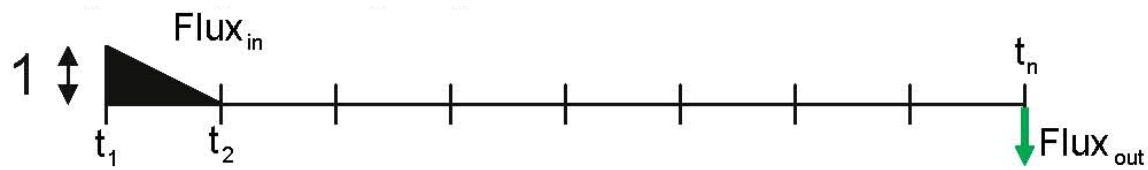

Figure 3-13 Decreasing Triangular Input Flux Profile

This equation was evaluated in Excel files for 128 different values of time, t_n; the integral (convolution, to be more precise) had to be evaluated numerically. The Excel files are described later. The situation was also modeled in the RESRAD-OFFSITE code using the inputs shown in Table 3-4. In addition, the erosion rate of the contaminated zone was increased so that the contaminated zone erodes away before the second time point. This produces the desired triangular input flux profile. Twenty-four (8 nuclides, each at 3 different distribution coefficients) temporal profiles of output flux were verified. The verification of four of these flux profiles is illustrated in Figures 3-14, 3-15, 3-16, and 3-17.

Table 3-4 RESRAD-OFFSITE Inputs and Intermediate Calculations That Pertain to Transport in the Saturated Zone to the Surface Water Body

Average transport distance	X (m)	**850**		
Length of contamination	L_x (m)	**100**		
Width of contamination	L_y (m)	**100**		
Saturated hydraulic conductivity	K_{sat} (m/yr)	**500**		
Hydraulic gradient		**.02**		
Darcy velocity	V_d (m/yr)	*10*		
Infiltration rate	I (m/yr)	*0.5*		
Depth of initial penetration of the contamination into the saturated zone	L_z (m)	*5*		
Total porosity	p_t	**0.4**		
Effective porosity	p_e	**0.2**		
Dry bulk density	ρ_b (g/cc)	**1.5**		
Distribution coefficient	K_d (cc/g)	**0**	**1**	**10**
Retardation factor	R_d	*1*	*4.75*	*38.5*
Contaminant transport velocity	V_c (m/yr)	*50*	*10.53*	*1.299*
Longitudinal dispersivity	d_x (m)	**20**		
Longitudinal dispersion coefficient of contaminants	D_{cx} (m^2/yr)	*1000*	*210.5*	*25.97*
Lateral horizontal dispersivity	d_y (m)	**3**		
Lateral horizontal dispersion coefficient of contaminants	D_{cy} (m^2/yr)	*150*	*31.58*	*3.896*
Lateral vertical dispersivity	d_y (m)	**0.15**		
Lateral vertical dispersion coefficient of contaminants	D_{cy} (m^2/yr)	*7.5*	*1.579*	*0.1048*
Time to peak flux	t_p (yr)	*14.5*	*54.3*	*211.9*
Distance from the plum centerline to right edge of surface waterbody	y_n (m)	**–150**		
Distance from the plum centerline to left edge of surface waterbody	y_f (m)	**150**		
Depth of aquifer intercepted by surface water body	d_s (m)	**5**		
Time horizon	(years)	**32**	**128**	**1024**
Number of time points		**128**		

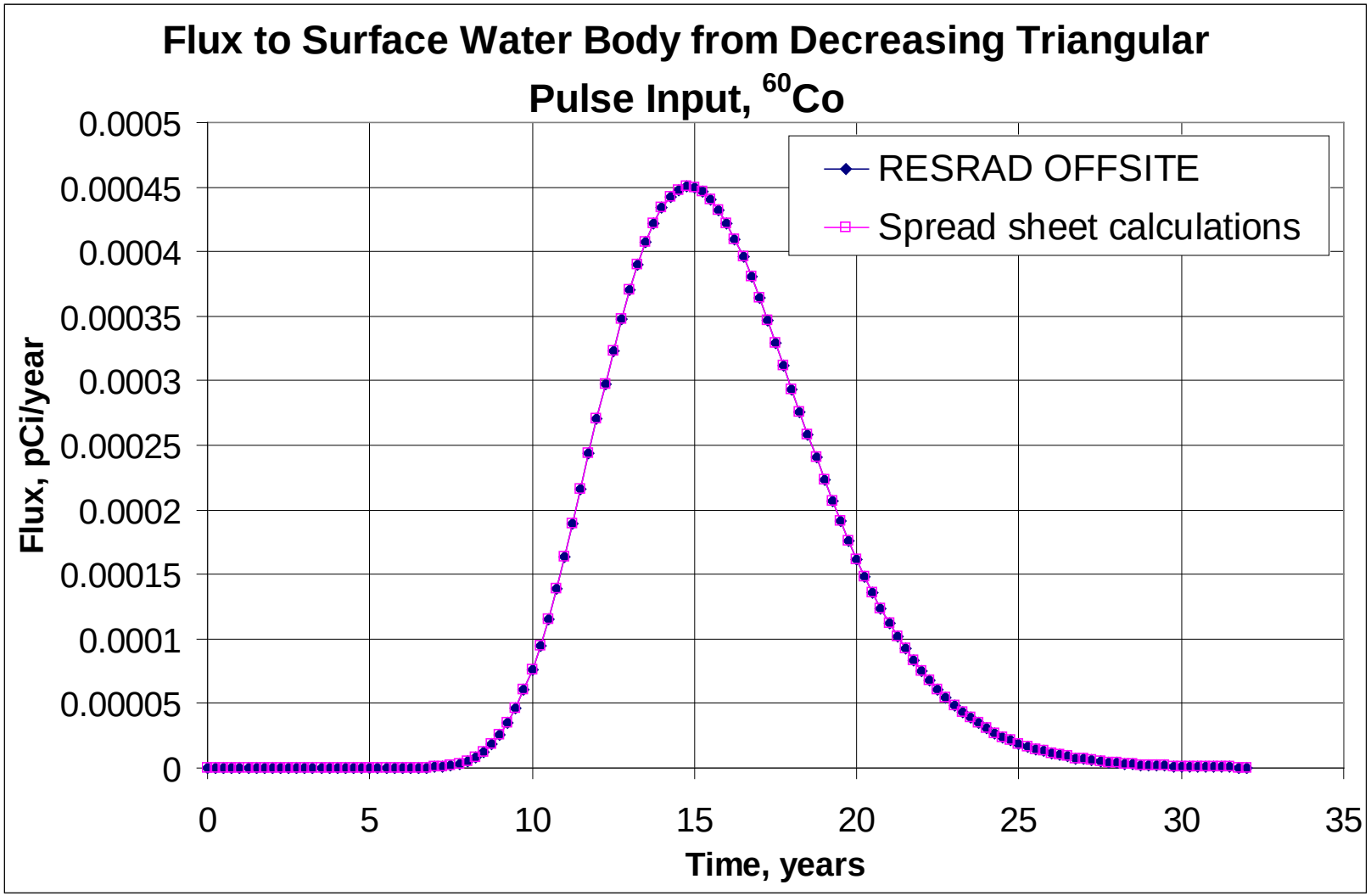

Figure 3-14 Verification of RESRAD-OFFSITE Computed Flux to the Surface Water Body Resulting from a Triangular Input Flux of ^{60}Co of Unity at Time Zero and of Zero at the First Time Point at the Water Table Using Spreadsheet Calculations

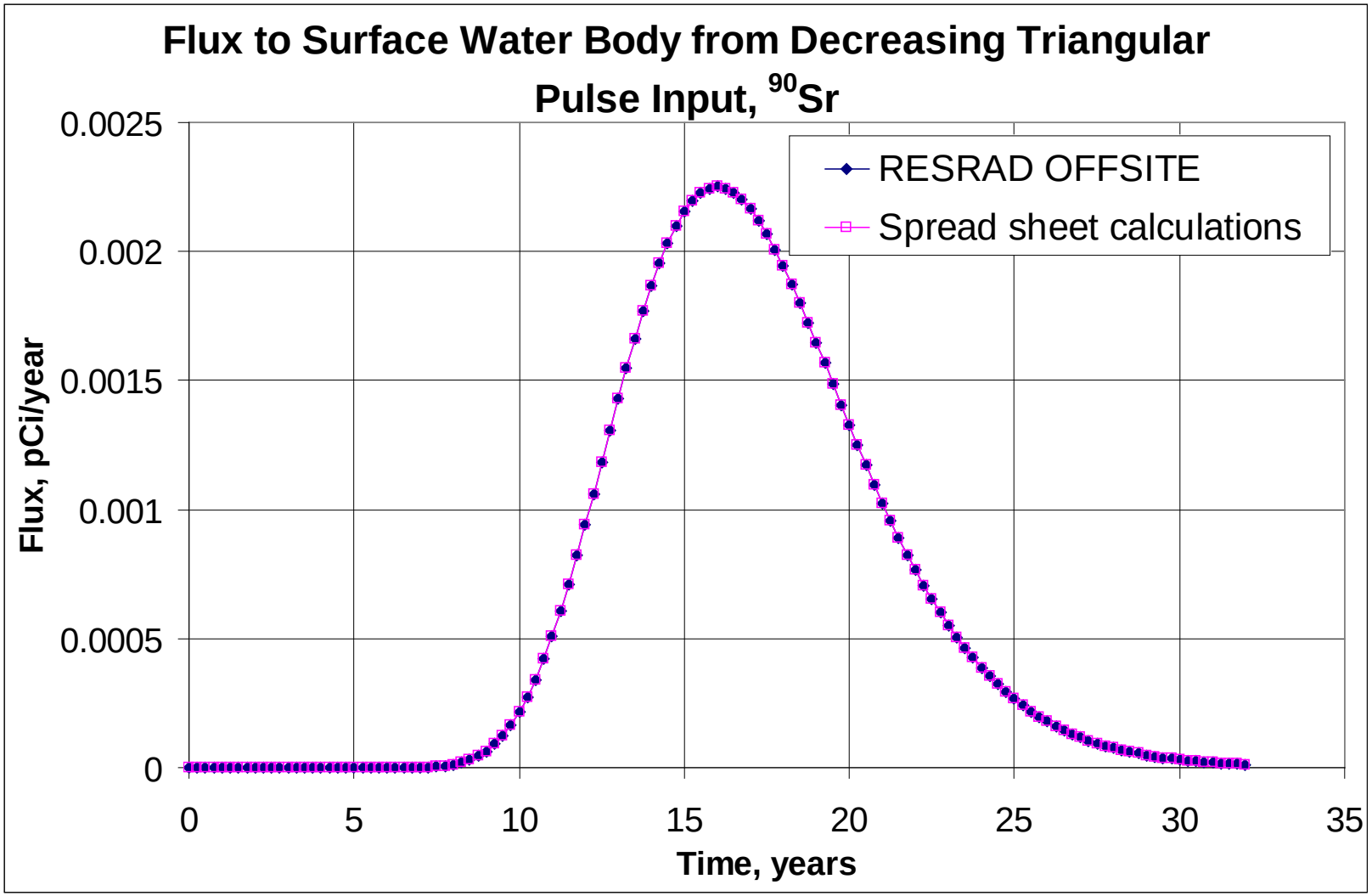

Figure 3-15 Verification of RESRAD-OFFSITE Computed Flux to the Surface Water Body Resulting from a Triangular Input Flux of ^{90}Sr of Unity at Time Zero and of Zero at the First Time Point at the Water Table Using Spreadsheet Calculations

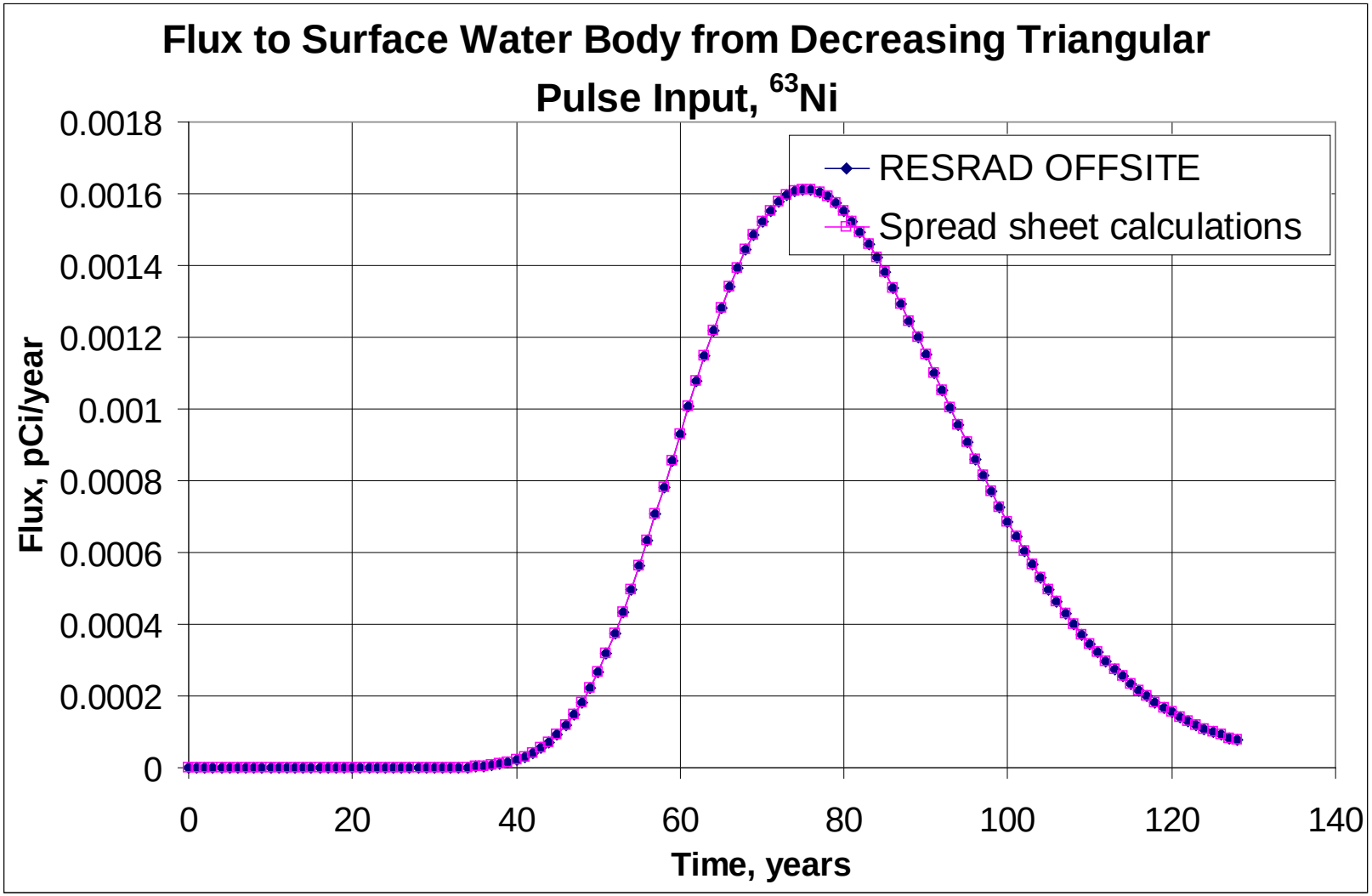

Figure 3-16 Verification of RESRAD-OFFSITE Computed Flux to the Surface Water Body Resulting from a Triangular Input Flux of ^{63}Ni of Unity at Time Zero and of Zero at the First Time Point at the Water Table Using Spreadsheet Calculations

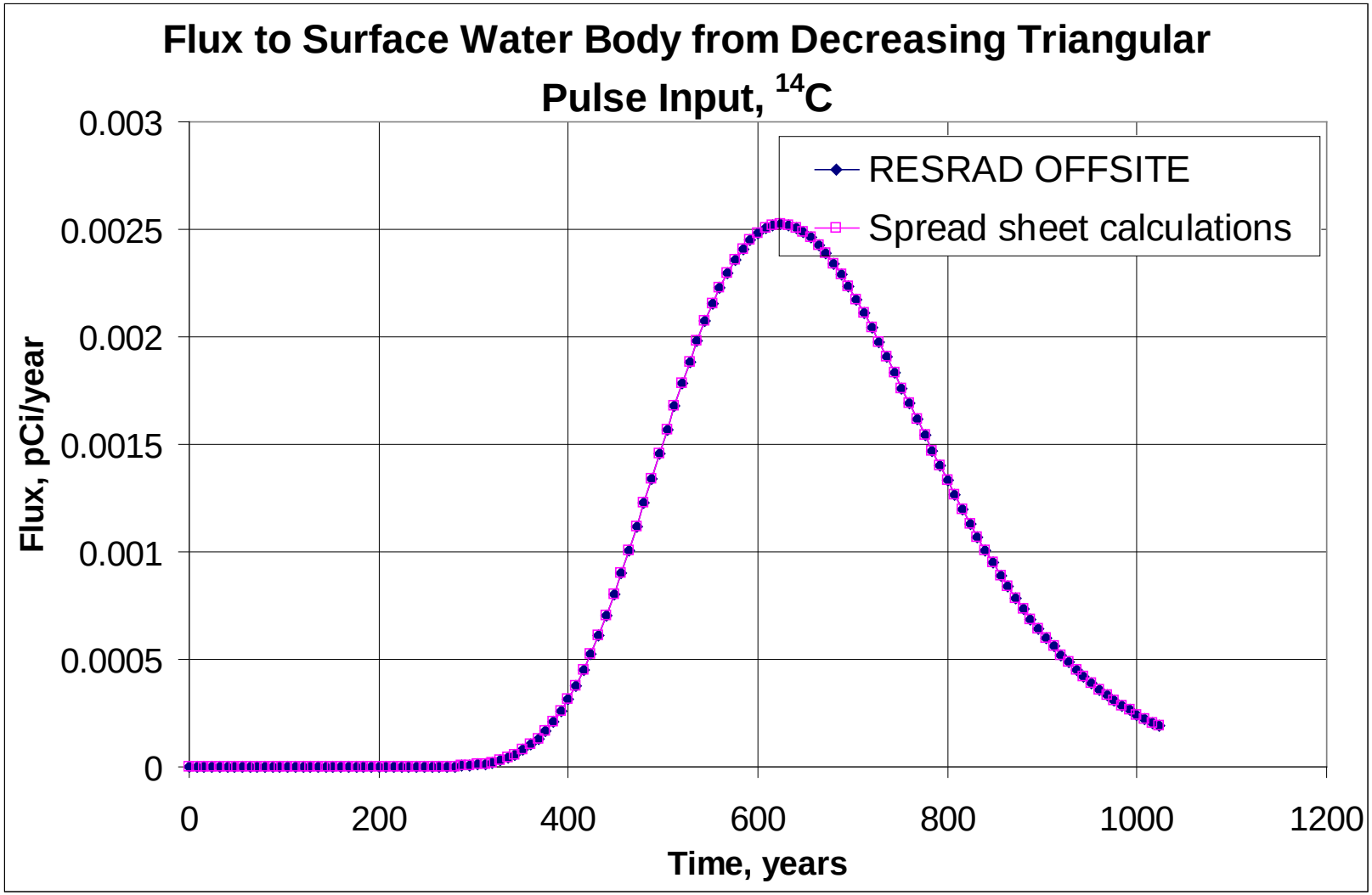

Figure 3-17 Verification of RESRAD-OFFSITE Computed Flux to the Surface Water Body Resulting from a Triangular Input Flux of ^{14}C of Unity at Time Zero and of Zero at the First Time Point at the Water Table Using Spreadsheet Calculations

3.2.2 Output Flux from an Increasing Triangular Input Flux

For the input flux shown in Figure 3-18, the expression for the output flux becomes

$$f_1(x,t_n) = \int_{t_n-t_2}^{t_n-t_1} \left(\frac{t_n - t_1 - \tau}{t_2 - t_1}\right) \frac{V_c e^{-\lambda\tau}}{2L_x} \left[erf\left(\frac{x + \frac{L_x}{2} - V_c\tau}{\sqrt{4D_x^c\tau}}\right) - erf\left(\frac{x - \frac{L_x}{2} - V_c\tau}{\sqrt{4D_x^c\tau}}\right)\right] d\tau$$
$$- \int_{t_n-t_2}^{t_n-t_1} \left(\frac{t_n - t_1 - \tau}{t_2 - t_1}\right) \sqrt{\frac{D_x^c}{4\pi\tau}} \frac{e^{-\lambda\tau}}{L_x} \left[e^{-\frac{\left(x+\frac{L_x}{2}-V_c\tau\right)^2}{4D_x^c\tau}} - e^{-\frac{\left(x-\frac{L_x}{2}-V_c\tau\right)^2}{4D_x^c\tau}} \right] d\tau \quad . \qquad \text{(Eq. 3.9)}$$

This equation was evaluated in Excel files for 128 different values of time, t_n; the integral (convolution, to be more precise) had to be evaluated numerically. The Excel files are described later. The situation was also modeled in the RESRAD-OFFSITE using the inputs shown in Table 3-4. It is not possible to obtain the desired increasing triangular input flux profile (Figure 3-18) using the release model of RESRAD-OFFSITE. The RESRAD-OFFSITE feature allowing an informed user to override the internal release model was utilized for this verification of the transport in the saturated zone. A double triangular input flux shown in Figure 3-19 was specified for the run. The increasing triangular input flux depicted in Figure 3-18 is equivalent to the difference between the double triangular input flux in Figure 3-19 and the decreasing triangular input flux in Figure 3-13 shifted by a time interval. Thus, the output flux corresponding to the increasing triangular input flux (Figure 3-18) is obtained as the difference between the output flux from the double triangular input flux (Figure 3-19) and the output flux from the decreasing triangular flux (Figure 3-13) shifted by a time interval.

Twenty-four (eight nuclides, each at three different distribution coefficients) temporal profiles of output flux were verified. The verification of four of these flux profiles is illustrated in Figures 3-20, 3-21, 3-22, and 3-23.

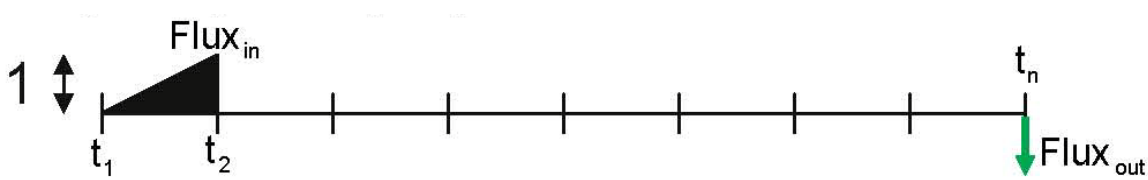

Figure 3-18 Increasing Triangular Input Flux Profile

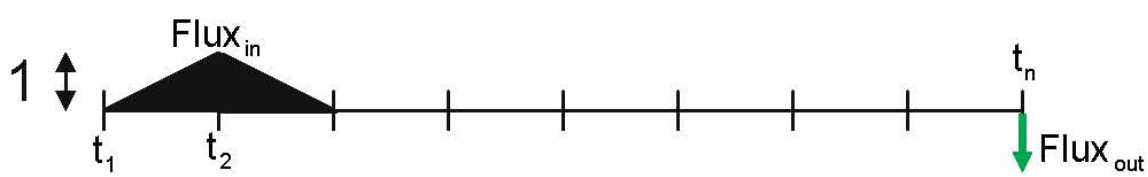

Figure 3-19 Double Triangular Input Flux Profile

3.2.3 Description of the Excel Files Used in This Verification

Three excel files, saturated 0.xls, saturated 1.xls, and saturated 10.xls, one for each value of the distribution coefficient, were used to verify the transport in the saturated zone. The first tab, "Ti," contains the inputs that pertain to transport in the saturated zone and some intermediate calculations; the inputs are in bold. The tabs "AQ 1," "AQ 2," and "AQ 21" are the temporal input fluxes used in RESRAD-OFFSITE and correspond to Figure 3-13, 3-18, and 3-19. "SWF 1" and "SWF 21" are the RESRAD-OFFSITE outputs of flux, out of the saturated zone into the surface water body, corresponding to the input fluxes in tabs "AQ 1" and "AQ 21." The temporal flux in tab "SWF 2" was obtained by subtracting from the fluxes in tab "SWF 21" the fluxes in tab "SWF 1" shifted by a time step.

The tab "Single Nuclide graph" compares the temporal output flux from RESRAD-OFFSITE code with that calculated in the spreadsheet. The comparisons are captured in two plots: the first one, the one at the top, anchored in cell "J4," compares the output flux from a decreasing triangular input flux over the first time interval; the second plot, anchored in cell "J35," compares the output flux from an increasing triangular input flux over the first time interval. The plots pertain to the nuclide shown in cell "C1," plots that pertain to the eight nuclides ^{60}Co, ^{3}H, ^{90}Sr, ^{137}Cs, ^{63}Ni, ^{226}Ra, ^{14}C, and ^{238}U can be viewed by typing in the numbers, 2, 4, 9, 3, 5, 6, 1, and 11, respectively, in cell "A1" and then launching the computational macro by clicking Ctrl-a. The computational macro evaluates the convolutions using numerical integration; the numerical integration method used in the code is described in Section 3.3.14 of the RESRAD-OFFSITE User's Manual. Note that the nuclide name will change in cell "C1" but not in the title of the plots. Plots of all 48 verifications that were performed can be viewed in turn in this fashion. A subset of these plots were shown in Figures 3-14 to 3-17 and 3-20 to 3-23.

3.3 Verification of Transport in the Saturated Zone to the Well

The general equation that needs to be verified is the dispersive-advective transport Eq. 3.71 of the RESRAD-OFFSITE User's Manual. This equation is reproduced below.

$$c_{well}(x_w, y_w, t_0) = c_{w,z} c_{w,y}(y_w) \frac{V_c}{2V_d L_y L_z L_x} \int_0^{t_n} f_{wt}(t_n - \tau)$$

$$\times\ e^{-\lambda\tau} \left[erf\left(\frac{x_w + L_x/2 - V_c\tau}{\sqrt{4D_x^c \tau}} \right) - erf\left(\frac{x_w - L_x/2 - V_c\tau}{\sqrt{4D_x^c \tau}} \right) \right] d\tau\,, \qquad \text{(Eq. 3.10)}$$

where:

$$c_{w,y}(y_w) = \frac{\sqrt{D_y^c t_p}}{\phi_w} \left(Interf\ \frac{2y_w + \phi_w + L_y}{\sqrt{16 D_y^c t_p}} - Interf\ \frac{2y_w + \phi_w - L_y}{\sqrt{16 D_y^c t_p}} - \right.$$

$$\left. Interf\ \frac{2y_w - \phi_w + L_y}{\sqrt{16 D_y^c t_p}} + Interf\ \frac{2y_w - \phi_w - L_y}{\sqrt{16 D_y^c t_p}} \right)$$

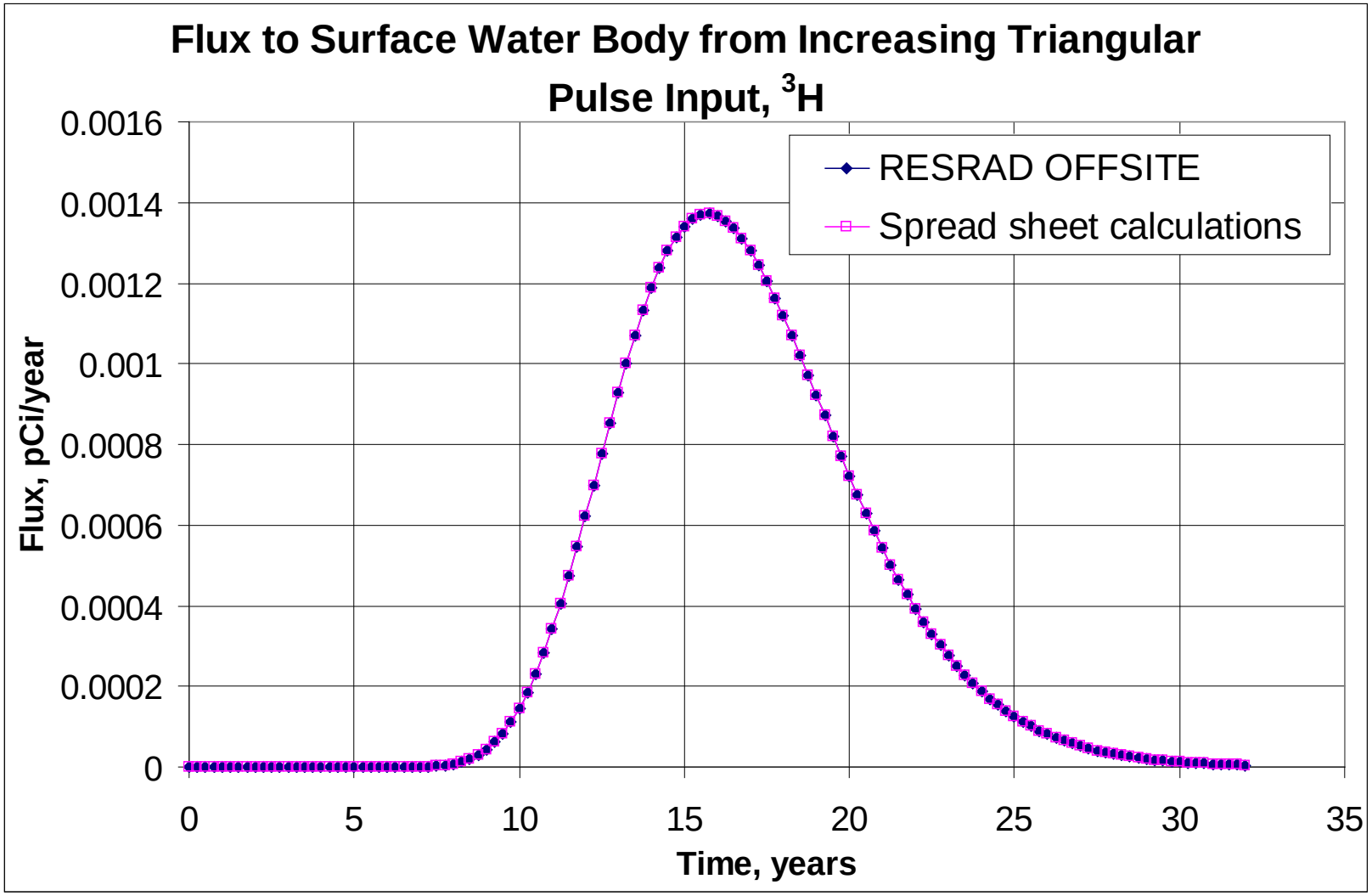

Figure 3-20 Verification of RESRAD-OFFSITE Computed Flux to the Surface Water BodyFResulting from a Triangular Input Flux of ^{3}H of Zero at Time Zero and of Unity at the First Time Point at the Water Table Using Spreadsheet Calculations

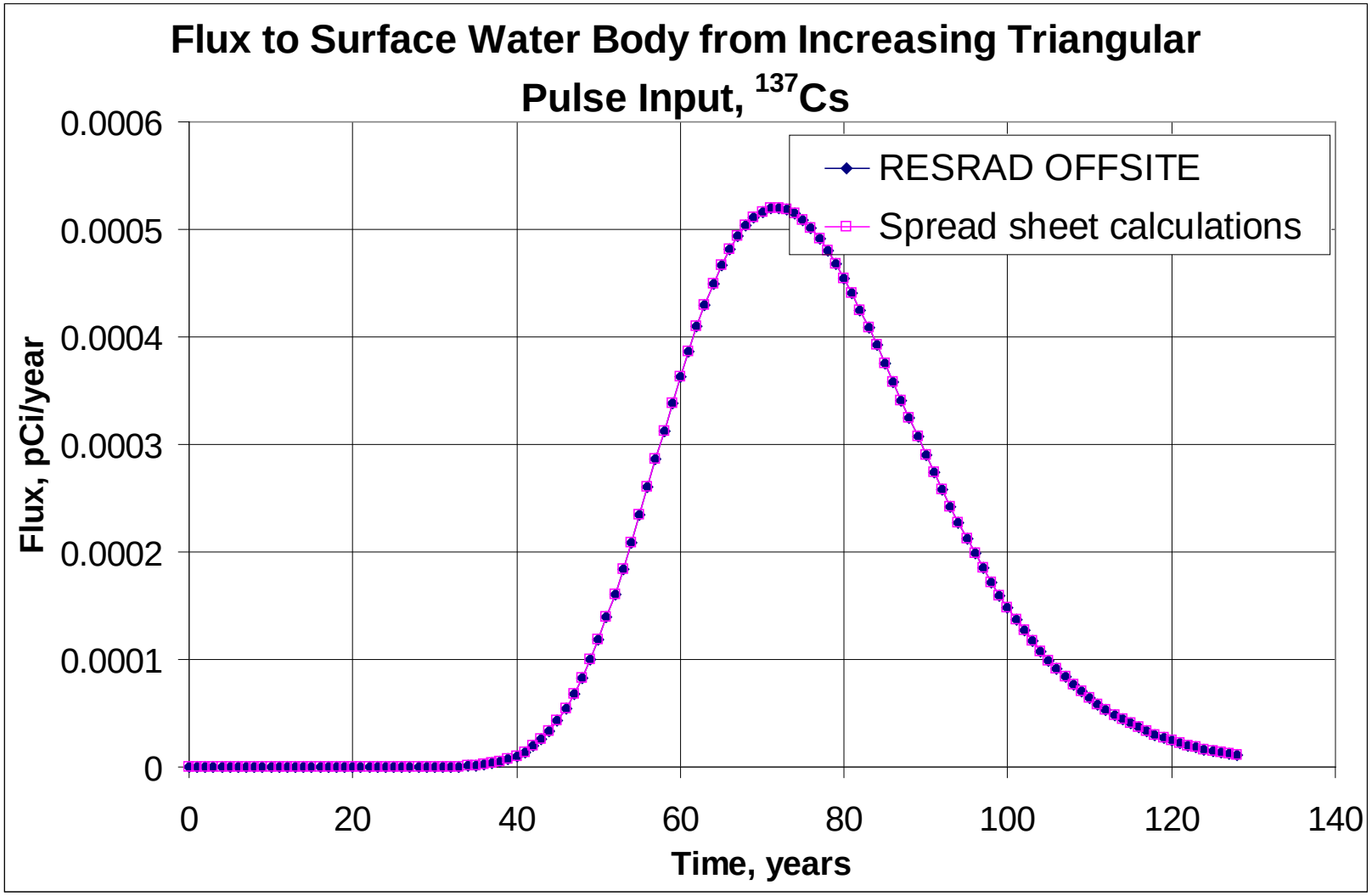

Figure 3-21 Verification of RESRAD-OFFSITE Computed Flux to the Surface Water Body Resulting from a Triangular Input Flux of ^{137}Cs of Zero at Time Zero and of Unity at the First Time Point at the Water Table Using Spreadsheet Calculations

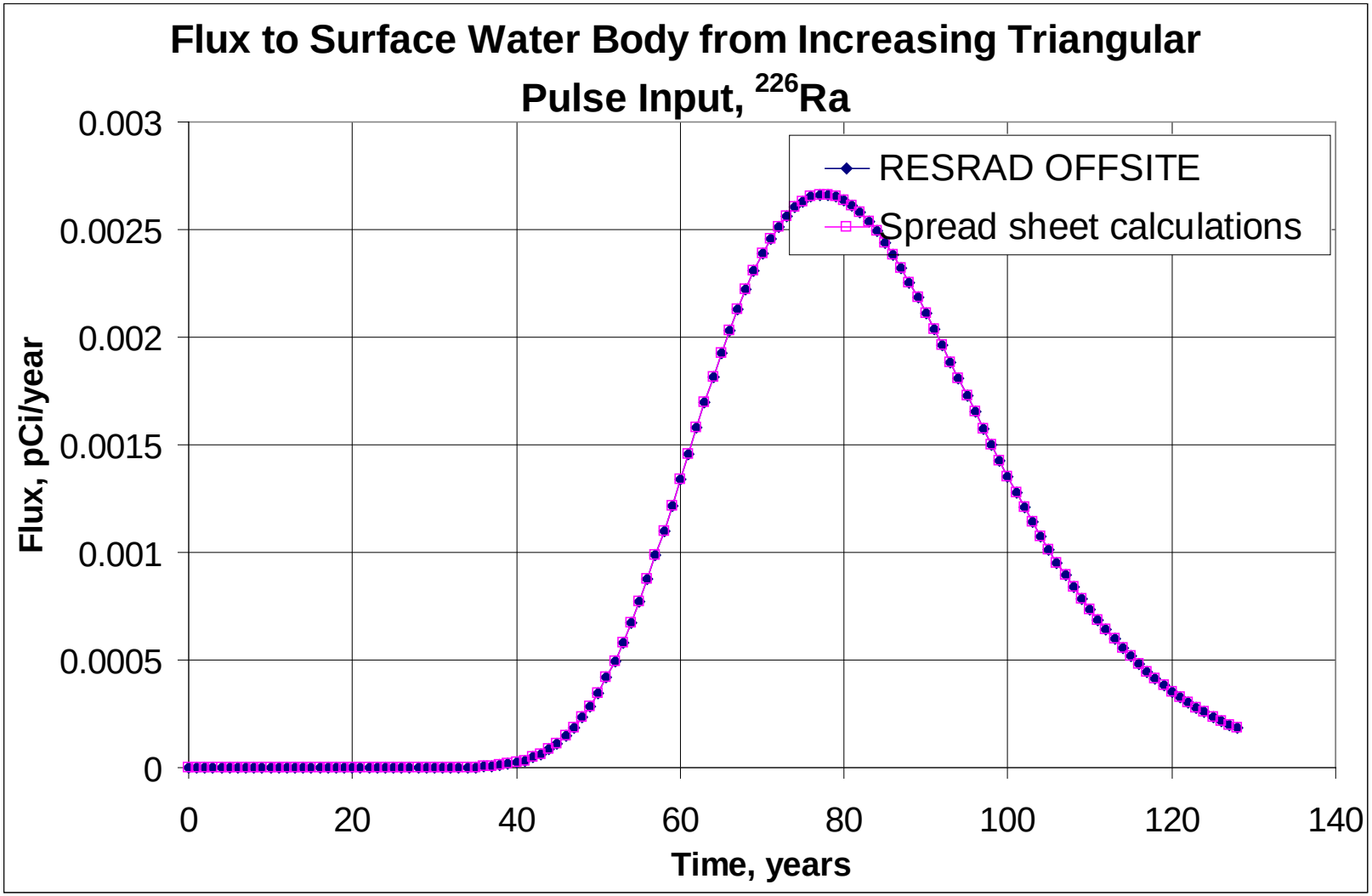

Figure 3-22 Verification of RESRAD-OFFSITE Computed Flux to the Surface Water Body Resulting from a Triangular Input Flux of ^{226}Ra of Zero at Time Zero and of Unity at the First Time Point at the Water Table Using Spreadsheet Calculations

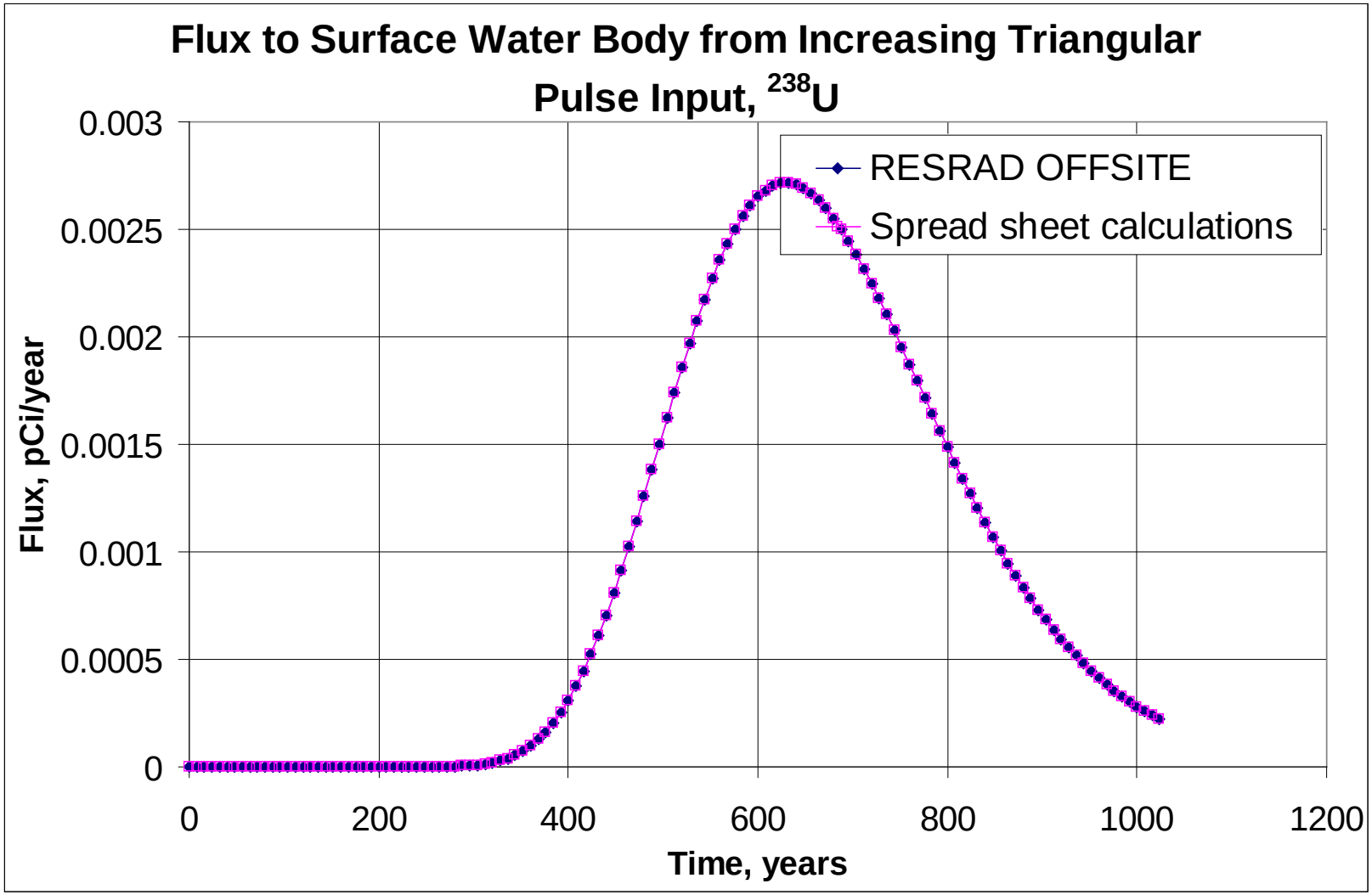

Figure 3-23 Verification of RESRAD-OFFSITE Computed Flux to the Surface Water Body Resulting from a Triangular Input Flux of ^{238}U of Zero at Time Zero and of Unity at the First Time Point at the Water Table Using Spreadsheet Calculations

and

$$c_{w,z} = \frac{\sqrt{D_z^c t_p}}{d_w}\left(Interf\,\frac{d_w + L_z}{\sqrt{4D_z^c t_p}} - Interf\,\frac{d_w - L_z}{\sqrt{4D_z^c t_p}} - Interf\,\frac{L_z}{\sqrt{4D_z^c t_p}} + Interf\,\frac{-L_z}{\sqrt{4D_z^c t_p}} \right)$$

This is the concentration in a well located at a distance x_w from the center of the primary contamination at time t_n, due to the input flux $f_{wt}(t)$ at the water table.

The convolution is simplified to the two expressions (Eqs. 3.72 and 3.73) for the two triangular input fluxes considered in the previous sections.

$$f_1(x, t_n - t_m) = \int_{t_n - t_m}^{t_n - t_{m-1}} \left(\frac{t_n - t_{m-1} - \tau}{t_m - t_{m-1}} \right) \frac{V_c e^{-\lambda\tau}}{2L_x V_d L_y L_z} \left[erf\left(\frac{x + L_x/2 - V_c\tau}{\sqrt{4D_x^c \tau}} \right) - erf\left(\frac{x - L_x/2 - V_c\tau}{\sqrt{4D_x^c \tau}} \right) \right] d\tau$$

(Eq. 3.11)

$$f_2(x, t_n - t_{m-1}) = \int_{t_n - t_m}^{t_n - t_{m-1}} \left(\frac{\tau - t_n + t_m}{t_m - t_{m-1}} \right) \frac{V_c e^{-\lambda\tau}}{2L_x V_d L_y L_z} \left[erf\left(\frac{x + L_x/2 - V_c\tau}{\sqrt{4D_x^c \tau}} \right) - erf\left(\frac{x - L_x/2 - V_c\tau}{\sqrt{4D_x^c \tau}} \right) \right] d\tau$$

The first is due to the input flux that increases linearly from zero at time t_{m-1} to one at time t_m. The second is due to the input flux that decreases linearly from one at time t_{m-1} to zero at time t_m.

The concentrations of eight different nuclides (Table 3-1) that represent a wide spectrum of half-lives were verified. The values used for the RESRAD-OFFSITE inputs that pertain to modeling the transport in the saturated zone to the well are in Table 3-5. The inputs are in bold, while the intermediate calculations are in italics. Three different runs with three different distribution coefficients were used for each of the nuclides to cover a wide range of conditions in this verification of transport in the saturated zone. Even so, this verification is not exhaustive; the Excel file that was used in this verification is available to verify other cases, should the need arise.

3.3.1 Output Flux from a Decreasing Triangular Input Flux

For the decreasing input flux profile shown in Figure 3-24, the expression for the concentration in the well becomes

$$f_2(x, t_n) = \frac{1}{V_d L_y L_z} \frac{V_c}{2L_x} \int_{t_n - t_2}^{t_n - t_1} \left(\frac{\tau - t_n + t_2}{t_2 - t_1} \right) e^{-\lambda\tau} \left[erf\left(\frac{x + L_x/2 - V_c\tau}{\sqrt{4D_x^c \tau}} \right) - erf\left(\frac{x - L_x/2 - V_c\tau}{\sqrt{4D_x^c \tau}} \right) \right] d\tau\,.$$

(Eq. 3.12)

This equation was evaluated in Excel files for 128 different values of time, t_n; the integral (convolution, to be more precise) had to be evaluated numerically. The Excel files are described later. The situation was also modeled in the RESRAD-OFFSITE code using the inputs shown in Table 3-5. In addition, the erosion rate of the contaminated zone was increased so that the contaminated zone erodes away before the

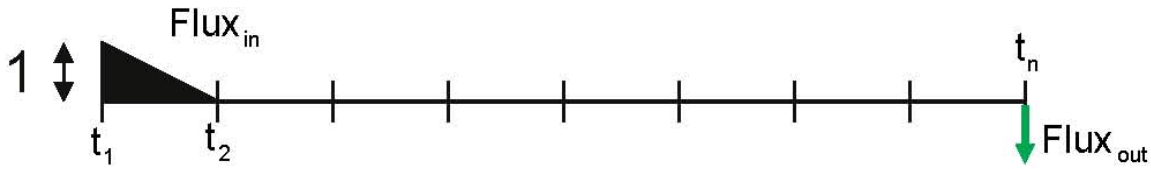

Figure 3-24 Decreasing Triangular Input Flux Profile

Table 3-5 RESRAD-OFFSITE Inputs and Intermediate Calculations That Pertain to Transport in the Saturated Zone to the Well

Average transport distance	x (m)	**850**		
Length of contamination	L_x (m)	**100**		
Width of contamination	L_y (m)	**100**		
Saturated hydraulic conductivity	K_{sat} (m/yr)	**500**		
Hydraulic gradient		**.02**		
Darcy velocity	V_d (m/yr)	*10*		
Infiltration rate	I (m/yr)	*0.5*		
Depth of initial penetration of the contamination into the saturated zone	L_z (m)	*5*		
Total porosity	p_t	**0.4**		
Effective porosity	p_e	**0.2**		
Dry bulk density	ρ_b (g/cc)	**1.5**		
Distribution coefficient	K_d (cc/g)	**0**	**1**	**10**
Retardation factor	R_d	*1*	*4.75*	*38.5*
Contaminant transport velocity	V_c (m/yr)	*50*	*10.53*	*1.299*
Longitudinal dispersivity	d_x (m)	**20**		
Longitudinal dispersion coefficient of contaminants	D_{cx} (m^2/yr)	*1,000*	*210.5*	*25.97*
Lateral horizontal dispersivity	d_y (m)	**3**		
Lateral horizontal dispersion coefficient of contaminants	D_{cy} (m^2/yr)	*150*	*31.58*	*3.896*
Lateral vertical dispersivity	d_y (m)	**0.15**		
Lateral vertical dispersion coefficient of contaminants	D_{cy} (m^2/yr)	*7.5*	*1.579*	*0.1048*
Time to peak flux	t_p (yr)	*14.5*	*54.3*	*211.9*
Distance from the plum centerline to well	y_w (m)	**0**		
Well pumping rate	U_w (m^3/yr)	**5,100**		
Depth of aquifer intercepted by well	d_w (m)	**5**		
Width of aquifer intercepted by well	ϕ_w (m)	*51*		
Time horizon	(years)	**32**	**128**	**1024**
Number of time points		**128**		

second time point. This produces the desired triangular input flux. Twenty-four (eight nuclides, each at three different distribution coefficients) temporal profiles of output flux were verified. The verification of four of these flux profiles is illustrated in Figures 3-25, 3-26, 3-27, and 3-28.

3.3.2 Output Flux from an Increasing Triangular Input Flux

For the increasing input flux profile shown in Figure 3-29, the expression for the concentration in the well then becomes

$$f_1(x,t_n) = \frac{1}{V_d L_y L_z} \frac{V_c}{2L_x} \int_{t_n - t_2}^{t_n - t_1} \left(\frac{t_n - t_1 - \tau}{t_2 - t_1} \right) e^{-\lambda\tau} \left[erf\left(\frac{x + L_x/2 - V_c\tau}{\sqrt{4D_x^c \tau}} \right) - erf\left(\frac{x - L_x/2 - V_c\tau}{\sqrt{4D_x^c \tau}} \right) \right] d\tau$$

(Eq. 3.13)

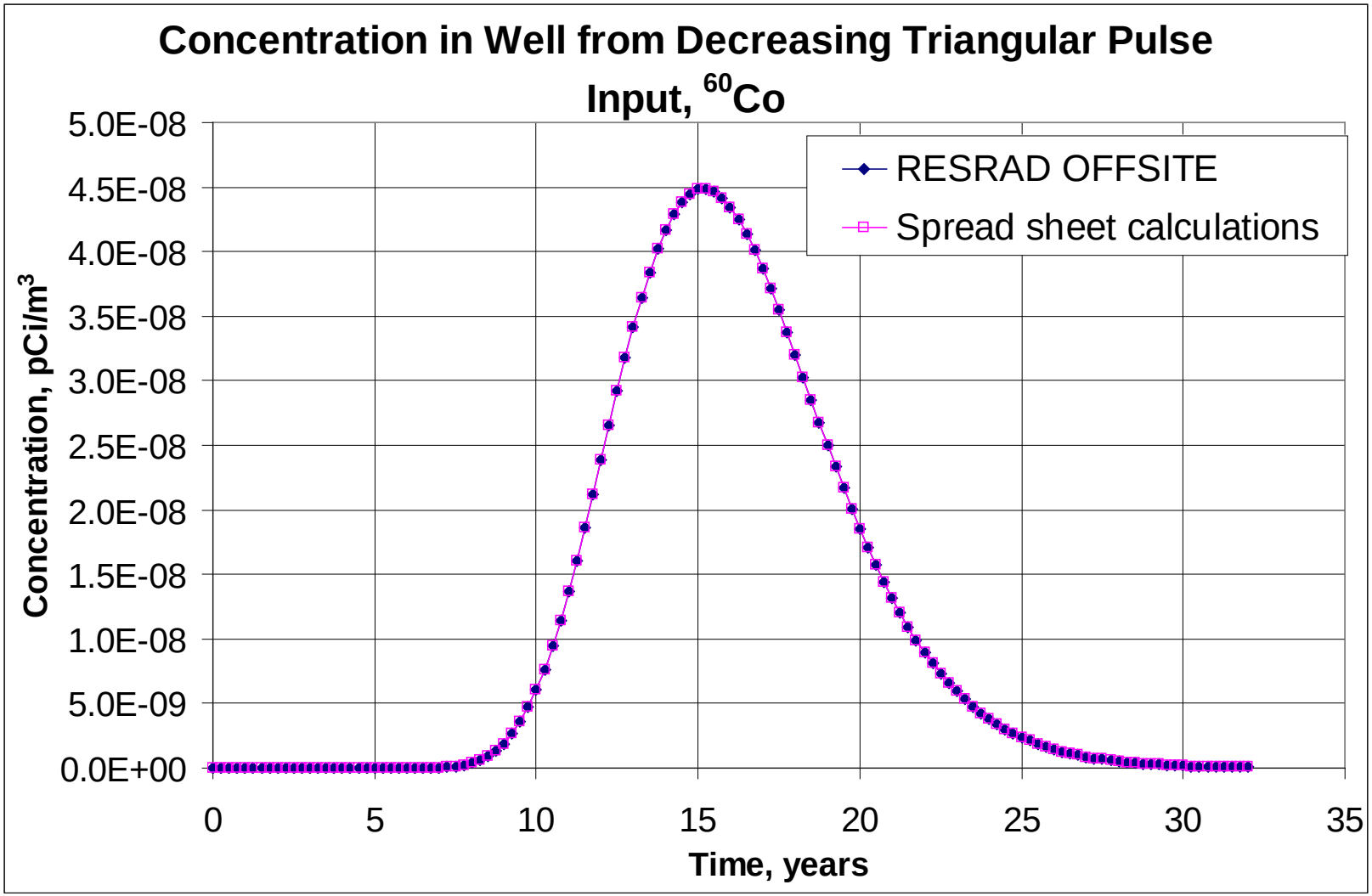

Figure 3-25 Verification of RESRAD-OFFSITE Computed Concentration in the Well Resulting from a Triangular Input Flux of ^{60}Co of Unity at Time Zero and of Zero at the First Time Point at the Water Table Using Spreadsheet Calculations

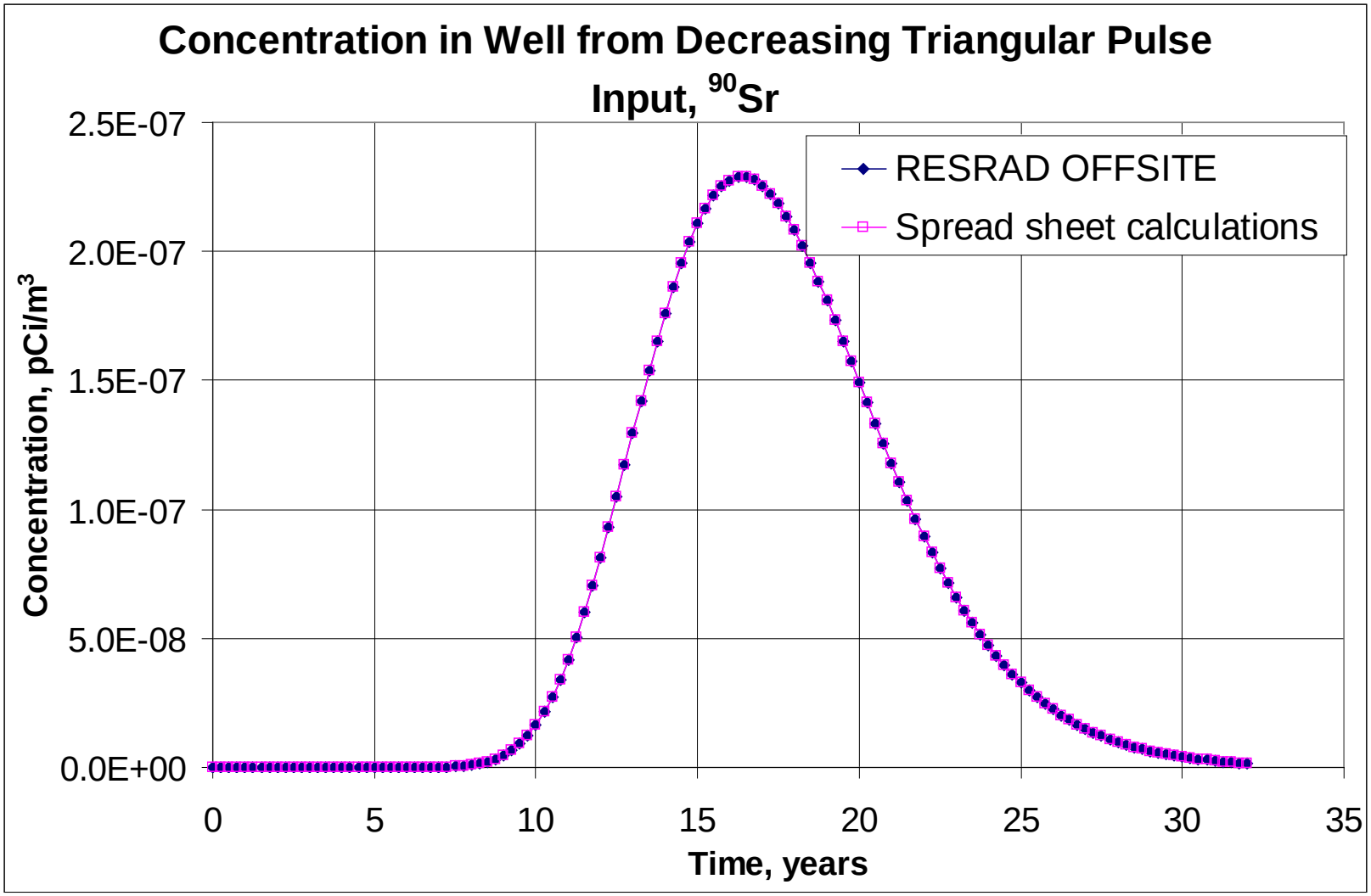

Figure 3-26 Verification of RESRAD-OFFSITE Computed Flux Concentration in the Well Resulting from a Triangular Input Flux of ^{90}Sr of Unity at Time Zero and of Zero at the First Time Point at the Water Table Using Spreadsheet Calculations

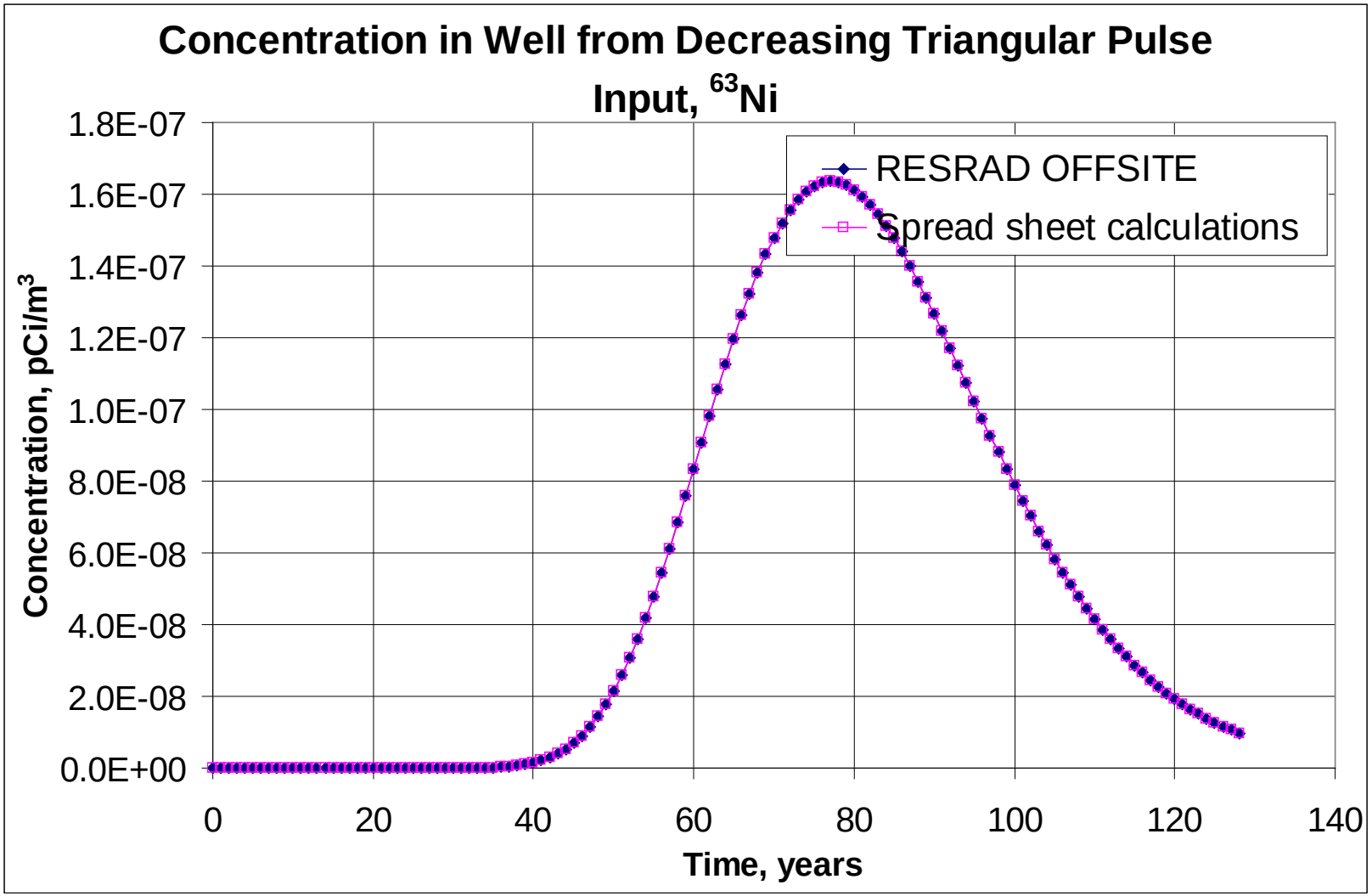

Figure 3-27 Verification of RESRAD-OFFSITE Computed Concentration in the Well Resulting from a Triangular Input Flux of ^{63}Ni of Unity at Time Zero and of Zero at the First Time Point at the Water Table Using Spreadsheet Calculations

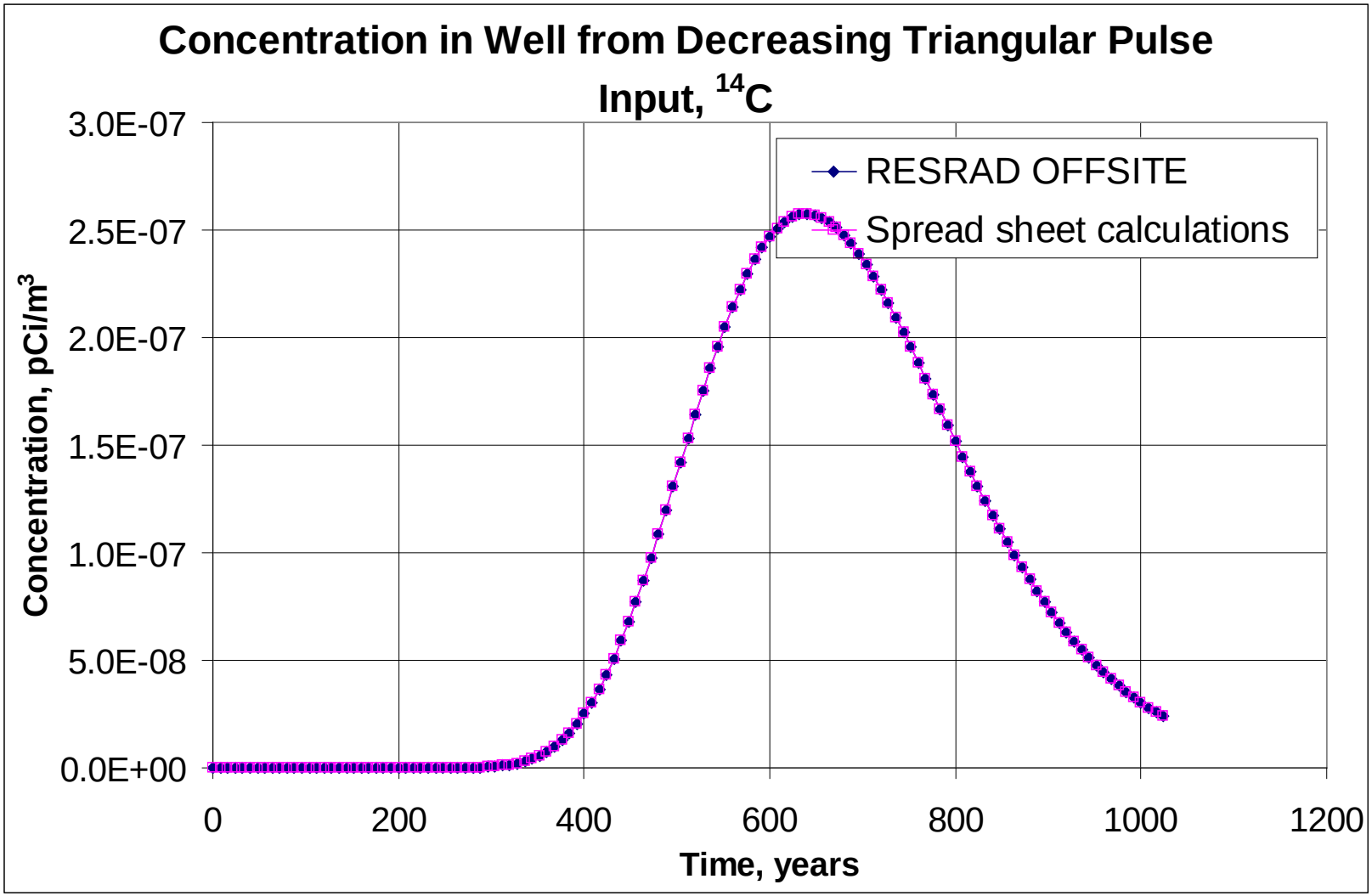

Figure 3-28 Verification of RESRAD-OFFSITE Computed Concentration in the Well Resulting from a Triangular Input Flux of ^{14}C of Unity at Time Zero and of Zero at the First Time Point at the Water Table Using Spreadsheet Calculations

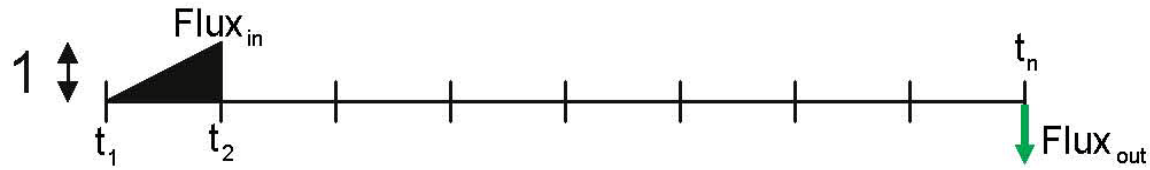

Figure 3-29 Increasing Triangular Input Flux Profile

This equation was evaluated in Excel files for 128 different values of time, t_n; the integral (convolution, to be more precise) had to be evaluated numerically. The Excel files are described later. The situation was also modeled in the RESRAD-OFFSITE code using the inputs shown in Table 3-5. It is not possible to obtain the desired increasing triangular input flux profile (Figure 3-29) using the release model of RESRAD-OFFSITE. The RESRAD-OFFSITE feature allowing an informed user to override the internal release model was utilized for this verification of the transport in the unsaturated zone. A double triangular input flux shown in Figure 3-30 was specified for the run. The increasing triangular input flux depicted in Figure 3-29 is equivalent to the difference between the double triangular input flux in Figure 3-30 and the decreasing triangular input flux in Figure 3-24 shifted by a time interval. Thus the output flux corresponding to the increasing triangular input flux (Figure 3-29) is obtained as the difference between the output flux from the double triangular input flux (Figure 3-30) and the output flux from the decreasing triangular flux (Figure 3-24) shifted by a time interval. Twenty-four (eight nuclides, each at three different distribution coefficients) temporal profiles of output flux were verified. The verification of four of these flux profiles is illustrated in Figures 3-31, 3-32, 3-33, and 3-34.

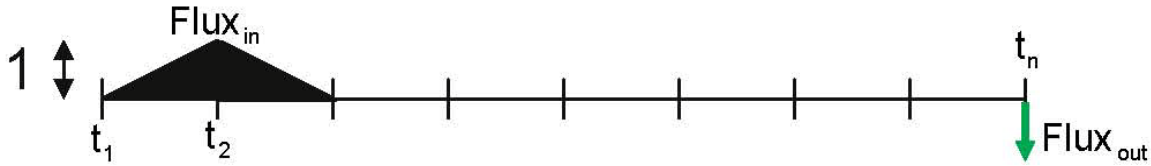

Figure 3-30 Double Triangular Input Flux Profile

3.3.3 Description of the Excel Files Used in This Verification

Three Excel files, saturated 0.xls, saturated 1.xls, and saturated 10.xls, one for each value of the distribution coefficient, were used to verify the transport in the saturated zone. The first tab, "Ti," contains the inputs that pertain to transport in the saturated zone and some intermediate calculations; the inputs are in bold. The tabs "AQ 1," "AQ 2," and "AQ 21" are the temporal input fluxes used in RESRAD-OFFSITE and correspond to Figures 3-24, 3-29, and 3-30. Tabs "WellConc 1" and "WellConc 21" are the RESRAD-OFFSITE concentrations in the well corresponding to the input fluxes in tabs "AQ 1" and "AQ 21." The temporal concentration in tab "WellConc 2" was obtained by subtracting from the concentrations in tab "WellConc 21" the concentrations in tab "WellConc 1" shifted by a time step.

The tab "Single Nuclide graph" compares the temporal concentrations from RESRAD-OFFSITE with that calculated in the spreadsheet. The comparisons are captured in two plots: the first one, anchored in cell "J66", compares the concentration in the well from a decreasing triangular input flux over the first time interval; the second plot, anchored in cell "J97," compares the concentration in the well from a increasing triangular input flux over the first time interval. The plots pertain to the nuclide shown in cell "C1"; plots

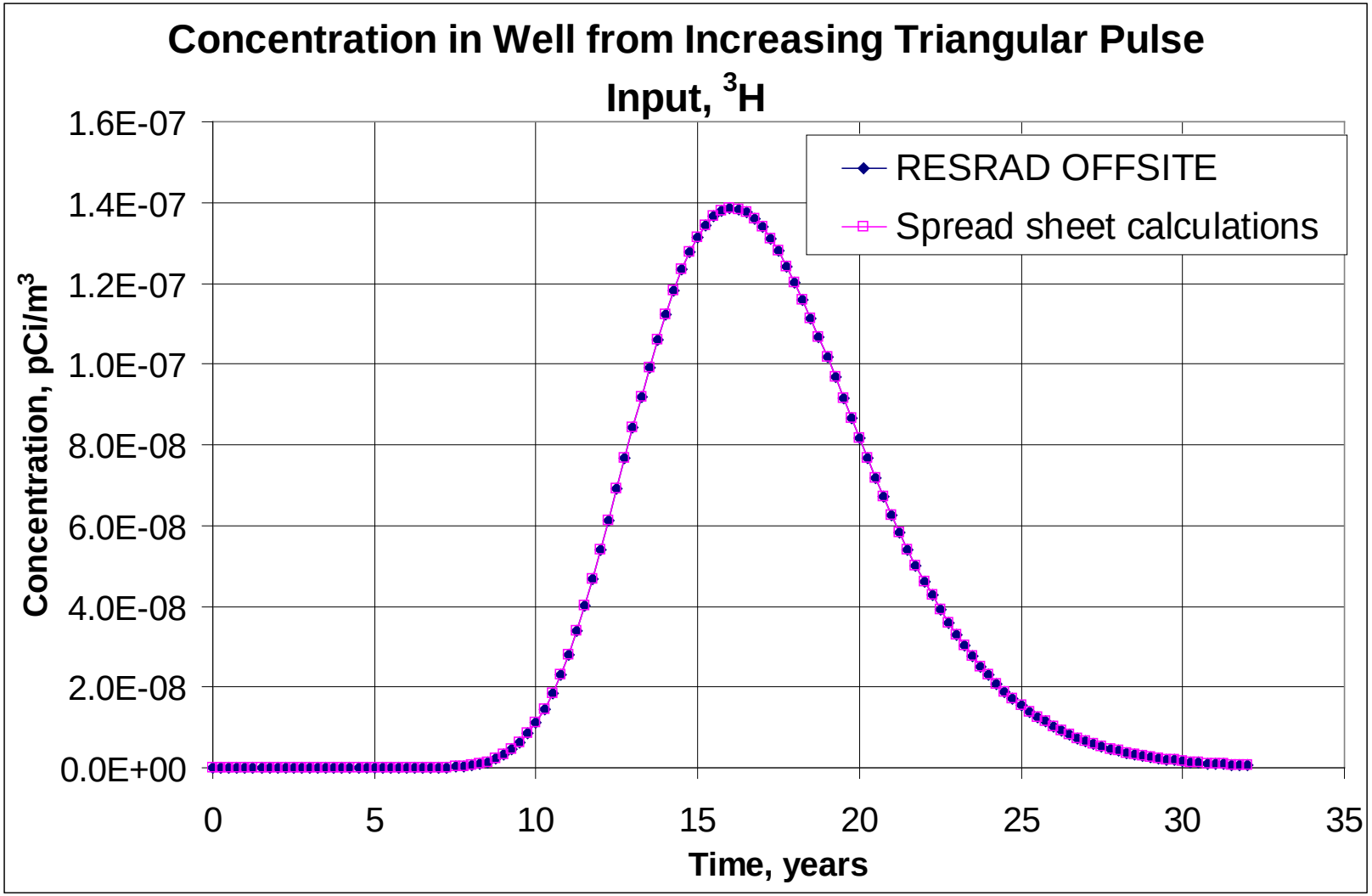

Figure 3-31 Verification of RESRAD-OFFSITE Computed Flux Concentration in the Well Resulting from a Triangular Input Flux of ^{3}H of Zero at Time Zero and of Unity at the First Time Point at the Water Table Using Spreadsheet Calculations

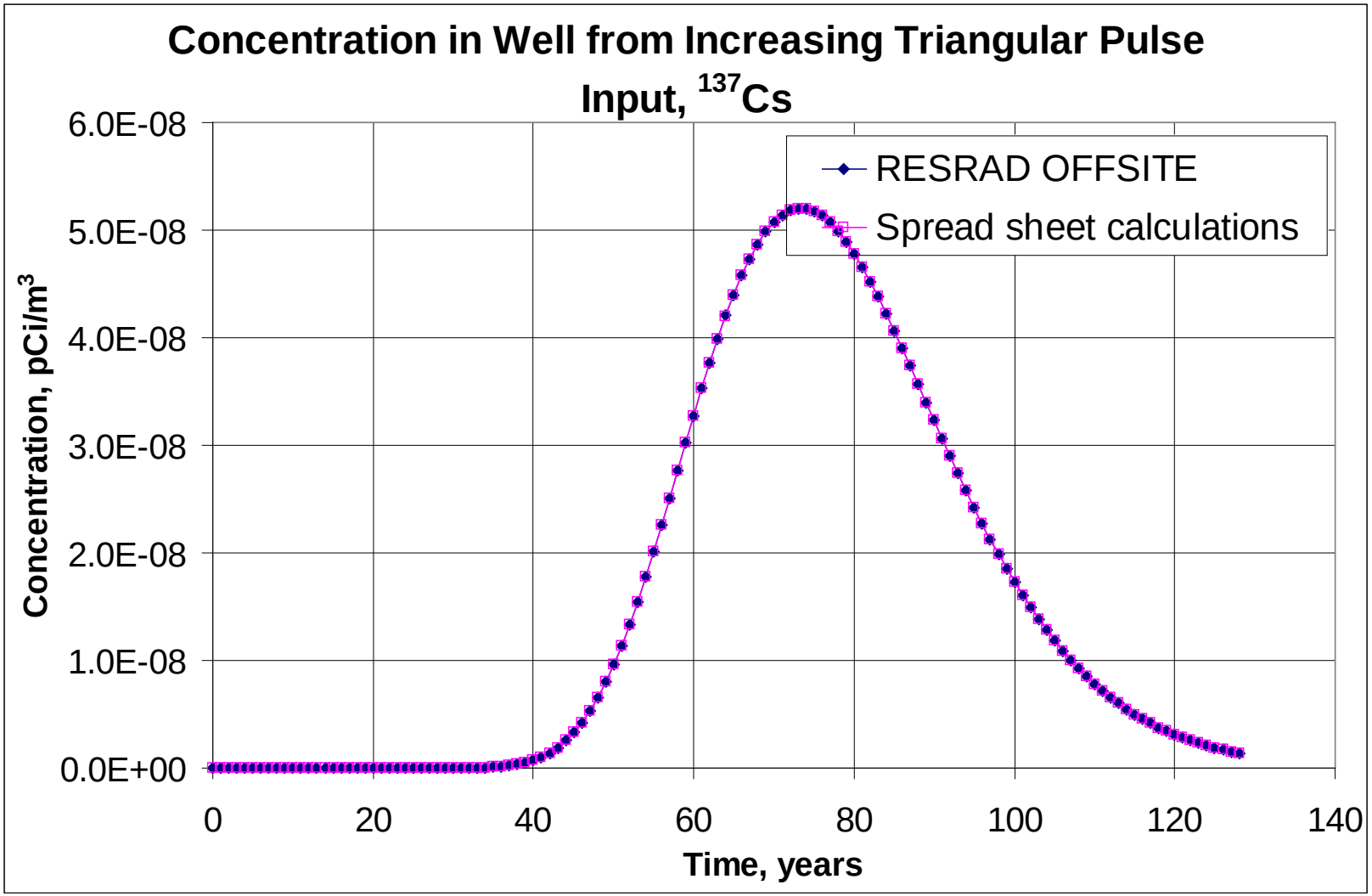

Figure 3-32 Verification of RESRAD-OFFSITE Computed Flux Concentration in the Well Resulting from a Triangular Input Flux of ^{137}Cs of Zero at Time Zero and of Unity at the First Time Point at the Water Table Using Spreadsheet Calculations

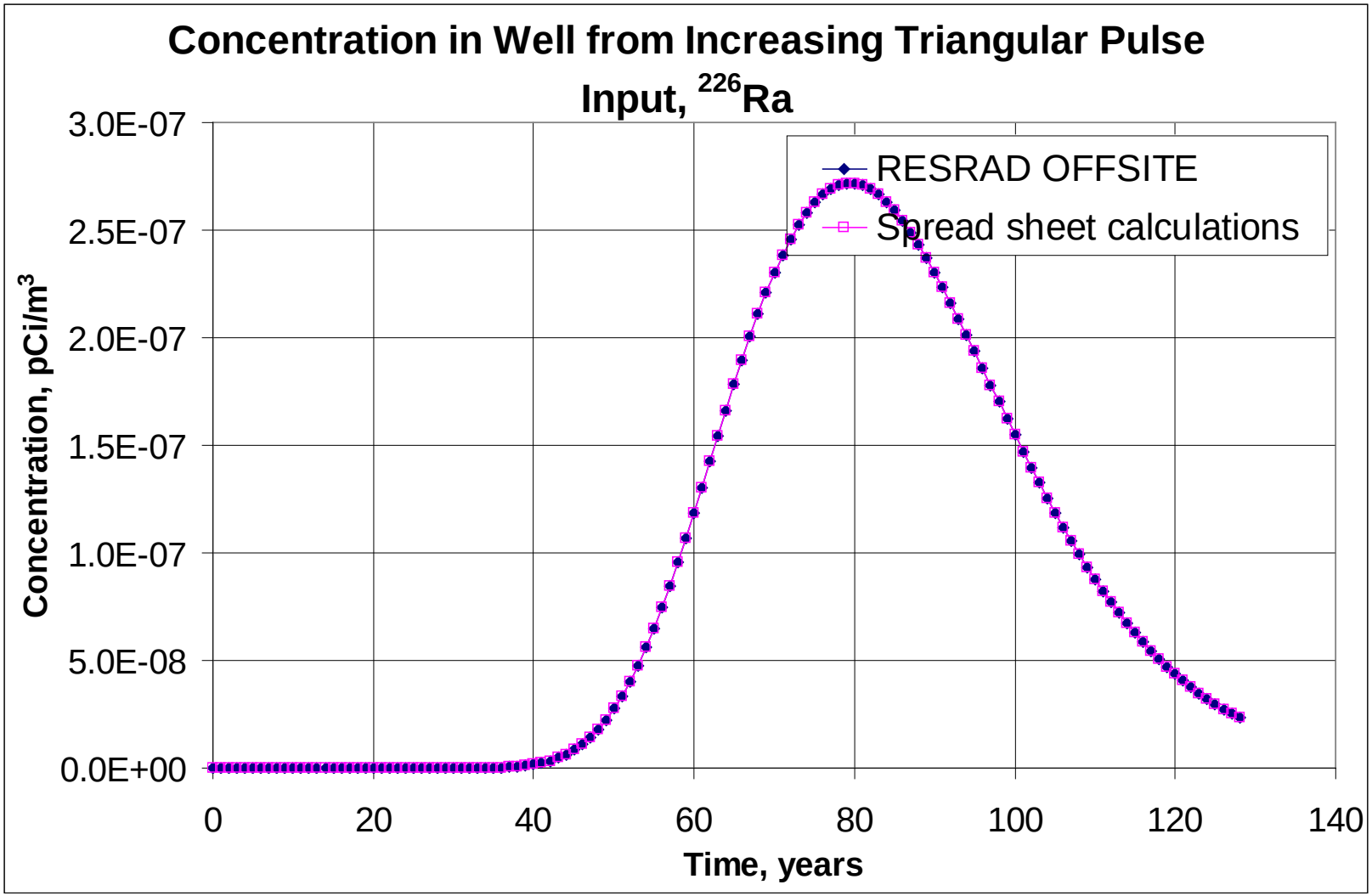

Figure 3-33 Verification of RESRAD-OFFSITE Computed Flux Concentration in the Well Resulting from a Triangular Input Flux of ^{226}Ra of Zero at Time Zero and of Unity at the First Time Point at the Water Table Using Spreadsheet Calculations

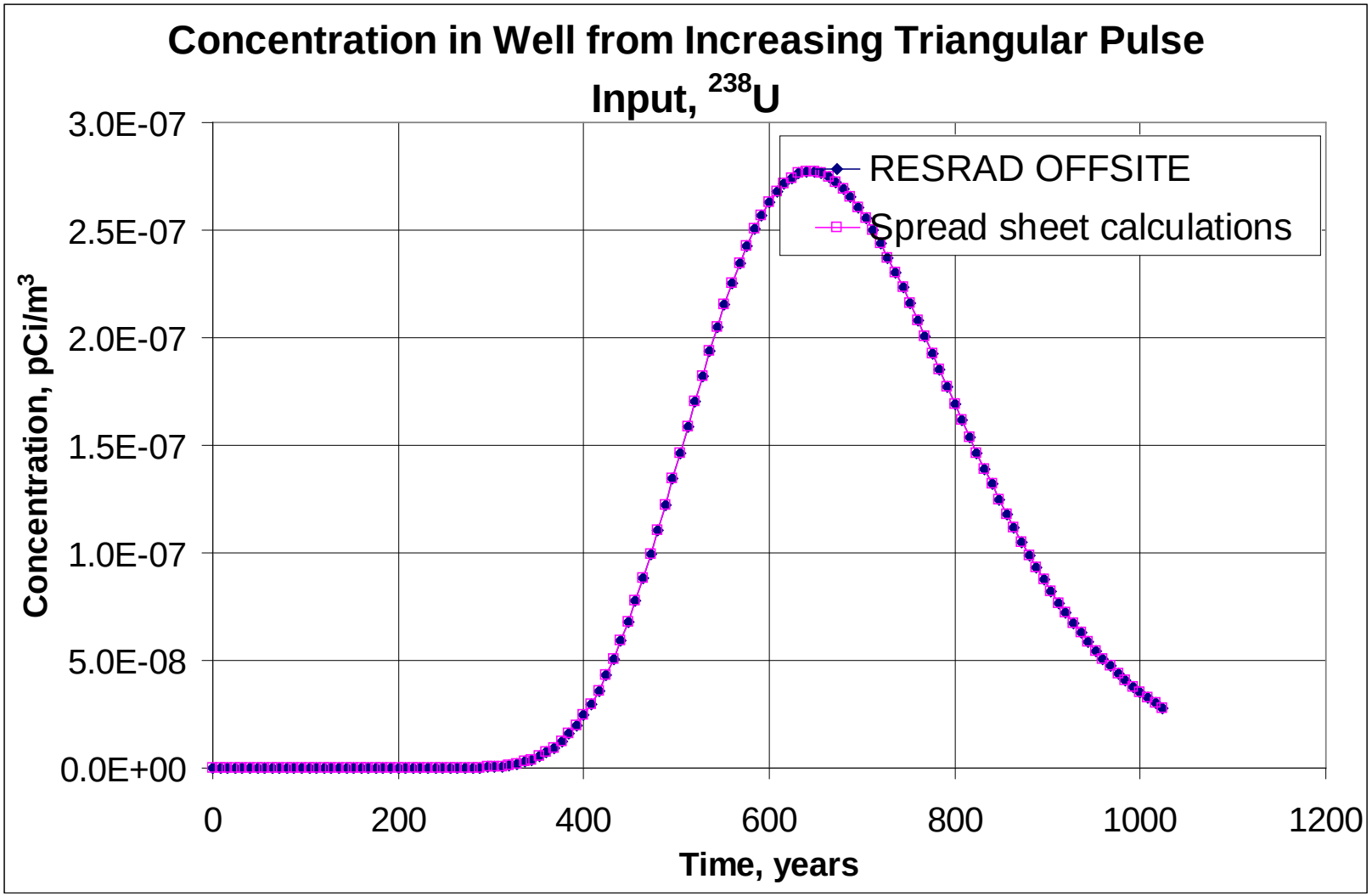

Figure 3-34 Verification of RESRAD-OFFSITE Computed Flux Concentration in the Well Resulting from a Triangular Input Flux of ^{238}U of Zero at Time Zero and of Unity at the First Time Point at the Water Table Using Spreadsheet Calculations

that pertain to the eight nuclides ^{60}Co, ^{3}H, ^{90}Sr, ^{137}Cs, ^{63}Ni, ^{226}Ra, ^{14}C, and ^{238}U can be viewed by typing in the numbers 2, 4, 9, 3, 5, 6, 1, and 11, respectively, in cell "A1" and then launching the computational macro by clicking Ctrl-a. The computational macro evaluates the convolutions using numerical integration; the numerical integration method used in the code is described in Section 3.3.14 of the RESRAD-OFFSITE User's Manual. Note that the nuclide name will change in cell "C1" but not in the title of the plots. Plots of all 48 verifications that were performed can be viewed in turn in this fashion. A subset of these plots were shown in Figures 3-25 through 3-34.

4.0 ATMOSPHERIC TRANSPORT MODEL

The atmospheric transport model used in RESRAD-OFFSITE is a Gaussian plume dispersion model based on an area source release. The model is used to estimate the normalized air concentrations at area locations downwind of a contaminated site. Details of the model are presented in Yu et al. (2007). This section presents the results of the verification study performed to show that the model was implemented correctly in the RESRAD-OFFSITE code.

RESRAD-OFFSITE assumes separate primary contamination source and receptor areas. For the calculation of downwind air concentrations, the source and receptor areas are first partitioned into grids having 1-m square resolution or greater. The center point of each grid square is used as the source or receptor point representing that small area. Air concentration calculations are performed for each receptor grid square for emissions from every source grid square, with an average chronic air concentration then calculated for each receptor grid square. The average air concentration over the entire receptor area is then taken to be the average value over all receptor grid squares. Each point-to-point calculation uses the appropriate wind direction and frequency for the specific points involved. Thus, no area source approximations are used. Rather, a series of point-to-point calculations are performed using a standard sector-averaged Gaussian plume equation. The proper evaluation of the point-to-point calculations is verified in Section 4.1. Section 4.2 examines the concentration averaging over the entire receptor area.

4.1 Sector-Average Gaussian Plume Model

An arbitrary set of baseline conditions were used to exercise a range of calculations in the computer code as shown in Table 4-1. The point-to-point calculations assumed source and receptor areas of 1 m^2. Air concentrations as a function of distance, direction, elevation, and wind frequency were estimated for a single run of the program.

The RESRAD-OFFSITE results were compared against spreadsheets using the code methodology as described in Yu et al. (2007). The normalized air concentrations (χ/Q values) calculated by the program can be found in the CHIOVERQ.OUT file after program execution in the directory containing the executable code. The first set of comparisons, as shown in Table 4-2, assumed a heat release flux (Q_h = 90 cal/s) with a grid spacing of 1 m (90 cal/m^2-s) to exercise the plume rise portion of the code. This value is consistent with heat fluxes from ground surfaces due to solar heating from direct sunlight during the summer months in the western United States on a clear day (NREL 2008).

The results in Table 4-2 are from three separate runs of the baseline verification input file. Run 1 was performed using Briggs rural dispersion coefficients with no dry or wet deposition assumed. Runs 2 and 3 were performed using the Pasquill-Gifford dispersion coefficients with dry deposition assumed. Wet deposition was not considered in Run 2 but was considered in Run 3. In all three cases, good agreement (< 2% difference) was shown between the RESRAD-OFFSITE results and the parallel spreadsheet calculations, with excellent agreement (about 0.2% or less) for distances of 500 m or greater.

A second set of runs were performed with the same baseline verification input file without the incorporation of plume rise (heat release term set to zero) and all receptor area elevations set to zero. Table 4-3 presents this second set of results, with good agreement (about 1% difference or less) between RESRAD-OFFSITE and independent spreadsheet results. In all cases, Runs 1 through 6, the differences in results could be considered to be within round-off error. Some differences may be due partially to the use of different integration methods in RESRAD-OFFSITE and the spreadsheet calculations, as discussed in the following example of a spreadsheet calculation.

Table 4-1 Baseline Site Layout and Atmospheric Transport Parameters Used to Verify RESRAD-OFFSITE Point-to-Point Air Dispersion Calculations

Receptor Area	Distance[a] (m)	Direction[b]	Elevation[c] (m)	Directional Frequency[d]	Stability Category[e]	Wind Speed (m/s)
Fruit, grain, nonleafy vegetables plot	100	North	0	0.05	A	0.89
Leafy vegetables plot	200	South	5	0.10	B	2.46
Pasture, silage growing area	500	East	10	0.25	D	6.93
Grain fields	1,000	West	15	0.20	C	4.47
Dwelling site	10,000	Northeast	20	0.40	F	9.61

[a] Distance from the release point.

[b] Direction from release point. Direction toward which the wind is blowing.

[c] Elevation with respect to the release point.

[d] Fraction of time the wind is blowing in a particular direction with a specific wind speed under a given stability category.

[e] Pasquill-Gifford atmospheric stability category designations.

An example spreadsheet calculation from the verification spreadsheet is provided here to illustrate the process used to check the proper operation of the RESRAD-OFFSITE air dispersion model. The calculation considered is that for the normalized air concentration over the grain fields in Run 3. The effective release height (Figure 4-1) is first calculated in an iterative process with the effective wind speed (Figure 4-2), which are then used to calculate values for the vertical dispersion coefficient (Figure 4-3) and the downwind depleted source strength (Figure 4-4) due to wet and dry deposition. In Eq. 4.31 (in Figure 4-4), the dry deposition $F(x)$ integral term was evaluated using a Simpson's rule approach in the spreadsheet as a secondary check, whereas it is performed by a Romberg integration routine (Press et al. 1992) in the code. The sector average plume equation shown in Figure 4-5 is then used to calculate the normalized air concentration at the specified location downwind. The equation numbers in the figures refer to their numbering in Yu et al. (2007).

4.2 Area Model

The site layout used for verification of the average normalized air concentration over a downwind receptor area is shown in Figure 4-6. RESRAD-OFFSITE computes the air concentration by averaging the values obtained from point-to-point estimates. In this case, a 30 × 30 m receptor area is centered 70 m north and 15 m east of a release point. With a grid spacing set to 10 m in the atmospheric transport input, the code should split the area into nine 10 × 10 m grids for evaluation. The calculation will involve computing the point-to-point air concentration from the release point to the center of each of the nine 10 × 10 m grid areas, summing the results, and dividing by nine to obtain the average air concentration. To verify proper operation, a separate set of nine individual calculations can be run, a calculation for transport from the release point to each of the nine distinct 10 × 10 m grid areas. The results can be manually summed and divided by nine for comparison with the calculation for the entire 30 × 30 m area with a 10 m grid spacing.

For the verification check, the receptor area was intentionally positioned straddling the dividing line between a wind direction of blowing towards the north and the north-northeast at the receptor

Table 4-2 Comparison of RESRAD-OFFSITE Normalized Air Concentrations (s/m^3) with Spreadsheet Verification Calculations (with Plume Rise)[a]

Receptor Area	Spreadsheet Calculation[b]	Spreadsheet × Directional Frequency[b]	RESRAD-OFFSITE	% Difference
Run 1 – Briggs rural dispersion coefficients, no dry or wet deposition				
Fruit, grain, nonleafy vegetables plot	1.120E-03	5.600E-05	5.683E-05	1.48
Leafy vegetables plot	1.698E-04	1.698E-05	1.690E-05	0.47
Pasture, silage growing area	2.552E-05	6.380E-06	6.391E-06	0.17
Grain fields	6.144E-06	1.229E-06	1.228E-06	0.07
Dwelling site	5.218E-07	2.087E-07	2.087E-07	0.01
Run 2 – Pasquill-Gifford dispersion coefficients with dry deposition, no wet deposition				
Fruit, grain, nonleafy vegetables plot	1.538E-03	7.690E-05	7.807E-05	1.52
Leafy vegetables plot	2.004E-04	2.004E-05	1.992E-05	0.60
Pasture, silage growing area	3.115E-05	7.788E-06	7.797E-06	0.12
Grain fields	7.256E-06	1.451E-06	1.449E-06	0.15
Dwelling site	4.340E-07	1.736E-07	1.737E-07	0.06
Run 3 – Pasquill-Gifford dispersion coefficients with dry and wet deposition				
Fruit, grain, nonleafy vegetables plot	1.512E-03	7.560E-05	7.678E-05	1.56
Leafy vegetables plot	1.980E-04	1.980E-05	1.968E-05	0.61
Pasture, silage growing area	3.082E-05	7.705E-06	7.714E-06	0.12
Grain fields	7.019E-06	1.404E-06	1.401E-06	0.20
Dwelling site	4.273E-07	1.709E-07	1.711E-07	0.11

[a] Note that the number of significant figures used are for comparison purposes only to check the accuracy of the RESRAD-OFFSITE calculations.

[b] The spreadsheet calculations do not incorporate the directional wind frequency, as shown in Table 4-1.

location. Thus, a different portion of the wind frequency data for each stability class in the meteorological data file will be used when calculating air concentrations within the north and north-northeast sectors. The IL_CHICAGO.str meteorological file was used in this example. The normalized air concentration values (s/m^3) obtained from separate runs involving each of the nine individual 10×10 m areas are listed within their respective areas in Figure 4-6. The average air concentration is then calculated to be 2.753×10^{-4} s/m^3. A single run for the 30×30 m area with a grid spacing set to 10 m as described above, computes a value of 2.747×10^{-4} s/m^3.

Thus, very good agreement is shown with about a 0.2% difference, well within any round-off errors that might be expected.

Table 4-3 Additional Comparison of RESRAD-OFFSITE Normalized Air Concentrations (s/m^3) with Spreadsheet Verification Calculations (without Plume Rise)[a]

Receptor Area	Spreadsheet Calculation[b]	Spreadsheet × Directional Frequency[b]	RESRAD-OFFSITE	% Difference
Run 4 – Pasquill-Gifford dispersion coefficients, no dry or wet deposition				
Fruit, grain, nonleafy vegetables plot	1.572E-03	7.860E-05	7.937E-05	0.98
Leafy vegetables plot	2.023E-04	2.023E-05	2.013E-05	0.49
Pasture, silage growing area	3.142E-05	7.855E-06	7.869E-06	0.18
Grain fields	7.342E-06	1.468E-06	1.467E-06	0.10
Dwelling site	4.524E-07	1.810E-07	1.810E-07	0.02
Run 5 – Pasquill-Gifford dispersion coefficients with dry deposition, no wet deposition				
Fruit, grain, nonleafy vegetables plot	1.546E-03	7.730E-05	7.807E-05	1.00
Leafy vegetables plot	2.005E-04	2.005E-05	1.994E-05	0.55
Pasture, silage growing area	3.116E-05	7.790E-06	7.801E-06	0.14
Grain fields	7.262E-06	1.452E-06	1.451E-06	0.10
Dwelling site	4.357E-07	1.743E-07	1.744E-07	0.07
Run 6 – Pasquill-Gifford dispersion coefficients with dry and wet deposition				
Fruit, grain, nonleafy vegetables plot	1.521E-03	7.605E-05	7.678E-05	0.96
Leafy vegetables plot	1.981E-04	1.981E-05	1.970E-05	0.56
Pasture, silage growing area	3.083E-05	7.708E-06	7.718E-06	0.14
Grain fields	7.025E-06	1.405E-06	1.403E-06	0.14
Dwelling site	4.291E-07	1.716E-07	1.717E-07	0.03

[a] Note that the number of significant figures used are for comparison purposes only to check the accuracy of the RESRAD-OFFSITE calculations. Pasquill-Gifford dispersion coefficients were used for all runs. All receptor area elevations were set to zero. Plume rise was not considered.

[b] The spreadsheet calculations do not incorporate the directional wind frequency as shown in Table 4-1.

Effective Release Height

$$\underset{H}{\boxed{0.62}}\,(m) = \underset{h}{\boxed{1.00}} + \underset{\Delta h}{\boxed{0.25}} - \left(1. - \underset{P_c}{\boxed{0.50}}\right) * \left[\min\left(\underset{h+\Delta h}{\boxed{1.25}}\ \underset{E_r - E_p}{\boxed{15.00}}\right)(m)\right] \quad \textbf{(4.1)}$$

Unstable/Neutral Conditons (A-D)

x <= 10 * stack height

$$\underset{\Delta h\,(m)}{\boxed{N/A}} = \frac{1.6}{\underset{U_H\,(m/s)}{\boxed{4.47}}} * \left[\underset{(m^4/cal\text{-}s^2)}{3.7 * 10^{-5}} * \underset{Q_h\,(cal/s)}{\boxed{90}} * \underset{x^2\,(m^2)}{\boxed{1000000}}\right]^{1/3} \quad \textbf{(4.2)}$$

x > 10 * stack height

$$\underset{\Delta h\,(m)}{\boxed{0.25}} = \frac{1.6}{\underset{U_H\,(m/s)}{\boxed{4.47}}} * \left[\underset{(m^4/cal\text{-}s^2)}{3.7 * 10^{-5}} * \underset{Q_h\,(cal/s)}{\boxed{90}} * 100 * \underset{h^2\,(m^2)}{\boxed{1.00}}\right]^{1/3} \quad \textbf{(4.3)}$$

Stable Conditions (E,F)

Still expanding [x <= 2.4*($U_H/s^{1/2}$) and U >= U_{test}]

$$\underset{\Delta h\,(m)}{\boxed{N/A}} = \frac{1.6}{\underset{U_H\,(m/s)}{\boxed{4.47}}} * \left[\underset{(m^4/cal\text{-}s^2)}{3.7 * 10^{-5}} * \underset{Q_h\,(cal/s)}{\boxed{90}} * \underset{x^2\,(m^2)}{\boxed{1000000}}\right]^{1/3} \quad \textbf{(4.4)}$$

Far limit [x > 2.4*($U_H/s^{1/2}$) and U >= U_{test}]

$$\underset{\Delta h\,(m)}{\boxed{N/A}} = 2.9 * \left[\frac{\underset{(m^4/cal\text{-}s^2)}{3.7 * 10^{-5}} * \underset{Q_h\,(cal/s)}{\boxed{90}}}{\underset{U_H\,(m/s)}{\boxed{4.47}} * \underset{s\,(s^{-2})}{\boxed{0.001204}}}\right]^{1/3} \quad \textbf{(4.5)}$$

Light wind, vertical rise (U < U_{test})

$$\underset{\Delta h\,(m)}{\boxed{N/A}} = 5.0 * \frac{\left[\underset{(m^4/cal\text{-}s^2)}{3.7 * 10^{-5}} * \underset{Q_h\,(cal/s)}{\boxed{90}}\right]^{1/4}}{\left[\underset{s\,(s^{-2})}{\boxed{0.001204}}\right]^{3/8}} \quad \textbf{(4.6)}$$

s: stability parameter [g/T * dθ/dz]

$$\underset{s\,(s^{-2})}{\boxed{0.001204}} = \frac{\underset{(m/s^2)}{9.80665}}{\underset{T_a(^oK)}{\boxed{285}}} * \underset{dT/dz + l\,(^oK/m)}{\boxed{0.035}} \quad \textbf{(4.7)}$$

wind speed cut-off

$$\underset{U_{test}}{\boxed{0.020218}}\,(m/s) = 0.195 * \left[\underset{(m^4/cal\text{-}s^2)}{3.7 * 10^{-5}} * \underset{Q_h\,(cal/s)}{\boxed{90}}\right]^{1/4} * \left[\underset{s\,(s^{-2})}{\boxed{0.001204}}\right]^{1/8} \quad \textbf{(4.8)}$$

Figure 4-1 Effective Release Height Calculation in RESRAD-OFFSITE

Effective Wind Speed

If H_{eff} <= 10 m

$$\underset{U_{eff}\ (m/s)}{\boxed{4.47}} = \underset{U\ (m/s)}{\boxed{4.47}}$$

else

$$\underset{U_{eff}\ (m/s)}{\boxed{N/A}} = \underset{U\ (m/s)}{\boxed{4.47}} * \left[\frac{\underset{H_{eff}\ (m)}{\boxed{0.62}}}{\underset{H_{Anem}\ (m)}{\boxed{10.00}}} \right]^{\underset{p}{\boxed{0.1}}} \qquad \textbf{(4.9)}$$

Figure 4-2 Calculation of the Effective Wind Speed (iteration of Eq. 4.9 with Eqs. 4.2 to 4.5 to obtain consistent effective wind speed and release height values)

Pasquill-Gifford σ_z

$$\underset{\sigma_z\ (m)}{\boxed{61.1}} = \underset{a}{\boxed{1.13E\text{-}01}} * \left(\underset{x\ (m)}{\boxed{1{,}000}} \right)^{\boxed{9.11E\text{-}01}\ b} + \underset{c}{\boxed{0.00E+00}} \qquad \textbf{(4.34)}$$

σ_z adjusted for buoyancy-induced dispersion

$$\underset{\sigma_{ze}\ (m)}{\boxed{61.1}} = \left(\underset{\sigma_z^2\ (m^2)}{\boxed{3.73E+03}} + \left(\underset{\Delta h\ (m)}{\boxed{0.25}} / 3.5 \right)^2 \right)^{1/2} \qquad \textbf{(4.36/4.37)}$$

Figure 4-3 Vertical Dispersion Coefficient Calculation

Washout Coefficient

$$\underset{V_w\ (1/s)}{\boxed{1.48E\text{-}04}} = \underset{W_C\ (1/s)(mm/h)^{-1}}{\boxed{1.00E\text{-}03}} * \underset{R\ (mm/h)}{\boxed{1.48E\text{-}01}} \qquad \textbf{(4.29)}$$

Depleted Source Strength **(4.31)**

$$\underset{Q_x\ (Ci)}{\boxed{9.56E\text{-}01}} = \underset{Q_0\ (Ci)}{\boxed{1.00E+00}} * \exp\left[- \left(\frac{\underset{V_w\ (1/s)}{\boxed{1.48E\text{-}04}} * \underset{x\ (m)}{\boxed{1000.0}}}{\underset{U_{eff}\ (m/s)}{\boxed{4.47}}} + \frac{\underset{V_d\ (m/s)}{\boxed{0.0010}}}{(\pi/2)^{1/2} * \underset{U_{eff}\ (m/s)}{\boxed{4.47E+00}}} * \boxed{66.91} \int_0^x F(x)dx \right) \right]$$

Figure 4-4 Calculation of the Depleted Source Strength Due to Wet and Dry Deposition

Plume reflection not considered if

$$\sigma_z(x) \;<=\; \frac{\left(1 - \dfrac{\boxed{0.62}}{H_{eff}\,(m)} \Big/ \dfrac{\boxed{400}}{L\,(m)}\right)^{1/2}}{1.2} * \frac{\boxed{400}}{L\,(m)} = \frac{\boxed{333.1}}{\sigma_{z,no\text{-}mix}\,(m)} \quad \textbf{[TRUE]} \qquad \textbf{(4.15)}$$

Then

$$\frac{\boxed{7.019E\text{-}06}}{C_{a,no\text{-}mix}\,(Ci/m^3)} = \frac{\dfrac{\boxed{9.56E\text{-}01}}{Q_x\,(Ci)}}{(2\pi)^{1/2} * \dfrac{\boxed{61.1}}{\sigma_z\,(m)} * \dfrac{\boxed{4.47E+00}}{U_{eff}\,(m/s)} * \dfrac{\boxed{1000}}{x\,(m)} * \tan(11.25^o)} * \exp\left[- \left(\frac{\dfrac{\boxed{3.89E\text{-}01}}{H_{eff}^2\,(m^2)}}{2 * \dfrac{\boxed{3.73E+03}}{\sigma_z^2\,(m^2)}} \right) \right] \qquad \textbf{(4.22)}$$

Figure 4-5 Normalized Air Concentration Calculation in RESRAD-OFFSITE

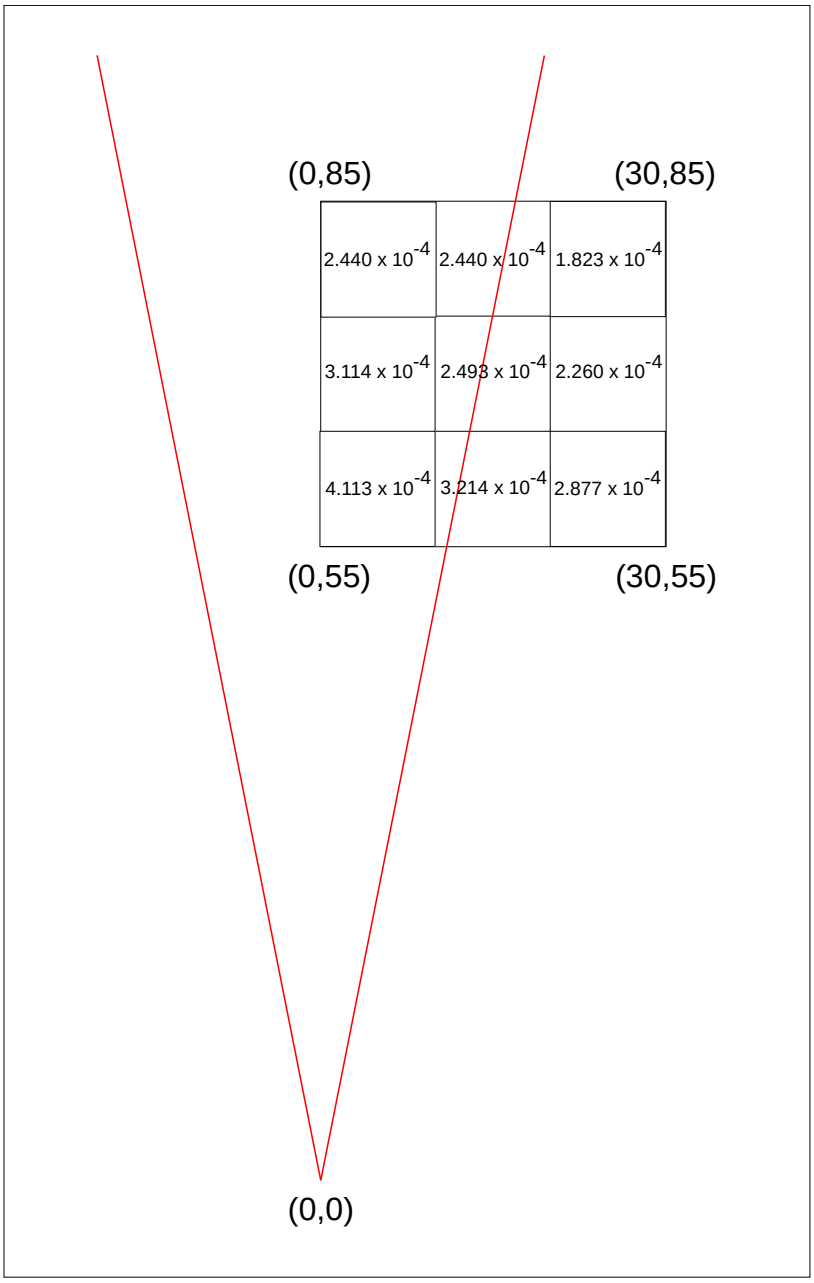

Figure 4-6 Site Layout for Verification of the Area Averaged Normalized Air Concentration

5.0 ACCUMULATION AT OFFSITE LOCATIONS AND IN FOOD

Accumulation at offsite surface soil and food was verified in this section. The results of spreadsheet calculations were compared with RESRAD-OFFSITE code results for different processes involved in accumulation. For example, in verifying accumulation in offsite surface soil, the accumulation in offsite surface soil from irrigation and deposition of particulates was verified first, then the total accumulation calculations were verified. Similarly, the calculations were first verified for the first member of the decay chain, and later verification was done for the second member of the decay chain. To simplify spreadsheet calculations, storage times for surface water, well water, fruit, grain, nonleafy vegetables, leafy vegetables, pasture and silage, livestock feed grain, meat, milk, fish, and crustaceans and mollusks were changed to zero from their defaults in the code. The spreadsheets were created for eight radionuclides (H-3, C-14, Co-60, Ni-63, Sr-90, Cs-137, Ra-226, and U-238) to capture the variability in radionuclide-dependent parameters. The subsequent sections show the results for one radionuclide only, but the calculations are done for all eight radionuclides in the Excel spreadsheets. Table 5-1 lists the radionuclide-independent parameters used in the calculations, and Table 5-2 lists the radionuclide-dependent parameters used in the calculations. Section 5.1 discusses the accumulation in offsite surface soil. Section 5.2 focuses on the accumulation in surface water. Plant accumulation is discussed in Section 5.3. Meat and milk accumulation is discussed in Section 5.4, and Section 5.5 focuses on accumulation in fish and aquatic food.

5.1 Accumulation in Offsite Surface Soil

Offsite surface soil gets contaminated due to irrigation with contaminated water and deposition of contaminated dust. Radiological transformations, soil mixing in the surface layer, erosion, and equilibrium desorption release are included when calculating surface soil concentration at offsite locations. Accumulation in offsite surface soil is calculated as described in Section 5.1 of RESRAD-OFFSITE User's Manual (Yu et al. 2007).

5.1.1 Accumulation in Offsite Surface Soil from Irrigation

The contaminant deposition rate (pCi/m^2/yr) at any time *t* of radionuclide *i* in offsite soil from irrigation water is given as (Eq. 5.11 in the RESRAD-OFFSITE User's Manual):

$$D_i(t) = q_{ir} w_i^{ir}(t)\left[1 - f_{int}\frac{1-\exp(-\lambda_w t_g)}{\lambda_w t_g}\right] \qquad \text{(Eq. 5.1)}$$

where:

q_{ir} = irrigation rate (m/yr),

$w_i^{ir}(t)$ = activity concentration of radionuclide *i* in contaminated irrigation water (pCi/m^3),

f_{int} = foliar interception factor,

λ_w = weathering constant (per yr),

Table 5-1 Parameters Used in the Verification of Accumulation in Offsite Soil, Surface Water, Plant, Meat, Milk, and Aquatic Food

General Parameters	Values
Deposition velocity (m/s)	0.001
Storage time (d)	0
Precipitation rate (m/yr)	1
Offsite soil parameters in different agricultural areas	
Fraction of area directly over primary contamination	0
Irrigation applied (m/yr)	0.2
Evapotranspiration coefficient	0.5
Runoff coefficient	0.2
Mixing depth (m)	0.15
Volumetric water content	0.3
Dry bulk density (g/cm^3)	1.5
Soil erodibility factor	0.4
Slope-length-steepness factor	0.4
Cover and management	0.003
Support practice factor	1
Surface water body parameters	
Volume of surface water body (m^3)	150,000
Area of surface water body (m^2)	90,000
Mean residence time of water (yr)	1
Sediment delivery ratio	1
Plant accumulation parameters	
Wet crop yield for fruit, grain, and leafy vegetables (kg/m^2)	0.7
Wet crop yield for leafy vegetables (kg/m^2)	1.5
Wet crop yield for pasture and silage (kg/m^2)	1.1
Wet crop yield for grain (kg/m^2)	0.7
Foliage to food transfer coefficient for fruit, grain, and leafy vegetables	0.1
Foliage to food transfer coefficient for leafy vegetables	1.0
Foliage to food transfer coefficient for pasture and grass	1.0
Foliage to food transfer coefficient for grain	0.1
Duration of growing season for fruit, grain, and leafy vegetables (yr)	0.17
Duration of growing season for leafy vegetables (yr)	0.25
Duration of growing season for pasture and grass (yr)	0.08
Duration of growing season for grain, yr	0.17
Weathering removal constant for all plant types (per yr)	20
Foliar interception factor for irrigation for all plant types[a]	0.25
Foliar interception factor for dust for all plant types	0.25
Meat and milk accumulation parameters	
Beef cattle water intake (L/d)	50
Dairy cow water intake (L/d)	160
Beef cattle pasture intake (kg/d)	14
Dairy cow pasture intake (kg/d)	44
Beef cattle grain intake (kg/d)	54
Dairy cow grain intake (kg/d)	11
Beef cattle soil intake from pasture and silage (kg/d)	0.1
Dairy cow soil intake from pasture and silage (kg/d)	0.4
Beef cattle soil intake from grain (kg/d)	0.4
Dairy cow soil intake from grain (kg/d)	0.1

[a] For C-14 and H-3, the foliar interception factor for irrigation = 0.

Table 5-2 Radionuclide Specific Parameters Used in the Verification of Accumulation in Offsite Soil, Surface Water Body, Plant, Meat, Milk, and Aquatic Food

Radionuclide	H-3	C-14	Co-60	Ni-63	Sr-90	Y-90	Cs-137	Ra-226	Pb-210	U-238	Th-234
Half life (yr)	12.35	5730	5.271	96	29.12	64 h	30	1600	22.3	4.47E+09	6.70E-02
Cut-off half life (d)	30	30	30	30	1	1	30	30	30	1	1
Distribution coefficient (cm^3/g)	0	0.1	1,000	1,000	30	720	4,600	70	100	50	60,000
Distribution coefficient of sediment in surface water (cm^3/g)	0	0.1	1,000	1,000	30	720	4,600	70	100	50	60,000
Plant root uptake transfer factor (pCi/kg per pCi/kg)	NR[a]	NR	0.08	0.05	0.3	0.0025	0.04	0.04	0.01	0.0025	0.001
Meat transfer factor (pCi/kg per pCi/d)	NR	NR	0.02	0.005	0.008	0.002	0.03	0.001	0.0008	0.00034	0.0001
Milk transfer factor (pCi/L per pCi/d)	NR	NR	0.002	0.02	0.002	2.00E-05	0.008	0.001	0.0003	0.0006	5.00E-07
Fish bioaccumulation factor (pCi/kg per pCi/L)	1	50,000	300	100	60	30	2,000	50	300	10	100
Crustacea bioaccumulation factor (pCi/kg per pCi/L)	1	9,100	200	100	100	1,000	100	250	100	60	500

[a] NR = not required.

t_g = duration of growing season (yr).

The deposition rate of radionuclide *i* by irrigation water at any time *t* is approximated by a linear function given as (Eq. 5.12; Yu et al. 2007):

$$D_i(t) = \alpha_i + \beta_i \times t \qquad \text{(Eq. 5.2)}$$

where α_i and β_i are constant between each pair of time points.

The soil concentration of first member of transformation chain at any time *t* is given as (Eq. 5.15; Yu et al. 2007):

$$s_1^o(t) = A_1^0 + A_1^1 \times t + C_1^1 e^{-(\lambda_1 + E^o + L_1^0)t} \qquad \text{(Eq. 5.3)}$$

where A_1^0, A_1^1, and C_1^1 are given as:

$$A_1^1 = \frac{\beta_1}{\rho_b^0 d_{mix}^o (\lambda_1 + E^o + L_1^o)} \qquad \text{(Eq. 5.4)}$$

$$A_1^0 = \frac{\alpha_1}{\rho_b^0 d_{mix}^o (\lambda_1 + E^o + L_1^o)} - \frac{A_1^1}{\lambda_1 + E^o + L_1^o} \qquad \text{(Eq. 5.5)}$$

$$C_1^1 = s_1^0(0) - A_1^0 \qquad \text{(Eq. 5.6)}$$

where:

ρ_b^0 = dry bulk density of soil at the offsite location (g/m^3),
d_{mix}^o = mixing depth at offsite location (m),
λ_1 = decay constant of the first member of transformation chain (/yr),
E^o = fraction of the mixing zone that is eroded each year (/yr),
L_1^o = rate at which the nuclide is leached out of the mixing layer (/yr).

The leach rate can be calculated as:

$$L_1^o = \frac{I^o / d_{mix}^o}{\theta_c^o + \rho_b^o K_{d_1}^o} \qquad \text{(Eq. 5.7)}$$

where:

I^o = infiltration rate at the offsite location (m/yr),

θ_c^o = volumetric water content at offsite location,

$K_{d_1}^o$ = distribution coefficient of radionuclide at offsite location cm^3/g.

The infiltration rate is calculated as (Eq. 3.18; Yu et al. 2007):

$$I = (1 - C_e) \times ((1 - C_r) \times P_r + q_{ir}) \quad \text{(Eq. 5.8)}$$

where:

C_e = evapotranspiration coefficient,

C_r = runoff coefficient,

P_r = precipitation rate m/yr.

Table 5-3 shows the results of spreadsheet calculations for few time steps for the accumulation in offsite surface soil from irrigation. The verification was done for C-14 (initial concentration = 1 pCi/g) and groundwater was used for irrigation. The results of spreadsheet calculations were compared with the RESRAD-OFFSITE results (Figure 5-1). For this comparison, the soil concentration in the fruit, grain, and non-leafy vegetable agricultural area was used. The parameters that were changed from their default values were: K_d was changed to 0.1 cm^3/g and the deposition velocity was set at 0. Figure 5-2 shows the individual steps of the calculation for one time step highlighted in Table 5-3. For this comparison radionuclide concentration in irrigation water was obtained from the code. There is practically no difference in the spreadsheet calculations and the results from RESRAD-OFFSITE code (see Table 5-3 and Figure 5-1).

5.1.2 Accumulation in Offsite Surface Soil from Deposition of Contaminated Dust

The contamination deposition rate ($pCi/m^2/yr$) at any time *t* of radionuclide *i* in offsite soil from contaminated dust is given as (Eq. 5.13 in the RESRAD-OFFSITE User's Manual):

$$D_i(t) = V_{dep} a_i(t)[1 - f_{\text{int}} \frac{1 - \exp(-\lambda_w t_g)}{\lambda_w}] \quad \text{(Eq. 5.9)}$$

where:

V_{dep} = deposition velocity of the contaminated dust particle (m/yr),

$a_i(t)$ = air concentration of radionuclide *i* above the agricultural area where plant is growing (pCi/m^3).

The soil concentration in the offsite location from deposition of contaminated dust can be calculated in the same way, as described in Section 5.1.1.

Table 5-3 Spreadsheet Calculations for C-14 Accumulation in Offsite Surface Soil from Irrigation

Time, yr	Irrigation Water Conc. from Code (pCi/m^3)	Deposition from Irrigation Water ($pCi/m^2/yr$)	α1	β1	A11	A10	C11	Soil Conc. Calculated	Soil Conc. from Code
0.00E+00	0.00E+00	0.00E+00	0.00E+00	0.00E+00	0.00E+00	0.00E+00	0.00E+00	0.00E+00	0.00E+00
4.88E-01	0.00E+00	0.00E+00	0.00E+00	0.00E+00	0.00E+00	0.00E+00	0.00E+00	0.00E+00	0.00E+00
9.77E-01	0.00E+00	0.00E+00	0.00E+00	0.00E+00	0.00E+00	0.00E+00	0.00E+00	0.00E+00	0.00E+00
1.46E+00	0.00E+00	0.00E+00	0.00E+00	0.00E+00	0.00E+00	0.00E+00	0.00E+00	0.00E+00	0.00E+00
1.95E+00	0.00E+00	0.00E+00	0.00E+00	0.00E+00	0.00E+00	0.00E+00	0.00E+00	0.00E+00	0.00E+00
2.44E+00	0.00E+00	0.00E+00	0.00E+00	0.00E+00	0.00E+00	0.00E+00	0.00E+00	0.00E+00	0.00E+00
2.93E+00	0.00E+00	0.00E+00	0.00E+00	0.00E+00	0.00E+00	0.00E+00	0.00E+00	0.00E+00	0.00E+00
3.42E+00	0.00E+00	0.00E+00	0.00E+00	0.00E+00	0.00E+00	0.00E+00	0.00E+00	0.00E+00	0.00E+00
3.91E+00	0.00E+00	0.00E+00	0.00E+00	0.00E+00	0.00E+00	0.00E+00	0.00E+00	0.00E+00	0.00E+00
4.39E+00	0.00E+00	0.00E+00	0.00E+00	0.00E+00	0.00E+00	0.00E+00	0.00E+00	0.00E+00	0.00E+00
4.88E+00	0.00E+00	0.00E+00	0.00E+00	0.00E+00	0.00E+00	0.00E+00	0.00E+00	0.00E+00	0.00E+00
5.37E+00	0.00E+00	0.00E+00	0.00E+00	0.00E+00	0.00E+00	0.00E+00	0.00E+00	0.00E+00	0.00E+00
5.86E+00	2.72E-06	5.44E-07	0.00E+00	1.11E-06	6.69E-13	-9.03E-14	9.03E-14	2.39E-13	2.39E-13
6.35E+00	2.70E-03	5.40E-04	5.44E-07	1.10E-03	6.63E-10	-8.92E-11	8.94E-11	2.37E-10	2.37E-10
6.84E+00	1.83E-01	3.66E-02	5.40E-04	7.39E-02	4.44E-08	-5.66E-09	5.90E-09	1.62E-08	1.62E-08
7.32E+00	1.43E+00	2.86E-01	3.66E-02	5.11E-01	3.06E-07	-1.94E-08	3.55E-08	1.31E-07	1.31E-07
7.81E+00	6.19E+00	1.24E+00	2.86E-01	1.95E+00	1.17E-06	1.38E-08	1.17E-07	5.88E-07	5.88E-07
8.30E+00[a]	2.01E+01	4.02E+00	1.24E+00	5.71E+00	3.42E-06	2.80E-07	3.08E-07	1.96E-06	1.96E-06
8.79E+00	5.47E+01	1.09E+01	4.02E+00	1.41E+01	8.49E-06	1.27E-06	6.92E-07	5.43E-06	5.43E-06

[a] The calculations for the highlighted time step are shown in Figure 5-2.

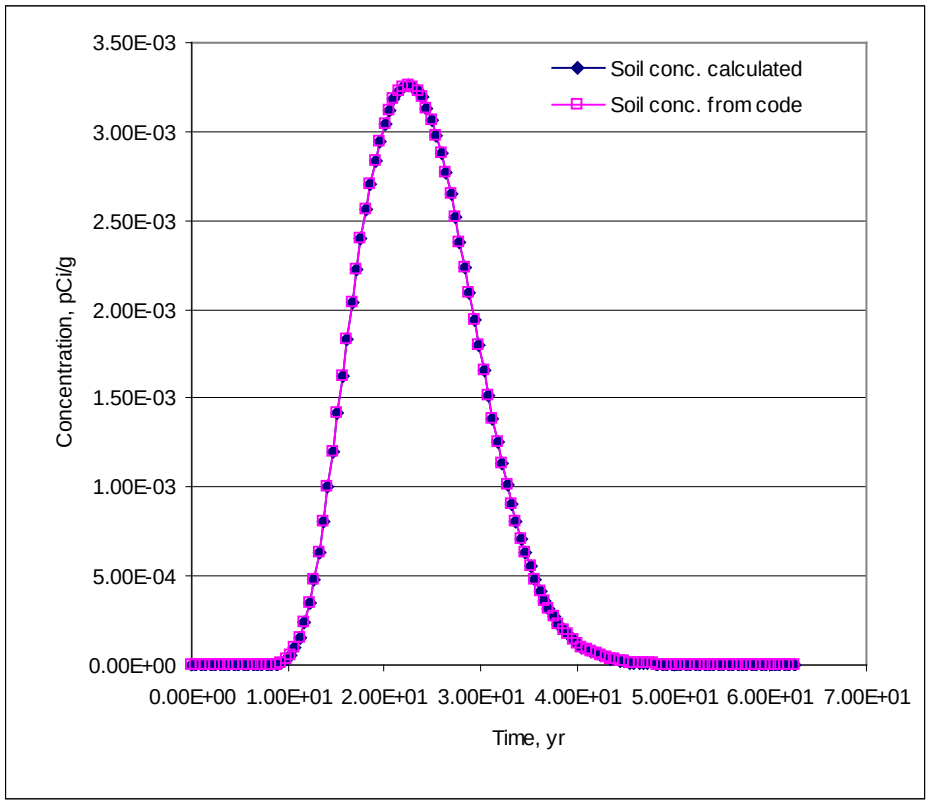

Figure 5-1 Accumulation of C-14 in Offsite Soil from Irrigation from Spreadsheet Calculations and from RESRAD-OFFSITE Code

Table 5-4 shows the results of spreadsheet calculations for few time steps for the accumulation in offsite surface soil from deposition. The verification was done for C-14. The results of spreadsheet calculations are compared with the RESRAD-OFFSITE results (Figure 5-3). For this comparison, the soil concentration in the fruit, grain, and nonleafy vegetable agricultural area was used. The irrigation rate in the agricultural area where fruit, grain, and nonleafy vegetables grow was set at 0 to only account for accumulation from deposition. Figure 5-4 shows the individual steps of the calculation for one time step highlighted in Table 5-4. For this comparison, radionuclide concentration in air was obtained from the code. There is practically no difference in the spreadsheet calculations and the results from RESRAD-OFFSITE code (see Table 5-4 and Figure 5-3).

For verifying the combined accumulation due to irrigation and deposition from contaminated dust, Sr-90 was selected (the results for other radionuclides are shown in the Excel spreadsheets). Table 5-5 shows the results of spreadsheet calculations for few time steps for the accumulation in offsite surface soil from irrigation and deposition. The verification was done for Sr-90 and surface water was used for irrigation. The cutoff half-life was changed to 1 day from its default setting of 30 days. All other parameters were kept at their default values. For this comparison, the soil concentration in the fruit, grain, and nonleafy vegetable agricultural area was used. The results of spreadsheet calculations are compared with the RESRAD-OFFSITE results (Figure 5-5). Figure 5-6 shows the individual steps of the calculation for one time step highlighted in Table 5-5. For this comparison, radionuclide concentrations in air and irrigation water were obtained from the code. There is practically no difference in the spreadsheet calculations and the results from RESRAD-OFFSITE code (see Table 5-6 and Figure 5-5).

Offsite Surface Soil Accumulation from Irrigation

3.4	=	20	×	0.17									
$\lambda_w t_g$		λ_w		t_g									
2.84E-01	=	(1	−	exp(-	3.4	)	/	3.4					
$\frac{1-\exp(-\lambda_w t_g)}{\lambda_w t_g}$					$\lambda_w t_g$			$\lambda_w t_g$					
4.02E+00	=	0.2	×	20.1208	×	(1	−	0	×	2.84E-01	)		(5.1)
$D_i(t)$		q_{ir}		$w_i^{ir}(t)$				f_{int}		$\frac{1-\exp(-\lambda_w t_g)}{\lambda_w t_g}$			
α1	=	1.23719											
5.71E+00	=	(	4.024	−	1.2372	)	/	(	8.30078	−	7.813	)	
β1			$D_i(t)$		α1				t2		t1		
0.5	=	(	1	−	0.5	)							
$(1-C_e)$					C_e								
0.8	=	(	1	−	0.2								
$(1-C_r)$					C_r								
0.5	=	0.5	×	(	0.8	×	1	+	0.2	)			(5.8)
I^o		$(1-C_e)$			$(1-C_r)$		P_r		q_{ir}				
7.41E+00	=	0.5	/	0.15	/	(	0.3	+	1.5	×	0.1	)	(5.7)
L_1^o		I^o		d_{mix}^o			θ_c^o		ρ_b^o		$K_{d_1}^o$		
7.41E+00	=	0.00012	+	7.65E-05	+	7.40741							
$\lambda_1 + E^o + L_1^o$		λ_1		E^o		L_1^o							
3.42E-06	=	5.70773	/	225000	/	7.4076							(5.4)
A11		β1		$\rho_b^0 d_{mix}^o$		$\lambda_1 + E^o + L_1^o$							
2.80E-07	=	1.23719	/	225000	/	7.4076	-	3.42E-06	/	7.407605			(5.5)
A10		α1		$\rho_b^0 d_{mix}^o$		$\lambda_1 + E^o + L_1^o$		A11		$\lambda_1 + E^o + L_1^o$			
3.08E-07	=	5.9E-07	−	2.80E-07									(5.6)
C11		S10		A10									
1.96E-06	=	2.80E-07	+	3.42E-06	x	0.48828	+	3.08E-07	x	0.026864			(5.3)
S1(t)		A10		A11		t		C11		$e^{-(\lambda_1+E^o+L_1^0)t}$			

Figure 5-2 Offsite Surface Soil Accumulation from Irrigation

Table 5-4 Spreadsheet Calculations for C-14 Accumulation in Offsite Surface Soil from Deposition

Time	Concentration in Air (pCi/m^3) from Code	Deposition Rate from Air ($pCi/m^2/yr$)	α1	β1	A11	A10	C11	Soil Conc. Calculated	Soil Conc. from Code
0.00E+00	3.03E-07	9.46E-03	0.00E+00	0.00E+00	0.00E+00	0.00E+00	0.00E+00	0.00E+00	0.00E+00
4.88E-01	4.63E-08	1.44E-03	9.46E-03	-1.64E-02	-9.85E-09	7.00E-09	-7.00E-09	2.01E-09	2.01E-09
9.77E-01	7.07E-09	2.20E-04	1.44E-03	-2.51E-03	-1.50E-09	1.07E-09	9.38E-10	3.60E-10	3.60E-10
1.46E+00	1.08E-09	3.37E-05	2.20E-04	-3.83E-04	-2.30E-10	1.63E-10	1.97E-10	5.65E-11	5.65E-11
1.95E+00	1.65E-10	5.14E-06	3.37E-05	-5.84E-05	-3.50E-11	2.49E-11	3.16E-11	8.66E-12	8.66E-12
2.44E+00	2.52E-11	7.85E-07	5.14E-06	-8.92E-06	-5.35E-12	3.81E-12	4.86E-12	1.32E-12	1.32E-12
2.93E+00	3.84E-12	1.20E-07	7.85E-07	-1.36E-06	-8.17E-13	5.81E-13	7.42E-13	2.02E-13	2.02E-13
3.42E+00	5.87E-13	1.83E-08	1.20E-07	-2.08E-07	-1.25E-13	8.87E-14	1.13E-13	3.09E-14	3.09E-14
3.91E+00	8.96E-14	2.79E-09	1.83E-08	-3.17E-08	-1.90E-14	1.35E-14	1.73E-14	4.71E-15	4.71E-15
4.39E+00	1.37E-14	4.26E-10	2.79E-09	-4.85E-09	-2.91E-15	2.07E-15	2.64E-15	7.19E-16	7.19E-16
4.88E+00	2.09E-15	6.51E-11	4.26E-10	-7.40E-10	-4.44E-16	3.16E-16	4.04E-16	1.10E-16	1.10E-16
5.37E+00	3.19E-16	9.94E-12	6.51E-11	-1.13E-10	-6.78E-17	4.82E-17	6.16E-17	1.68E-17	1.68E-17
5.86E+00	4.87E-17	1.52E-12	9.94E-12	-1.72E-11	-1.03E-17	7.36E-18	9.41E-18	2.56E-18	2.56E-18
6.35E+00	7.43E-18	2.32E-13	1.52E-12	-2.63E-12	-1.58E-18	1.12E-18	1.44E-18	3.91E-19	3.91E-19
6.84E+00	1.13E-18	3.54E-14	2.32E-13	-4.02E-13	-2.41E-19	1.71E-19	2.19E-19	5.96E-20	5.96E-20
7.32E+00	1.73E-19	5.40E-15	3.54E-14	-6.13E-14	-3.68E-20	2.62E-20	3.35E-20	9.11E-21	9.11E-21
7.81E+00	2.64E-20	8.24E-16	5.40E-15	-9.37E-15	-5.62E-21	4.00E-21	5.11E-21	1.39E-21	1.39E-21
8.30E+00[a]	4.03E-21	1.26E-16	8.24E-16	-1.43E-15	-8.58E-22	6.10E-22	7.80E-22	2.12E-22	2.12E-22
8.79E+00	6.16E-22	1.92E-17	1.26E-16	-2.18E-16	-1.31E-22	9.31E-23	1.19E-22	3.24E-23	3.24E-23

[a] The calculations for the highlighted time step are shown in Figure 5-4.

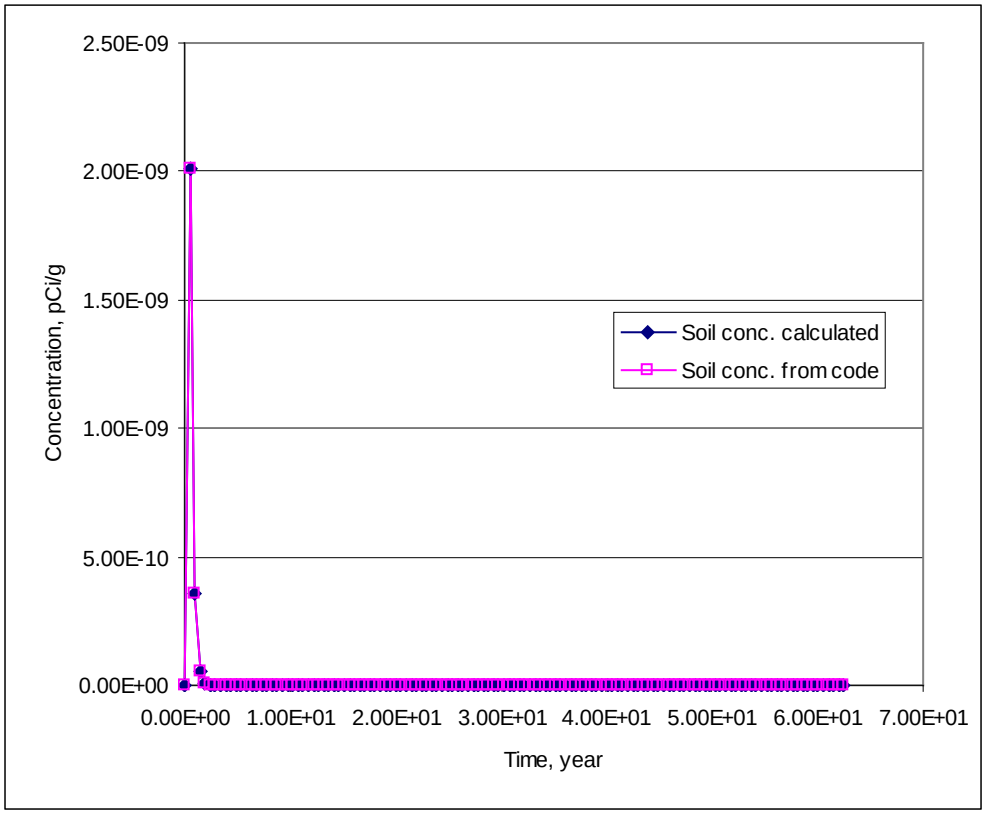

Figure 5-3 Accumulation of C-14 in Offsite Soil from Deposition from Spreadsheet Calculations and from RESRAD-OFFSITE Code

5.1.3 Accumulation in Offsite Surface Soil for the Second Member of the Transformation Chain

The soil concentration of second member of the transformation chain at any time *t* is given as (Eq. 5.18 in RESRAD-OFFSITE User's Manual):

$$s_2^o(t) = A_2^0 + A_2^1 \times t + C_2^1 e^{-(\lambda_1 + E^o + L_1^0)t} + C_2^2 e^{-(\lambda_2 + E^o + L_2^0)t} \tag{5.10}$$

where A_2^0, A_2^1, C_2^1, and C_2^2 are given as:

$$A_2^0 = \frac{\alpha_2}{\rho_b^0 d_{mix}^o (\lambda_2 + E^o + L_2^o)} + \frac{\lambda_2 A_1^0}{\lambda_2 + E^o + L_2^o} - \frac{A_2^1}{\lambda_2 + E^0 + L_2^o} \tag{5.11}$$

$$A_2^1 = \frac{\beta_2}{\rho_b^0 d_{mix}^o (\lambda_2 + E^o + L_2^o)} + \frac{\lambda_2 A_1^1}{\lambda_2 + E^o + L_2^o} \tag{5.12}$$

$$C_2^1 = \frac{\lambda_2 C_1^1}{\lambda_2 + L_2^o - \lambda_1 - L_1^o} \tag{5.13}$$

Offsite Surface Soil Accumulation from Paticulate Deposition

3.4	=	20	×	0.17									
$\lambda_w t_g$		λ_w		t_g									
		/yr		yr									
4.83E-02	=	(1	−	exp(-	3.4	)	/	20					
$\frac{1-\exp(-\lambda_w t_g)}{\lambda_w}$					$\lambda_w t_g$			λ_w					
1.26E-16	=	31557.6	×	4.034E-21	×	(1	−	0.25	×	4.83E-02	)		(5.9)
$D_i(t)$		V_{dep}		$a_i(t)$				f_{int}		$\frac{1-\exp(-\lambda_w t_g)}{\lambda_w}$			
pCi/m²/yr		m/yr		pCi/m³									
α1	=	8.239E-16											
-1.43E-15	=	(	$D_i(t)$ 5	−	8.24E-16	)	/	(	8.30078	−	7.8125	)	
β1					α1				t2		t1		
pCi/m²			pCi/m²/yr		pCi/m²/yr				yr		yr		
0.5	=	(	1	−	0.5	)							
$(1-C_e)$					C_e								
0.8	=	(	1	−	0.2								
$(1-C_r)$					C_r								
0.5	=	0.5	×	(	0.8	×	1	+	0.2	)			(5.8)
I^o		$(1-C_e)$			$(1-C_e)$		P_r		q_{1r}				
m/yr							m/yr		m/yr				
7.41E+00	=	0.5	/	0.15	/	(	0.3	+	1.5	×	0.1	)	(5.7)
L_1^o		I^o		d_{mix}^o			θ_c^o		ρ_b^o		$K_{d_1}^o$		
/yr		m/yr		m					g/cm³				
7.41E+00	=		+	0.000121	+	7.65E-05	+	7.407407					
$\lambda_1 + E^o + L_1^o$				λ_1		E^o		L_1^o					
/yr				/yr		/yr		/yr					
-8.58E-22	=	-1.43E-15	/	225000	/	7.407605							(5.4)
A11		β1		$\rho_b^0 d_{mix}^o$		$\lambda_1 + E^o + L_1^o$							
pCi/g/yr		pCi/m²		g/m²		/yr							
6.10E-22	=	8.239E-16	/	225000	/	7.407605	-	-8.6E-22	/	7.4076			(5.5)
A10		α1		$\rho_b^0 d_{mix}^o$		$\lambda_1 + E^o + L_1^o$		A11		$\lambda_1 + E^o + L_1^o$			
7.80E-22	=	1.39E-21	−	6.10E-22									(5.6)
C11		S10		A10									
pCi/g		pCi/g		pCi/g/yr									
2.12E-22	=	6.10E-22	+	-8.58E-22	x	0.48828	+	7.80E-22	x	0.02686			(5.3)
S1(t)		A10		A11		t		C11		$e^{-(\lambda_1+E^o+L_1^0)t}$			
pCi/g		pCi/g		pCi/g/yr		yr		pCi/g					

Figure 5-4 Offsite Surface Soil Accumulation from Deposition

Table 5-5 Spreadsheet Calculations for Sr-90 Accumulation in Offsite Surface Soil from both Irrigation and Deposition

Time	Sr-90 Concentration in Irrigation Water (pCi/m^3)	Sr-90 Concentration in Air from Code (pCi/m^3)	Influx Entering Offsite Soil ($pCi/m^2/yr$)	α1	β1	A11	A10	C11	Soil Conc. Calculated	Soil Conc. from Code
0.00E+00	0.00E+00	3.03E-05	9.46E-01	0.00E+00	0.00E+00	0.00E+00	0.00E+00	0.00E+00	0.00E+00	0.00E+00
4.88E-01	4.37E+01	2.99E-05	9.06E+00	9.46E-01	1.66E+01	7.58E-04	-7.73E-03	7.73E-03	1.07E-05	1.07E-05
9.77E-01	6.97E+01	2.95E-05	1.39E+01	9.06E+00	9.83E+00	4.48E-04	-4.19E-03	4.20E-03	3.45E-05	3.45E-05
1.46E+00	8.48E+01	2.91E-05	1.67E+01	1.39E+01	5.72E+00	2.61E-04	-2.04E-03	2.08E-03	6.52E-05	6.53E-05
1.95E+00	9.33E+01	2.86E-05	1.82E+01	1.67E+01	3.23E+00	1.47E-04	-7.52E-04	8.17E-04	9.92E-05	9.92E-05
2.44E+00	9.79E+01	2.82E-05	1.91E+01	1.82E+01	1.72E+00	7.85E-05	2.54E-05	7.38E-05	1.34E-04	1.34E-04
2.93E+00	1.00E+02	2.78E-05	1.95E+01	1.91E+01	8.12E-01	3.70E-05	4.90E-04	-3.56E-04	1.69E-04	1.69E-04
3.42E+00	1.01E+02	2.74E-05	1.96E+01	1.95E+01	2.62E-01	1.20E-05	7.65E-04	-5.96E-04	2.02E-04	2.02E-04
3.91E+00	1.01E+02	2.71E-05	1.96E+01	1.96E+01	-6.75E-02	-3.08E-06	9.25E-04	-7.23E-04	2.34E-04	2.34E-04
4.39E+00	1.00E+02	2.67E-05	1.94E+01	1.96E+01	-2.64E-01	-1.21E-05	1.02E-03	-7.81E-04	2.65E-04	2.65E-04
4.88E+00	9.92E+01	2.63E-05	1.92E+01	1.94E+01	-3.81E-01	-1.74E-05	1.06E-03	-7.99E-04	2.93E-04	2.93E-04
5.37E+00	9.81E+01	2.59E-05	1.90E+01	1.92E+01	-4.48E-01	-2.04E-05	1.09E-03	-7.94E-04	3.20E-04	3.20E-04
5.86E+00	9.69E+01	2.55E-05	1.88E+01	1.90E+01	-4.86E-01	-2.22E-05	1.09E-03	-7.75E-04	3.46E-04	3.46E-04
6.35E+00	9.56E+01	2.52E-05	1.85E+01	1.88E+01	-5.06E-01	-2.31E-05	1.09E-03	-7.48E-04	3.69E-04	3.69E-04
6.84E+00	9.43E+01	2.48E-05	1.83E+01	1.85E+01	-5.15E-01	-2.35E-05	1.09E-03	-7.17E-04	3.91E-04	3.91E-04
7.32E+00	9.30E+01	2.45E-05	1.80E+01	1.83E+01	-5.17E-01	-2.36E-05	1.08E-03	-6.85E-04	4.11E-04	4.11E-04
7.81E+00	9.17E+01	2.41E-05	1.78E+01	1.80E+01	-5.16E-01	-2.35E-05	1.06E-03	-6.53E-04	4.30E-04	4.30E-04
8.30E+00[a]	9.04E+01	2.38E-05	1.75E+01	1.78E+01	-5.12E-01	-2.34E-05	1.05E-03	-6.21E-04	4.48E-04	4.48E-04
8.79E+00	8.91E+01	2.34E-05	1.73E+01	1.75E+01	-5.07E-01	-2.31E-05	1.04E-03	-5.89E-04	4.64E-04	4.64E-04

[a] The calculations for the highlighted time step are shown in Figure 5-6.

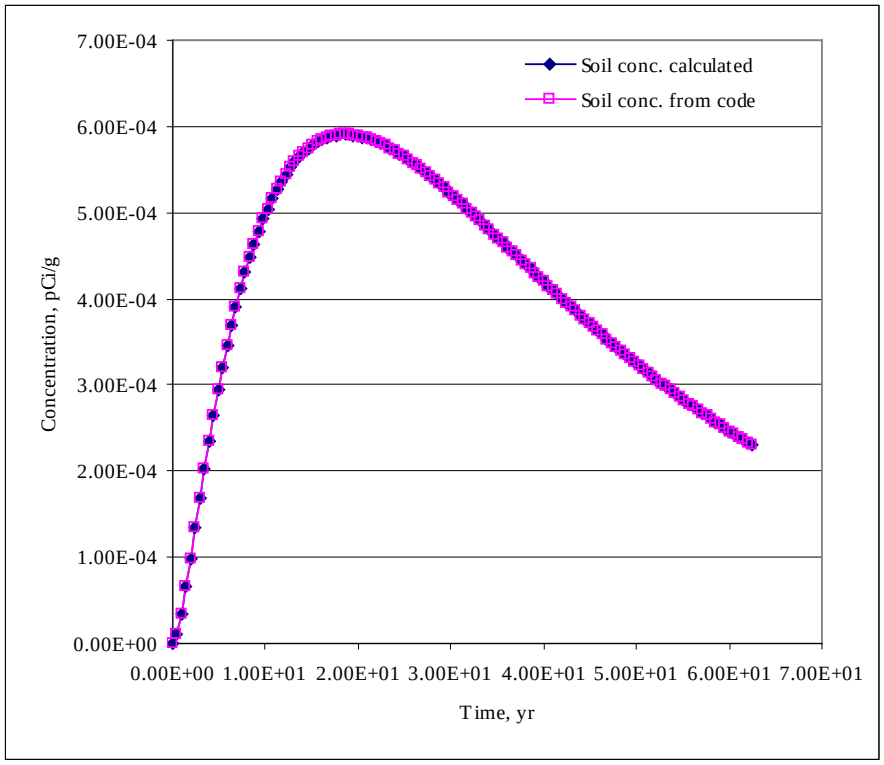

Figure 5-5 Accumulation of Sr-90 in Offsite Soil from Both Irrigation and Deposition from Spreadsheet Calculations and from RESRAD-OFFSITE Code

$$C_2^2 = s_2^0(0) - A_2^0 - C_2^1 \tag{5.14}$$

For verifying the offsite surface accumulation for the second member of the transformation chain, Sr-90 was selected and the concentration for its progeny Y-90 was verified. Table 5-6 shows the results of spreadsheet calculations for a few time steps for the accumulation in offsite surface soil from irrigation and deposition. For this comparison, the soil concentration in the fruit, grain, and nonleafy vegetable agricultural area was used. The results of spreadsheet calculations are compared with the RESRAD-OFFSITE results (Figure 5-7). Figure 5-8 shows the individual steps of the calculation for one time step highlighted in Table 5-6. For this comparison, radionuclide concentrations in air and irrigation water were obtained from the code. There is practically no difference in the spreadsheet calculations and the results from RESRAD-OFFSITE code (see Table 5-6 and Figure 5-7).

5.2 Accumulation in Surface Water

The contaminants can reach the surface water body from surface runoff, from contaminated groundwater flow, and by atmospheric deposition of contaminated dust. Radiological transformations and the removal of contaminant by the outflow of contaminated water are included when calculating surface water concentration, as described in Section 5.2 of the RESRAD-OFFSITE User's Manual. The rate contaminants enter the surface water body can be given as:

$$I_i^{sw}(t) = \frac{R_i^{sr}(t)SDR + f_s(t) + a_i(t)V_{dep}A^{sw}}{V_i^{sw}(t)} \tag{5.15}$$

Offsite Surface Soil Accumulation from both Irrigation and Particulate Deposition for the First Member of Transformation Chain

3.4	=	20	×	0.17										
$\lambda_w t_g$		λ_w		t_g										
		/yr		yr										
4.83E-02	=	(1	−	exp(-	3.4	)	/	20						
$\frac{1-\exp(-\lambda_w t_g)}{\lambda_w}$					$\lambda_w t_g$			λ_w						
7.41E-01	=	31557.6	×	2.38E-05	×	(1	−	0.25	×	4.83E-02	)			(5.9)
$D_i(t)_air$		V_{dep}		$a_i(t)$				f_{int}		$\frac{1-\exp(-\lambda_w t_g)}{\lambda_w}$				
pCi/m²/yr		m/yr		pCi/m³										
2.84E-01	=	(1	−	exp(-	3.4	)	/	3.4						
$\frac{1-\exp(-\lambda_w t_g)}{\lambda_w t_g}$					$\lambda_w t_g$			$\lambda_w t_g$						
1.68E+01	=	0.2	×	90.4078	×	(1	−	0.25	×	2.84E-01	)			(5.1)
$D_i(t)_irrigation$		q_{ir}		$w_i^{ir}(t)$				f_{int}		$\frac{1-\exp(-\lambda_w t_g)}{\lambda_w t_g}$				
pCi/m²/yr		m/yr		pCi/m³										
α1	=	17.78792												
-5.12E-01	=	(	1.75E+01	−	17.787916	)	/	(	8.3008	−	7.8125	)		
β1			$D_i(t)_tot$		α1				t2		t1			
pCi/m²					pCi/m²/yr				yr		yr			
0.5	=	(	1	−	0.5	)								
$(1-C_e)$					C_e									

0.8	=	(	1	−	0.2									
$(1-C_r)$					C_r									
0.5	=	0.5	×	(	0.8	×	1	+	0.2	)				(5.8)
I^o		$(1-C_e)$			$(1-C_e)$		P_r		q_{ir}					
m/yr							m/yr		m/yr					
7.36E-02	=	0.5	/	0.15	/	(	0.3	+	1.5	×	30	)		(5.7)
L_1^o		I^o		d_{mix}^o			θ_c^o		ρ_b^o		$K_{d_1}^o$			
/yr		m/yr		m					g/cm^3		cm^3/g			
9.75E-02	=		(	0.023803	+	8E-05	+	0.0735835	)					
$\lambda_1 + E^o + L_1^o$				λ_1		E^o		L_1^o						
/yr				/yr		/yr		/yr						
-2.34E-05	=	-0.51223	/	225000	/	0.0975								(5.4)
A11		β1		$\rho_b^0 d_{mix}^o$		$\lambda_1 + E^o + L_1^o$								
pCi/g/yr		pCi/m^2		g/m^2		/yr								
1.05E-03	=	17.78792	/	225000	/	0.0975	-	-2.34E-05	/	0.097463				(5.5)
A10		α1		$\rho_b^0 d_{mix}^o$		$\lambda_1 + E^o + L_1^o$		A11		$\lambda_1 + E^o + L_1^o$				
-6.21E-04	=	0.00043	−	1.05E-03										(5.6)
C11		S10		A10										
pCi/g		pCi/g		pCi/g/yr										
4.48E-04	=	1.05E-03	+	-2.34E-05	x	0.4883	+	-6.21E-04	x	0.953525				(5.3)
S1(t)		A10		A11		t		C11		$e^{-(\lambda_1+E^o+L_1^0)t}$				
pCi/g		pCi/g		pCi/g/yr		yr		pCi/g						

Figure 5-6 Offsite Surface Soil Accumulation from both Irrigation and Particulate Deposition for the First Member of Transformation Chain (the highlighted values correlate with the values in Table 5-5)

Table 5-6 Spreadsheet Calculations for Y-90 Accumulation in Offsite Surface Soil from Both Irrigation and Deposition

Time	Y-90 Concentration in Irrigation Water (pCi/m^3)	Y-90 Concentration in Air from Code (pCi/m^3)	Y-90 Influx Entering Offsite Soil ($pCi/m^2/yr$)	α2	β2	A21	A20	C21	C22	Soil Conc. Calculated	Soil Conc. from Code
0.00E+00	0.00E+00	0.00E+00	0.00E+00							0.00E+00	0.00E+00
4.88E-01	4.37E+01	2.99E-05	9.05E+00	0.00E+00	1.85E+01	7.59E-04	-7.74E-03	7.74E-03	4.53E-08	1.07E-05	1.07E-05
9.77E-01	6.96E+01	2.95E-05	1.39E+01	9.05E+00	9.83E+00	4.49E-04	-4.19E-03	4.20E-03	-9.48E-10	3.45E-05	3.45E-05
1.46E+00	8.47E+01	2.91E-05	1.66E+01	1.39E+01	5.70E+00	2.61E-04	-2.05E-03	2.08E-03	-4.65E-12	6.53E-05	6.53E-05
1.95E+00	9.32E+01	2.87E-05	1.82E+01	1.66E+01	3.21E+00	1.47E-04	-7.52E-04	8.18E-04	6.19E-13	9.93E-05	9.93E-05
2.44E+00	9.77E+01	2.82E-05	1.90E+01	1.82E+01	1.71E+00	7.86E-05	2.54E-05	7.39E-05	8.00E-13	1.34E-04	1.34E-04
2.93E+00	9.99E+01	2.78E-05	1.94E+01	1.90E+01	7.96E-01	3.70E-05	4.90E-04	-3.56E-04	6.92E-13	1.69E-04	1.69E-04
3.42E+00	1.01E+02	2.74E-05	1.95E+01	1.94E+01	2.47E-01	1.20E-05	7.66E-04	-5.97E-04	5.70E-13	2.02E-04	2.02E-04
3.91E+00	1.00E+02	2.71E-05	1.95E+01	1.95E+01	-8.20E-02	-3.08E-06	9.26E-04	-7.24E-04	5.75E-13	2.35E-04	2.35E-04
4.39E+00	9.98E+01	2.67E-05	1.94E+01	1.95E+01	-2.78E-01	-1.21E-05	1.02E-03	-7.82E-04	4.35E-13	2.65E-04	2.65E-04
4.88E+00	9.88E+01	2.63E-05	1.92E+01	1.94E+01	-3.94E-01	-1.74E-05	1.07E-03	-8.00E-04	3.77E-13	2.94E-04	2.94E-04
5.37E+00	9.77E+01	2.59E-05	1.90E+01	1.92E+01	-4.61E-01	-2.05E-05	1.09E-03	-7.95E-04	2.74E-13	3.21E-04	3.21E-04
5.86E+00	9.64E+01	2.56E-05	1.87E+01	1.90E+01	-4.98E-01	-2.22E-05	1.10E-03	-7.75E-04	2.50E-13	3.46E-04	3.46E-04
6.35E+00	9.51E+01	2.52E-05	1.85E+01	1.87E+01	-5.17E-01	-2.31E-05	1.09E-03	-7.49E-04	2.70E-13	3.69E-04	3.69E-04
6.84E+00	9.38E+01	2.48E-05	1.82E+01	1.85E+01	-5.26E-01	-2.35E-05	1.09E-03	-7.18E-04	1.89E-13	3.91E-04	3.91E-04
7.32E+00	9.25E+01	2.45E-05	1.79E+01	1.82E+01	-5.28E-01	-2.36E-05	1.08E-03	-6.86E-04	1.73E-13	4.12E-04	4.12E-04
7.81E+00	9.12E+01	2.41E-05	1.77E+01	1.79E+01	-5.26E-01	-2.36E-05	1.07E-03	-6.53E-04	2.25E-13	4.31E-04	4.31E-04
8.30E+00[a]	8.98E+01	2.38E-05	1.74E+01	1.77E+01	-5.22E-01	-2.34E-05	1.05E-03	-6.21E-04	1.86E-13	4.48E-04	4.48E-04
8.79E+00	8.85E+01	2.35E-05	1.72E+01	1.74E+01	-5.17E-01	-2.31E-05	1.04E-03	-5.90E-04	1.29E-13	4.64E-04	4.64E-04

[a] The calculations for the highlighted time step are shown in Figure 5-8.

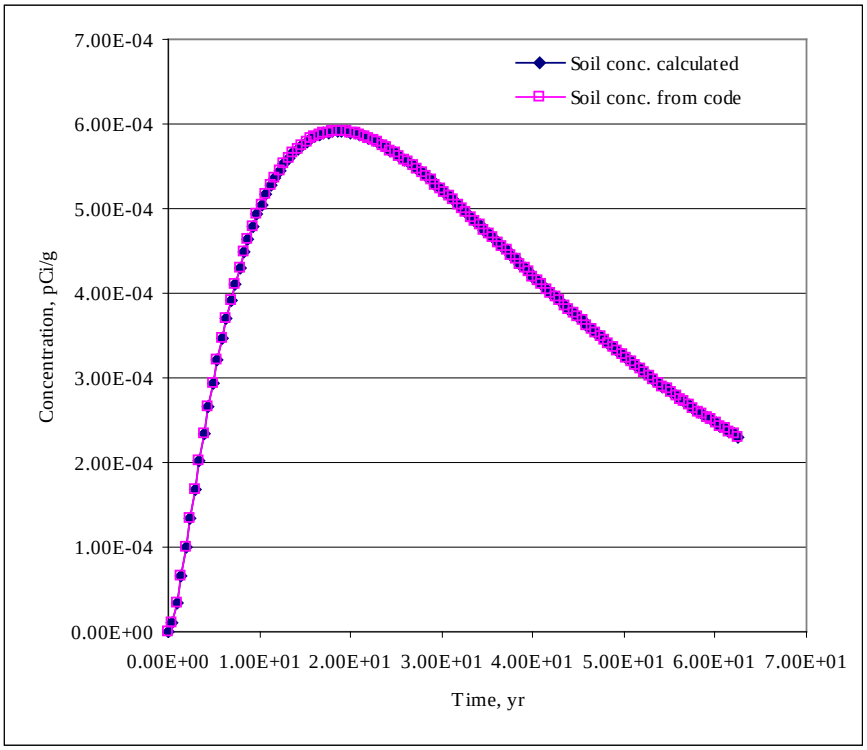

Figure 5-7 Accumulation of Y-90 in Offsite Soil from Both Irrigation and Deposition from Spreadsheet Calculations and from RESRAD-OFFSITE Code

where:

$R_i^{sr}(t)$ = release rate of nuclide *i* due to erosion of the surface soil above the primary contamination (pCi/yr),

SDR = sediment delivery ratio,

$f_s(t)$ = flux of nuclide *i* carried by groundwater entering the surface water body (pCi/yr),

$a_i(t)$ = air concentration of radionuclide *i* above the surface water body (pCi/m^3),

A^{sw} = surface area of the surface water body (m^2),

$V_i^{sw}(t)$ = surface water body volume at time *t* (m^3) (given in Eq. 5.29 in RESRAD-OFFSITE User's Manual):

$$V_i^{sw}(t) = V^{sw} + m^{sd}(t)K_d^i/10^6 \tag{5.16}$$

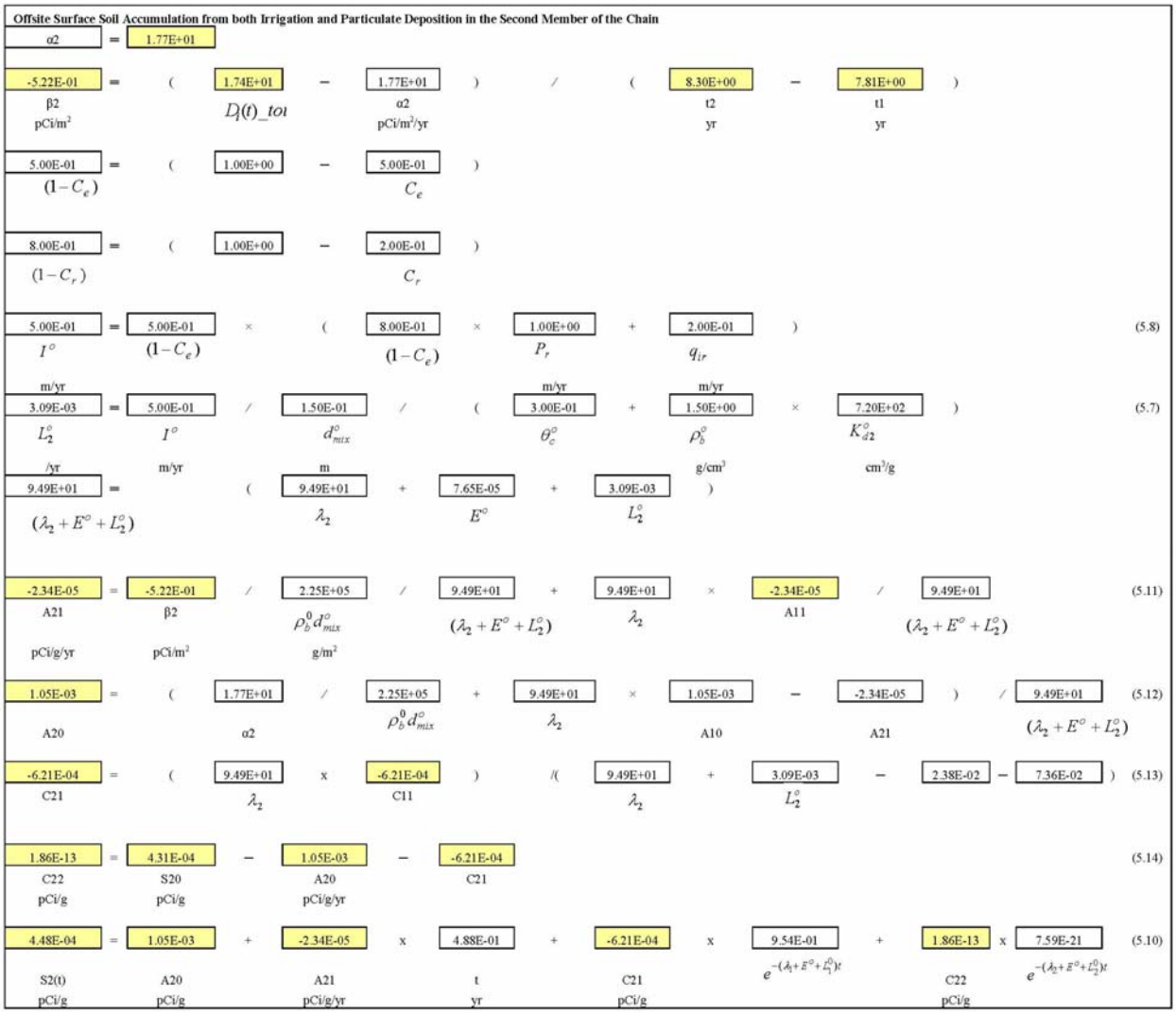

Figure 5-8 Offsite Surface Soil Accumulation from Both Irrigation and Particulate Deposition in the Second Member of the Chain (the highlighted values correlate with the values in Table 5-6)

where:

$$m^{sd}(t) = m^{sd}(0) + \frac{dm^{sd}(t)}{dt}\Delta t$$

V^{sw} = initial volume of water in the surface water body (m^3),

$m^{sd}(t)$ = cumulative mass of contaminated soil deposited into surface water body (g),

K_d^i = distribution coefficient of deposited radionuclide (cm^3/g).

The rate contaminants enter the water body can be approximated by a linear function of time *t* given as:

$$I_i^{sw}(t) = \alpha_i + \beta_i \times t \tag{5.17}$$

where α_i and β_i are constant between each pair of time points.

The surface water concentration of the first member of the transformation chain at any time *t* is given as (Eq. 5.37 in the RESRAD-OFFSITE User's Manual):

$$w_1^{sw}(t) = A_1^0 + A_1^1 \times t + C_1^1 e^{-(\lambda_1 + \lambda_1^{sw} + \lambda_1^{sw})t} \tag{5.18}$$

where A_1^0, A_1^1, and C_1^1 are given as:

$$A_1^0 = \frac{\alpha_1 - A_1^1}{\lambda_1 + \lambda_1^{sw} + \lambda_1^{sd}} \tag{5.19}$$

$$A_1^1 = \frac{\beta_1}{(\lambda_1 + \lambda_1^{sw} + \lambda_1^{sd})} \tag{5.20}$$

$$C_1^1 = w_1^{sw}(0) - A_1^0 \tag{5.21}$$

where:

λ_i^{sw} = rate constant for the removal of nuclide *i* with the water flowing out of the surface water body (/yr),

λ_i^{sd} = equivalent rate constant for the change in partitioning caused by the additional mass of eroded soil into the surface water body (/yr),

$$\lambda_i^{sw} = \frac{q_{sw}}{V_i^{sw}(t)} \tag{5.22}$$

$$\lambda_i^{sd} = \frac{10^{-6} K_d^i}{V_i^{sw}} \frac{dm^{sd}(t)}{dt} \tag{5.23}$$

$$q_{sw} = \frac{V^{sw}}{mean_residence_time} \tag{5.24}$$

For verifying the surface water concentration from the initial contamination, Ra-226 was selected. Table 5-7 shows the results of spreadsheet calculations for few time steps for the accumulation in surface water. All parameters were kept at their default values. The results of spreadsheet calculations are compared with the RESRAD-OFFSITE results (Figure 5-9). Figure 5-10 shows the individual steps of the calculation for one time step highlighted in Table 5-7. For this comparison, additional mass deposition, erosion flux, air concentration above the surface water area, and flux from groundwater to surface water body were taken as input from the code. There is practically no difference in the spreadsheet calculations and the results from RESRAD-OFFSITE code (see Table 5-7 and Figure 5-9). The spreadsheet calculations for other radionuclides are provided in Excel spreadsheets.

The surface water concentration of the second member of transformation chain at any time *t* is given as (Equation 5.40 in the RESRAD-OFFSITE User's Manual):

$$w_2^{sw}(t) = A_2^0 + A_2^1 \times t + C_2^1 e^{-(\lambda_1+\lambda_1^{sw}+\lambda_1^{sd})t} + C_2^2 e^{-(\lambda_2+\lambda_2^{sw}+\lambda_2^{sd})t} \tag{5.25}$$

where A_2^0, A_2^1, C_2^1, and C_2^2 are given as:

$$A_2^0 = \frac{\alpha_2}{(\lambda_2+\lambda_2^{sw}+\lambda_2^{sd})} + \frac{[\frac{V_1^{sw}(t)}{V_2^{sw}(t)}]\lambda_2 A_1^0}{(\lambda_2+\lambda_2^{sw}+\lambda_2^{sd})} - \frac{A_2^1}{(\lambda_2+\lambda_2^{sw}+\lambda_2^{sd})} \tag{5.26}$$

$$A_2^1 = \frac{\beta_2}{(\lambda_2+\lambda_2^{sw}+\lambda_2^{sd})} + \frac{[\frac{V_1^{sw}(t)}{V_2^{sw}(t)}]\lambda_2 A_1^1}{(\lambda_2+\lambda_2^{sw}+\lambda_2^{sd})} \tag{5.27}$$

$$C_2^1 = [\frac{V_1^{sw}(t)}{V_2^{sw}(t)}]\frac{\lambda_2 C_1^1}{\lambda_2+\lambda_2^{sw}+\lambda_2^{sd}-\lambda_1-\lambda_1^{sw}-\lambda_1^{sd}} \tag{5.28}$$

$$C_2^2 = w_2^{sw}(0) - A_2^0 - C_2^1 \tag{5.29}$$

For verifying the surface water concentration for the second member of the transformation chain, Ra-226 was selected and the concentration for its progeny Pb-210 was verified. Table 5-8 shows the results of spreadsheet calculations for a few time steps for the accumulation in surface water for the second member of the chain (Pb-210). The results of spreadsheet calculations are compared with the RESRAD-OFFSITE results (Figure 5-11). For this comparison, erosion flux, air concentration above the surface water area, and flux from groundwater to surface water body were taken as input from the code. There is practically no difference in the spreadsheet calculations and the results from RESRAD-OFFSITE code (see Table 5-8 and Figure 5-11). The spreadsheet calculations for other radionuclides are provided in Excel spreadsheets.

5.3 Accumulation in Plants

Plant foods get contaminated due to root uptake from offsite contaminated soil, foliar uptake from overhead irrigation, and foliar uptake from contaminated dust in the agricultural area. RESRAD-OFFSITE has four food types: fruit, grain, and nonleafy vegetables; leafy vegetables; pasture and silage; and grain. Fruit, grain, and nonleafy and leafy vegetables are for human consumption, while pasture and silage and grain are for livestock intake. Accumulation in plant food is calculated as described in Section 5.3 of the RESRAD-OFFSITE User's Manual.

The activity concentration in the edible part of the plant from root uptake of the contaminated offsite soil is given as (Eq. 5.44 in the RESRAD-OFFSITE User's Manual):

Table 5-7 Spreadsheet Calculations for Ra-226 Accumulation in Surface Water

Time	V_1^{sw}	$M^{sd}(t)$	λ_1^{sw}	λ_1^{sd}	Erosion Flux from the Code (pCi/yr)	Additional Mass Deposited from the Code (g/yr)	Air Concentration above SW Area from Code (pCi/m^3)	Flux from Groundwater to Surface Water Body from Code (pCi/yr)	Flux Entering Surface Water Body (pCi/yr/m^3)	α1	β1	A11	A10	C11	First Member Surface Water Conc. Calculated (pCi/m^3)	First Member Surface Water Conc. from Code (pCi/m^3)
0	150000	0.00E+00	1.00E+00	8.03E-05	1.72E+05	1.72E+05	1.37E-08	0.00E+00	1.15E+00						0.00E+00	0.00E+00
0.4883	150006	8.40E+04	1.00E+00	8.03E-05	1.72E+05	1.72E+05	1.37E-08	0.00E+00	1.15E+00	1.15E+00	-3.31E-03	-3.31E-03	1.15E+00	-1.15E+00	4.43E-01	4.43E-01
0.9766	150012	1.68E+05	1.00E+00	8.03E-05	1.72E+05	1.72E+05	1.37E-08	0.00E+00	1.14E+00	1.15E+00	-3.31E-03	-3.30E-03	1.15E+00	-7.06E-01	7.14E-01	7.14E-01
1.4648	150018	2.52E+05	1.00E+00	8.03E-05	1.71E+05	1.72E+05	1.36E-08	0.00E+00	1.14E+00	1.14E+00	-3.30E-03	-3.30E-03	1.15E+00	-4.33E-01	8.80E-01	8.80E-01
1.9531	150024	3.36E+05	1.00E+00	8.03E-05	1.71E+05	1.72E+05	1.36E-08	0.00E+00	1.14E+00	1.14E+00	-3.30E-03	-3.29E-03	1.15E+00	-2.66E-01	9.81E-01	9.81E-01
2.4414	150029	4.20E+05	1.00E+00	8.03E-05	1.71E+05	1.72E+05	1.36E-08	0.00E+00	1.14E+00	1.14E+00	-3.29E-03	-3.29E-03	1.14E+00	-1.63E-01	1.04E+00	1.04E+00
2.9297	150035	5.04E+05	1.00E+00	8.03E-05	1.71E+05	1.72E+05	1.36E-08	0.00E+00	1.14E+00	1.14E+00	-3.29E-03	-3.29E-03	1.14E+00	-1.00E-01	1.08E+00	1.08E+00
3.418	150041	5.88E+05	1.00E+00	8.03E-05	1.70E+05	1.72E+05	1.36E-08	0.00E+00	1.14E+00	1.14E+00	-3.28E-03	-3.28E-03	1.14E+00	-6.15E-02	1.10E+00	1.10E+00
3.9063	150047	6.72E+05	1.00E+00	8.03E-05	1.70E+05	1.72E+05	1.35E-08	0.00E+00	1.13E+00	1.14E+00	-3.28E-03	-3.28E-03	1.14E+00	-3.77E-02	1.11E+00	1.11E+00
4.3945	150053	7.56E+05	1.00E+00	8.03E-05	1.70E+05	1.72E+05	1.35E-08	0.00E+00	1.13E+00	1.13E+00	-3.27E-03	-3.27E-03	1.14E+00	-2.32E-02	1.12E+00	1.12E+00
4.8828	150059	8.40E+05	1.00E+00	8.03E-05	1.70E+05	1.72E+05	1.35E-08	0.00E+00	1.13E+00	1.13E+00	-3.27E-03	-3.27E-03	1.14E+00	-1.43E-02	1.13E+00	1.13E+00
5.3711[a]	150065	9.24E+05	1.00E+00	8.02E-05	1.69E+05	1.72E+05	1.35E-08	0.00E+00	1.13E+00	1.13E+00	-3.26E-03	-3.26E-03	1.13E+00	-8.80E-03	1.13E+00	1.13E+00
5.8594	150071	1.01E+06	1.00E+00	8.02E-05	1.69E+05	1.72E+05	1.35E-08	0.00E+00	1.13E+00	1.13E+00	-3.26E-03	-3.26E-03	1.13E+00	-5.44E-03	1.13E+00	1.13E+00
6.3477	150076	1.09E+06	9.99E-01	8.02E-05	1.69E+05	1.72E+05	1.34E-08	0.00E+00	1.13E+00	1.13E+00	-3.25E-03	-3.25E-03	1.13E+00	-3.38E-03	1.13E+00	1.13E+00
6.8359	150082	1.18E+06	9.99E-01	8.02E-05	1.69E+05	1.72E+05	1.34E-08	0.00E+00	1.12E+00	1.13E+00	-3.25E-03	-3.25E-03	1.13E+00	-2.11E-03	1.13E+00	1.13E+00
7.3242	150088	1.26E+06	9.99E-01	8.02E-05	1.69E+05	1.72E+05	1.34E-08	0.00E+00	1.12E+00	1.12E+00	-3.24E-03	-3.24E-03	1.13E+00	-1.34E-03	1.13E+00	1.13E+00
7.8125	150094	1.34E+06	9.99E-01	8.02E-05	1.68E+05	1.72E+05	1.34E-08	0.00E+00	1.12E+00	1.12E+00	-3.24E-03	-3.24E-03	1.13E+00	-8.60E-04	1.12E+00	1.12E+00
8.3008	150100	1.43E+06	9.99E-01	8.02E-05	1.68E+05	1.72E+05	1.34E-08	0.00E+00	1.12E+00	1.12E+00	-3.24E-03	-3.24E-03	1.12E+00	-5.67E-04	1.12E+00	1.12E+00

[a] The calculations for the highlighted time step are shown in Figure 5-10.

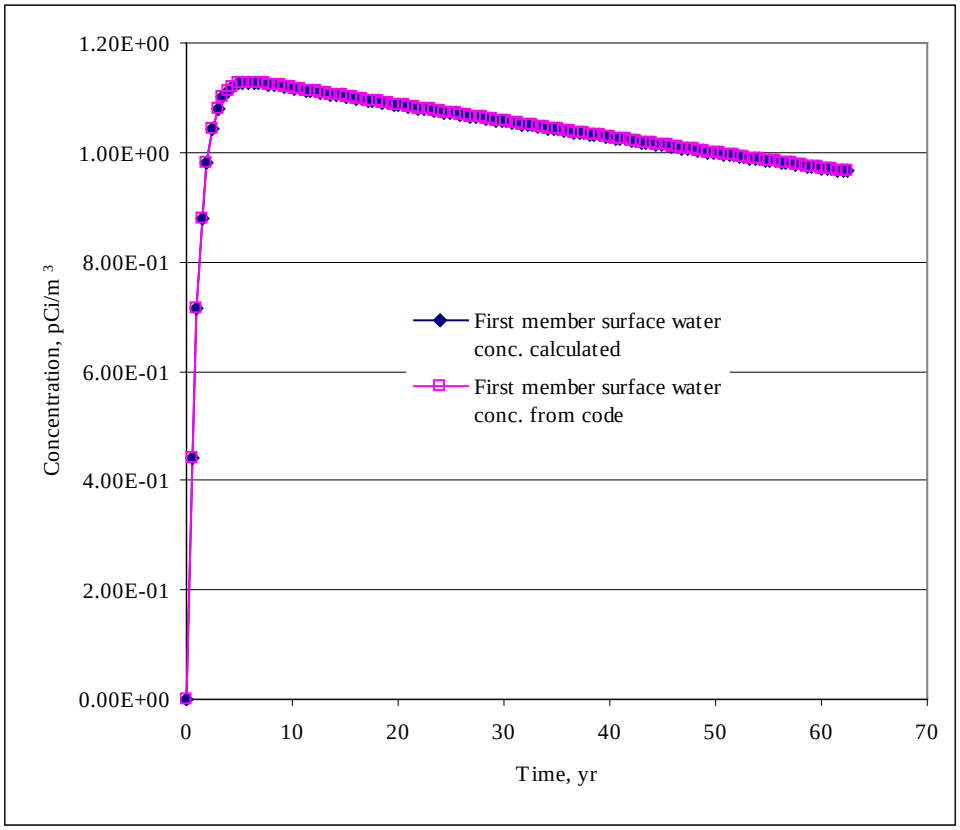

Figure 5-9 Accumulation of Ra-226 in Surface Water from Spreadsheet Calculations and from RESRAD-OFFSITE Code

$$p_i^{offsoil}(t) = rtf_i s_i^0(t) \tag{5.30}$$

where:

$p_i^{offsoil}(t)$ = activity concentration of radionuclide *i* in plant from root uptake at time *t* (pCi/kg),

rtf_i = plant transfer factor (root uptake factor) of radionuclide *i* (pCi/kg per pCi/kg),

$s_i^0(t)$ = radionuclide *i* concentration in offsite soil where plant good is grown at time *t* (pCi/kg).

The activity concentration in the edible part of the plant from foliar uptake from overhead irrigation is given as (Eq. 5.45 in the RESRAD-OFFSITE User's Manual):

$$p_i^{oi}(t) = \frac{f_{\text{int}} f_{tl}}{Y} \frac{1-\exp(-\lambda_w t_g)}{\lambda_w} \frac{q_{ir}}{t_g} w_i^{ir}(t) \tag{5.31}$$

where:

Accumulation in Surface Water for the First Member of Transformation Chain

9.24E+05	=	8.40E+05	+	(	1.72E+05	×	(	5.37E+00	−	4.88E+00	))			(5.16a)
$m^{sd}(t)$		$m^{sd}(0)$			$\frac{dm^{sd}(t)}{dt}$			t2		t1				
1.50E+05	=	1.50E+05	+	(	9.24E+05	×	7.00E+01	/	1.00E+06	)				(5.16)
$V_i^{sw}(t)$		V^{sw}			$m^{sd}(t)$		K_d^i							
1.50E+05	=	1.50E+05	/	1.00E+00										(5.24)
q_{sw}		V^{sw}		$mean_residence_time$										
1.00E+00	=	1.50E+05	/	1.50E+05										(5.22)
λ_i^{sw}		q_{sw}		$V_i^{sw}(t)$										
8.02E-05	=	(	1.00E-06	×	7.00E+01	/	1.50E+05	×	1.72E+05	)				(5.23)
λ_i^{sd}					K_d^i		$V_i^{sw}(t)$		$\frac{dm^{sd}(t)}{dt}$					
1.00E+00	=	4.33E-04	+	1.00E+00	+	8.02E-05								
$\lambda_1 + \lambda_1^{sw} + \lambda_1^{sd}$		λ_1		λ_i^{sw}		λ_i^{sd}								
1.69E+05	=	1.69E+05	×	1.00E+00										
$R_i^{sr}(t)SDR$		$R_i^{sr}(t)$		SDR										
3.83E+01	=	1.35E-08	×	3.16E+04	×	9.00E+04								
$a_i(t)V_{dep}A^{sw}$		$a_i(t)$		V_{dep}		A^{sw}								
1.13E+00	=	(	1.69E+05	+	0.00E+00	+	3.83E+01	)	/	1.50E+05				(5.15)
$I_i^{sw}(t)$			$R_i^{sr}(t)SDR$		$f_s(t)$		$a_i(t)V_{dep}A^{sw}$			$V_i^{sw}(t)$				
α1	=	1.13E+00												
-3.26E-03	=	(	1.13E+00	−	1.13E+00	)	/	(	5.37E+00	−	4.88E+00	)		
β1														
-3.26E-03	=	-3.26E-03	/	1.00E+00										(5.19)
A11		β1		$\lambda_1 + \lambda_1^{sw} + \lambda_1^{sd}$										
1.13E+00	=	(	1.13E+00	−	-3.26E-03	)	/	1.00E+00						(5.20)
A10			α1		A11			$\lambda_1 + \lambda_1^{sw} + \lambda_1^{sd}$						
-8.80E-03	=	1.13E+00	−	1.13E+00										(5.21)
C11		$w_1^{sw}(0)$		A10										
1.13E+00	=	1.13E+00	+	-1.59E-03	+	-8.80E-03	×	6.14E-01						(5.18)
$w_1^{sw}(t)$		A10		$A_1^1(t)$		C11		$e^{-(\lambda_1+\lambda_1^{sw}+\lambda_1^{sw})t}$						

Figure 5-10 Accumulation in Surface Water for the First Member of Transformation Chain (the highlighted values correlate with the values in Table 5-7)

$p_i^{oi}(t)$ = activity concentration of radionuclide *i* in the edible portion of the plant resulting from foliar uptake of overhead irrigation (pCi/kg),

f_{int} = foliar interception factor,

f_{tl} = fraction of the contaminant that is translocated from the foliage to the edible part of the plant,

Y = wet crop yield (kg/m^2),

Table 5-8 Spreadsheet Calculations for Pb-210 Accumulation in Surface Water

Time, yr	V_2^{sw}	λ_2^{sw}	λ_2^{sd}	Erosion Flux from the Code (pCi/yr)	Air Concentration above SW Area from Code (pCi/m^3)	Flux from Groundwater to Surface Water Body from Code (pCi/yr)	Flux Entering Surface Water Body (pCi/yr/m^3)	α2	β2	A21	A20	C21	C22	Second Member Surface Water Conc. Calculated, (pCi/m^3)	Second Member Surface Water Conc. from Code (pCi/m^3)
0	1.50E+05	1.00E+00	1.15E-04	0.00E+00	0.00E+00	0.00E+00	0.00E+00							0.00E+00	0.00E+00
0.488	1.50E+05	1.00E+00	1.15E-04	2.59E+03	2.06E-10	0.00E+00	1.73E-02	0.00E+00	3.53E-02	3.42E-02	1.52E-03	-1.17E+00	1.16E+00	6.66E-03	6.66E-03
0.977	1.50E+05	1.00E+00	1.15E-04	5.13E+03	4.08E-10	0.00E+00	3.42E-02	1.73E-02	3.47E-02	3.36E-02	1.88E-02	-7.15E-01	7.03E-01	2.13E-02	2.13E-02
1.465	1.50E+05	1.00E+00	1.15E-04	7.63E+03	6.07E-10	0.00E+00	5.09E-02	3.42E-02	3.41E-02	3.30E-02	3.57E-02	-4.39E-01	4.25E-01	3.91E-02	3.91E-02
1.953	1.50E+05	1.00E+00	1.15E-04	1.01E+04	8.03E-10	0.00E+00	6.73E-02	5.09E-02	3.35E-02	3.24E-02	5.24E-02	-2.70E-01	2.56E-01	5.78E-02	5.78E-02
2.441	1.50E+05	1.00E+00	1.15E-04	1.25E+04	9.95E-10	0.00E+00	8.33E-02	6.73E-02	3.30E-02	3.19E-02	6.88E-02	-1.66E-01	1.55E-01	7.62E-02	7.62E-02
2.93	1.50E+05	1.00E+00	1.15E-04	1.49E+04	1.18E-09	0.00E+00	9.92E-02	8.33E-02	3.24E-02	3.13E-02	8.49E-02	-1.02E-01	9.30E-02	9.40E-02	9.40E-02
3.418	1.50E+05	1.00E+00	1.15E-04	1.72E+04	1.37E-09	0.00E+00	1.15E-01	9.92E-02	3.18E-02	3.08E-02	1.01E-01	-6.25E-02	5.57E-02	1.11E-01	1.11E-01
3.906	1.50E+05	1.00E+00	1.15E-04	1.95E+04	1.55E-09	0.00E+00	1.30E-01	1.15E-01	3.13E-02	3.02E-02	1.16E-01	-3.84E-02	3.32E-02	1.28E-01	1.28E-01
4.395	1.50E+05	9.99E-01	1.15E-04	2.17E+04	1.73E-09	0.00E+00	1.45E-01	1.30E-01	3.07E-02	2.97E-02	1.32E-01	-2.36E-02	1.96E-02	1.43E-01	1.43E-01
4.883	1.50E+05	9.99E-01	1.15E-04	2.40E+04	1.91E-09	0.00E+00	1.60E-01	1.45E-01	3.02E-02	2.92E-02	1.47E-01	-1.45E-02	1.14E-02	1.59E-01	1.59E-01
5.371	1.50E+05	9.99E-01	1.15E-04	2.61E+04	2.08E-09	0.00E+00	1.74E-01	1.60E-01	2.96E-02	2.87E-02	1.61E-01	-8.97E-03	6.43E-03	1.74E-01	1.74E-01
5.859	1.50E+05	9.99E-01	1.15E-04	2.83E+04	2.25E-09	0.00E+00	1.88E-01	1.74E-01	2.91E-02	2.82E-02	1.76E-01	-5.55E-03	3.43E-03	1.88E-01	1.88E-01
6.348	1.50E+05	9.99E-01	1.15E-04	3.04E+04	2.42E-09	0.00E+00	2.02E-01	1.88E-01	2.86E-02	2.77E-02	1.90E-01	-3.45E-03	1.62E-03	2.02E-01	2.02E-01
6.836	1.50E+05	9.99E-01	1.15E-04	3.24E+04	2.58E-09	0.00E+00	2.16E-01	2.02E-01	2.81E-02	2.72E-02	2.04E-01	-2.16E-03	5.39E-04	2.16E-01	2.16E-01
7.324	1.50E+05	9.99E-01	1.15E-04	3.45E+04	2.74E-09	0.00E+00	2.30E-01	2.16E-01	2.76E-02	2.67E-02	2.18E-01	-1.36E-03	-1.12E-04	2.30E-01	2.30E-01
7.813	1.50E+05	9.99E-01	1.15E-04	3.64E+04	2.90E-09	0.00E+00	2.43E-01	2.30E-01	2.71E-02	2.62E-02	2.31E-01	-8.79E-04	-4.99E-04	2.43E-01	2.43E-01
8.301	1.50E+05	9.99E-01	1.15E-04	3.84E+04	3.06E-09	0.00E+00	2.56E-01	2.43E-01	2.66E-02	2.58E-02	2.45E-01	-5.80E-04	-7.26E-04	2.56E-01	2.56E-01
8.789	1.50E+05	9.99E-01	1.15E-04	4.03E+04	3.21E-09	0.00E+00	2.69E-01	2.56E-01	2.62E-02	2.53E-02	2.58E-01	-3.97E-04	-8.57E-04	2.69E-01	2.69E-01
9.277	1.50E+05	9.99E-01	1.15E-04	4.22E+04	3.36E-09	0.00E+00	2.81E-01	2.69E-01	2.57E-02	2.48E-02	2.70E-01	-2.84E-04	-9.31E-04	2.82E-01	2.82E-01
9.766	1.50E+05	9.99E-01	1.15E-04	4.41E+04	3.51E-09	0.00E+00	2.93E-01	2.81E-01	2.52E-02	2.44E-02	2.83E-01	-2.15E-04	-9.69E-04	2.94E-01	2.94E-01
10.25	1.50E+05	9.99E-01	1.15E-04	4.59E+04	3.65E-09	0.00E+00	3.06E-01	2.93E-01	2.48E-02	2.40E-02	2.95E-01	-1.72E-04	-9.85E-04	3.06E-01	3.06E-01

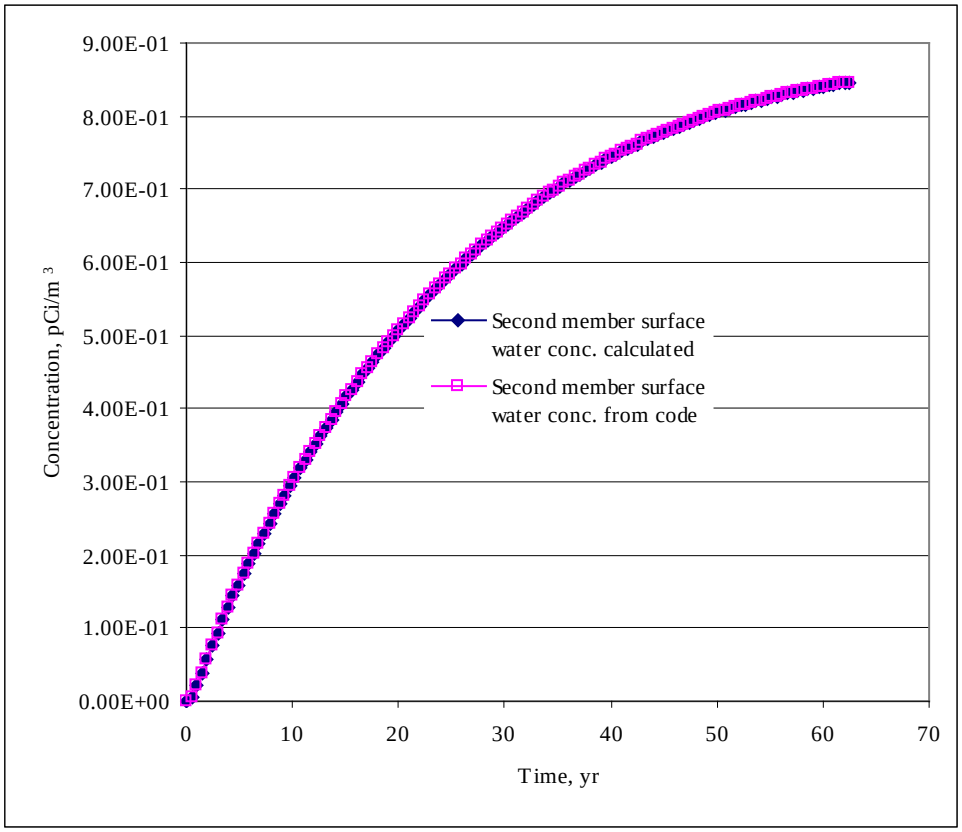

Figure 5-11 Accumulation of Pb-210 in Surface Water from Spreadsheet Calculations and from RESRAD-OFFSITE Code

λ_w = weathering constant (per yr),

t_g = duration of growing season (yr),

q_{ir} = irrigation rate (m/yr),

$w_i^{ir}(t)$ = activity concentration of radionuclide *i* in contaminated irrigation water (pCi/m^3).

The activity concentration in the edible part of the plant from foliar uptake from contaminated dust is given as (Eq. 5.51 in the RESRAD-OFFSITE User's Manual):

$$p_i^{dust}(t) = \frac{f_{\text{int}} f_{tl}}{Y} \frac{1-\exp(-\lambda_w t_g)}{\lambda_w} V_{dep} a_i(t) \qquad 5.32)$$

where:

$p_i^{dust}(t)$ = activity concentration of radionuclide *i* at time *t* in the edible portion of the plant from foliar interception of dust (pCi/kg),

Table 5-9 Spreadsheet Calculations for U-238 Accumulation in Fruit, Grain, and Nonleafy Vegetables – Grown in Area 1

Time (year)	Soil Conc. from Code (pCi/g)	Irrigation Water Conc. from Code (pCi/L)	Air Conc. from Code (pCi/m^3)	Plant Conc. from Root Uptake (pCi/g)	Plant Conc. from Irrigation (pCi/g)	Plant Conc. from Dust (pCi/g)	Fruit, Grain, Nonleafy Conc. Calculated (pCi/kg)	Fruit, Grain, Nonleafy Conc. from Code (pCi/kg)
0.00E+00	0.00E+00	0.00E+00	3.03E-07	0.00E+00	0.00E+00	1.65E-08	1.65E-05	1.65E-05
4.88E-01	1.09E-07	4.43E-04	3.03E-07	2.72E-10	8.99E-07	1.65E-08	9.16E-04	9.16E-04
9.77E-01	3.58E-07	7.14E-04	3.02E-07	8.94E-10	1.45E-06	1.65E-08	1.47E-03	1.47E-03
1.46E+00	6.88E-07	8.79E-04	3.02E-07	1.72E-09	1.79E-06	1.64E-08	1.80E-03	1.80E-03
1.95E+00	1.06E-06	9.80E-04	3.01E-07	2.66E-09	1.99E-06	1.64E-08	2.01E-03	2.01E-03
2.44E+00	1.46E-06	1.04E-03	3.01E-07	3.66E-09	2.11E-06	1.64E-08	2.13E-03	2.13E-03
2.93E+00[a]	1.88E-06	1.08E-03	3.00E-07	4.69E-09	2.19E-06	1.64E-08	2.21E-03	2.21E-03
3.42E+00	2.29E-06	1.10E-03	3.00E-07	5.73E-09	2.23E-06	1.63E-08	2.26E-03	2.26E-03
3.91E+00	2.70E-06	1.11E-03	2.99E-07	6.76E-09	2.26E-06	1.63E-08	2.28E-03	2.28E-03
4.39E+00	3.11E-06	1.12E-03	2.99E-07	7.78E-09	2.27E-06	1.63E-08	2.30E-03	2.30E-03
4.88E+00	3.51E-06	1.12E-03	2.98E-07	8.78E-09	2.28E-06	1.63E-08	2.31E-03	2.31E-03
5.37E+00	3.90E-06	1.13E-03	2.98E-07	9.76E-09	2.29E-06	1.62E-08	2.31E-03	2.31E-03
5.86E+00	4.29E-06	1.13E-03	2.97E-07	1.07E-08	2.29E-06	1.62E-08	2.31E-03	2.31E-03
6.35E+00	4.67E-06	1.12E-03	2.97E-07	1.17E-08	2.28E-06	1.62E-08	2.31E-03	2.31E-03
6.84E+00	5.03E-06	1.12E-03	2.97E-07	1.26E-08	2.28E-06	1.62E-08	2.31E-03	2.31E-03
7.32E+00	5.39E-06	1.12E-03	2.96E-07	1.35E-08	2.28E-06	1.61E-08	2.31E-03	2.31E-03
7.81E+00	5.75E-06	1.12E-03	2.96E-07	1.44E-08	2.28E-06	1.61E-08	2.31E-03	2.31E-03
8.30E+00	6.09E-06	1.12E-03	2.95E-07	1.52E-08	2.27E-06	1.61E-08	2.30E-03	2.30E-03

[a] The calculations for the highlighted time step are shown in Figure 5-13.

V_{dep} = deposition velocity of the contaminated dust particle (m/yr),

$a_i(t)$ = air concentration of radionuclide *i* at time *t* above the agricultural area where plant is growing (pCi/m^3).

U-238 was selected for this pathway verification. First, the plant concentration from the sub-pathways was calculated and finally added together to compare the results of the total plant concentration. The initial soil concentration in the primary contaminated area was 1 pCi/g. Surface water was the source of water for all uses. Other parameters were at their default values. The calculations were done for all four food types. The sub-pathways considered were: root uptake from offsite contaminated soil, foliar uptake from overhead irrigation, and foliar uptake from contaminated dust in the agricultural area. For this comparison, radionuclide concentration in soil, irrigation water, and air in the agricultural area where the plants were grown were obtained from the code. Tables 5-9 to 5-12 show the spreadsheet calculations for U-238 accumulation in four different food types grown in four different agricultural areas.

Figure 5-12 shows the U-238 accumulations in fruit, grain, and nonleafy vegetables grown in agricultural area 1 from both spreadsheet calculations and from the RESRAD-OFFSITE code. Figure 5-13 shows the individual steps of the calculation for one time step highlighted in Table 5-9 for U-238 accumulation in fruit, grain, and nonleafy vegetables.

Table 5-10 Spreadsheet Calculations for U-238 Accumulation in Leafy Vegetables – Grown in Area 2

Time (year)	Soil Conc. from Code (pCi/g)	Irrigation Water Conc. from Code (pCi/L)	Air Conc. from Code (pCi/m^3)	Plant Conc. from Root Uptake (pCi/g)	Plant Conc. from Irrigation (pCi/g)	Plant Conc. from Dust (pCi/g)	Leafy Conc. Calculated (pCi/kg)	Leafy Conc. from Code (pCi/kg)
0.00E+00	0.00E+00	0.00E+00	2.35E-07	0.00E+00	0.00E+00	6.14E-08	6.14E-05	6.14E-05
4.88E-01	1.06E-07	4.43E-04	2.35E-07	2.66E-10	2.93E-06	6.13E-08	2.99E-03	2.99E-03
9.77E-01	3.56E-07	7.14E-04	2.34E-07	8.90E-10	4.73E-06	6.12E-08	4.79E-03	4.79E-03
1.46E+00	6.89E-07	8.79E-04	2.34E-07	1.72E-09	5.82E-06	6.11E-08	5.89E-03	5.89E-03
1.95E+00	1.07E-06	9.80E-04	2.33E-07	2.67E-09	6.49E-06	6.10E-08	6.55E-03	6.55E-03
2.44E+00	1.47E-06	1.04E-03	2.33E-07	3.69E-09	6.90E-06	6.09E-08	6.96E-03	6.96E-03
2.93E+00[a]	1.89E-06	1.08E-03	2.33E-07	4.73E-09	7.14E-06	6.08E-08	7.21E-03	7.21E-03
3.42E+00	2.31E-06	1.10E-03	2.32E-07	5.78E-09	7.29E-06	6.07E-08	7.35E-03	7.35E-03
3.91E+00	2.73E-06	1.11E-03	2.32E-07	6.82E-09	7.37E-06	6.06E-08	7.44E-03	7.44E-03
4.39E+00	3.14E-06	1.12E-03	2.31E-07	7.85E-09	7.42E-06	6.05E-08	7.48E-03	7.48E-03
4.88E+00	3.55E-06	1.12E-03	2.31E-07	8.87E-09	7.44E-06	6.04E-08	7.51E-03	7.51E-03
5.37E+00	3.95E-06	1.13E-03	2.31E-07	9.86E-09	7.45E-06	6.03E-08	7.52E-03	7.52E-03
5.86E+00	4.34E-06	1.13E-03	2.30E-07	1.08E-08	7.45E-06	6.02E-08	7.52E-03	7.52E-03
6.35E+00	4.72E-06	1.12E-03	2.30E-07	1.18E-08	7.45E-06	6.01E-08	7.52E-03	7.52E-03
6.84E+00	5.09E-06	1.12E-03	2.30E-07	1.27E-08	7.44E-06	6.00E-08	7.51E-03	7.51E-03
7.32E+00	5.45E-06	1.12E-03	2.29E-07	1.36E-08	7.43E-06	5.99E-08	7.51E-03	7.51E-03
7.81E+00	5.81E-06	1.12E-03	2.29E-07	1.45E-08	7.42E-06	5.98E-08	7.50E-03	7.50E-03
8.30E+00	6.16E-06	1.12E-03	2.29E-07	1.54E-08	7.41E-06	5.97E-08	7.49E-03	7.49E-03

[a] The calculations for the highlighted time step are shown in Figure 5-15.

Figure 5-14 shows the U-238 accumulations in leafy vegetables grown in agricultural area 2 from both spreadsheet calculations and from the RESRAD-OFFSITE code. Figure 5-15 shows the individual steps of the calculation for one time step highlighted in Table 5-10 for U-238 accumulation in leafy vegetables.

Figure 5-16 shows the U-238 accumulations in pasture and silage grown in agricultural area 3 from both spreadsheet calculations and from the RESRAD-OFFSITE code. Figure 5-17 shows the individual steps of the calculation for one time step highlighted in Table 5-11 for U-238 accumulation in pasture and silage.

Figure 5-18 shows the U-238 accumulations in grain grown in agricultural area 4 from both spreadsheet calculations and from the RESRAD-OFFSITE code. Figure 5-19 shows the individual steps of the calculation for one time step highlighted in Table 5-12 for U-238 accumulation in grain.

There is practically no difference in the RESRAD-OFFSITE code results and spreadsheet calculations for all plant types.

Table 5-11 Spreadsheet Calculations for U-238 Accumulation in Pasture and Silage – Grown in Area 3

Time (year)	Soil Conc. from Code (pCi/g)	Irrigation Water Conc. from Code (pCi/L)	Air Conc. from Code (pCi/m^3)	Plant Conc. from Root Uptake (pCi/g)	Plant Conc. from Irrigation (pCi/g)	Plant Conc. from Dust (pCi/g)	Pasture, Silage Conc. Calculated (pCi/kg)	Pasture Silage Conc. from Code (pCi/kg)
0.00E+00	0.00E+00	0.00E+00	4.59E-08	0.00E+00	0.00E+00	1.31E-08	1.31E-05	1.31E-05
4.88E-01	8.66E-08	4.43E-04	4.59E-08	2.16E-10	1.00E-05	1.31E-08	1.01E-02	1.01E-02
9.77E-01	3.05E-07	7.14E-04	4.58E-08	7.63E-10	1.62E-05	1.31E-08	1.62E-02	1.62E-02
1.46E+00	6.01E-07	8.79E-04	4.57E-08	1.50E-09	1.99E-05	1.31E-08	2.00E-02	2.00E-02
1.95E+00	9.41E-07	9.80E-04	4.56E-08	2.35E-09	2.22E-05	1.31E-08	2.22E-02	2.22E-02
2.44E+00	1.30E-06	1.04E-03	4.56E-08	3.26E-09	2.36E-05	1.30E-08	2.36E-02	2.36E-02
2.93E+00[a]	1.68E-06	1.08E-03	4.55E-08	4.19E-09	2.44E-05	1.30E-08	2.45E-02	2.45E-02
3.42E+00	2.05E-06	1.10E-03	4.54E-08	5.13E-09	2.49E-05	1.30E-08	2.50E-02	2.50E-02
3.91E+00	2.43E-06	1.11E-03	4.53E-08	6.07E-09	2.52E-05	1.30E-08	2.53E-02	2.53E-02
4.39E+00	2.80E-06	1.12E-03	4.53E-08	7.00E-09	2.54E-05	1.30E-08	2.54E-02	2.54E-02
4.88E+00	3.16E-06	1.12E-03	4.52E-08	7.91E-09	2.55E-05	1.29E-08	2.55E-02	2.55E-02
5.37E+00	3.52E-06	1.13E-03	4.51E-08	8.80E-09	2.55E-05	1.29E-08	2.55E-02	2.55E-02
5.86E+00	3.87E-06	1.13E-03	4.50E-08	9.68E-09	2.55E-05	1.29E-08	2.55E-02	2.55E-02
6.35E+00	4.22E-06	1.12E-03	4.50E-08	1.05E-08	2.55E-05	1.29E-08	2.55E-02	2.55E-02
6.84E+00	4.55E-06	1.12E-03	4.49E-08	1.14E-08	2.55E-05	1.29E-08	2.55E-02	2.55E-02
7.32E+00	4.88E-06	1.12E-03	4.48E-08	1.22E-08	2.55E-05	1.28E-08	2.55E-02	2.55E-02
7.81E+00	5.20E-06	1.12E-03	4.48E-08	1.30E-08	2.54E-05	1.28E-08	2.54E-02	2.54E-02
8.30E+00	5.51E-06	1.12E-03	4.47E-08	1.38E-08	2.54E-05	1.28E-08	2.54E-02	2.54E-02

[a] The calculations for the highlighted time step are shown in Figure 5-17.

5.4 Accumulation in Meat and Milk

Accumulation in meat and milk at offsite locations is calculated as described in Section 5.4 of the RESRAD-OFFSITE User's Manual. Assuming that agricultural areas are not in the primary contamination zone, accumulation is given as (Eq. 5.52 in the RESRAD-OFFSITE User's Manual):

$$m_i(t) = imf_i[q_{ing}^p p_i(t) + q_{ing}^s s_i^o(t) + q_{ing}^w w_i^{if}(t)] \tag{5.33}$$

where:

$m_i(t)$ = activity concentration of radionuclide *i* in meat or milk at time *t* (pCi/kg),

imf_i = meat or milk transfer factor of radionuclide *i* (pCi/kg per pCi/d),

q_{ing}^p = plant ingestion rate by the livestock (kg/d),

$p_i(t)$ = radionuclide *i* concentration in plant food (pCi/kg),

Table 5-12 Spreadsheet Calculations for U-238 Accumulation in Grain – Grown in Area 4

Time (year)	Soil Conc. from Code (pCi/g)	Irrigation Water Conc. from Code (pCi/L)	Air Conc. from Code (pCi/m^3)	Plant Conc. from Root Uptake (pCi/g)	Plant Conc. from Irrigation (pCi/g)	Plant Conc. from Dust (pCi/g)	Grain Conc. Calculated (pCi/kg)	Grain Conc. from Code (pCi/kg)
0.00E+00	0.00E+00	0.00E+00	1.19E-07	0.00E+00	0.00E+00	6.50E-09	6.50E-06	6.50E-06
4.88E-01	9.66E-08	4.43E-04	1.19E-07	2.41E-10	8.99E-07	6.49E-09	9.06E-04	9.06E-04
9.77E-01	3.33E-07	7.14E-04	1.19E-07	8.33E-10	1.45E-06	6.47E-09	1.46E-03	1.46E-03
1.46E+00	6.52E-07	8.79E-04	1.19E-07	1.63E-09	1.79E-06	6.46E-09	1.79E-03	1.79E-03
1.95E+00	1.02E-06	9.80E-04	1.18E-07	2.54E-09	1.99E-06	6.45E-09	2.00E-03	2.00E-03
2.44E+00	1.41E-06	1.04E-03	1.18E-07	3.52E-09	2.11E-06	6.44E-09	2.12E-03	2.12E-03
2.93E+00[a]	1.81E-06	1.08E-03	1.18E-07	4.52E-09	2.19E-06	6.43E-09	2.20E-03	2.20E-03
3.42E+00	2.21E-06	1.10E-03	1.18E-07	5.53E-09	2.23E-06	6.42E-09	2.25E-03	2.25E-03
3.91E+00	2.61E-06	1.11E-03	1.18E-07	6.53E-09	2.26E-06	6.41E-09	2.27E-03	2.27E-03
4.39E+00	3.01E-06	1.12E-03	1.18E-07	7.52E-09	2.27E-06	6.40E-09	2.29E-03	2.29E-03
4.88E+00	3.40E-06	1.12E-03	1.17E-07	8.50E-09	2.28E-06	6.39E-09	2.30E-03	2.30E-03
5.37E+00	3.78E-06	1.13E-03	1.17E-07	9.46E-09	2.29E-06	6.38E-09	2.30E-03	2.30E-03
5.86E+00	4.16E-06	1.13E-03	1.17E-07	1.04E-08	2.29E-06	6.37E-09	2.30E-03	2.30E-03
6.35E+00	4.53E-06	1.12E-03	1.17E-07	1.13E-08	2.28E-06	6.36E-09	2.30E-03	2.30E-03
6.84E+00	4.89E-06	1.12E-03	1.17E-07	1.22E-08	2.28E-06	6.35E-09	2.30E-03	2.30E-03
7.32E+00	5.24E-06	1.12E-03	1.16E-07	1.31E-08	2.28E-06	6.34E-09	2.30E-03	2.30E-03
7.81E+00	5.58E-06	1.12E-03	1.16E-07	1.40E-08	2.28E-06	6.33E-09	2.30E-03	2.30E-03
8.30E+00	5.92E-06	1.12E-03	1.16E-07	1.48E-08	2.27E-06	6.32E-09	2.29E-03	2.29E-03

[a] The calculations for the highlighted time step are shown in Figure 5-19.

q_{ing}^{s} = soil ingestion rate by the livestock (kg/d),

$s_i^0(t)$ = radionuclide *i* concentration in soil ingested by livestock at time *t* (pCi/kg),

q_{ing}^{w} = water ingestion rate by the livestock (kg/L),

$w_i^{if}(t)$ = radionuclide *i* concentration in water ingested by livestock at time *t* (pCi/L).

Livestock eat grains as well as pasture and silage, and the soil ingested would be from both agricultural areas where livestock feed is grown. Cs-137 was selected for this pathway verification. The initial soil concentration in the primary contaminated area was 1 pCi/g. Surface water was the source of water for all uses. Other parameters were at their default values. First the accumulation from the sub-pathways was calculated and finally added together to compare the results of the total meat and milk concentrations (see Tables 5-13 and 5-14). The sub-pathways considered were: pasture and silage ingestion, grain ingestion, soil ingestion from pasture and silage agricultural area, soil ingestion from grain agricultural area, and water ingestion. For this comparison, radionuclide concentration in plant, soil, and water was obtained from the code. Figure 5-20 shows the Cs-137 accumulations in meat, and Figure 5-21 shows the Cs-137 accumulation in milk. Figure 5-22 shows the individual steps of the calculation for one time step highlighted in Table 5-13 for Cs-137 accumulation in meat. Figure 5-23 shows the individual steps of the calculation for one time step highlighted in Table 5-14 for Cs-137 accumulation in milk.

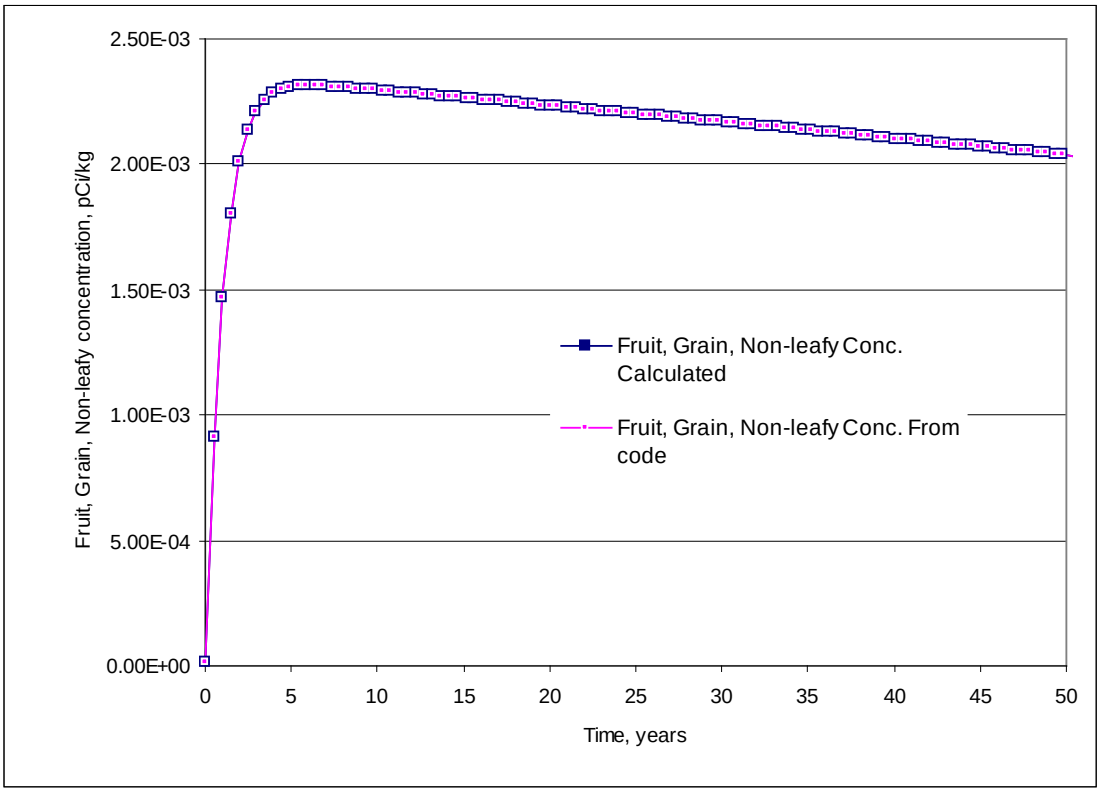

Figure 5-12 Accumulation of U-238 in Fruit, Grain, and Nonleafy Vegetables from Spreadsheet Calculations and from RESRAD-OFFSITE Code

There is practically no difference in the RESRAD-OFFSITE code results and spreadsheet calculations for meat and milk accumulation.

5.5 Accumulation in Fish and Aquatic Foods

Accumulation in fish and aquatic food is calculated as described in Section 5.5 of the RESRAD-OFFSITE User's Manual by the following equation:

$$aqf_i(t) = baf_i \times w_i^{sw}(t) \tag{5.34}$$

where:

$aqf_i(t)$ = activity concentration of radionuclide *i* in aquatic food at time *t* (pCi/kg),

$w_i^{sw}(t)$ = surface water concentration at any time *t* (pCi/L), and

baf_i = bioaccumulation factor in fish or aquatic food (pCi/kg per pCi/L).

Cobalt-60 was selected for this pathway verification. The initial concentration was 1 pCi/g. The rest of the parameters were at their default values. The surface water concentration at different times was obtained from the code. Table 5-15 shows the results from the spreadsheet calculations and compares the

Plant Concentration Calculations – Fruir, Grain, and Non-leafy Vegetables

3.4	=	20	×	0.17
$\lambda_w t_g$		λ_w		t_g
		/yr		yr

4.83E-02	=	(1	−	exp(-	3.4	)	/	20
$\frac{1-\exp(-\lambda_w t_g)}{\lambda_w}$					$\lambda_w t_g$			λ_w
yr								/yr

3.57E-02	=	0.25	×	0.1	/	0.7
$\frac{f_{\text{int}} f_{tl}}{Y}$		f_{int}		f_{tl}		Y
(m^2/kg)						kg/m^2

Root uptake from off-site contaminated soil

4.69E-06	=	2.50E-03	×	1.88E-03	(5.30)
$p_i^{offsoil}(t)$		rtf_i		$s_i^0(t)$	
		pCi/kg per			
(pCi/kg)		pCi/kg		(pCi/kg)	

Foliar uptake from overhead irrigation

2.19E-03	=	3.57E-02	×	4.83E-02	×	1.08E+00	×	0.2	/	0.17	(5.31)
$p_i^{oi}(t)$		$\frac{f_{\text{int}} f_{tl}}{Y}$		$\frac{1-\exp(-\lambda_w t_g)}{\lambda_w}$		$w_i^{ir}(t)$		q_{ir}		t_g	
(pCi/kg)		(m^2/kg)		(yr)		(pCi/m^3)		(m)		(yr)	

Foliar uptake from contaminated dust

1.64E-05	=	3.57E-02	×	4.83E-02	×	3.00E-07	×	31557.6	(5.32)
$p_i^{dust}(t))$		$\frac{f_{\text{int}} f_{tl}}{Y}$		$\frac{1-\exp(-\lambda_w t_g)}{\lambda_w}$		$a_i(t)$		V_{dep}	
(pCi/kg)		(m^2/kg)		(yr)		(pCi/m^3)		(m/yr)	

Figure 5-13 Plant Concentration Calculations for Fruit, Grain, and Nonleafy Vegetables

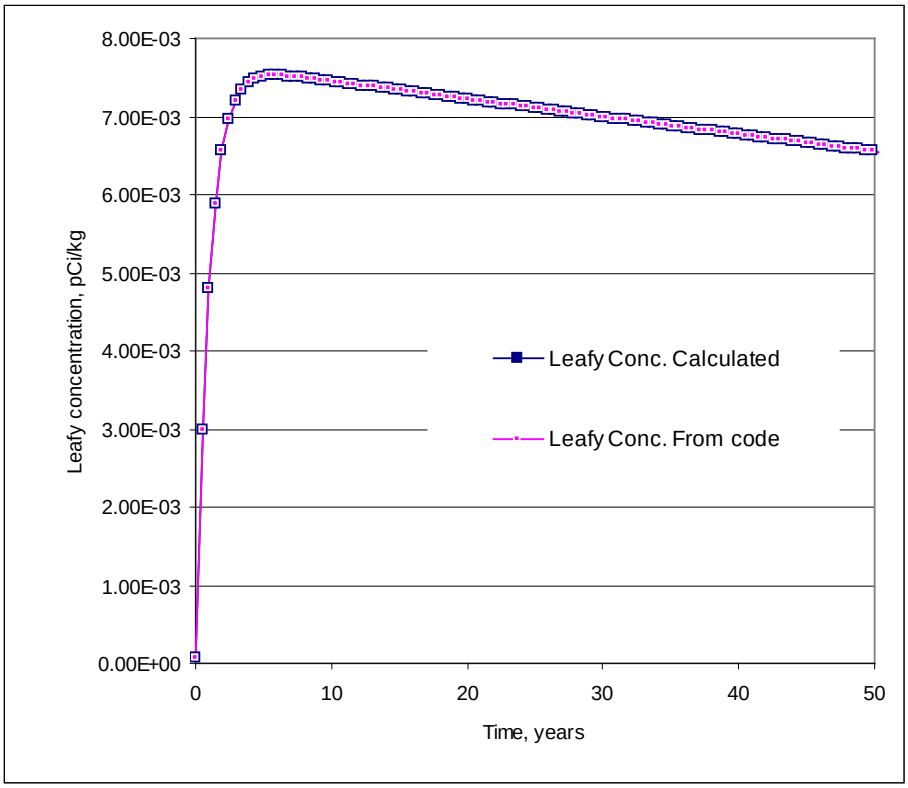

Figure 5-14 Accumulation of U-238 in Leafy Vegetables from Spreadsheet Calculations and from RESRAD-OFFSITE Code

results from the code for different time steps. Figure 5-24 shows the accumulation concentration calculations in fish and aquatic food. Figure 5-25 compares the results for fish concentration, and Figure 5-26 compares the spreadsheet calculated results for crustacea concentration.

Plant Concentration Calculations - Leafy Vegetables

5	=	20	×	0.25
$\lambda_w t_g$		λ_w		t_g
		/yr		yr

4.97E-02	=	(1	−	exp(-	5	)	/	20
$\frac{1-\exp(-\lambda_w t_g)}{\lambda_w}$					$\lambda_w t_g$			λ_w
yr								/yr

1.67E-01	=	0.25	×	1	/	1.5
$\frac{f_{\text{int}} f_{tl}}{Y}$		f_{int}		f_{tl}		Y
(m^2/kg)						kg/m^2

Root uptake from off-site contaminated soil

4.73E-06	=	2.50E-03	×	1.89E-03	(5.30)
$p_i^{offsoil}(t)$		rtf_i		$s_i^0(t)$	
(pCi/kg)		pCi/kg per pCi/kg		(pCi/kg)	

Foliar uptake from overhead irrigation

7.14E-03	=	1.67E-01	×	4.97E-02	×	1.08E+00	×	0.2	/	0.25	(5.31)
$p_i^{oi}(t)$		$\frac{f_{\text{int}} f_{tl}}{Y}$		$\frac{1-\exp(-\lambda_w t_g)}{\lambda_w}$		$w_i^{ir}(t)$		q_{ir}		t_g	
(pCi/kg)		(m^2/kg)		(yr)		(pCi/m^3)		(m)		(yr)	

Foliar uptake from contaminated dust

6.08E-05	=	1.67E-01	×	4.97E-02	×	2.33E-07	×	31557.6	(5.32)
$p_i^{dust}(t)$		$\frac{f_{\text{int}} f_{tl}}{Y}$		$\frac{1-\exp(-\lambda_w t_g)}{\lambda_w}$		$a_i(t)$		V_{dep}	
(pCi/kg)		(m^2/kg)		(yr)		(pCi/m^3)		(m/yr)	

Figure 5-15 Plant Concentration Calculations for Leafy Vegetables

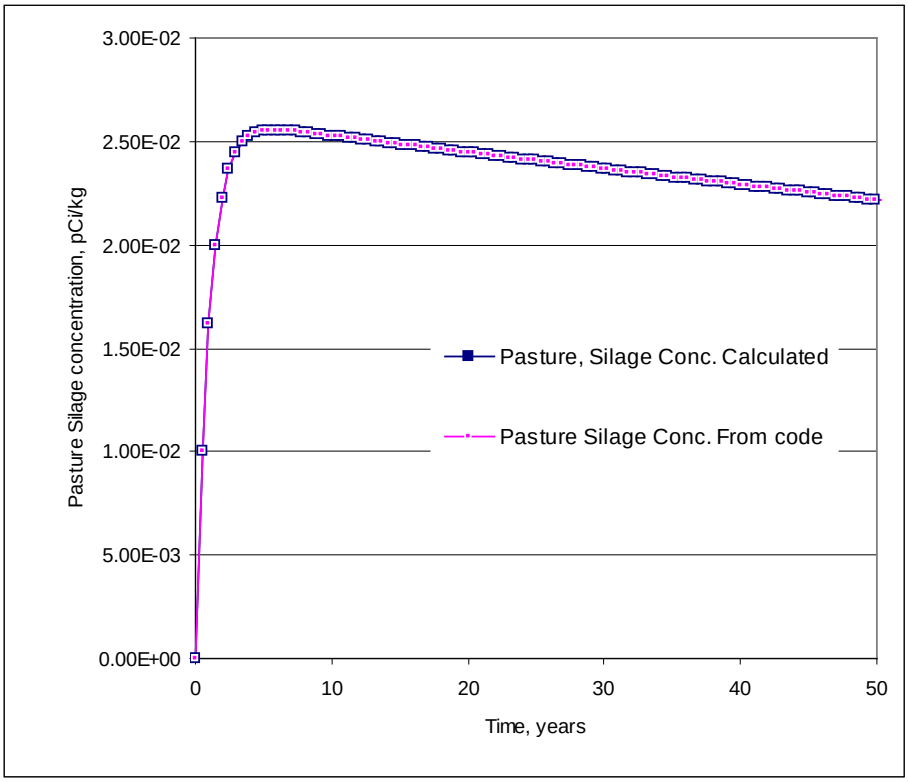

Figure 5-16 Accumulation of U-238 in Pasture and Silage from Spreadsheet Calculations and from RESRAD-OFFSITE Code

Plant Concentration Calculations - Pasture and Silage

1.6	=	20	×	0.08
$\lambda_w t_g$		λ_w		t_g
		/yr		yr

3.99E-02	=	(1	−	exp(-	1.6	)	/	20
$\frac{1-\exp(-\lambda_w t_g)}{\lambda_w}$					$\lambda_w t_g$			λ_w
yr								/yr

2.27E-01	=	0.25	×	1	/	1.1
$\frac{f_{\text{int}} f_{tl}}{Y}$		f_{int}		f_{tl}		Y
(m^2/kg)						kg/m^2

Root uptake from off-site contaminated soil

4.19E-06	=	2.50E-03	×	1.68E-03	(5.30)
$p_i^{offsoil}(t)$		rtf_i		$s_i^0(t)$	
(pCi/kg)		pCi/kg per pCi/kg		(pCi/kg)	

Foliar uptake from overhead irrigation

2.44E-02	=	2.27E-01	×	3.99E-02	×	1.08E+00	×	0.2	/	0.08	(5.31)
$p_i^{oi}(t)$		$\frac{f_{\text{int}} f_{tl}}{Y}$		$\frac{1-\exp(-\lambda_w t_g)}{\lambda_w}$		$w_i^{ir}(t)$		q_{ir}		t_g	
(pCi/kg)		(m^2/kg)		(yr)		(pCi/m^3)		(m)		(yr)	

Foliar uptake from contaminated dust

1.30E-05	=	2.27E-01	×	3.99E-02	×	4.55E-08	×	31557.6	(5.32)
$p_i^{dust}(t)$		$\frac{f_{\text{int}} f_{tl}}{Y}$		$\frac{1-\exp(-\lambda_w t_g)}{\lambda_w}$		$a_i(t)$		V_{dep}	
(pCi/kg)		(m^2/kg)		(yr)		(pCi/m^3)		(m/yr)	

Figure 5-17 Plant Concentration Calculations for Pasture and Silage

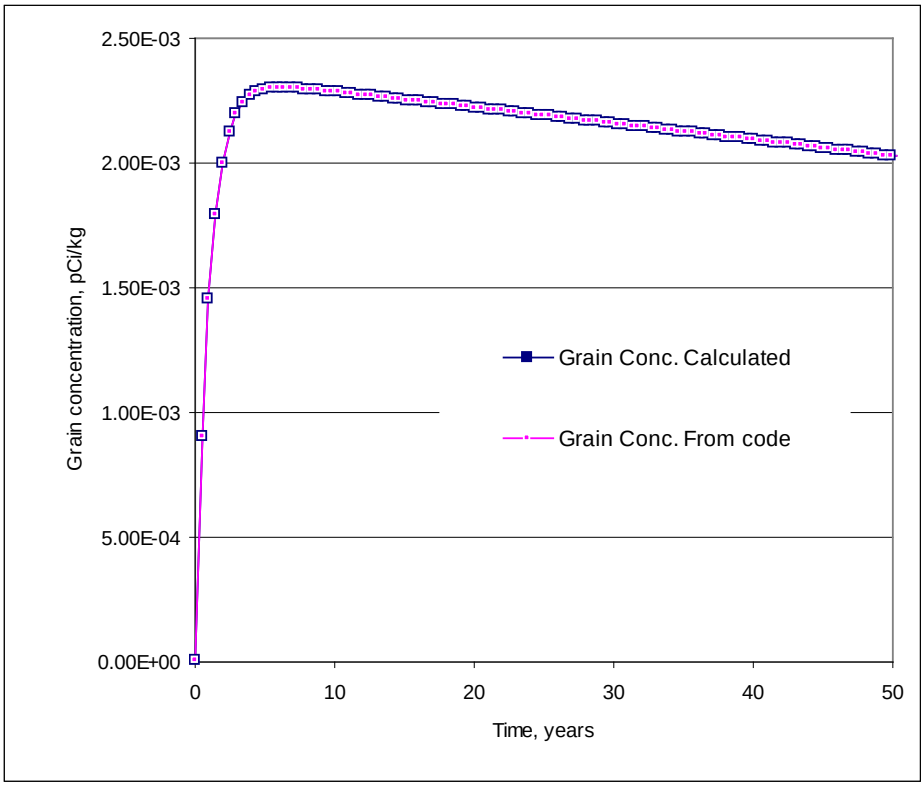

Figure 5-18 Accumulation of U-238 in Grain from Spreadsheet Calculations and from RESRAD-OFFSITE Code

Plant Concentration Calculations - Grain

3.4	=	20	×	0.17
$\lambda_w t_g$		λ_w		t_g
		/yr		yr

4.83E-02	=	(1	−	exp(-	1.6	)	/	20
$\frac{1-\exp(-\lambda_w t_g)}{\lambda_w}$					$\lambda_w t_g$			λ_w
yr								/yr

3.57E-02	=	0.25	×	0.1	/	0.7
$\frac{f_{\text{int}} f_{tl}}{Y}$		f_{int}		f_{tl}		Y
(m^2/kg)						kg/m^2

Root uptake from off-site contaminated soil

4.52E-06	=	2.50E-03	×	1.81E-03	(5.30)
$p_i^{offsoil}(t)$		rtf_i		$s_i^0(t)$	
(pCi/kg)		pCi/kg per pCi/kg		(pCi/kg)	

Foliar uptake from overhead irrigation

2.19E-03	=	3.57E-02	×	4.83E-02	×	1.08E+00	×	0.2	/	0.17	(5.31)
$p_i^{oi}(t)$		$\frac{f_{\text{int}} f_{tl}}{Y}$		$\frac{1-\exp(-\lambda_w t_g)}{\lambda_w}$		$w_i^{ir}(t)$		q_{ir}		t_g	
(pCi/kg)		(m^2/kg)		(yr)		(pCi/m^3)		(m)		(yr)	

Foliar uptake from contaminated dust

6.43E-06	=	3.57E-02	×	4.83E-02	×	1.18E-07	×	31557.6	(5.32)
$p_i^{dust}(t))$		$\frac{f_{\text{int}} f_{tl}}{Y}$		$\frac{1-\exp(-\lambda_w t_g)}{\lambda_w}$		$a_i(t)$		V_{dep}	
(pCi/kg)		(m^2/kg)		(yr)		(pCi/m^3)		(m/yr)	

Figure 5-19 Plant Concentration Calculations for Grain

Table 5-13 Spreadsheet Calculations for Cs-137 Meat Concentration

Time (year)	Pasture Conc. (pCi/kg)	Grain Conc. (pCi/kg)	Water Conc. (pCi/L)	Soil Conc. in Grain Area (pCi/g)	Soil Conc. in Pasture Area (pCi/g)	Meat Conc. from Pasture Intake (pCi/kg)	Meat Conc. from Grain Intake (pCi/kg)	Meat Conc. from Water Intake (pCi/kg)	Meat Conc. from Soil Intake with Grain (pCi/kg)	Meat Conc. from Soil Intake with Pasture (pCi/kg)	Total Meat Conc. Calculated (pCi/kg)	Meat Conc. from Code (pCi/kg)
0.00E+00	1.31E-05	6.50E-06	0.00E+00	0.00E+00	0.00E+00	5.52E-06	1.05E-05	0.00E+00	0.00E+00	0.00E+00	1.60E-05	1.60E-05
4.88E-01	9.93E-03	8.98E-04	4.37E-04	9.58E-08	8.58E-08	4.17E-03	1.46E-03	6.56E-04	1.15E-06	2.57E-07	6.28E-03	6.28E-03
9.77E-01	1.58E-02	1.43E-03	6.97E-04	3.30E-07	3.02E-07	6.65E-03	2.32E-03	1.05E-03	3.96E-06	9.07E-07	1.00E-02	1.00E-02
1.46E+00	1.93E-02	1.76E-03	8.49E-04	6.44E-07	5.94E-07	8.10E-03	2.85E-03	1.27E-03	7.73E-06	1.78E-06	1.22E-02	1.22E-02
1.95E+00	2.13E-02	1.95E-03	9.37E-04	1.00E-06	9.27E-07	8.94E-03	3.16E-03	1.41E-03	1.20E-05	2.78E-06	1.35E-02	1.35E-02
2.44E+00	2.24E-02	2.06E-03	9.85E-04	1.38E-06	1.28E-06	9.41E-03	3.34E-03	1.48E-03	1.66E-05	3.85E-06	1.42E-02	1.42E-02
2.93E+00	2.30E-02	2.13E-03	1.01E-03	1.78E-06	1.65E-06	9.65E-03	3.45E-03	1.51E-03	2.13E-05	4.94E-06	1.46E-02	1.46E-02
3.42E+00	2.32E-02	2.16E-03	1.02E-03	2.17E-06	2.01E-06	9.76E-03	3.51E-03	1.53E-03	2.60E-05	6.04E-06	1.48E-02	1.48E-02
3.91E+00	2.33E-02	2.18E-03	1.02E-03	2.56E-06	2.38E-06	9.78E-03	3.54E-03	1.53E-03	3.07E-05	7.14E-06	1.49E-02	1.49E-02
4.39E+00	2.32E-02	2.19E-03	1.02E-03	2.95E-06	2.74E-06	9.75E-03	3.55E-03	1.53E-03	3.54E-05	8.22E-06	1.49E-02	1.49E-02
4.88E+00	2.31E-02	2.19E-03	1.01E-03	3.33E-06	3.10E-06	9.70E-03	3.56E-03	1.52E-03	3.99E-05	9.29E-06	1.48E-02	1.48E-02
5.37E+00[a]	2.29E-02	2.19E-03	1.00E-03	3.70E-06	3.44E-06	9.62E-03	3.55E-03	1.51E-03	4.44E-05	1.03E-05	1.47E-02	1.47E-02
5.86E+00	2.27E-02	2.19E-03	9.95E-04	4.07E-06	3.78E-06	9.54E-03	3.54E-03	1.49E-03	4.88E-05	1.14E-05	1.46E-02	1.46E-02
6.35E+00	2.25E-02	2.18E-03	9.85E-04	4.42E-06	4.12E-06	9.45E-03	3.53E-03	1.48E-03	5.31E-05	1.24E-05	1.45E-02	1.45E-02
6.84E+00	2.23E-02	2.17E-03	9.74E-04	4.77E-06	4.44E-06	9.36E-03	3.52E-03	1.46E-03	5.73E-05	1.33E-05	1.44E-02	1.44E-02
7.32E+00	2.21E-02	2.17E-03	9.64E-04	5.11E-06	4.76E-06	9.26E-03	3.51E-03	1.45E-03	6.14E-05	1.43E-05	1.43E-02	1.43E-02
7.81E+00	2.18E-02	2.16E-03	9.53E-04	5.44E-06	5.07E-06	9.17E-03	3.50E-03	1.43E-03	6.53E-05	1.52E-05	1.42E-02	1.42E-02
8.30E+00	2.16E-02	2.15E-03	9.43E-04	5.77E-06	5.37E-06	9.07E-03	3.48E-03	1.41E-03	6.92E-05	1.61E-05	1.41E-02	1.41E-02

[a] The calculations for the highlighted time step are shown in Figure 5-22.

Table 5-14 Spreadsheet Calculations for Cs-137 Milk Concentration

Time (year)	Pasture Conc. (pCi/kg)	Grain Conc. (pCi/kg)	Water Conc. (pCi/L)	Soil Conc. in Grain Area (pCi/g)	Soil Conc. in Pasture Area (pCi/g)	Milk Conc. from Pasture Intake (pCi/kg)	Milk Conc. from Grain Intake (pCi/kg)	Milk Conc. from Water Intake (pCi/kg)	Milk Conc. from Soil Intake with Grain (pCi/kg)	Milk Conc. from Soil Intake with Pasture (pCi/kg)	Total Milk Conc. Calculated (pCi/kg)	Milk Conc. from Code (pCi/kg)
0.00E+00	1.31E-05	6.50E-06	0.00E+00	0.00E+00	0.00E+00	4.63E-06	5.72E-07	0.00E+00	0.00E+00	0.00E+00	5.20E-06	5.20E-06
4.88E-01	9.93E-03	8.98E-04	4.37E-04	9.58E-08	8.58E-08	3.50E-03	7.91E-05	5.60E-04	7.66E-08	2.75E-07	4.14E-03	4.14E-03
9.77E-01	1.58E-02	1.43E-03	6.97E-04	3.30E-07	3.02E-07	5.57E-03	1.26E-04	8.92E-04	2.64E-07	9.67E-07	6.59E-03	6.59E-03
1.46E+00	1.93E-02	1.76E-03	8.49E-04	6.44E-07	5.94E-07	6.79E-03	1.55E-04	1.09E-03	5.15E-07	1.90E-06	8.03E-03	8.03E-03
1.95E+00	2.13E-02	1.95E-03	9.37E-04	1.00E-06	9.27E-07	7.49E-03	1.71E-04	1.20E-03	8.02E-07	2.97E-06	8.87E-03	8.87E-03
2.44E+00	2.24E-02	2.06E-03	9.85E-04	1.38E-06	1.28E-06	7.89E-03	1.81E-04	1.26E-03	1.11E-06	4.10E-06	9.33E-03	9.33E-03
2.93E+00	2.30E-02	2.13E-03	1.01E-03	1.78E-06	1.65E-06	8.09E-03	1.87E-04	1.29E-03	1.42E-06	5.27E-06	9.57E-03	9.57E-03
3.42E+00	2.32E-02	2.16E-03	1.02E-03	2.17E-06	2.01E-06	8.18E-03	1.91E-04	1.31E-03	1.74E-06	6.45E-06	9.68E-03	9.68E-03
3.91E+00	2.33E-02	2.18E-03	1.02E-03	2.56E-06	2.38E-06	8.20E-03	1.92E-04	1.31E-03	2.05E-06	7.62E-06	9.71E-03	9.71E-03
4.39E+00	2.32E-02	2.19E-03	1.02E-03	2.95E-06	2.74E-06	8.17E-03	1.93E-04	1.30E-03	2.36E-06	8.77E-06	9.68E-03	9.68E-03
4.88E+00	2.31E-02	2.19E-03	1.01E-03	3.33E-06	3.10E-06	8.13E-03	1.93E-04	1.30E-03	2.66E-06	9.91E-06	9.63E-03	9.63E-03
5.37E+00[a]	2.29E-02	2.19E-03	1.00E-03	3.70E-06	3.44E-06	8.07E-03	1.93E-04	1.29E-03	2.96E-06	1.10E-05	9.56E-03	9.56E-03
5.86E+00	2.27E-02	2.19E-03	9.95E-04	4.07E-06	3.78E-06	8.00E-03	1.93E-04	1.27E-03	3.25E-06	1.21E-05	9.48E-03	9.48E-03
6.35E+00	2.25E-02	2.18E-03	9.85E-04	4.42E-06	4.12E-06	7.92E-03	1.92E-04	1.26E-03	3.54E-06	1.32E-05	9.39E-03	9.39E-03
6.84E+00	2.23E-02	2.17E-03	9.74E-04	4.77E-06	4.44E-06	7.84E-03	1.91E-04	1.25E-03	3.82E-06	1.42E-05	9.30E-03	9.30E-03
7.32E+00	2.21E-02	2.17E-03	9.64E-04	5.11E-06	4.76E-06	7.76E-03	1.91E-04	1.23E-03	4.09E-06	1.52E-05	9.21E-03	9.21E-03
7.81E+00	2.18E-02	2.16E-03	9.53E-04	5.44E-06	5.07E-06	7.68E-03	1.90E-04	1.22E-03	4.36E-06	1.62E-05	9.11E-03	9.11E-03
8.30E+00	2.16E-02	2.15E-03	9.43E-04	5.77E-06	5.37E-06	7.60E-03	1.89E-04	1.21E-03	4.62E-06	1.72E-05	9.02E-03	9.02E-03

[a] The calculations for the highlighted time step are shown in Figure 5-23.

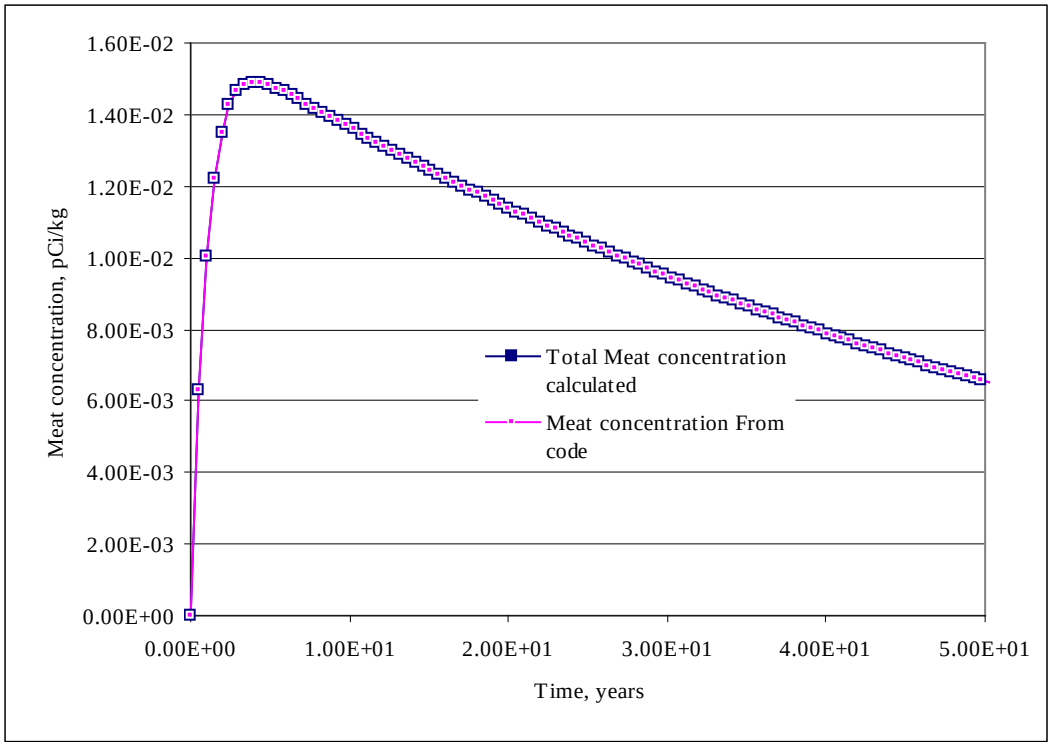

Figure 5-20 Accumulation of Cs-137 in Meat from Spreadsheet Calculations and from RESRAD-OFFSITE Code

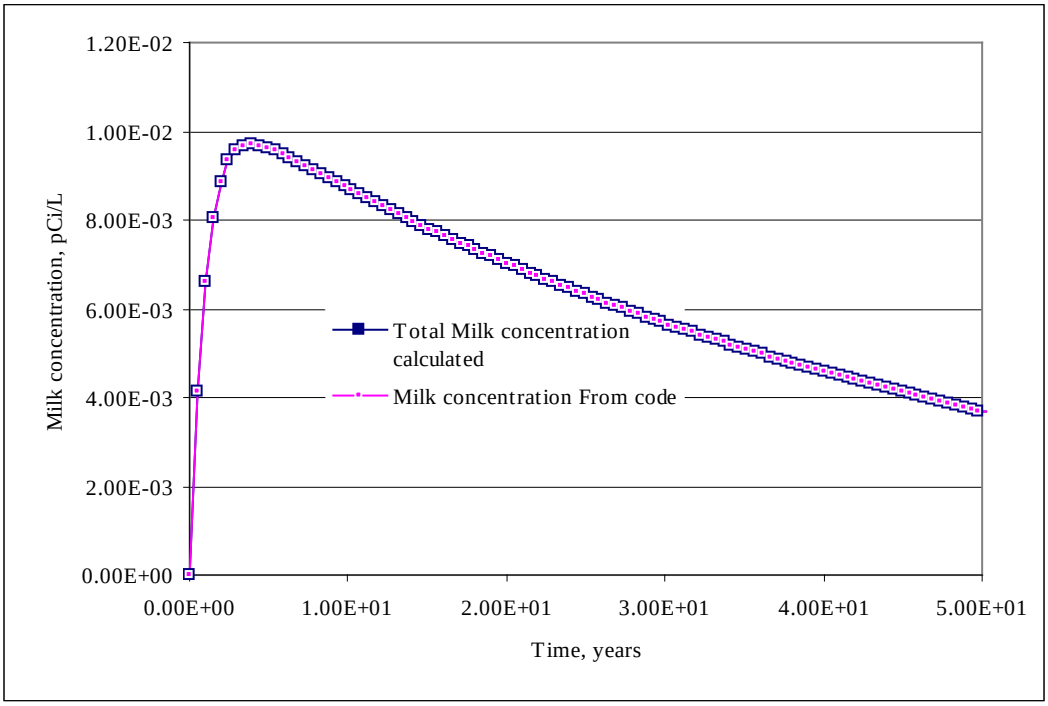

Figure 5-21 Accumulation of Cs-137 in Milk from Spreadsheet Calculations and from RESRAD-OFFSITE Code

Meat Concentration Calculations

Meat concentration from pasture intake

9.62E-03	=	0.03	x	14	x	2.29E-02	(5.33)
$m_i(t)$		imf_i		q_{ing}^{p}		$p_i(t)$	
pCi/kg		pCi/kg per pCi/d		kg/d		pCi/kg	

Meat concentration from grain intake

3.55E-03	=	0.03	x	54	x	2.19E-03	(5.33)
$m_i(t)$		imf_i		q_{ing}^{p}		$p_i(t)$	
pCi/kg		pCi/kg per pCi/d		kg/d		pCi/kg	

Meat concentration from soil intake in pasture agricultural area

1.03E-05	=	0.03	x	0.1	x	3.44E-03	(5.33)
$m_i(t)$		imf_i		q_{ing}^{s}		$s_i^o(t)$	
pCi/kg		pCi/kg per pCi/d		kg/d		pCi/kg	

Meat concentration from soil intake in grain agricultural area

4.44E-05	=	0.03	x	0.4	x	3.70E-03	(5.33)
$m_i(t)$		imf_i		q_{ing}^{s}		$s_i^o(t)$	
pCi/kg		pCi/kg per pCi/d		kg/d		pCi/kg	

Meat concentration from water intake

1.51E-03	=	0.03	x	50	x	1.00E-03	(5.33)
$m_i(t)$		imf_i		q_{ing}^{w}		$w_i^{if}(t)$	
pCi/kg		pCi/kg per pCi/d		L/d		pCi/kg	

Figure 5-22 Meat Concentration Calculations

Milk Concentration Calculations

Milk concentration from pasture intake

8.07E-03	=	0.008	X	44	x	2.29E-02	(5.33)
$m_i(t)$		imf_i		q_{ing}^{p}		$p_i(t)$	
pCi/kg		pCi/kg per pCi/d		kg/d		pCi/kg	

Milk concentration from grain intake

1.93E-04	=	0.008	X	11	x	2.19E-03	(5.33)
$m_i(t)$		imf_i		q_{ing}^{p}		$p_i(t)$	
pCi/kg		pCi/kg per pCi/d		kg/d		pCi/kg	

Milk concentration from soil intake in pasture agricultural area

1.10E-05	=	0.008	X	0.4	x	3.44E-03	(5.33)
$m_i(t)$		imf_i		q_{ing}^{s}		$s_i^{o}(t)$	
pCi/kg		pCi/kg per pCi/d		kg/d		pCi/kg	

Milk concentration from soil intake in grain agricultural area

2.96E-06	=	0.008	X	0.1	x	3.70E-03	(5.33)
$m_i(t)$		imf_i		q_{ing}^{s}		$s_i^{o}(t)$	
pCi/kg		pCi/kg per pCi/d		kg/d		pCi/kg	

Milk concentration from water intake

1.29E-03	=	0.008	X	160	x	1.00E-03	(5.33)
$m_i(t)$		imf_i		q_{ing}^{w}		$w_i^{if}(t)$	
pCi/kg		pCi/kg per pCi/d		L/d		pCi/kg	

Figure 5-23 Milk Concentration Calculations

Table 5-15 Spreadsheet Calculations for Co-60 Accumulation in Fish and Aquatic Foods

Time (year)	Surface Water Conc. from Code (pCi/L)	Fish Conc. Calculated (pCi/kg)	Crustacea Conc. Calculated (pCi/kg)	Fish Conc. from Code (pCi/kg)	Crustacea Conc. from Code (pCi/kg)
0	0.00E+00	0.00E+00	0.00E+00	0.00E+00	0.00E+00
0.49	4.16E-04	1.25E-01	8.31E-02	1.25E-01	8.31E-02
0.98	6.29E-04	1.89E-01	1.26E-01	1.89E-01	1.26E-01
1.46[a]	7.27E-04	2.18E-01	1.45E-01	2.18E-01	1.45E-01
1.95	7.61E-04	2.28E-01	1.52E-01	2.28E-01	1.52E-01
2.44	7.59E-04	2.28E-01	1.52E-01	2.28E-01	1.52E-01
2.93	7.38E-04	2.21E-01	1.48E-01	2.21E-01	1.48E-01
3.42	7.07E-04	2.12E-01	1.41E-01	2.12E-01	1.41E-01
3.91	6.72E-04	2.02E-01	1.34E-01	2.02E-01	1.34E-01
4.39	6.35E-04	1.90E-01	1.27E-01	1.90E-01	1.27E-01
4.88	5.98E-04	1.79E-01	1.20E-01	1.79E-01	1.20E-01
5.37	5.63E-04	1.69E-01	1.13E-01	1.69E-01	1.13E-01
5.86	5.29E-04	1.59E-01	1.06E-01	1.59E-01	1.06E-01
6.35	4.96E-04	1.49E-01	9.93E-02	1.49E-01	9.93E-02
6.84	4.66E-04	1.40E-01	9.31E-02	1.40E-01	9.31E-02
7.32	4.37E-04	1.31E-01	8.74E-02	1.31E-01	8.74E-02
7.81	4.10E-04	1.23E-01	8.20E-02	1.23E-01	8.20E-02
8.30	3.84E-04	1.15E-01	7.69E-02	1.15E-01	7.69E-02
8.79	3.60E-04	1.08E-01	7.21E-02	1.08E-01	7.21E-02
9.28	3.38E-04	1.01E-01	6.76E-02	1.01E-01	6.76E-02
9.77	3.17E-04	9.51E-02	6.34E-02	9.51E-02	6.34E-02
10.25	2.97E-04	8.92E-02	5.94E-02	8.92E-02	5.94E-02

[a] The calculations for the highlighted time step are shown in Figure 5-24.

Fish Concentration Calculations for Co-60

2.18E-01	=	300	x	7.27E-04	(5.34)
$aqf_i(t)$		baf_i		$w_i^{sw}(t)$	
(pCi/kg)		pCi/kg per pCi/L		pCi/L	

Crustacea Concentration Calculations for Co-60

1.45E-01	=	200	x	7.27E-04	(5.34)
$aqf_i(t)$		baf_i		$w_i^{sw}(t)$	
(pCi/kg)		pCi/kg per pCi/L		pCi/L	

Figure 5-24 Fish and Aquatic Foods Concentration Calculations

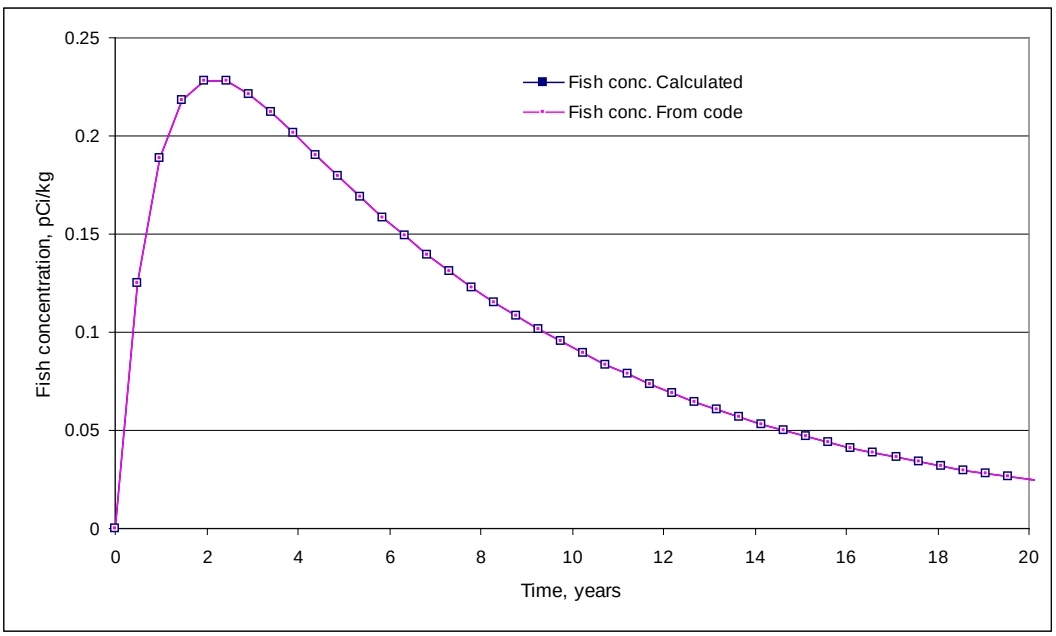

Figure 5-25 Accumulation of Co-60 in Fish from Spreadsheet Calculations and from RESRAD-OFFSITE Code

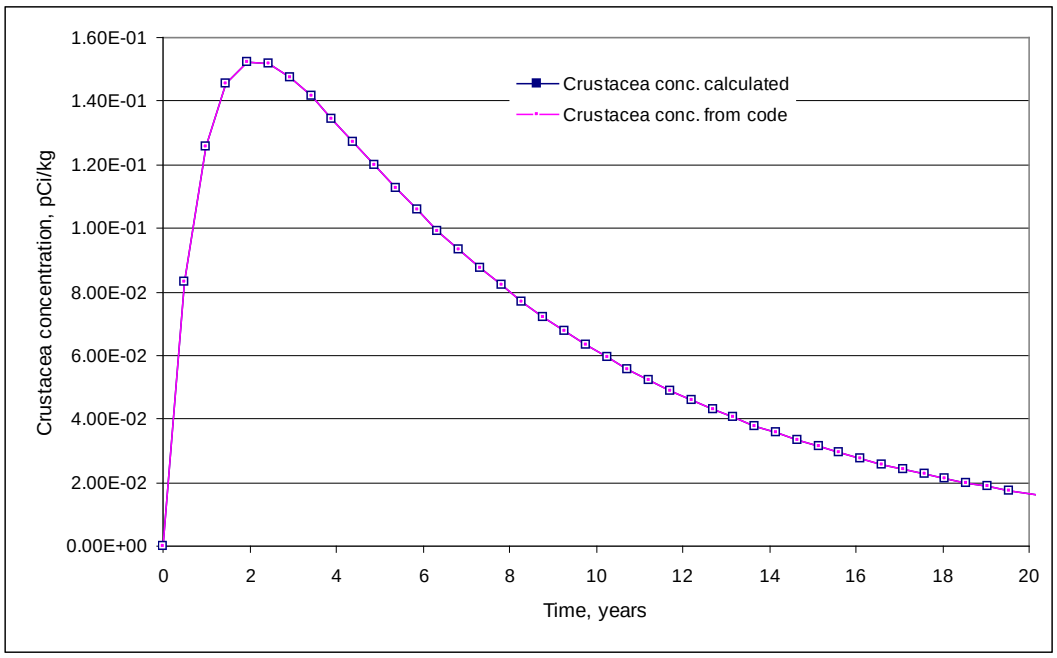

Figure 5-26 Accumulation of Co-60 in Crustacea from Spreadsheet Calculations and from RESRAD-OFFSITE Code

6 REFERENCES

BIOMOVS (Biosphere Model Validation Study) II, 1995, *Long-Term Contaminant Migration and Impacts from Uranium Mill Tailings — Comparison of Computer Models Using a Hypothetical Dataset*, BIOMOVS II Technical Report No. 4, Biosphere Model Validation Study Steering Committee, Swedish Radiation Protection Institute, Stockholm, Sweden.

BIOMOVS II, 1996, *Long-Term Contaminant Migration and Impacts from Uranium Mill Tailings — Comparison of Computer Models Using a Realistic Dataset*, BIOMOVS II Technical Report No. 5, Biosphere Model Validation Study Steering Committee, Swedish Radiation Protection Institute, Stockholm, Sweden.

Cheng, J.J., et al., 1995, *Benchmarking Analysis of Three Multimedia Models: RESRAD, MMSOILS, and MEPAS*, DOE/ORO-2033, U.S. Department of Energy, Washington, D.C.

Gnanapragasam, E., and C. Yu, 1997, *Analysis of BIOMOVS II Uranium Mill Tailings Scenario 1.07 with the RESRAD Computer Code*, ANL/EAD/TM-66, Argonne National Laboratory, Argonne, Ill.

Gnanapragasam, E., et al., 2000, "Comparison of Multimedia Model Predictions for a Contaminant Plume Migration Scenario," *J. Contaminant Hydrology* 46(1–2):17–38.

Halliburton NUS (Halliburton NUS Corporation), 1994, *Verification of RESRAD: A Code for Implementing Residual Radioactive Material Guidelines, Version 5.03*, HNUS-ARPD-94-174, Gaithersburg, Md.

Mills, W.B., et al., 1997, "Multimedia Benchmarking Analysis for Three Risk Assessment Models: RESRAD, MMSOILS, and MEPAS," *Risk Analysis* 17(2):187–201.

NREL (National Renewable Energy Laboratory), 2008, "Concentrating Solar Power Resource Maps," Sept. Available at http://www.nrel.gov/csp/maps.html. Accessed July 1, 2009.

Press, W.H., et al., 1992, *Numerical Recipes in FORTRAN, The Art of Scientific Computing*, Cambridge University Press, New York.

Whelan, G., et al., 1999a, "Benchmarking of the Saturated-Zone Module Associated with Three Risk Assessment Models: RESRAD, MMSOILS, and MEPAS," *Environmental Engineering Science* 16(1):67–80.

Whelan, G., et al., 1999b, "Benchmarking of the Vadose-Zone Module Associated with Three Risk Assessment Models: RESRAD, MMSOILS, and MEPAS," *Environmental Engineering Science* 16(1):81–91.

Yu, C., et al., 1993, *Manual for Implementing Residual Radioactive Material Guidelines Using RESRAD, Version 5.0*, ANL/EAD/LD-2, Argonne National Laboratory, Argonne, Ill.

Yu, C., et al., 2000, *Development of Probabilistic RESRAD 6.0 and RESRAD-Build 3.0 Computer Codes*, NUREG/CR-6697, ANL/EAD/TM-98, Argonne National Laboratory, Argonne, Ill., Nov.

Yu, C., et al., 2001, *User's Manual for RESRAD Version 6*, ANL/EAD-4, Argonne National Laboratory, Argonne, Ill.

Yu, C., et al., 2003, *User's Manual for RESRAD-BUILD Version 3*, ANL/EAD/03-1, Argonne National Laboratory, Argonne, Ill., June.

Yu, C., et al., 2006, *Benchmarking of RESRAD-OFFSITE: Transition from RESRAD (onsite) to RESRAD-OFFSITE and Comparison of RESRAD-OFFSITE Predictions with Peer Codes*, ANL/EVS/TM/05-1, Argonne National Laboratory, Argonne, Ill., June.

Yu, C., et al., 2007, *User's Manual for RESRAD-OFFSITE Version 2*, ANL/EVS/TM/07-1, DOE/HS-0005, NUREG/CR-6937, DOE/HS-0005, Environmental Science Division, Argonne National Laboratory, Argonne, Ill., June.